THE UNIVERSITY OF CALGARY

Analytical and Experimental Studies of the Stability Limits of Nonpremixed Flames in a Co-Flowing Stream

by

Massoumeh Karbassi

A DISSERTATION

SUBMITTED TO THE FACULTY OF GRADUATE STUDIES

IN PARTIAL FULFILLMENT OF THE REQUIREMENTS FOR THE

DEGREE OF DOCTOR OF PHILOSOPHY

DEPARTMENT OF MECHANICAL ENGINEERING

CALGARY, ALBERTA

SEPTEMBER, 1997

0-612-24541-1

Abstract

Stability limits of non-premixed jet flames into a co-flowing oxidizing stream have been studied both experimentally and analytically in this work.

The combined effect of jet velocity and co-flowing stream velocity on flame stability were investigated experimentally for methane, propane, ethylene and hydrogen as jet fuels. Four different types of flame stability limits were observed: liftoff, reattachment, blowout of *lifted* flames and blowout of *attached* flames. Depending on the value of the co-flowing stream velocity, three different regions were recognized. At low co-flowing stream velocities, blowout of *lifted* flames was observed while at higher co-flowing stream velocities, blowout of *attached* flames took place. For mid values of stream velocities, both types of blowout were experienced.

It was found that the conditions prior to ignition, such as co-flowing stream and jet velocities and position of the ignitor, have significant effects on the flame stabilization mechanism. Furthermore, the optimum ignition conditions for achieving higher blowout limits were explored experimentally and an ignition limit for attached flames was recognized.

Experiments indicated that the addition of diluents to a jet fuel or surrounding air stream could decrease the blowout limits of methane jet flames. Nitrogen, carbon dioxide and helium were employed as the diluents. Introduction of hydrogen into a methane jet flame increased the blowout limits of both lifted and attached flames. The effect of premixing a fuel with the surrounding air stream was also studied. Addition of an auxiliary fuel into a co-flowing air stream increased the blowout limits of lifted and attached flames for a methane jet. Methane, propane, ethylene and hydrogen were

used as auxiliary fuels. The effect of nozzle configuration on the stability limits of jet flames was investigated for a range of co-flowing air stream velocities.

Two different models were proposed to predict the stability limits of jet flames in a co-flowing stream. The need for two different models arises from the fact that the nozzle far-field conditions are responsible for blowout of *lifted* flames, while the nozzle near-field conditions affect the blowout of *attached* flames, liftoff and reattachment.

In the present study, a model for blowout of *lifted* flames was proposed based on a well-recognized criterion. According to this criterion, blowout occurs when the ratio of the mixing time scale to characteristic chemical time scale falls below a critical value. The advantage of this model stem from utilization of a different expression for the mixing time. The predictions of this model was fairly accurate over different operational conditions established by variations in surrounding stream velocity and composition, jet fuel composition, nozzle diameter and combustor size.

A dimensionless criterion was also proposed to predict liftoff, reattachment and blowout of *attached* flames in a co-flowing air stream. It was shown that these phenomena take place as the value of this criterion becomes equal to its critical value. The predicted stability limits using this criterion agreed fairly accurately with experimental data for (the fuels tried) methane, propane, ethylene and hydrogen jet flames over a range of co-flowing air stream velocities and jet diameters.

Acknowledgments

As with any undertaking, the five-year work which went into the completion of this dissertation could not have been done without the support and interest of a number of people.

My supervisor, Dr. I. Wierzba, must be especially acknowledged for her scholarly advice, sacrifice of time and thoughtful editing of this manuscript. Her extensive experience put my research onto the correct path to achieve a solution for an important practical problem. Her generous financial support ensured my peace of mind during the whole course of study.

Dr. G. A. Karim was an invaluable resource. I am deeply indebted to him for sharing his insights into problems related to this project. Dr. J. A. C. Kentfield, not only made interesting comments, but also provided an unlimited supply of encouragement. The laboratory work was supported ably by R. Gustafson, A. Moherle, G. East, B. Stephens, V. Nick, D. Forre and K.T. Wong. I offer warm thanks to our graduate secretary, Ms. Lynn Banach, for her swift replies to my numerous inquiries and to Ms. Maria Berry, Ms. Nareeza Khan, Ms. Rhonda Harbidge and Ms. Margaret Tefledzuk for their help with administrative matters related to my academic work.

I am deeply grateful to all my dear friends who helped me in many ways during this endeavor. I would especially like to thank Nancy Papanikolauo for her help during my experiments and her kind support, and Bhakta Ale, Eric Clavelle, Emad Khalil, Ramsey Bunama, Alireza Alizadeh Attar, Mehrdad Farid, Reza Babayi, Ian Potter, Yan Wong and Kai Chen for a five-year collaboration in various ways.

The financial support of the University of Calgary, Natural Science and Engineering Research Council of Canada and Zonta International Foundation are also acknowledged.

My parents have always given me the encouragement to learn more and employ my knowledge in practical ways. I am grateful to them for the many sacrifices they have made for me.

Finally, thanks must go to my husband Faramarz who allowed me to meet the challenge I encountered in pursuing this research work. He was always a full partner in this endeavor.

To
My Parents and My husband

Contents

List of Tables

List of Figures

List of Symbols

Notation

A	Mole of air
a_L	Constant, Equation (5.51)
Ct	Velocity ratio, Equation (5.27)
c	Mass fraction
d	Diameter (mm)
F	Mole of fuel
H	Constant, Equation (5.52)
I_1, I_2	Constant, Equations (5.19) and (5.20)
k	Dimensionless group, Equation (4.3)
k_B	Criterion for blowout limits of lifted flames, Equation (5.34)
k_B^*	Criterion for blowout limits of lifted flames, Equation (5.10)
$k_{B,Cr}$	Critical value of k_B
$k_{B,Cr}^*$	Critical value of k_B^*
k_{LBR}	Criterion for liftoff, blowout of attached flames and reattachment limits, Equation (6.1)
$(k_{LBR})_{Cr}$	Critical value of k_{LBR}
L_{DF}	Lean flammability limit of fuel-diluent mixture in air (% by volume)

L_F	Lean flammability limit of fuel in air (% by volume)
L_{F_1}	Lean flammability limit of the first fuel in air (% by volume)
L_{F_2}	Lean flammability limit of the second fuel in air (% by volume)
$L_{F_1 D}$	Lean flammability limit of the first fuel-diluent mixture in air (% by volume)
$L_{F_1 F_2}$	Lean flammability limit of jet fuel mixture (first and second fuel) in air (% by volume)
$L_{F_1 F_2 D}$	Lean flammability limit of jet fluid (mixture of the first, the second fuel and diluent) in air (% by volume)
$L_{F_J F_S}$	Lean flammability limit of fuel mixture (jet fuel and surrounding fuel) in air (% by volume)
L_{F_J}	Lean flammability limit of jet fuel in air (% by volume)
L_{F_S}	Lean flammability limit of surrounding fuel in air (% by volume)
L_{St}	Stoichiometric mixture of fuel in air (% by volume)
ℓ	Characteristic size of turbulent large eddies (m)
M	Molecular weight
m	Mass flow rate (kg/s)
P	Pressure (kPa)
Q	Volumetric flow rate (m^3/s)
Re_S	Reynolds number of co-flowing oxidizing stream
r	Radius (m)
S_L	Laminar burning velocity of fuel in air (m/s)
$S_{L,max}$	Maximum laminar burning velocity of fuel in air (m/s)
$S_{L,St}$	Stochiometric laminar burning velocity of fuel in air (m/s)
T	Temperature (K)

u	Velocity (m/s)
u_d	Dynamic velocity, Equation (5.29), (m/s)
u_k	Kinematic velocity, Equation (5.28), (m/s)
X	Normalized axial distance
X_r	Function, Equation (5.25)
X_u	Function, Equation (5.26)
x	Axial distance from jet exit (m)
Y	Mole fraction
Y_{AT}	Mole fraction of air in total mixture
Y_{DA}	Mole fraction of diluent in diluent-air mixture
Y_{DF}	Mole fraction of diluent in fuel-diluent mixture
Y_{DF_1}	Mole fraction of diluent in mixture of the first fuel and diluent
Y_{DT}	Mole fraction of diluent in total mixture
Y_{F_1}	Mole fraction of the first fuel in jet fuel mixture
Y_{F_1T}	Mole fraction of the first fuel in total mixture of fuels and diluent
Y_{F_2T}	Mole fraction of the second fuel in total mixture of fuels and diluent
Y_{F_SA}	Mole fraction of surrounding fuel in mixture of surrounding fuel and air
Y_{F_JT}	Mole fraction of jet fuel in total mixture of jet fuel, surrounding fuel and air
Y_{F_SF}	Mole fraction of surrounding fuel in mixture of jet fuel and surrounding fuel
Y_{F_ST}	Mole fraction of surrounding fuel in total mixture of jet fuel, surrounding fuel and air
Y_{FT}	Mole fraction of jet fuel in total mixture of jet fuel, surrounding

diluent and air

$U_{L,L}$ Liftoff jet velocity at limiting co-flowing stream velocity (m/s)

$U_{R,L}$ Reattachment jet velocity at limiting co-flowing stream velocity (m/s)

$U_{S,L}$ Limiting co-flowing stream velocity (m/s)

u_S Co-flowing stream velocity (m/s)

α Thermal diffusivity (m^2/s)

Δ Nozzle lip-thickness (mm)

δ_c Jet concentration-half radius (m)

δ_u Jet velocity-half radius (m)

ε Energy dissipation rate per unit mass (m^2/s^3)

η Normalized radical distance

ν Kinematic viscosity (m^2/s)

ρ Density (kg/m^3)

τ_c Characteristic chemical time (s)

τ_k Kolmogorov microscale of time (s)

τ_m Characteristic mixing time (s)

ϕ Equivalence ratio

Subscripts

A Air

ave Average

D Diluent

F Fuel

F_1 First fuel

F_2 Second fuel

F_J	Jet fuel
F_S	Surrounding (auxiliary) fuel
J	Jet
m	Jet axis
mix	Mixture
o	Jet exit
ref	Reference
S	Stream
St	Stochiometric
T	Total
∞	Co-flowing stream

Chapter 1

Introduction

1.1 Scope of the Present Work

Turbulent non-premixed jet flames (also known as diffusion flames) constitute an important class of flames in theoretical and experimental studies as well as practical applications such as gas turbine combustors, rocket motors, ram jets, industrial furnaces, diesel engines, petrochemical flares, etc. For the efficient and safe operation of these combustion devices, the jet flames should be stable over the whole range of operating conditions. A sudden blowout of flame can have serious implications.

In non-premixed jet flames the fuel and oxidizer are initially separated and then are mixed within the flame zone through molecular and turbulent diffusion. The combustion processes are controlled by the entrainment of surrounding oxidizer into the mixture of jet fuel and hot products of combustion until a flammable mixture is reached. A jet flame discharging into an effectively "infinite" quiescent atmosphere is called a free jet flame, while a jet flame discharging into an enclosed atmosphere of oxidizing stream is a confined jet flame.

An increase in the fuel jet velocity results in detachment - liftoff - of the flame from the burner rim. With further increase of the jet velocity, the lifted flame blows out, while a decrease in the jet velocity can lead to reattachment of lifted flames. When the air stream velocity exceeds a certain value with increasing the jet velocity, the flame attached to the rim blows out suddenly with no liftoff, i.e., blowout of attached flames occurs. The stability limits of jet flames particularly liftoff and blowout are of fundamental importance, since they define the operating limitation of combustion systems for an efficient usage of fuels. Research on the stability of jet flames has attracted much attention in the past with a renewed and vigorous attention recently. However, the actual physical and chemical processes affecting flame stability are very complex and many fundamental questions about their nature remain unanswered.

In many industrial applications, combustion of a jet fuel occurs in the presence of a co-flowing oxidizing stream. Adding a co-flowing oxidizing stream increases the efficiency of the combustion process, shortens the flame length and reduces the residence time for NO_x formation [1], but it increases the local gas velocity and destabilizes the flame. Although various models have been proposed for flame stability in the literature, they tend to have serious limitations, especially in dealing with *jet flames in co-flowing streams.* These models are incapable of predicting accurately all the experimental observations. At the present time, there is no model available to predict liftoff and blowout of attached flames in confined co-flowing streams as well as an observed hysteresis phenomenon in reattachment of lifted flames. Moreover, the model available for predicting blowout of lifted flames [2] cannot predict accurately enough the experimental trends over a wide range of operating conditions. Relatively limited experimental information is available on the stability limits of jet flames in a co-flowing air stream to validate a model. In spite of several experimental studies on the effect of confined co-flowing stream velocity on the stability limits of jet flames, there is no firm report of a thorough measurement of various phenomena such as liftoff, blowout and reattachment over a range of jet and stream velocity combinations for which a jet fuel can be ignited and sustained.

Due to pollution legislations, new alternatives such as mixtures of methane-hydrogen are of practical importance as potential sources of fuel. Due to insufficient data on the stability limits of these mixtures experimental and analytical studies are required to identify these limits for various compositions and to predict the improving effect of hydrogen addition to a methane jet on the flame stability limits.

In combustion systems, it is always desirable to enhance the stability limits of jet flames. One effective technique to improve these limits is the introduction of a secondary fuel into a surrounding air stream [3–5]. Accurate modeling is required to explain this phenomenon.

With the increasing availability and utilization of fuel mixtures as well as low heating value gaseous fuels containing a substantial amount of diluent (e.g. biogas), there is a need to estimate reliably the effect of the fuel composition on the blowout limits of non-premixed jet flames. There are also situations where the co-flowing air contains a small concentration of a diluent or a fuel. For example in gas turbines and internal combustion engines, some exhaust gas recirculation can be utilized to control NO_x emissions. The exhaust gas which contains a significant amount of carbon dioxide, nitrogen and water vapor vitiates the co-flowing combustion air resulting in a lower stability limit for jet flames. Only limited information is available about the flame stability limits in such conditions at the present time.

1.2 Objectives

The above section reveals that more measurements and modeling are needed to describe the stability of jet flames. The goal of the current research is to develop a simple yet comprehensive model predicting the blowout limits of *lifted* jet flames in a wide range of jet fuel compositions, fuel nozzle geometries and co-flowing stream velocities and compositions. The other purpose of this research is to obtain a dimensionless criterion for predicting the effect of fuel type and co-flowing stream velocities on the liftoff, reattachment and blowout of *attached* flames.

Experimental investigation of stability limits of jet flames in a co-flowing stream is required to gain more insight about the effect of a co-flowing stream on the flame stability characteristics as well as to validate the developed models. The proposed models should be validated against the available experimental data in the literature as well.

Chapter 2

Literature Survey

The stability limits of non-premixed jet flames - liftoff, reattachment, blowout of lifted or attached flames - have been subjects of numerous research efforts and have been studied through experiments [1–39] and semi-empirical modeling or computation [2,40–62]. A review of these efforts is summarized in this chapter.

2.1 Experimental Studies of Flame Stability

Simple Free Jet Flames. Various experimental investigations have been carried out to assess the stability limits of jet flames in different operational conditions. However, most of these investigations have been related to the combustion of fuel jets in an unconfined quiescent medium (simple free jet flames) [7–12, 40–43, 63]. Vanquickenborne and Van Tiggelen [40] have reported extensive experimental results for unignited and ignited methane jet flames for a range of jet velocities and jet diameters. Jet blowout limits and liftoff heights were reported as well. Their results for lifted flames showed that fuel concentration at the stabilization point is close to stoichiometric composition.

Similar measurements were conducted by Gunther et al [41, 42], and the liftoff, blowout and reattachment data for natural gas and mixtures of hydrogen and natural gas were reported. The liftoff heights for methane and ethylene jets diluted with air were measured by Mike-Lye and Hammer [43] and it was shown that liftoff heights increase with an increase in either jet velocity or amount of dilution.

The most extensive experimental investigation for liftoff and blowout limits of jet flames is reported by Kalghatgi [7, 8] for a variety of gaseous fuels and jet diameters. His results show that liftoff height is independent of jet diameter, increases linearly with an increase in jet velocity and decreases with an increase in burning velocity of a jet fuel, while jet blowout velocity increases with an increase with jet diameter and the burning velocity of a gaseous jet fuel.

Gollahalli et al [9] have studied the flame structure and hysteresis characteristic of lifting and reattaching for propane jet flames. They stated that the dynamics of organized structures control the reattachment process. In addition, the effect of fuel type and nozzle size on liftoff and reattachment velocity was investigated using propane and methane as a jet fuel and three different nozzle diameters of 5.53, 8.74 and 12.36 mm. Their experimental results revealed that liftoff and reattachment velocities for a methane jet are larger than those for a propane jet and these velocities decrease with an increase in nozzle size. Savas and Gollahalli [11] reported that jet flame liftoff and reattachment velocities depend on the shape of the velocity profile at the burner exit and on the ratio of the length to diameter of the nozzle tubes. Both liftoff and reattachment velocities increased with an increase in the length.

Unconfined Co-flowing Jet Flames. The effect of an unconfined, co-flowing air stream on stability limits of non-premixed jet flames was studied experimentally by many researchers [1, 6, 13–19, 44–46]. Among these studies, only Varnos et al [13] and Yuasa [14] investigated thoroughly the flame stability limit curves of liftoff, blowout of lifted flames, blowout of attached flames and reattachment over a considerable range of co-flowing stream velocity for hydrogen and methane as a jet fuel. Their findings show that an increase in the velocity of co-flowing air stream decreased the blowout limits of lifted flames significantly, while it had a minor effect on reattachment limits. In comparison, liftoff and blowout of attached flames are almost insensitive to stream velocities.

The effect of burner configurations on liftoff and blowout velocities of attached flames for hydrogen/air and methane/air co-flowing jet flames have been investigated by Takahashi et al [17, 18] and Varnos et al [13]. Their measurements on a variety of nozzle diameters and lip-thicknesses show that these velocities increase with a decrease in the nozzle diameter and an increase in the nozzle lip-thickness.

Addition of diluents to a hydrogen jet or to an external air flow was investigated by Takahashi et al [15,16]. Nitrogen, argon and helium were used as diluents. When a diluent was added to a hydrogen jet flame, the most detrimental effect on the stability limits of attached flames were observed for argon and nitrogen and then for helium as diluents; on the other hand, the presence of a diluent in unconfined co-flowing air stream decreased these limits more with nitrogen followed by helium and argon. In the case when a diluent was added to both jet fuel and co-flowing air stream, the most detrimental effect on these limits was observed with nitrogen followed by argon and helium. However, they did not offer an explanation to the different trends observed with these diluents in each case.

Confined Co-flowing Jet Flames. The stability limits of non-premixed jet flames in a confined co-flowing oxidizing stream were investigated experimentally over many years [2,3,5,20–30,38,39,64]. Most of these studies were limited to a relatively narrow or low range of stream velocities (up to 0.6 m/s) [21–26]. Very few studies were conducted over a wider range of stream velocities [5,27,28,30].

The blowout limits of jet flames for a wide range of co-flowing stream velocities were reported by Wierzba and Oladipo [27] for methane, propane, ethylene and hydrogen and for small jet diameters (ranged from 1 mm to 2 mm) and by Yoon et al [28] for hydrogen and for a large jet diameter (7 mm). Their results show that the type of flame before blowout (lifted or attached) depends on the value of the co-flowing stream velocity. An increase in co-flowing stream velocity decreased blowout limits to a larger degree for lifted flames than for attached flames. In spite of several flame stability measurements [5, 27, 28, 30], no plot of flame stability regions was provided to compare the effect of co-flowing stream velocity on liftoff, reattachment and blowout limits of lifted and attached flames all on the same diagram.

The effects of jet fuel composition and surrounding air stream composition on the jet flame stability have been the subject of many investigations [3–5, 22,26,29,30,61,64]. The effect of addition of an auxiliary fuel to a co-flowing air stream on blowout limits was studied by Karim et al [3,4] for relatively small stream velocities. Wierzba et al [5] showed that at higher co-flowing stream velocities and auxiliary fuel concentrations, the blowout limit can either increase or decrease depending on the type of blowout (blowout of attached or lifted flames).

The effect of variations in burner lip-thickness on blowout limits was reported by Yoon et al [28] for a hydrogen jet of 7 mm diameter and by Papanikolaou and Wierzba et al [30] for a methane jet of 3.18 mm diameter. Both concluded that for burners with larger lip-thicknesses, the blowout limits of attached flames could be extended into higher air velocity regime, while the blowout limits of lifted flames were not affected by burner lip-thickness.

2.2 Theoretical Studies of Flame Stability

Over decades, many attempts were made to identify the underlying physical mechanisms responsible for the stability of non-premixed jet flames, and to develop predictive models for them. However, much of the attention has been directed toward the modeling of the stability limits of simple jet flames issuing into a quiescent medium [40, 41, 43, 44, 47–53] and only a few theoretical studies have been conducted for jet flames into a co-flowing oxidizing atmosphere, either confined or unconfined [2, 46]. The available predictive models for liftoff and blowout are based on concepts of premixed combustion, laminar flamelets quenching, velocity gradient, small-scale structures and large scale mixing structures.

Premixed Combustion Models. The early work of Vanquickenborne and Van Tiggelen [40] used the concept of premixed combustion to explain the stability mechanism of turbulent lifted diffusion flames. A lifted flame stabilizes at a downstream position where the fuel-air mixture is in a stoichiometric proportion and the turbulent flame speed for the premixed fuel-air mixture is equal to the local jet velocity. To implement this concept, a vast knowledge of gas composition, gas velocity and turbulence parameters (such as intensity and scale) is required. They verified the proposed hypothetical stabilization mechanism with conducting extensive experimental measurements for a methane jet issued into a quiescent environment. Furthermore, they have shown that with further increase in gas velocity, the location of flame stabilization was forced toward a downstream position where the stoichiometry contour reaches its maximum width. In this condition, flame blowout will occur since the intensity of turbulence and therefore turbulent burning velocity no longer increases sufficiently in order to balance the local gas velocity.

Utilizing the same stabilization mechanism, Günther et al [41,42] studied the lifting phenomenon for jets of natural gas and hydrogen. Also, Kalghatgi [7,8] used this flame stability model as well as dimensional analysis to derive an empirical formula for correlating his experimental data on blowout limits and liftoff heights of different fuels over a range of jet nozzle diameters. Eickoff et al [10] and Schefer et al [35,36] supported the premixed concept by measurement of concentration, temperature and velocity around the flame stabilization region for lifted flames.

Recently, Kaplan et al [47] used numerical simulations of an axisymmetric co-flowing methane jet flame to study the flame liftoff phenomenon. The effect of jet velocity on liftoff height was simulated numerically at a constant co-flowing stream velocity. Their computations showed that the base of a lifted flame was located on the stoichiometric surface at a height where the local axial velocity was approximately equal to the turbulent burning velocity. The computed liftoff heights were in reasonable agreement with the experimental data of Kalghatgi [8]. They concluded that the results verify the premixed theory of Vanquickenborne and Van Tiggelen [40].

Laminar Flamelets and Partially Premixed Flamelets Models. Peters and Williams [55] questioned the validity of the concept of premixed combustion and argued that the degree of mixing in turbulent jets was insufficient to approach a uniform mixture of reactants upstream to the base of lifted flame. These authors proposed instead, the laminar flamelets model. In this model, a turbulent diffusion flame is considered to be an ensemble of laminar diffusion flamelets which can be quenched at strain rates above a critical value. As the jet exit velocity increases, the flamelets are stretched more and more. This may result in the extinction of a large fraction of laminar diffusion flamelets at the rim of an attached flame and lead to liftoff. The flame will be stabilized somewhere downstream of the nozzle exit where the strain rates are sufficiently low, so a reasonable fraction of the laminar diffusion flamelets remains unextinguished.

Based on this model, laminar diffusion flamelets cannot exist when the rate of dissipation of the (scalar) mixture fraction (defined to have a value of zero in the ambient atmosphere and unity at the nozzle exit) at its stoichiometric value exceeds a critical value. However, they chose an arbitrary functional form for the critical scalar dissipation rate to produce a better agreement of theoretical predictions with the data on liftoff heights for methane jet flames in a still air.

Muller, Breitbach and Peters [50] used the theory of partially premixed flamelets to predict the experimental flame liftoff height reported by Kalghatgi [8] and Miake-Lye and Hammer [43] for a simple methane jet flame. Peters et al [49, 50] concluded that both stabilization models of partially premixed flame propagation and laminar flamelets quenching can remain relevant.

Sanders and Lamers [51] used the laminar diffusion flamelets concept of Peters and William [55] to model the liftoff height of jet flames. They showed that the calculated results of Peters and Williams [55] do not predict accurately the slope of experimental liftoff height as a function of jet velocity curve. Therefore, they proposed the usage of the strain rate of the smallest eddies as a criterion for the flamelets quenching instead of the scalar dissipation rate. They reported that the modified model predicted accurately the experimental trend existing between flame liftoff height and jet exit velocity. In this model the coefficient for the strain rate was chosen by comparing and fitting calculated results to experimental ones.

Velocity Gradient Model. The concept of velocity-gradient proposed by Lewis and von Elbe [65] was employed by different researchers to predict the blowout limits of premixed and non-premixed flames. According to this concept, flame extinction will occur when the jet velocity gradient at the boundary of the nozzle wall exceeds a characteristic value. This model was later extended by Putman and Jensen [66] to yield a dimensionless parameter consisting of two Peclet numbers; one based on jet velocity and the other based on burning velocity. This dimensionless group as a blowout criterion was later applied to unconfined, co-flowing jet flames by Kremer et al [44]. Their experimental results showed that there is an optimum value of coaxial air velocity with respect to blowout limits for each employed nozzle. Since only this optimum blowout velocity was predicted for different nozzle geometries, it is not clear whether their developed procedure is also able to predict the effect of co-flowing stream velocity on blowout limits. A similar method was employed by Rawe and Kremer [45] for flame stabilization of unconfined turbulent diffusion flames with swirl.

Small-Scale Structure Based Models. Byggstoyl and Magnussen [48,56] proposed a model for local extinction of a simple free jet flame based on the Eddy Dissipation Concept (EDC) in turbulent flow. Extinction is assumed to take place in fine (small-scale) structures which are responsible for the dissipation of turbulence into heat. According to this extinction model, a lifted diffusion flame will be stabilized at the stoichiometric contour and at the position where the turbulent fine structure time scale equals the chemical time scale. The quenching time scale used in this model was obtained from the experimental data which was then used to predict the flame liftoff heights versus jet exit velocity.

Large-Scale Structure Based Models. A different physical mechanism based on the nature of large scale motions in turbulent jets was proposed by Broadwell et al [52] to explain the flame blowout phenomenon of simple jet diffusion flames. In this model, large scale flow structures brings ambient air in contact with a mixture of fuel and hot reaction products and after a certain time this mixture reaches the Kolmogorov scale in turbulence cascade. Blowout is expected when the local air and the hot mixture of products and fuel homogenize very rapidly and as a result there will be insufficient time for ignition before the temperature and concentration of radical species drops below a critical value. In this condition, the ratio of the local mixing time, τ_m, to a characteristic chemical time, τ_c, becomes less than a critical value at a distance proportional to flame length. Based on this proposed flame blowout criterion, an expression for jet blowout velocity was derived which accurately predicted the experimental findings of Kalghatgi [7] for a free jet flame. An expression was also derived for liftoff height as a function of jet exit velocity, but the validity of this expression was not verified by them.

Miake-Lye and Hammer [43] argued that due to the one dimensionality of the model of Broadwell et al [52], it is not directly applicable to the liftoff height. Accordingly, they developed a model based on the strain rate of large-scale coherent motions in a lifted turbulent jet flame to predict a linear relationship between the liftoff height and the jet exit velocity for a simple free axisymmetric jet flame. The results of this model were reported to be in agreement with previously measured liftoff heights for a variety of pure fuels.

Dahm and Mayman [46] modified the model of Broadwell et al [52] to include the effect of an unconfined, coaxial air flow on flame blowout limits. The experimental blowout limits for a range of geometries, fuels and diluents showed a fairly good agreement with their predicted data. The Dahm and Mayman [46] analysis was also used by Feikema et al [1] to predict the flame blowout limits for pure fuels as well as methane-hydrogen mixtures. For pure fuels, the blowout curves were properly predicted but for methane-hydrogen mixtures, the predicted curves did not agree with experimental measurements.

All the above models were developed for free jet flames which do not include the effect of confined co-flowing stream. However, many industrial applications involve jet flames in a confined, co-flowing air stream. A review by Pitts [67] also summarized the published experimental results and theoretical models for a simple jet flame and showed that none of the available models is completely satisfactory in correlating the existing experimental results.

Dahm and Dibble [2] applied Broadwell et al [52] concept for the flame stabilization to develop a predictive procedure for evaluating the blowout limits of lifted flames in a confined, co-flowing stream of air. By using velocity and concentration profiles for a jet in a co-flowing stream measured by Biringen [68], they calculated the position where the local flame stabilization mechanism fails and leads to blowout. This position was assumed to be at the last large coherent structure within the jet at which the concentration of jet fuel reaches its stoichiometric value. At this position, the ratio of mixing time to chemical time is less than a critical value for flame blowout conditions. Comparison of the predicted blowout limits obtained from their analysis with the experimentally-measured ones showed that this critical value is approximately constant for propane and methane jets discharged from nozzles of 3.3 and 5.2 mm diameters. The proposed blowout mechanism could predict the experimentally-obtained reduction in the blowout limits with increasing co-flowing stream velocity.

It can be seen from this literature survey that:

- majority of the available models are related to the free jet flames.
- all the models are semi-empirical and include coefficients determined from the experiments. Therefore, their applications are limited only to specific types of operating conditions.
- majority of the proposed models predict the liftoff height as a function of the jet exit velocity, but they do not predict the jet liftoff velocity.
- none of these models describe the hysteresis phenomenon of flame liftoff and reattachment.

Chapter 3

Experimental Apparatus and Procedure

The objectives of the experimental part of the present study were to investigate for non-premixed jet flames in a co-flowing stream:

- the stability curves and ignition characteristics for single and multi-component gaseous fuels,
- the effect of diluent addition to the jet fuel on the stability limits,
- the effect of diluent or fuel addition to the surrounding stream on the stability limits,
- the effect of nozzle geometry on the stability limits.

To meet these objectives, a laboratory combustion set-up was employed with capabilities to:

1. produce various fuel mixtures and fuel-diluent mixtures as the jet fuel and control their composition.

2. produce and control co-flowing stream velocity,
3. mix homogeneously the auxiliary fuel or diluent with air and control its concentration in the surrounding stream,
4. conduct flame visualization studies.

Detailed descriptions of the experimental apparatus and the procedure employed for evaluating the stability of a confined, co-flowing non-premixed flame are presented in the following sections.

3.1 Experimental Apparatus

An existing experimental well developed facility was employed [27, 29, 69]. The schematic diagram of the experimental apparatus is presented in Figure 3.1. The experimental apparatus consists of a vertical combustor, fuel and air supply systems and different flow control and metering systems.

The stability limits of circular non-premixed jet flames in a co-flowing oxidizing stream were determined in a vertical stainless steel combustor of a square cross section of $127 \times 127\,\mathrm{mm}^2$, 1300 mm tall and open to the atmosphere. The combustor was fitted with long quartz windows for flame visualization. At the base of the combustor a honeycomb straightener was installed to ensure uniform velocity of the air stream.

The surrounding air stream was generated using a centrifugal blower driven by an induction motor. The air flow rate was measured using a sharp-edged orifice plate. Througout the thesis, all cited values of the co-flowing stream velocities were "the mean stream velocity at the entry to the combustor". The apparatus permits the homogeneous mixing of an auxiliary fuel or

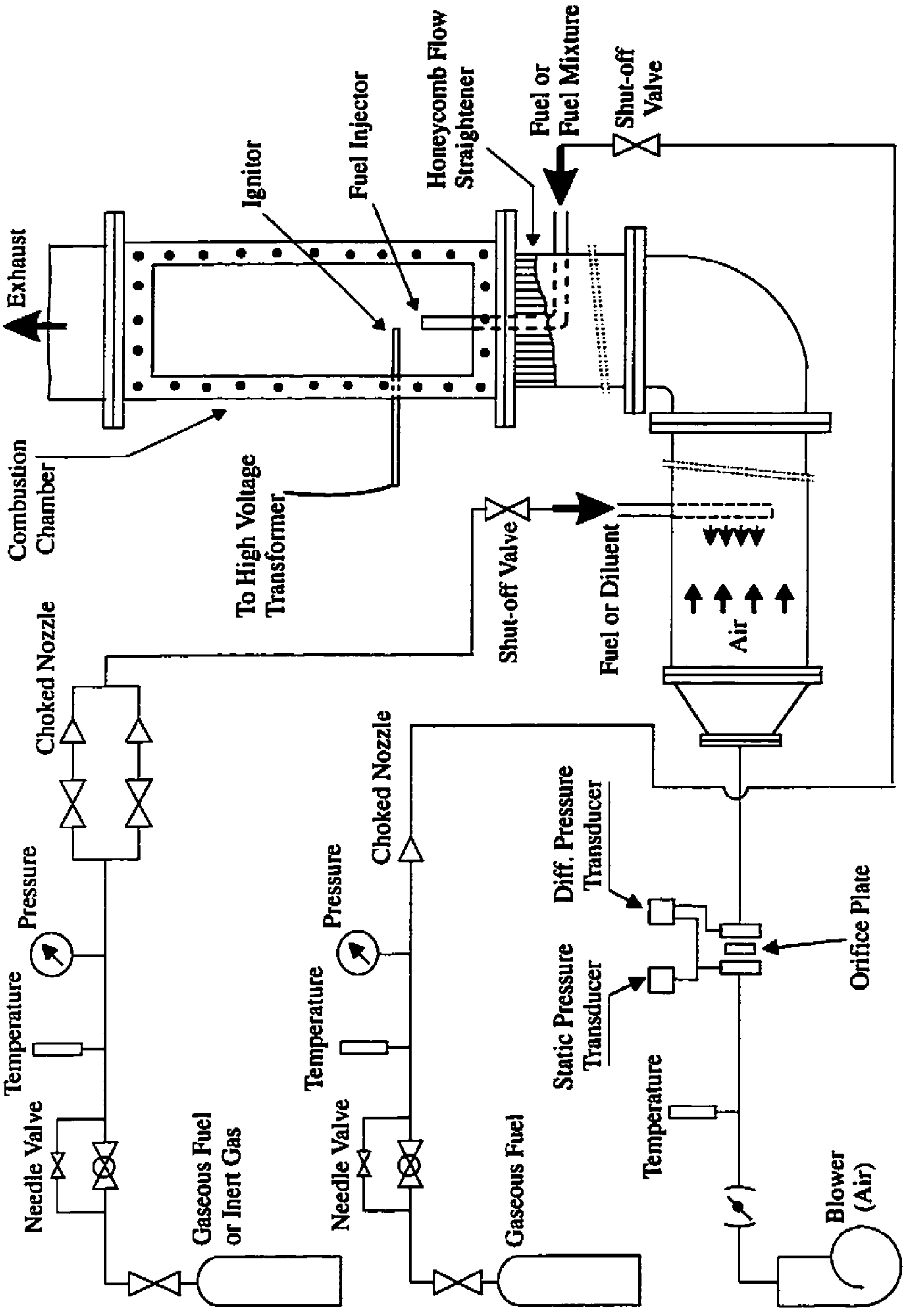

Figure 3.1: A schematic diagram of the experimental apparatus.

a diluent gas with the air stream at a point far upstream of the entry to the combustor.

Various fuels and diluents were supplied from high pressure cylinders and were carried to the jet and surrounding stream through seven independent feed lines. For simplicity, only two feed lines have been shown in Figure 3.1. All feed lines contained pressure regulars, flow control valves, temperature sensors, pressure gauges and choked nozzles. The flow rates of fuels and diluents were monitored using the calibrated choked nozzles. Altogether eleven choked nozzles were installed in these feed lines to provide measurements over a wide range of flow rates of different gases. The benefit of employing choked nozzles is that variations in the back pressure will not affect the accuracy of the flow rate measurement.

The jet was discharged vertically upward along the center line of the combustor from a circular brass nozzle. The jet was ignited by an electric spark. The location of the ignitor could be varied during tests from a point at the outer rim of the fuel nozzle up to 40 mm downstream.

The jet nozzles employed were of 2.00 and 2.82 mm inside diameter, d_o, with a lip-thickness, Δ, of 1.82 mm and 1.33 mm, respectively. Also a sharp-edged circular nozzle of 2.00 mm inside diameter with a lip-thickness of 0.20 mm was used to investigate the effect of nozzle geometry on the stability limits of a non-premixed flame. The schematic diagram of these two types of nozzles are shown in Figure 3.2.

Gaseous fuels employed in the experiments were commercially pure metane, ethylene, propane and hydrogen, while nitrogen, carbon dioxide and helium were used as diluents. All experiments were conducted at ambient temperature and pressure conditions (approximately $T \cong 296$ K and $P \cong 89$ kPa).

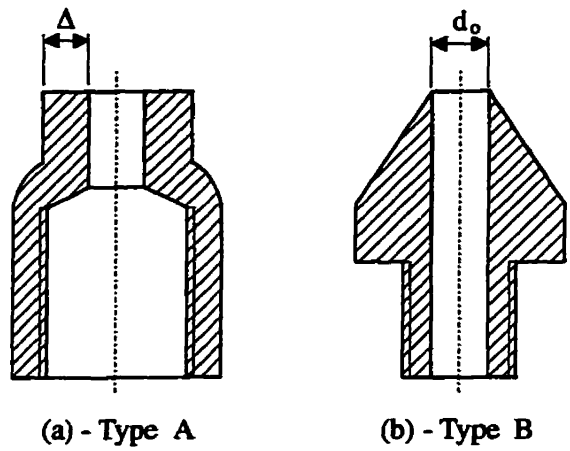

Figure 3.2: A schematic diagram of jet nozzles employed.

3.2 Experimental Procedure

The stability limits - liftoff, reattachment and blowout - of single and multi-component jet fuels were determined at different stream velocities and different fuel or diluent concentrations in the surrounding air stream by employing the following procedures.

Liftoff Limit of Attached Flames. The liftoff limits of single and multi-component fuels were determined visually as follows. The co-flowing stream velocity was first set at the desired level and the jet was electrically ignited at a low jet flow rate. Then, the jet flow rate was gradually increased until the flame lifted and stabilized at a distance downstream from the burner rim. The jet flow rate associated with sudden flame liftoff from the burner rim was recorded as the liftoff limit.

Reattachment Limit of Lifted Flames. The reattachment limit of a lifted flame at the desired stream velocity was measured visually by gradually decreasing the jet flow rate until the flame was returned to the burner rim.

Blowout Limit of Lifted Flames. Generally, two procedures can be followed to measure the blowout limits of lifted flames:

1. by gradually increasing the jet flow rate and keeping the stream flow rate constant,

2. by gradually increasing the stream flow rate and keeping the jet flow rate constant.

The results obtained with these two procedures were within an experimental uncertainty of approximately 5%. The blowout limits of lifted flames for *single component fuel* jets were determined visually using the first procedure. For the sake of simplicity, in tests with *fuel mixtures* as the jet fuel, the blowout of lifted flames was achieved by gradually increasing the air flow rate while keeping the jet flow rate and composition constant (the second procedure).

Blowout Limit of Attached Flames. To measure the blowout limits of attached flames, the jet flames were ignited at a reduced jet flow rate and at the desired level of co-flowing stream velocity. Then, the jet fuel flow rate was increased gradually until the flame blowout was observed.

Fuel or Diluent in Surrounding Stream. The stability limits of the non-premixed jet flames within a co-flowing stream of air containing an auxiliary fuel or a diluent were established by first setting the flow rate of air as desired and then introducing the required quantity of the auxiliary fuel or the diluent into the air stream. After ignition of the jet fuel, the liftoff and/or blowout limits were determined by increasing the jet flow rate, while the reattachment limit was determined by decreasing the jet flow rate.

Chapter 4

Experimental Results and Discussions

The effects of different parameters such as co-flowing stream velocity and composition, jet fuel composition and nozzle geometry on the stability limits of a non-premixed jet flame were investigated. The effect of the co-flowing stream velocity on these limits is discussed in Section 4.1 for four different jet fuels. Also, the effect of nozzle geometry on methane stability limits is investigated in this section. Section 4.2 focuses on the effect of hydrogen addition to a methane jet on the stability limits together with discussions about some observed phenomena. Introducing a secondary fuel, commonly known as **auxiliary fuel**, into the surrounding air stream can be an effective technique for improving the stability limits of jet flames. The results for a methane jet flame and different auxiliary fuels are presented and discussed in Section 4.3. The effect of addition of different inert gases to either jet fuel or surrounding air stream on the jet flame characteristics is discussed in Section 4.4. Nitrogen, carbon dioxide and helium were used as the diluent gas.

4.1 Flame Stability Curves for Pure Fuel Jets

Generally, two different types of non-premixed jet flames can be observed depending on the values of jet and co-flowing stream velocities. At sufficiently low jet velocities, regardless of stream velocity, the flame is stabilized at the burner rim. This is an **attached flame**. A photograph of an attached non-premixed ethylene flame is shown in Figure 4.1.

At sufficiently high jet velocities and relatively low stream velocities, the flame is lifted from the rim and stabilized at a certain distance downstream of the nozzle exit. This is a **lifted flame**. With an increase in jet flow rate, **liftoff distance** (the distance from the burner rim to the flame base) increases. An example of a lifted ethylene flame is shown in the photograph in Figure 4.2.

The stability limits of lifted and attached flames for different fuels in a co-flowing air stream were determined experimentally. The experiments were conducted with a nozzle of 2 mm diameter and 1.82 mm lip-thickness. The configuration of this nozzle is shown in Figure 3.2a.

4.1.1 Stability Curves for Methane Jet

The stability limits of a methane jet flame in a co-flowing air stream are shown in Figure 4.3. It can be seen that the co-flowing air stream velocity affects the stability limits very significantly. Three different regions named I, II and III can be recognized depending on the value of the co-flowing air stream velocity. The Reynolds numbers for the co-flowing stream, Re_S, shown in the figure are calculated based on the combustor hydraulic diameter of 0.127 m and the air kinematic viscosity of 15 mm^2/s.

Figure 4.1: Photograph of an attached ethylene nonpremixed flame in a co-flowing stream of air. The jet and stream velocities are 17.7 m/s and 0.94 m/s, respectively. The jet nozzle diameter is 4.5 mm.

Figure 4.2: Photograph of a lifted ethylene nonpremixed flame in a co-flowing stream of air. Jet and stream velocities are 19.65 m/s and 1.52 m/s, respectively. Jet nozzle diameter is 4.5 mm.

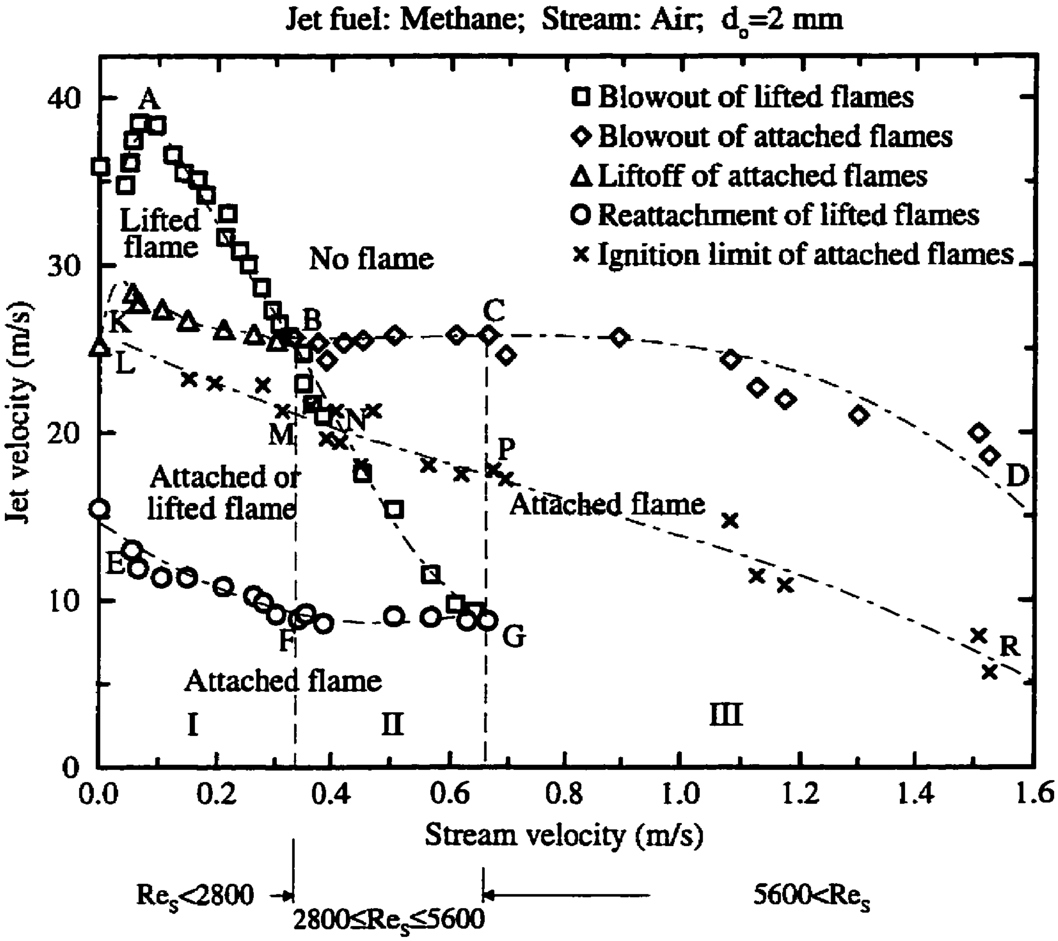

Figure 4.3: Stability limits of a methane non-premixed flame as a function of co-flowing air stream velocity. Jet diameter = 2.00 mm.

Region I. At co-flowing stream velocities less than ~0.34 m/s ($Re_S \sim$ 2800), both lifted and attached stable flames can be observed. The jet can be ignited at all possible stream-jet velocity combinations, but the type of a flame resulting from the spark ignition depended on the co-flowing air stream and jet velocities at the moment of ignition and the ignitor location as well.

At jet velocity values below those shown by line EF, ignition of the jet resulted in only attached flames irrespective of the ignitor position (up to 40 mm downstream of the jet exit). At jet velocities above those shown by line LM but less than line AB, ignition of the jet resulted in lifted flames only for ignitor positions up to 40 mm downstream of jet exit. Line LM is called the **ignition limit of attached flames** since no attached flames could be produced by ignition at jet velocities higher than the values represented by this line (Figure 4.3).

Ignition of a jet within the region of LMFE could result in an attached or lifted flame depending on the distance of the ignitor from the nozzle exit. A lifted flame was produced by ignition of the jet at a certain distance downstream of the burner rim. This distance which depends on the jet velocity is a maximum (at 40 mm downstream of burner rim) for jet velocities shown by line EF and is a minimum (at burner rim) for jet velocities shown by line LM. An attached flame was produced by ignition of the jet at the burner rim. The attached flames always suddenly lifted off when the jet velocity exceeded the values shown by line KB. Line KB is generally accepted as the **liftoff limit** of jet flames. It can be seen that the liftoff limit decreases slightly with an increase in the surrounding stream velocity.

The jet velocity beyond which a stable flame can not exist is known as the **blowout limit**. The blowout limits of lifted flames are indicated by line AB (square symbols) in Figure 4.3. The blowout limits of lifted flames improve up to a certain value at very low stream velocities. A further increase in the air stream velocity causes a large reduction in the blowout limit of lifted flames. Similar trends in variations of these limits with a co-flowing stream velocity were also reported [2,25,27,30].

With decreasing jet velocity , lifted flame can reattach to the nozzle rim. The **reattachment limits** are shown as line EF (circle symbols) in Figure 4.3. The same difference between the liftoff (line KB) and reattachment (line EF) limits was also observed by other researchers for non-premixed flames in quiescent medium [9, 10, 21, 23, 42, 63] as well as for premixed flames [70]. This hysteresis phenomenon can be explained in terms of significant differences in the distance between the nozzle rim and the point of transition from the laminar-to-turbulent conditions for flames and nonignited jets having the same jet velocity [63]. It has been reported that the distance from the nozzle rim to the point of transition for a flame is larger than that for a corresponding unignited jet [20,63].

Region II. Like in region I, for co-flowing stream velocities of 0.34 m/s $\leq u_s \leq$ 0.66 m/s, both lifted and attached flames can be observed. The type of a flame resulting from the ignition is dependent on the values of the co-flowing air stream and fuel jet velocities at the moment of ignition and the location of the ignitor. It should be noted that no ignition was possible within region BNPC. At the conditions within triangle NPG, ignition of the jet resulted in *attached* flames only. These *attached* flames could not be lifted from the burner rim at all. Within region MNB, the ignition of the jet resulted in lifted flames only. In region MNGF, both lifted and attached flames can be produced.

Generally, in region II, if ignition resulted in an attached flame, this flame would blow out with increasing jet velocity as an attached flame (line BC). If ignition resulted in a lifted flame, this flame would blow out as a lifted flame (line BG). Line BC, the **blowout limit of attached flames**, can be considered as a continuation of line KB, the liftoff limit of attached flames. The blowout limits of the *attached* flames in this region are considerably higher than those of the *lifted* flames. This fact has obvious serious implications in situations where the flame stability limits control the operational limits of combustion devices and in the case of sudden flame blowout and reignition processes. The blowout limits of *attached* flames are much less sensitive to the changes in the co-flowing stream velocities than the blowout limits of *lifted* flames. Consequently, the *lifted* flames should be avoided in this region, i.e., it is advantageous to ignite jets at as low jet velocities as possible or to locate the ignitor at the burner rim, since both of these cases always resulted in attached flames.

The value of the stream velocity at point B, which separates region I from II, will be called as **limiting co-flowing stream velocity** (Figure 4.3). The importance of this velocity stems from the fact that it is the minimum co-flowing stream velocity at which the blowout of *attached* flames can occur. It was reported that the limiting stream velocity depends on the nozzle size and the type of the fuel [27, 30]. The value of the stream velocity at point G (separating region II from region III) represents the maximum stream velocity beyond which lifted flames do not exist.

Region III. At co-flowing stream velocities higher than ~ 0.66 m/s, only attached stable flames were observed and these flames remained attached to the rim at blowout. The blowout limits of these flames are shown as line CD (Figure 4.3). As can be seen the flame blowout limit was decreasing with an increase in the co-flowing stream velocity and beyond a certain value of the co-flowing stream velocity, the stable flame could not exist at all.

It was not possible to ignite a jet when its velocity exceeded the values shown by line PR. Moreover, at stream velocities higher than $\sim$ 1.3 m/s, the ignition of the jet was achieved with difficulty even at very small jet velocities.

Ignition conditions and flame types at the moment of ignition and blowout in the different regions of I, II and III are listed in Table 4.1.

4.1.1.1 Effect of Nozzle Geometry

Effect of Nozzle Shape. In the present study, the effect of nozzle shape on stability limits was investigated employing relatively small nozzles of 2 mm diameter. The results of stability limits for two nozzles of the same diameter but of a different shape and lip-thickness (Figure 3.2a and 3.2b) are shown in Figure 4.4. As can be seen, the stability behavior trends for these nozzles are similar. The shape of a nozzle had much smaller effect on the blowout limit of lifted flames than on those of attached flames. This was rather expected, since the position of the flame stabilization region for lifted flames was located far downstream of the nozzle rim. In contrast, the nozzle near-field conditions are responsible for stabilization of attached flames and the effect of variation in nozzle configuration on the liftoff and blowout limits of attached flames could be very significant. For thick-walled nozzles, the recirculation zone formed between co-flowing air and fuel jet provides a

Table 4.1: A summary of ignition conditions and flame types at the moment of ignition and blowout at different co-flowing stream velocities for a methane non-premixed flame. For the definition of lines and regions refer to Figure 4.3.

No.	Ignition Conditions			Flame Type at		Blowout Limit (line)
	Coflowing Stream Velocity, (m/s)	**Jet Velocity**	**Ignitor Position from rim (mm)**	**Ignition**	**Blowout**	
1	Region I ($u_s \leq 0.34$)	below line EF	up to 40	attached	lifted	AB
2		within region LMFE	at the rim	attached	lifted	AB
3		within region ABFE	40	lifted	lifted	AB
4		within region ABML	up to 40	lifted	lifted	AB
5	Region II ($0.34 \leq u_s \leq 0.66$)	below line FG	up to 40	attached	attached	BC
6		below line MNP	at the rim	attached	attached	BC
7		within region BGF	40	lifted	lifted	BG
8		within region BCPN	up to 40	no ignition was possible		–
9	Region III ($u_s \geq 0.66$)	below line PR	up to 40	attached	attached	CD
10		within region CDRP	up to 40	no ignition was possible		–

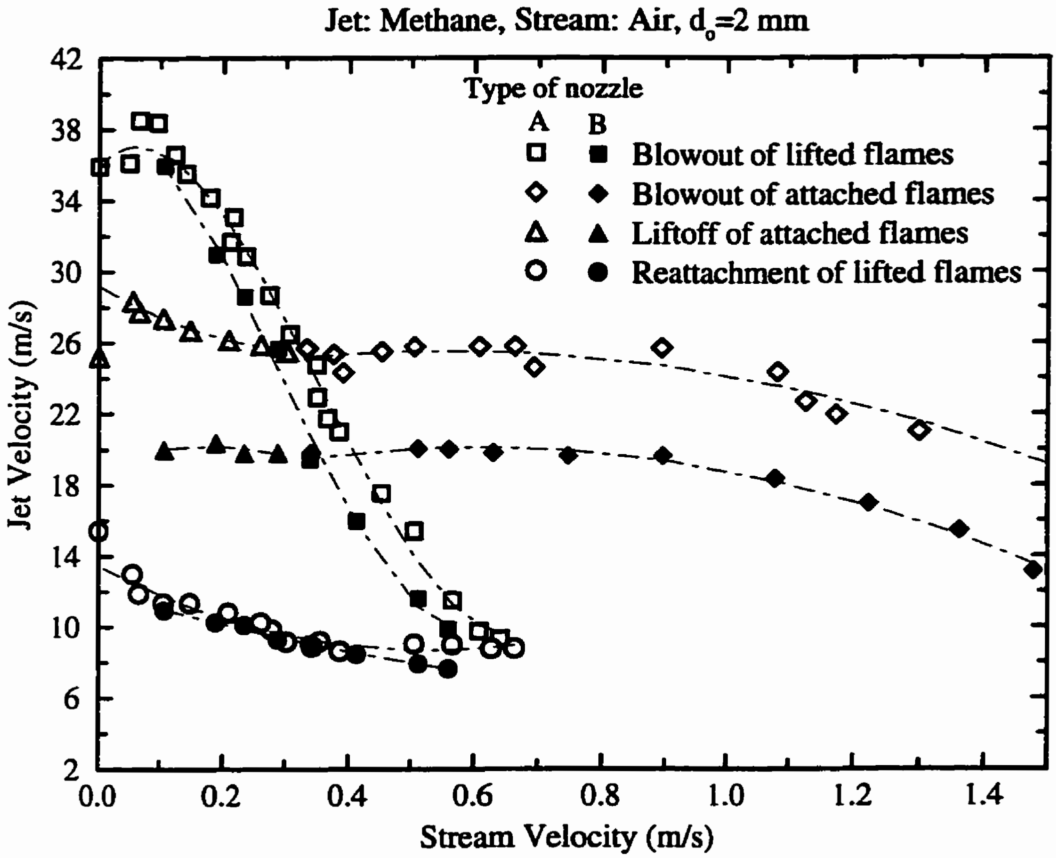

Figure 4.4: Stability limits of a methane non-premixed flame as a function of co-flowing stream velocity for two different nozzle shapes. Jet diameter = 2.00 mm. Symbols: open - Nozzle A (Figure 3.2a), solid - Nozzle B (Figure 3.2b).

significant stabilizing effect on attached flames [18]. Consequently, the liftoff and blowout limits of attached flames were higher for nozzle A than those for nozzle B.

As can be seen in Figure 4.4, variation in nozzle shape resulted in about 20 percent change in blowout limits of attached flames while it led to only 10 percent change in blowout limits of lifted flames. Variations in the nozzle configuration did not affect the value of limiting co-flowing stream velocity.

Effect of Nozzle Size. The blowout limits of lifted flames increased with increasing the nozzle A (Figure 3.2a) diameter from 2 mm to 2.82 mm (Figure 4.5). The rate of increase in the blowout limits of lifted flames can be very significant especially for small co-flowing stream velocities. The blowout limits for these two jet flames are close to each other at higher co-flowing stream velocities.

In comparison, the liftoff and blowout limits of attached flames showed a reverse trend with an increase in the nozzle size. The liftoff and blowout limits of attached flames were smaller for the larger nozzle over the entire range of co-flowing stream velocities considered. A similar trend was observed by other researchers as well [27,30]. The limiting co-flowing stream velocity increased somewhat with an increase in the nozzle diameter.

4.1.2 Stability Curves for Other Common Fuels

Stability curves similar to those described for methane jet flame were also obtained for propane, ethylene and hydrogen. They are shown in Figures 4.6, 4.7 and 4.8. Regions I, II and III can be identified for all these fuels, however, their relative size depends on the type of a fuel. These regions were also observed for an unconfined, co-flowing hydrogen jet flame in air [14].

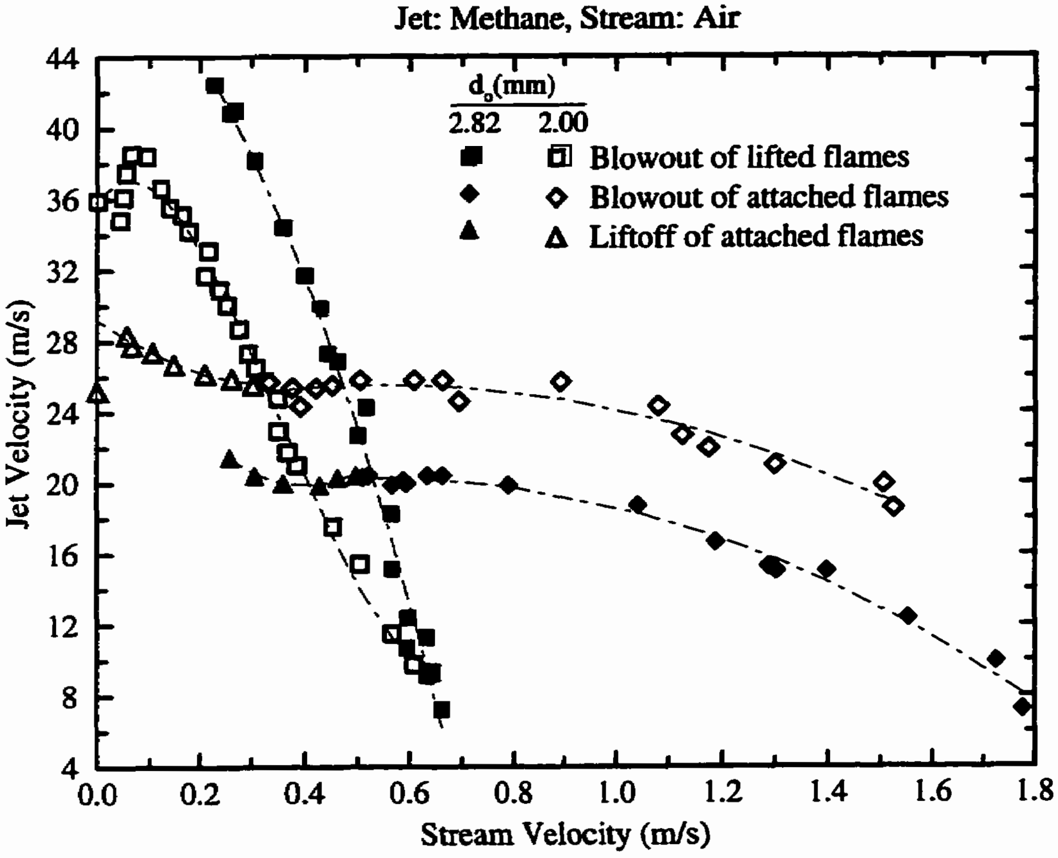

Figure 4.5: Stability limits of a methane non-premixed flame as a function of co-flowing stream velocity for two different sizes of nozzle A (Figure 3.2a).

The blowout limits of flames at zero stream velocity were ~36 m/s, ~51 m/s and ~ 119 m/s, for methane, propane and ethylene, respectively. For the same jet diameter, these values are approximately consistent with the values reported in [7] as ~35.5 m/s, ~57 m/s and ~124 m/s, respectively.

The blowout limits of lifted flames were the highest for hydrogen followed by ethylene, propane and methane (Figure 4.9). These hydrogen flames were also sustained at much higher co-flowing stream velocities. The reattachment limits, the liftoff limits and the blowout limits of attached flames were the highest for hydrogen jet followed by ethylene, methane and propane as shown in Figures 4.10 and 4.11.

4.1.3 Limiting Co-flowing Stream Velocity

As defined previously, the limiting co-flowing stream velocity is the minimum co-flowing stream velocity at which blowout of attached flames can occur. This velocity which is associated with the stream velocity of point B or F is shown for four different fuels in Figures 4.3, 4.6, 4.7 and 4.8. An attempt was made to correlate the experimentally obtained values of the limiting co-flowing **stream** velocities, $U_{S,L}$, and corresponding **jet** velocities at liftoff, $U_{L,L}$, and reattachment, $U_{R,L}$, for different fuels and nozzle diameters.

Stream Velocity. The limiting co-flowing stream velocities, $U_{S,L}$, were correlated in terms of jet diameter, d_o, the square root of jet fuel to co-flowing air density ratio, $(\rho_o/\rho_\infty)^{1/2}$ and the square of the maximum laminar burning velocity, $(S_{L,max})^2$. This can be expressed as:

$$U_{S,L} = 0.16 \times 10^4 \cdot d_o(\frac{\rho_o}{\rho_\infty})^{1/2}(S_{L,max})^2 \qquad (4.1)$$

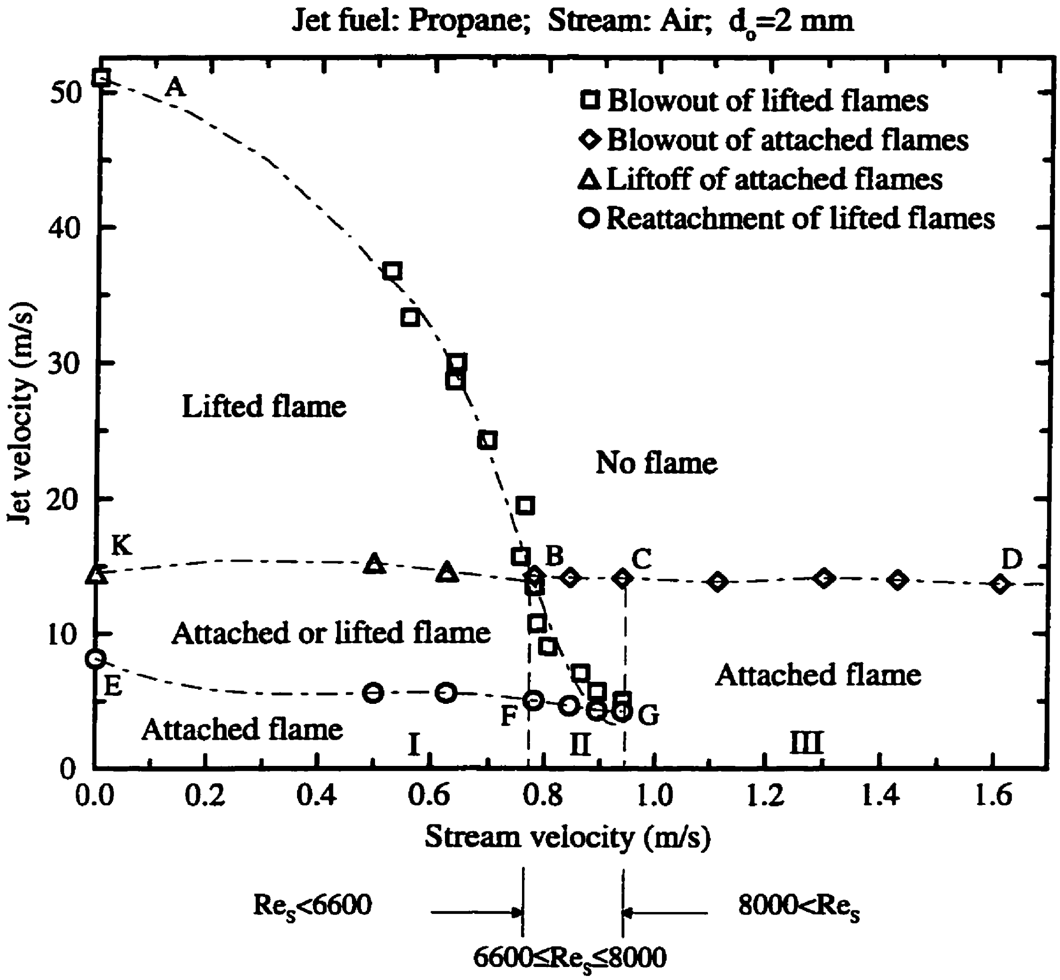

Figure 4.6: Stability limits of a propane non-premixed flame as a function of co-flowing air stream velocity. Jet diameter = 2.00 mm.

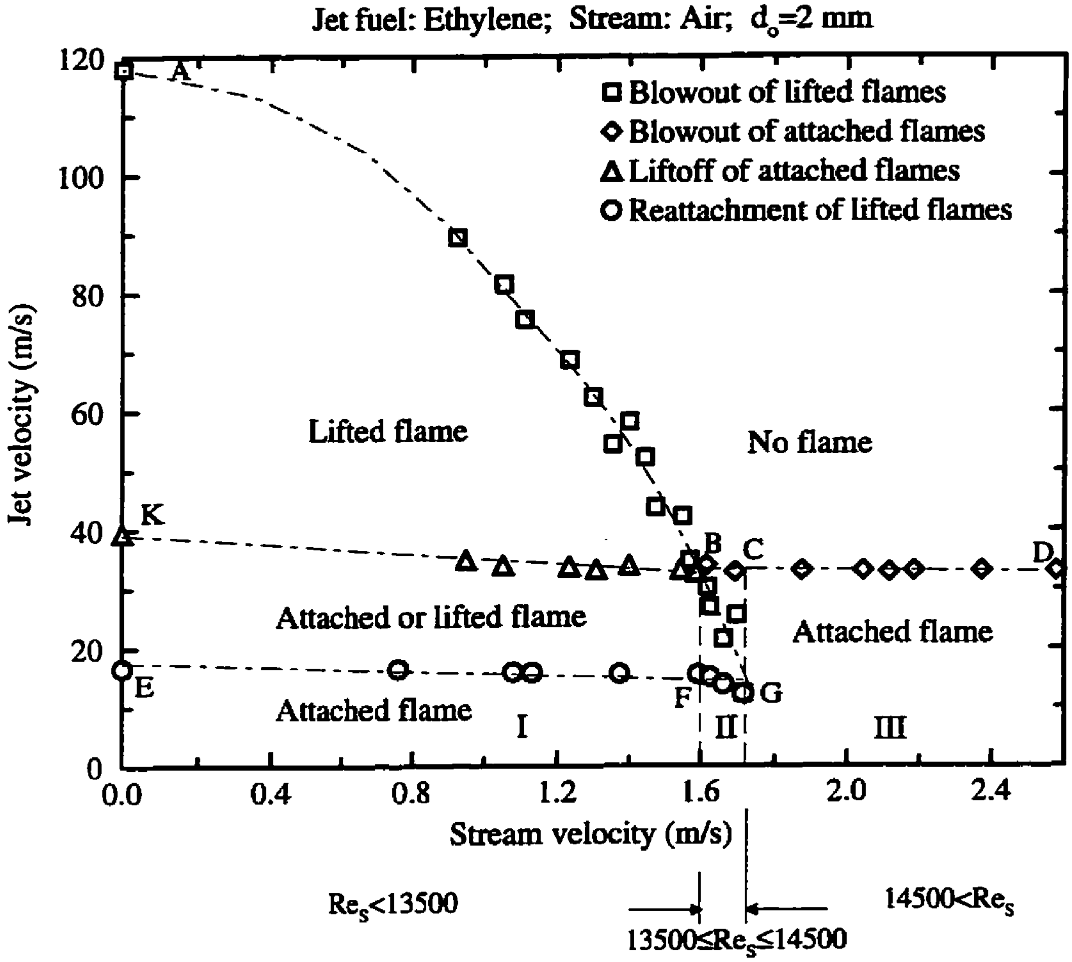

Figure 4.7: Stability limits of an ethylene non-premixed flame as a function of co-flowing air stream velocity. Jet diameter = 2.00 mm.

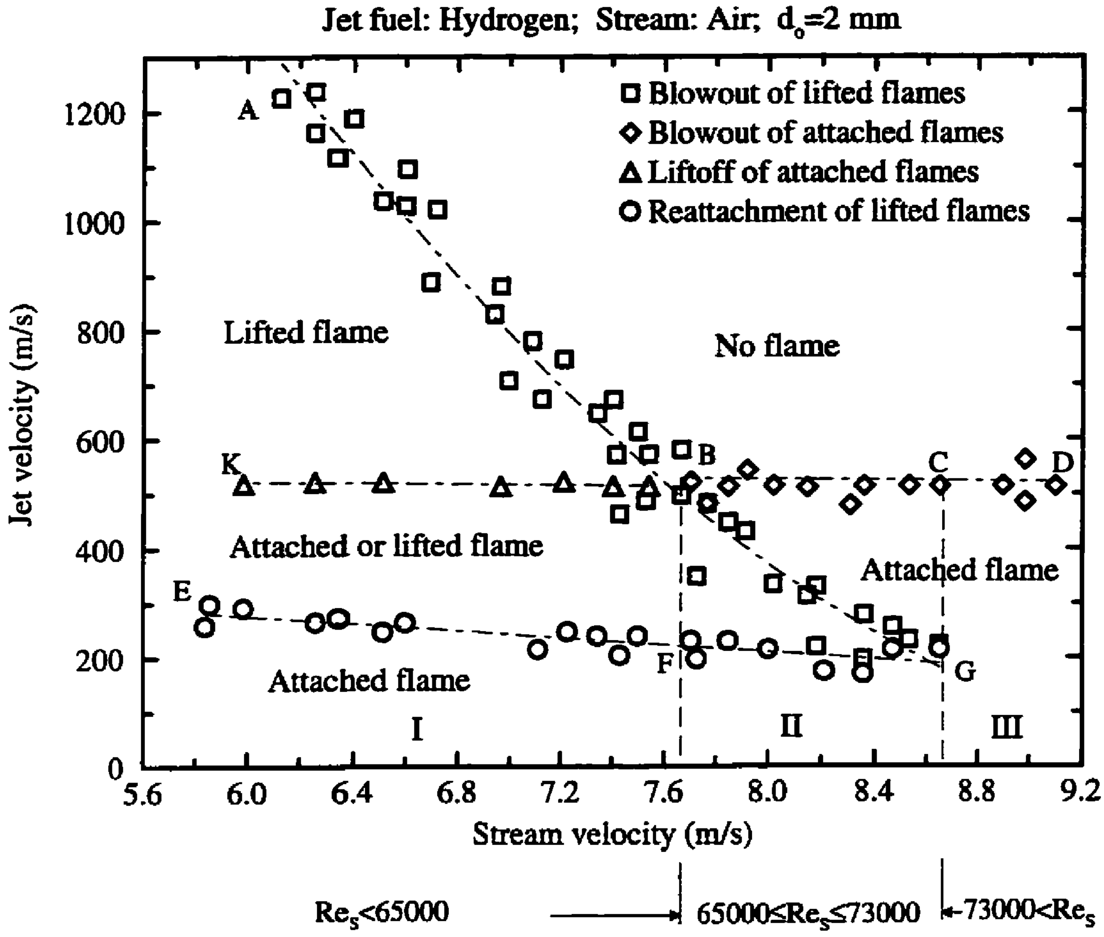

Figure 4.8: Stability limits of a hydrogen non-premixed flame as a function of co-flowing air stream velocity. Jet diameter = 2.00 mm.

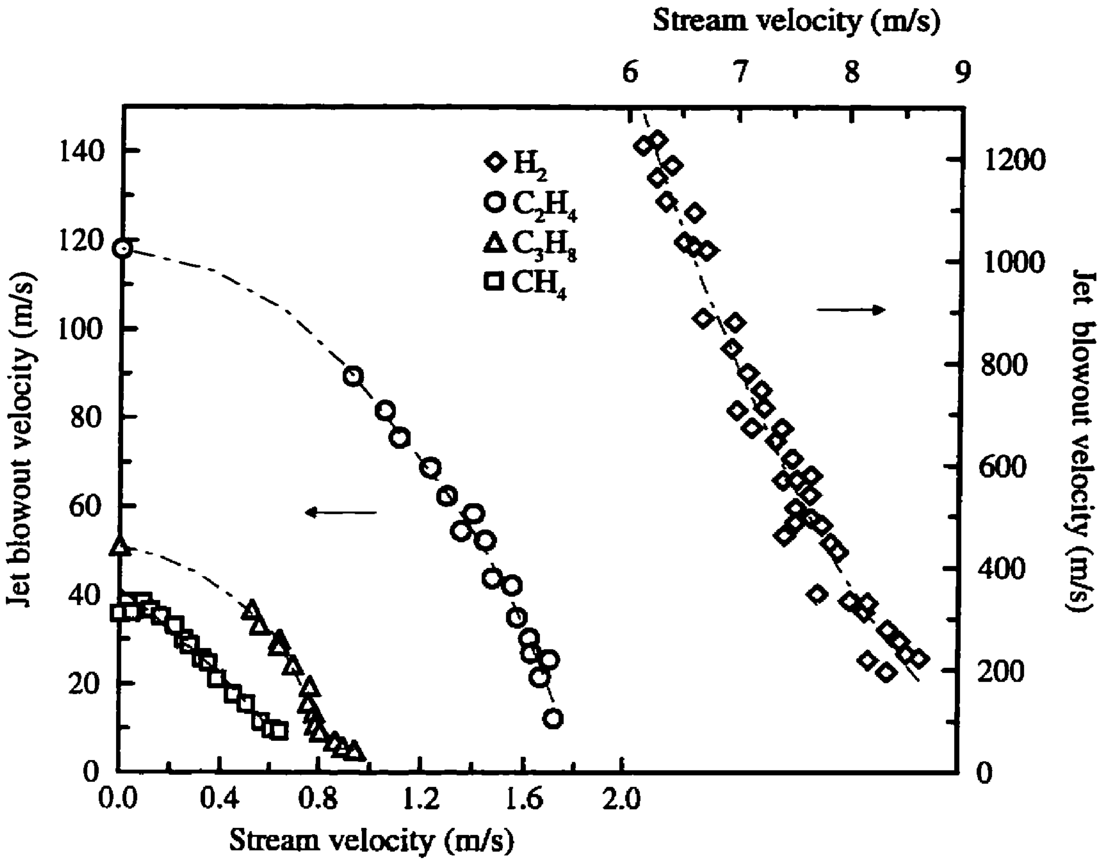

Figure 4.9: The blowout limits of lifted flames for different fuels as a function of co-flowing air stream velocity. Jet diameter = 2.00 mm.

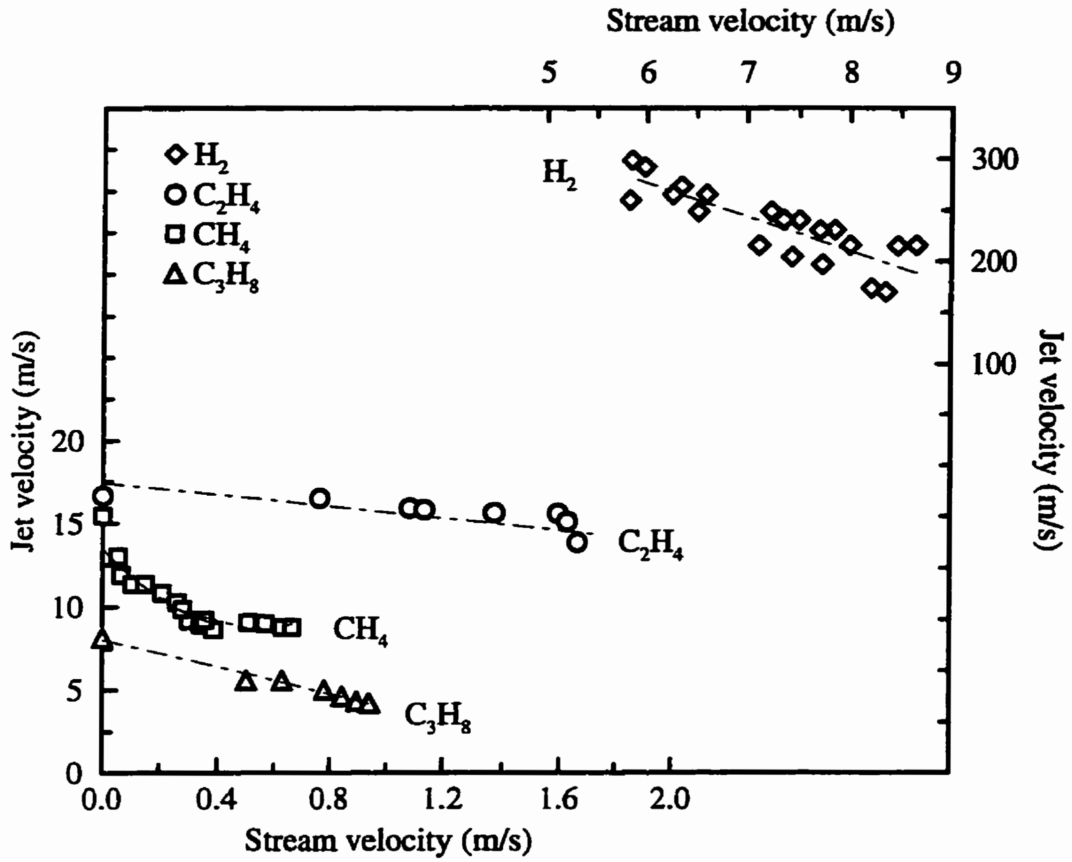

Figure 4.10: The reattachment limits of lifted flames for different fuels as a function of co-flowing air stream velocity. Jet diameter = 2.00 mm.

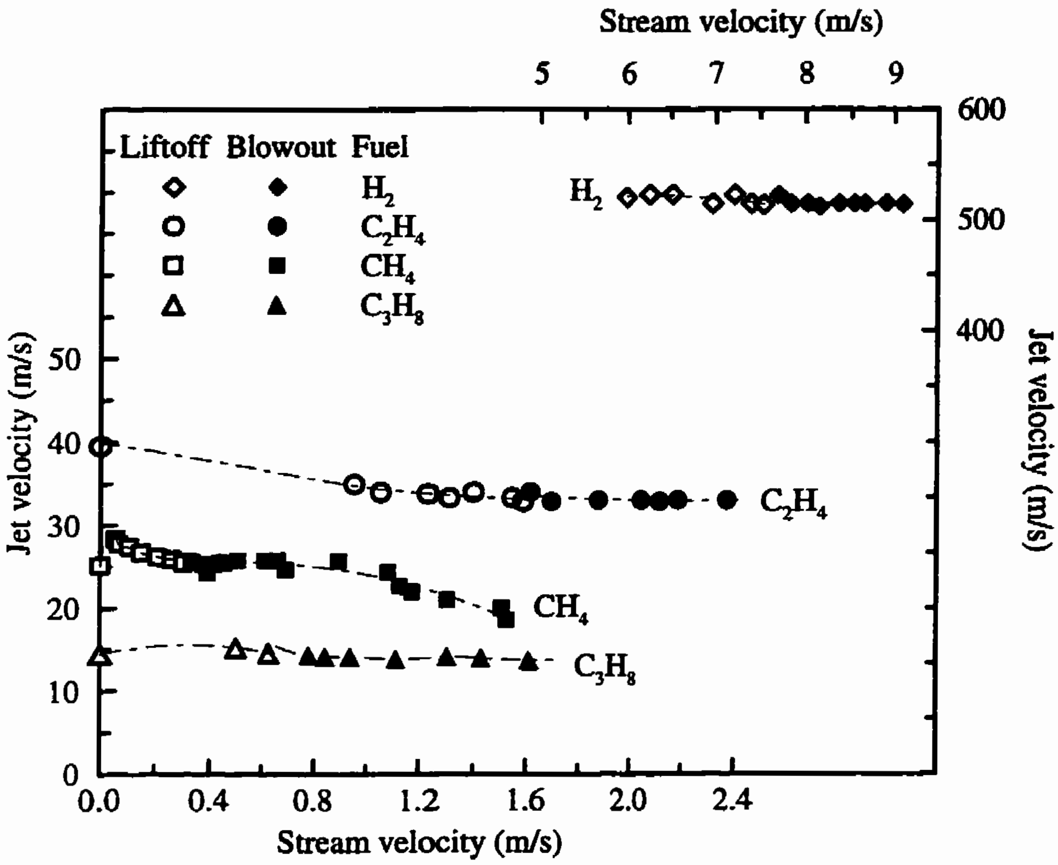

Figure 4.11: The liftoff and blowout limits of attached flames for different fuels as a function of co-flowing air stream velocity. Jet diameter = 2.00 mm.

The term $d_o(\rho_o/\rho_\infty)^{1/2}$ represents the rate of decay of the jet flow. A lower value for this term results in a faster decay of the jet flow [71–73], as can be easily seen for a jet discharged into a quiescent medium [71],

$$\frac{u_m}{u_o} \sim \frac{d_o}{x}\left(\frac{\rho_o}{\rho_\infty}\right)^{1/2} \tag{4.2}$$

where u_m is the maximum axial velocity (at the jet axis) at any downstream distance x from the nozzle and u_o is the jet velocity at the nozzle exit. A faster decay of jet flow results in a smaller mixing time scale (the time required to mix reactants and hot products). Also, the reciprocal of $(S_{L,max})^2$ is proportional to the chemical time scale for a given fuel burning in air (see the following chapter). Therefore, the limiting co-flowing stream velocity can be related to the ratio of mixing time to chemical time. A smaller value of this ratio results in a smaller limiting co-flowing stream velocity. The developed correlation is shown in Figure 4.12. The experimental data obtained in the present study as well as the data available in the literature [27, 30] are also included. In calculations, the maximum burning velocity of methane, propane, ethylene and hydrogen were taken as 0.41, 0.46, 0.79 and 3.0 m/s, respectively [74–76].

Jet Velocities of Liftoff and Reattachment. Experimental jet flame liftoff and reattachment velocities corresponding to the limiting co-flowing stream velocity (point B and F in the stability diagrams) can be correlated using the following dimensionless parameter:

$$k = \frac{u_m \cdot \delta_u}{S_{L,max}(r_o \cdot r_\infty)^{1/2}} \tag{4.3}$$

where r_o and r_∞ are the nozzle and combustor radius, respectively. The local jet flow width, δ_u, is linearly increasing with downstream distance, x, (for

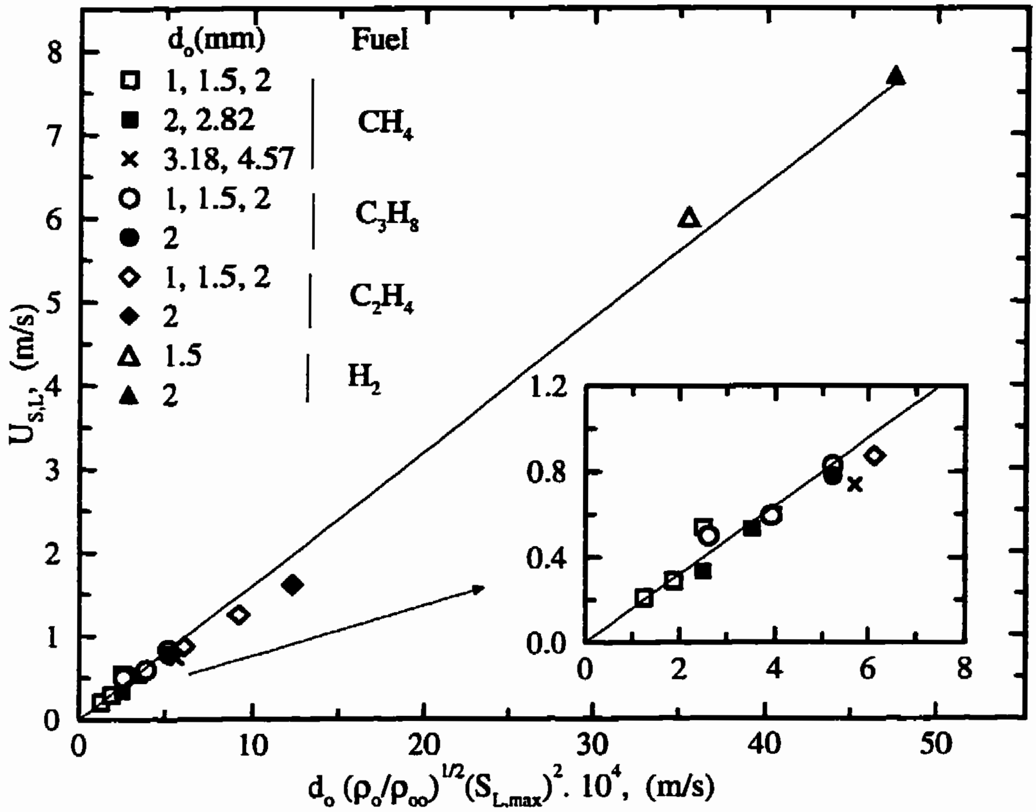

Figure 4.12: The limiting co-flowing air stream velocity for different fuels and jet diameters. Open symbols: from Ref. [27] for jet diameter of 1.00, 1.50 and 2.00 mm; Cross symbols: from Ref. [30] for jet diameter of 3.18 and 4.57 mm; Solid symbols: the present study for jet diameter of 2.00 and 2.82 mm.

simplicity, a jet into a quiescent medium was considered) as [2]:

$$\delta_u \sim x \tag{4.4}$$

The centerline velocity, u_m is also linearly decaying with distance, x (equation 4.2). Combining Equation (4.2) and (4.4),

$$u_m \cdot \delta_u \sim u_o \cdot d_o \cdot (\frac{\rho_o}{\rho_\infty})^{1/2} \tag{4.5}$$

Substituting the above relation into equation (4.3) and rearranging results in:

$$u_o = k \cdot (S_{L,max})(\frac{\rho_\infty}{\rho_o})^{1/2}(\frac{r_\infty}{r_o})^{1/2} \tag{4.6}$$

The density ratio can be expressed in terms of molecular weight and temperature ratios as:

$$u_o = k \cdot (S_{L,max})(\frac{M_\infty}{M_o})^{1/2}(\frac{T_o}{T_\infty})^{1/2}(\frac{r_\infty}{r_o})^{1/2} \tag{4.7}$$

where T_∞ = 300 K and k is a constant which is calculated as follows. By replacing $u_o = U_{L,L}$ for the liftoff jet velocity ($U_{L,L}$ extracted from the experimental data) and T_o = 2000 K, k = 2.2 can be obtained. Since before liftoff the jet flow near the nozzle is hot, T_o = 2000 K is used in this case. In the same way, constant k can be calculated to be equal to 2.2 for the reattachment jet velocity by replacing $u_o = U_{R,L}$ ($U_{R,L}$ extracted from the experimental data) and T_o = 300 K. Due to the fact that before reattachment the jet flow near the nozzle is cold, T_o = 300 K is used in this case. Calculating parameter k for various combinations of the fuel type and nozzle diameters reveals that this parameter is equal to 2.2 as long as the nozzles have the same configurations. Therefore, the above correlation can be written for the reattachment jet velocity as follows:

$$U_{R,L} = 2.2(S_{L,max})(\frac{M_\infty}{M_o})^{1/2}(\frac{\tau_\infty}{\tau_o})^{1/2} \tag{4.8}$$

and for the liftoff jet velocity as:

$$U_{L,L} = 2.2(S_{L,max})(\frac{M_\infty}{M_o})^{1/2}(\frac{T_o}{T_\infty})^{1/2}(\frac{\tau_\infty}{\tau_o})^{1/2} \tag{4.9}$$

or

$$U_{L,L} = U_{R,L} \cdot (\frac{T_o}{T_\infty})^{1/2} \tag{4.10}$$

where T_o = 2000 K. The liftoff and reattachment jet velocities calculated using Equations (4.9) and (4.8) are plotted in Figures 4.14 and 4.13. The corresponding experimentally obtained values are also shown for comparison. The values of maximum laminar burning velocities are the same as the values given in Section 6.3.

4.2 Stability Curves for Methane-Hydrogen Jets

It was shown that the stability limits for hydrogen are much higher than the stability limits for methane (Figures 4.3 and 4.8). Moreover, stable flames can also be sustained at much higher co-flowing air stream velocities for hydrogen compared to methane. For example, the maximum blowout velocity of the attached flame was $\sim$ 550 m/s for hydrogen, while it was about $\sim$ 26 m/s

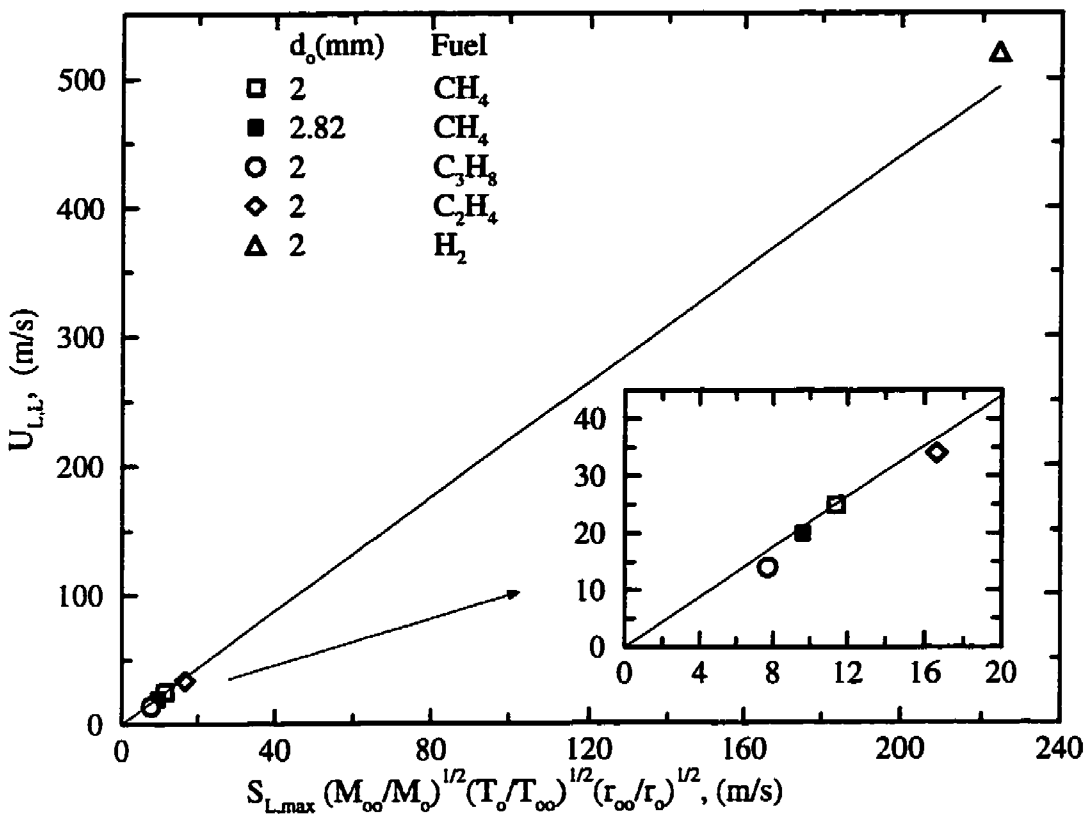

Figure 4.13: The liftoff limits of attached flames at the limiting co-flowing air stream velocity for different fuels and jet diameters. Jet diameters are 2.00 and 2.82 mm.

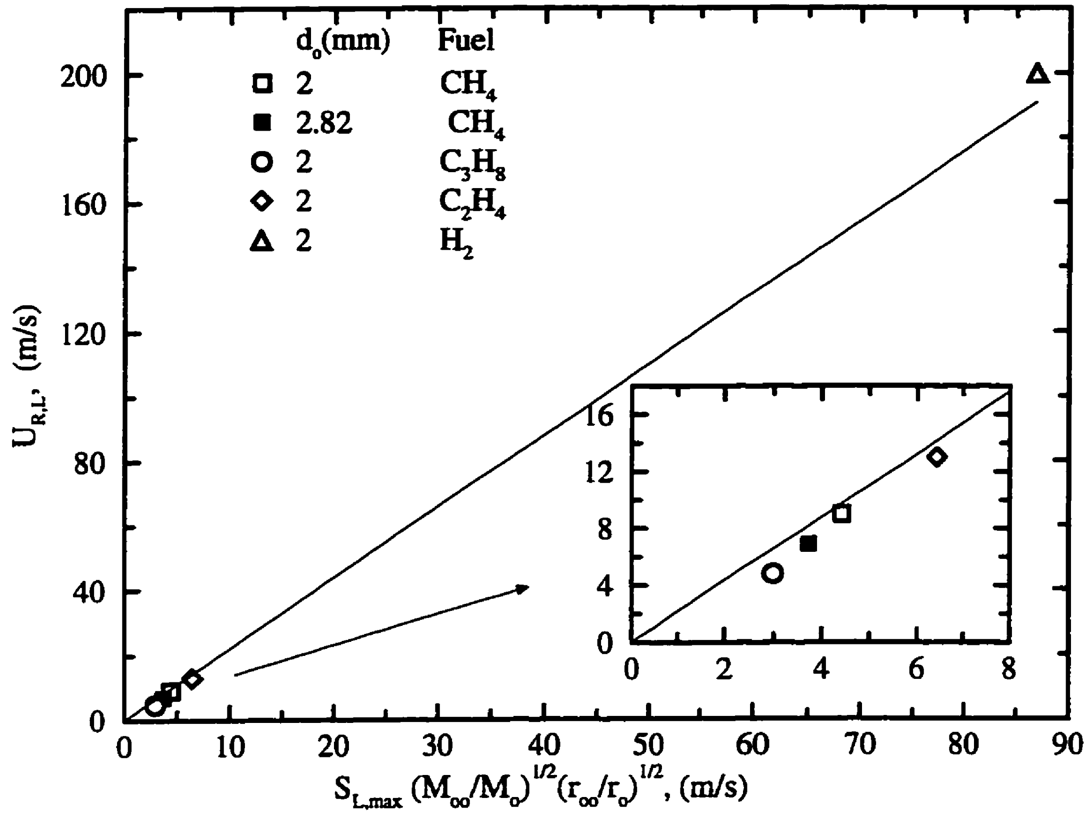

Figure 4.14: The reattachment limits of lifted flames at the limiting co-flowing air stream velocity for different fuels and jet diameters. Jet diameters are 2.00 and 2.82 mm.

for methane. The limiting stream velocity for the hydrogen flame was also very high ($\sim$ 7.70 m/s compared to $\sim$ 0.34 m/s for methane). An addition of hydrogen to methane can improve its stability limits. In addition, since hydrogen is a "clean" fuel, it is always desirable to burn fuels with higher content of hydrogen.

To investigate the effect of hydrogen addition to methane on its stability limits, tests were conducted for different methane-hydrogen mixtures. The blowout limits of a mixture containing 15 percent of hydrogen obtained using a 2.00 mm nozzle B (Figure 3.2b) are shown in Figure 4.15. The blowout limits for methane-hydrogen mixtures containing 25, 50 and 75 percent of hydrogen obtained using a 2 mm nozzle A (Figure 3.2a) are shown in Figures 4.16, 4.17 and 4.18, respectively.

The blowout limits of lifted flames and attached flames for different methane-hydrogen mixtures are also shown in Figure 4.19 together with those for pure methane and pure hydrogen for comparison. The presence of larger amount of hydrogen in the jet fuel provided higher blowout limits of the flame at all co-flowing stream velocities. For example, at a stream velocity of 1.00 m/s, an addition of 25 and 50 percent of hydrogen to methane increased the blowout limit of attached flames from $\sim$ 25 m/s (for pure methane) to $\sim$67 m/s and $\sim$125 m/s, respectively.

As can be seen in Figures 4.15, 4.16, 4.17, for mixtures containing 50 percent or less hydrogen only regions II and III were observed. For these mixtures, it was not possible to liftoff the attached flames by simply increasing the jet velocity. The lifted flames could only result from ignition at relatively high jet velocities with the ignitor located away from the nozzle rim. Similar observations were also reported in [6] for methane-hydrogen jets

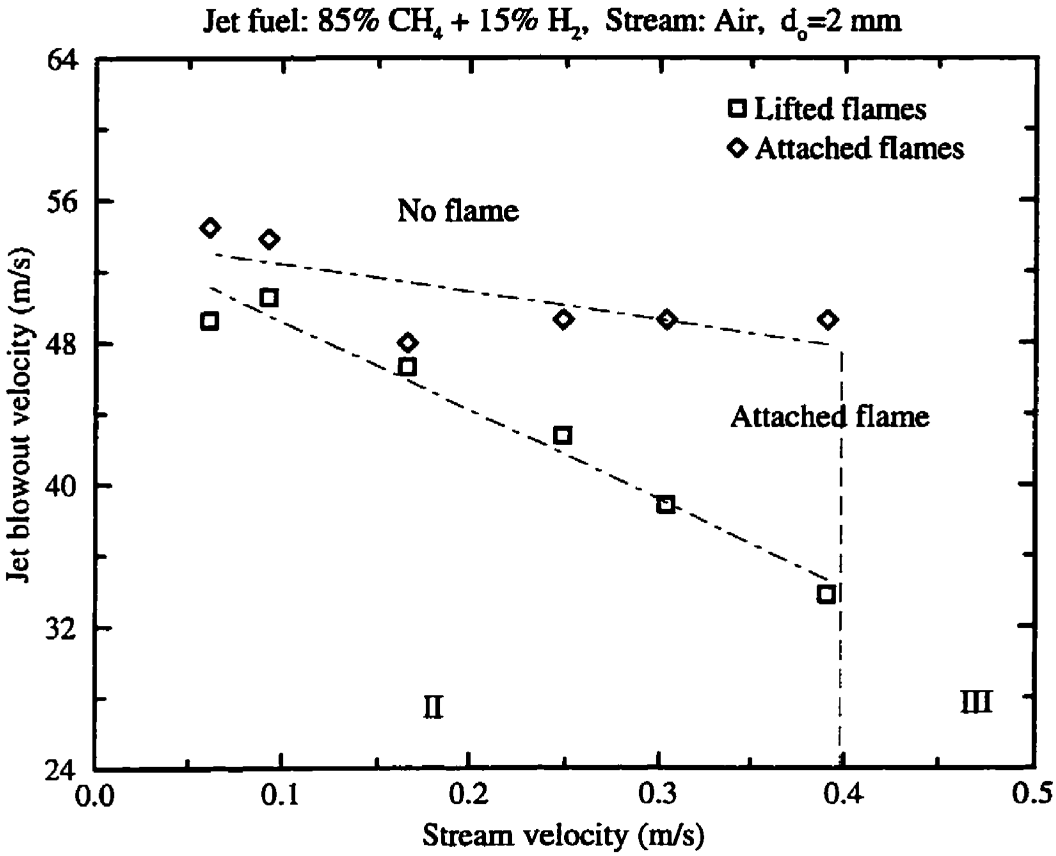

Figure 4.15: Flame blowout limits as a function of co-flowing stream velocity for a fuel mixture containing 85% of methane and 15% of hydrogen. Jet diameter = 2.00 mm.

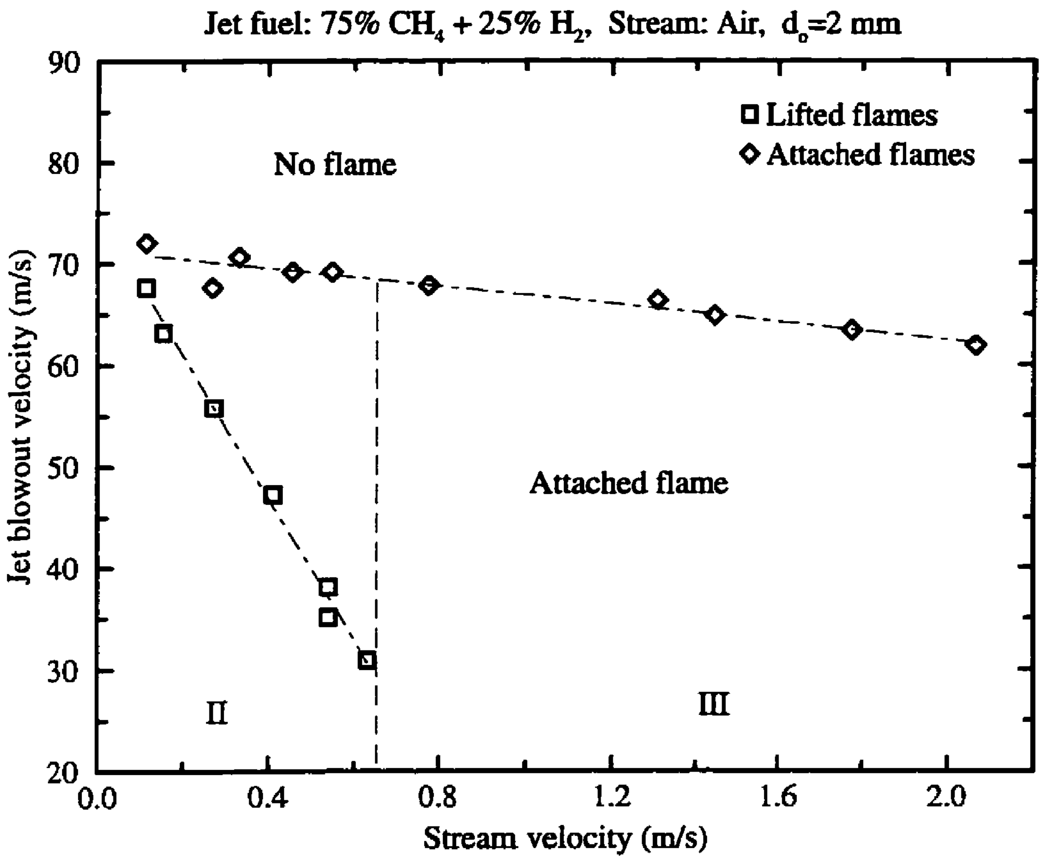

Figure 4.16: Flame blowout limits as a function of co-flowing stream velocity for a fuel mixture containing 75% of methane and 25% of hydrogen. Jet diameter = 2.00 mm.

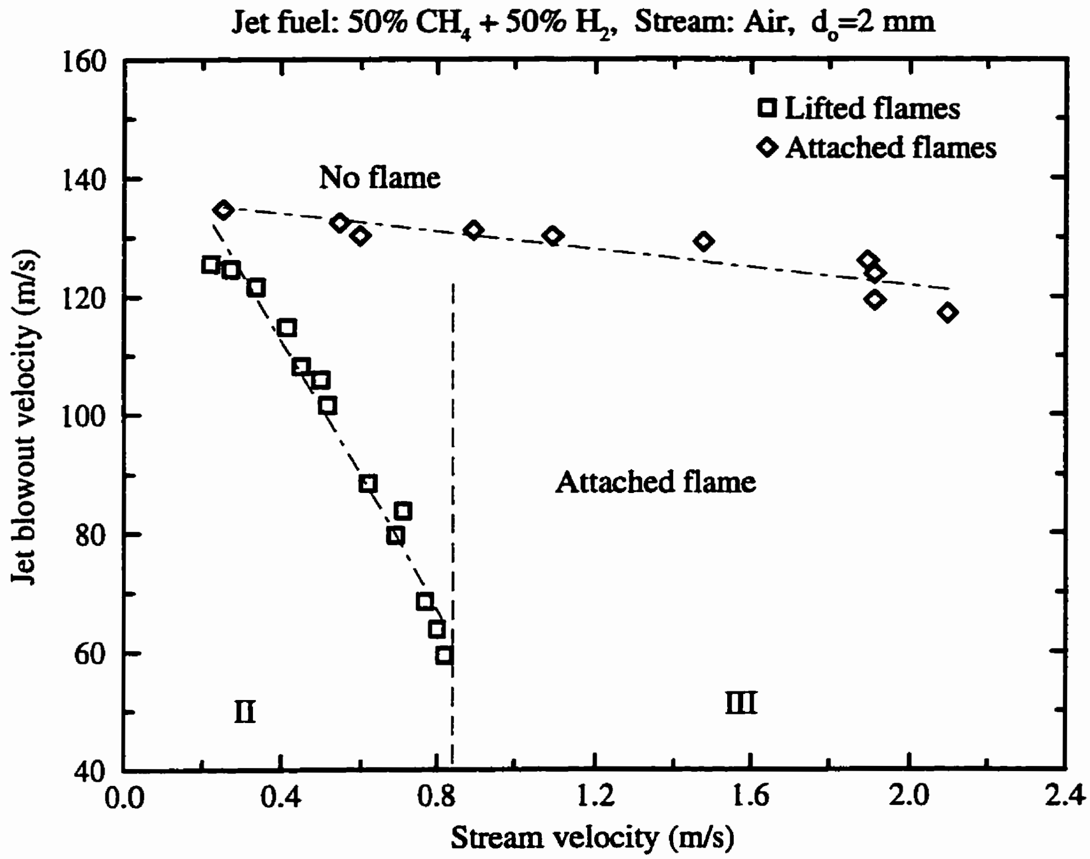

Figure 4.17: Flame blowout limits as a function of co-flowing stream velocity for a fuel mixture containing 50% of methane and 50% of hydrogen. Jet diameter = 2.00 mm.

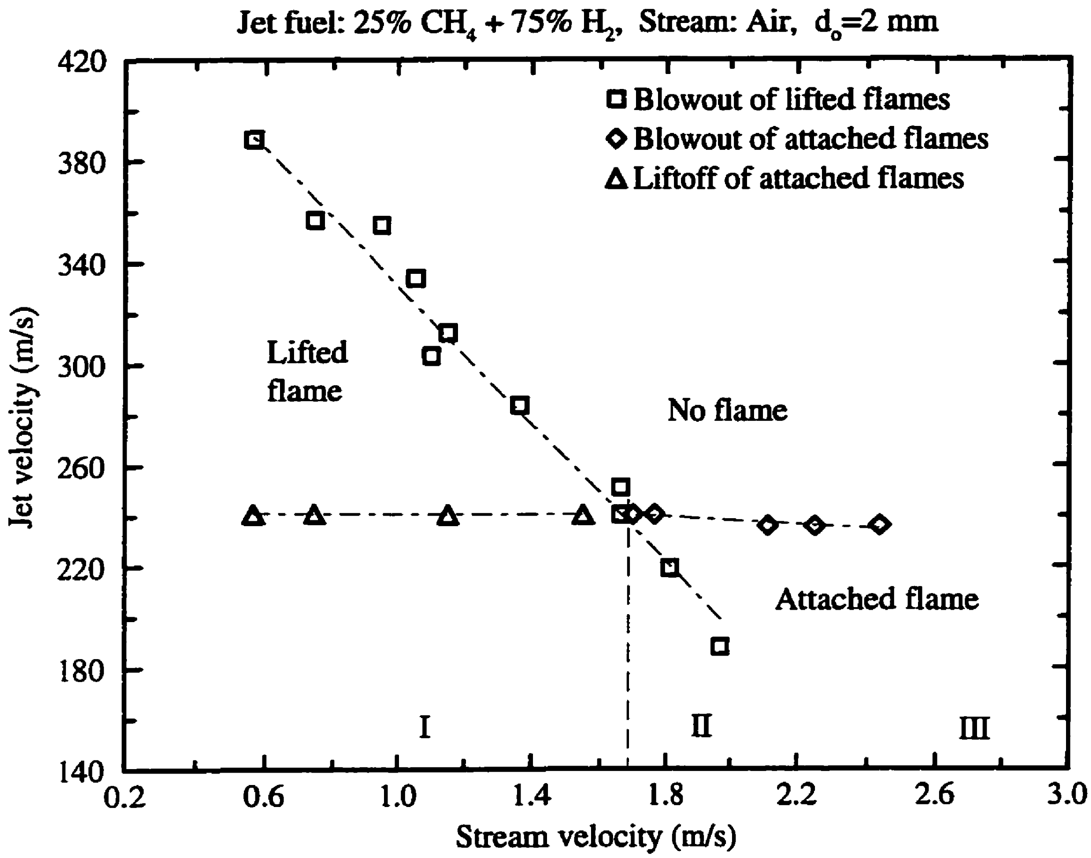

Figure 4.18: Stability limits as a function of co-flowing stream velocity for a fuel mixture containing 25% of methane and 75% of hydrogen. Jet diameter = 2.00 mm.

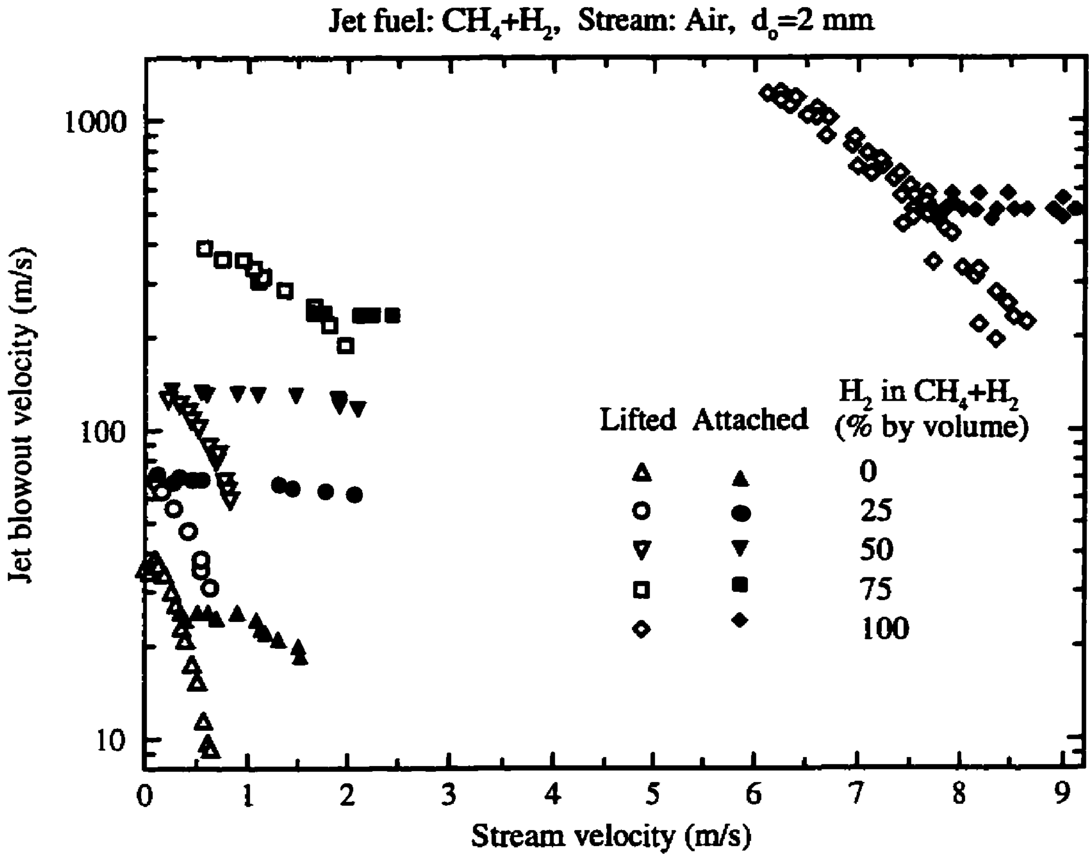

Figure 4.19: Flame blowout velocities as a function of co-flowing stream velocity for different methane-hydrogen mixtures. Jet diameter = 2.00 mm.

containing 33 and 55 percent of hydrogen using a nozzle of 2.2 mm diameter.

As in the case of pure fuel jets, the blowout limits of attached flames for different methane-hydrogen mixtures in region II were higher than those of lifted flames especially at higher co-flowing stream velocities. In addition, the blowout limits of the attached flames were much less sensitive to the changes in the co-flowing air stream velocity than those of the lifted flames. This makes them attractive to the operation in practical combustion devices. Lifted flames are usually avoided and considered unstable in practice. However, there is a need to estimate the limits for their existance in combustion devices.

The effect of hydrogen addition to the methane jet on limiting co-flowing stream velocity, $U_{S,L}$ is shown in Figure 4.20. It was unexpected that hydrogen addition up to 50 percent would not result in an increase in the limiting co-flowing stream velocity.

Effect of Nozzle Diameter. Similar trends for the stability limits were also observed for a jet diameter of 2.82 mm (Figure 4.21). Addition of 25 percent hydrogen to a methane jet flame increased the stability limits of jet flame and also decreased the limiting co-flowing stream velocity. However, the limiting stream velocities for both fuels (methane and methane-hydrogen mixture) were higher than the corresponding limiting stream velocities for a smaller jet of 2 mm diameter (Figure 4.19).

Furthermore for a jet diameter of 2.82 mm, stability region I was recognized even for fuel mixtures with 25 percent of hydrogen (Figure 4.21). It was reported in [30] that for a larger diameter of 4.57 mm, region I was recognized for a methane-hydrogen jet containing only 15 percent of hydrogen.

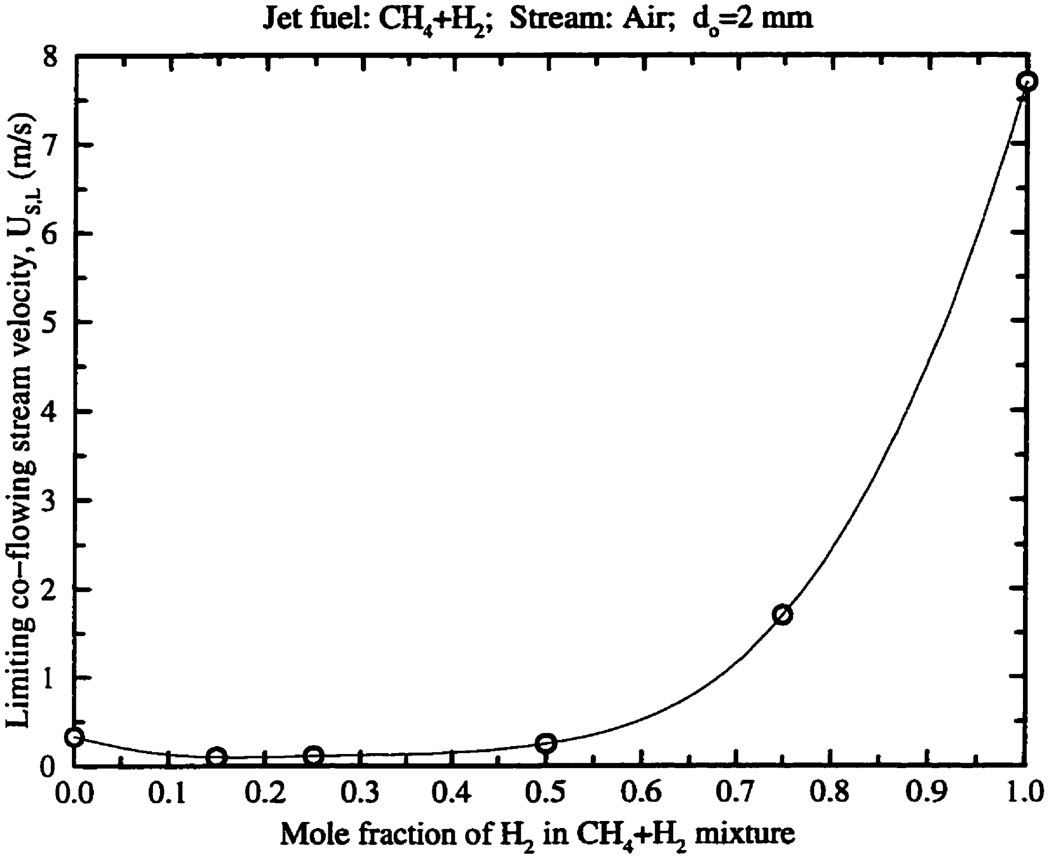

Figure 4.20: The limiting co-flowing stream velocity as a function of the mole fraction of hydrogen in methane-hydrogen mixture for different methane-hydrogen jet flames in air stream. Jet diameter = 2.00 mm.

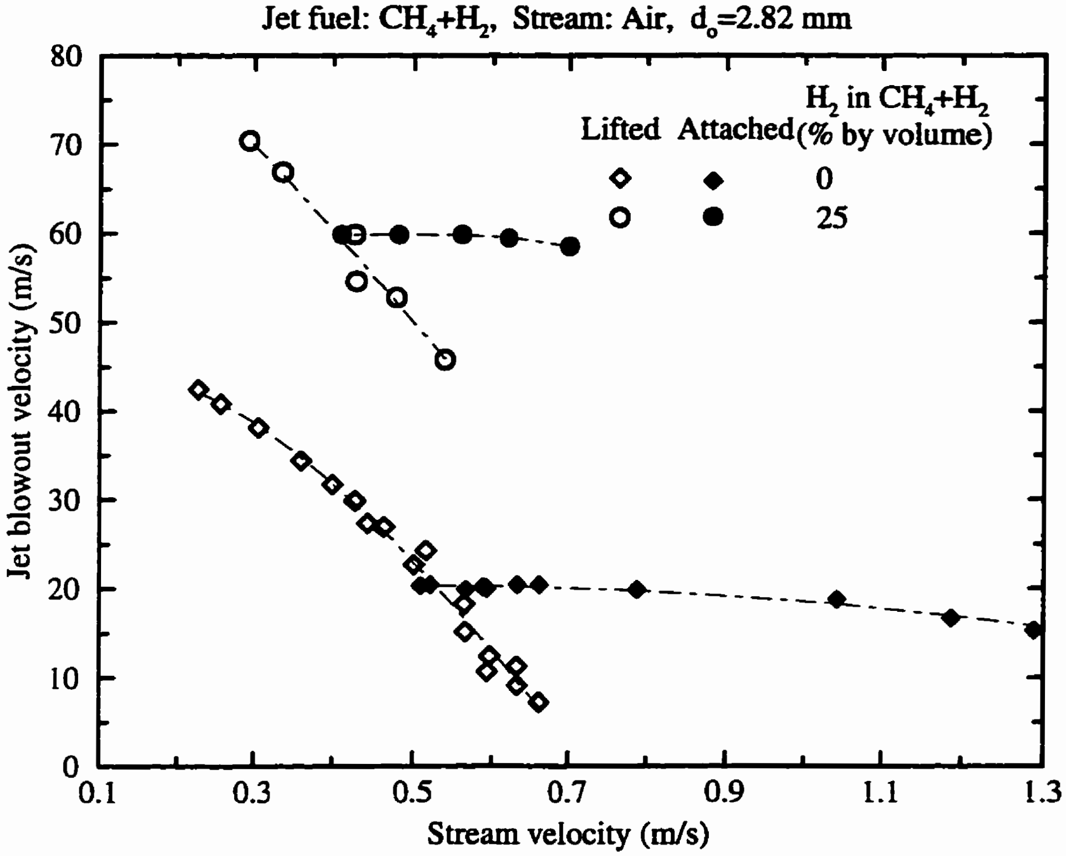

Figure 4.21: The jet flame blowout velocity as a function of co-flowing stream velocity for two different fuel mixtures.

4.3 Effect of Fuel in the Surrounding Stream

It is known that the addition of a fuel (auxiliary fuel or surrounding fuel) into a surrounding air stream can substantially enhance the stability of non-premixed flames [3,5,25,29]. This effect was also investigated experimentally in the present study to obtain consistent data for validation of the developed model for predicting the blowout limits of non-premixed jet flames. The experiments were conducted with a methane jet flame in a co-flowing stream containing an auxiliary fuel homogeneously mixed with the air. Methane, hydrogen, ethylene and propane were used as the auxiliary fuels. The results are presented in Figures 4.22, 4.23, 4.24 and 4.25.

It can be seen that the flame blowout limits increased significantly with a small increase in the concentration of the fuel in the surrounding stream. The limiting co-flowing stream velocity was also increased with an increase in the concentration of the fuel added to the surrounding stream. For example, an addition of 3 percent of methane to co-flowing stream increased the limiting co-flowing stream velocity from 0.34 m/s to 0.7 m/s.

An addition of an auxiliary fuel into the co-flowing air stream enhanced the blowout limits of the *lifted* flames more significantly than those of the *attached* flames. This enhancement is more significant at smaller co-flowing stream velocities. For example, at a stream velocity of 0.4 m/s, the ratio of the blowout limit of methane lifted flame in the presence of surrounding fuel (2% of methane) to the blowout limit of methane lifted flame without surrounding fuel is about 2.5, while this ratio at the stream velocity of 0.6 m/s is only 1.75 (Figure 4.22).

As it can be seen in Figures 4.26 and 4.27, the extent of improvement in

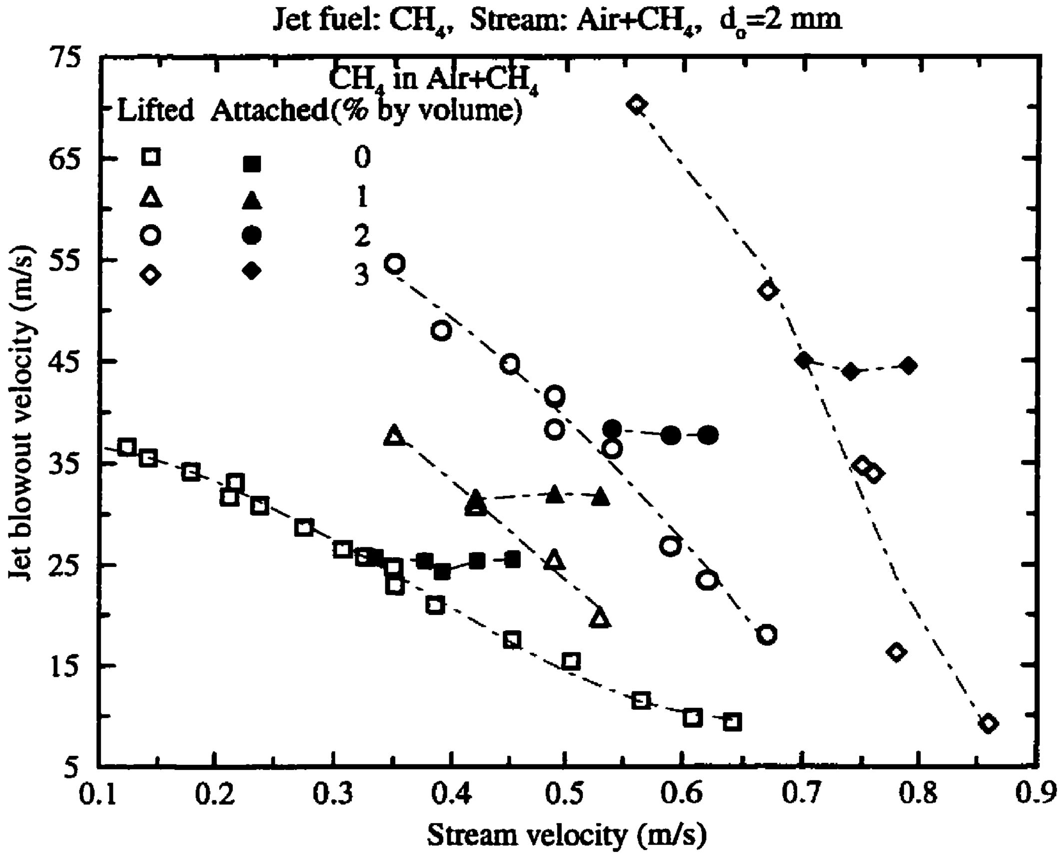

Figure 4.22: The blowout limits of a methane jet flame as a function of co-flowing stream velocity for different concentrations of methane in the co-flowing stream.

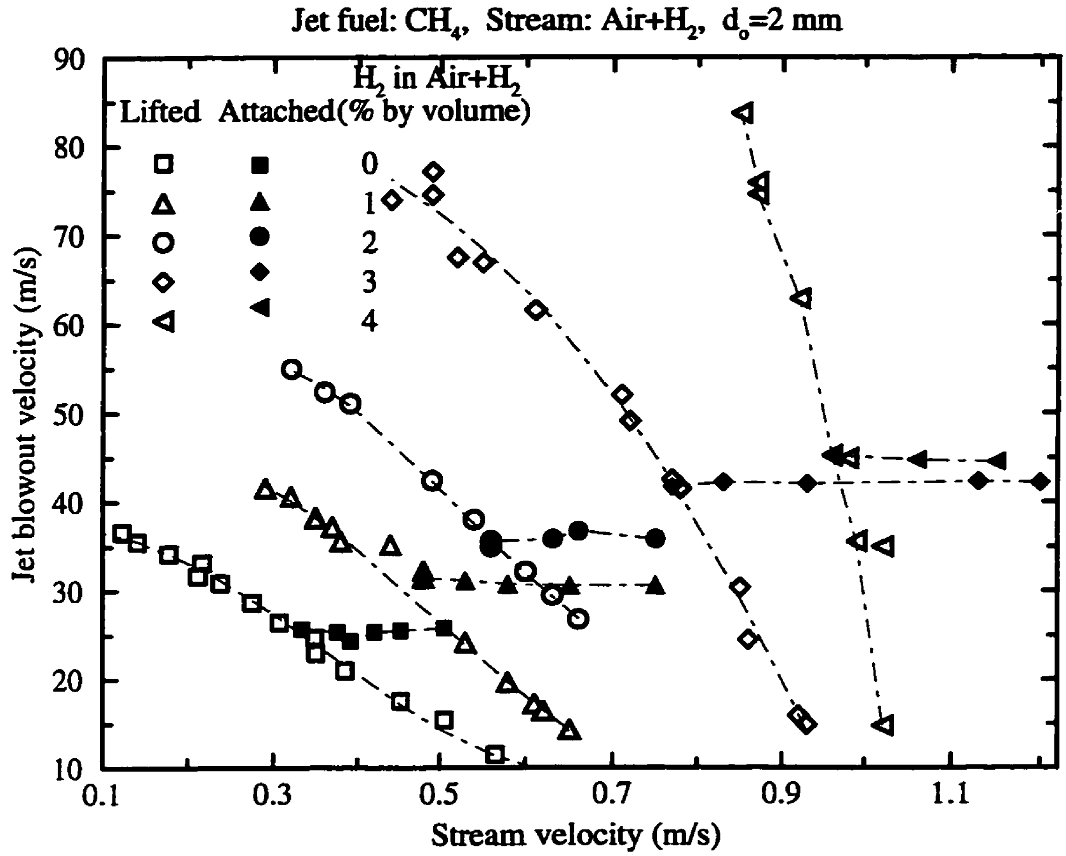

Figure 4.23: The blowout limits of a methane jet flame as a function of co-flowing stream velocity for different concentrations of hydrogen in the co-flowing stream.

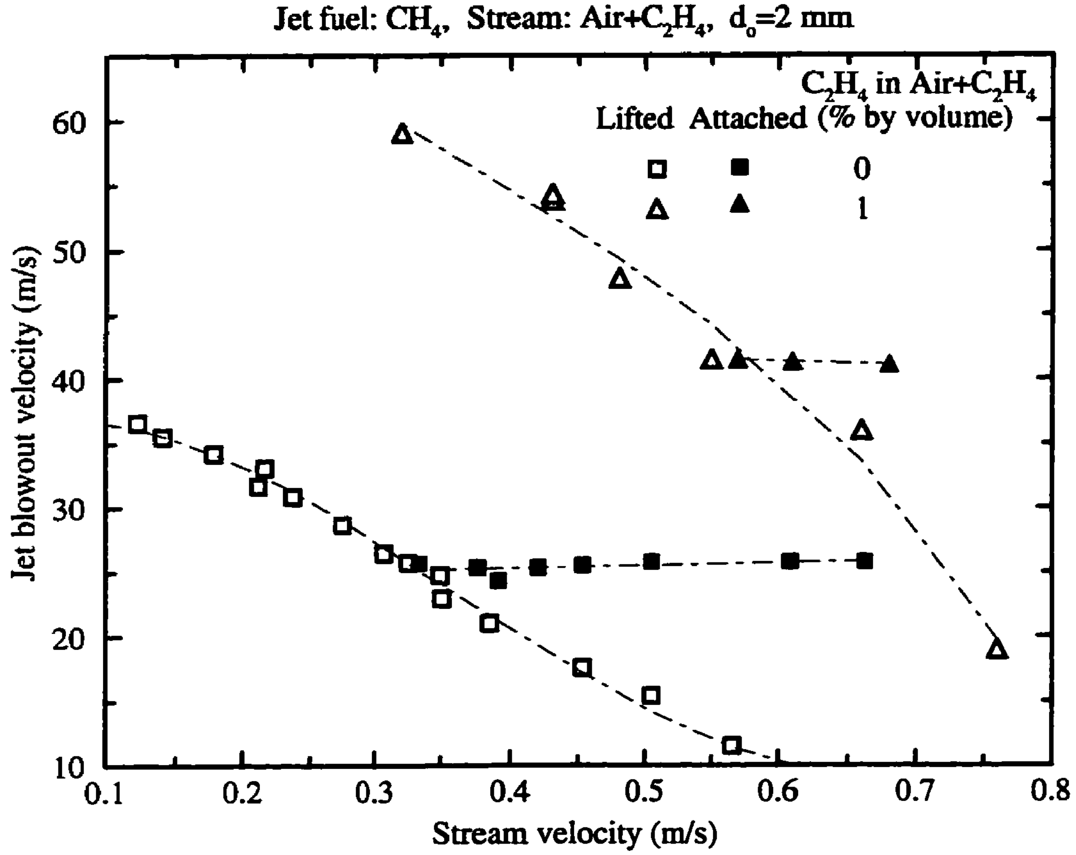

Figure 4.24: The blowout limits of a methane jet flame as a function of co-flowing stream velocity for different concentrations of ethylene in the co-flowing stream.

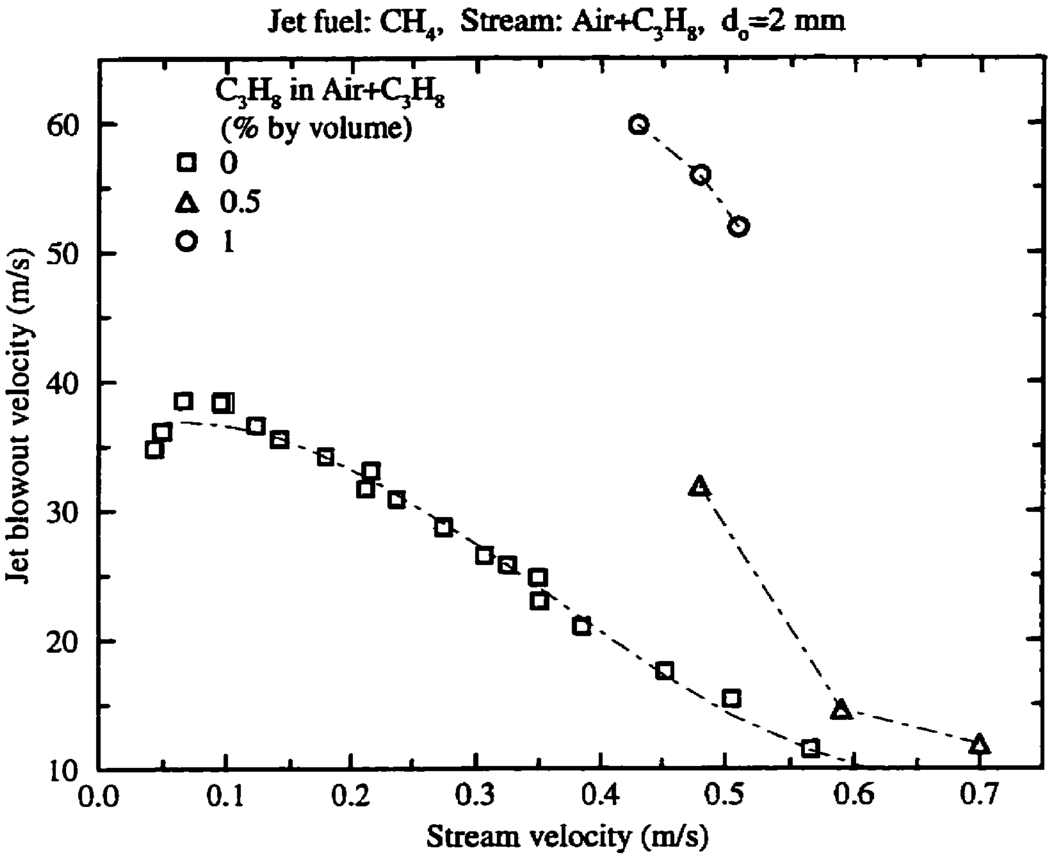

Figure 4.25: The blowout limits of methane lifted flames as a function of co-flowing stream velocity for different concentrations of propane in the co-flowing stream.

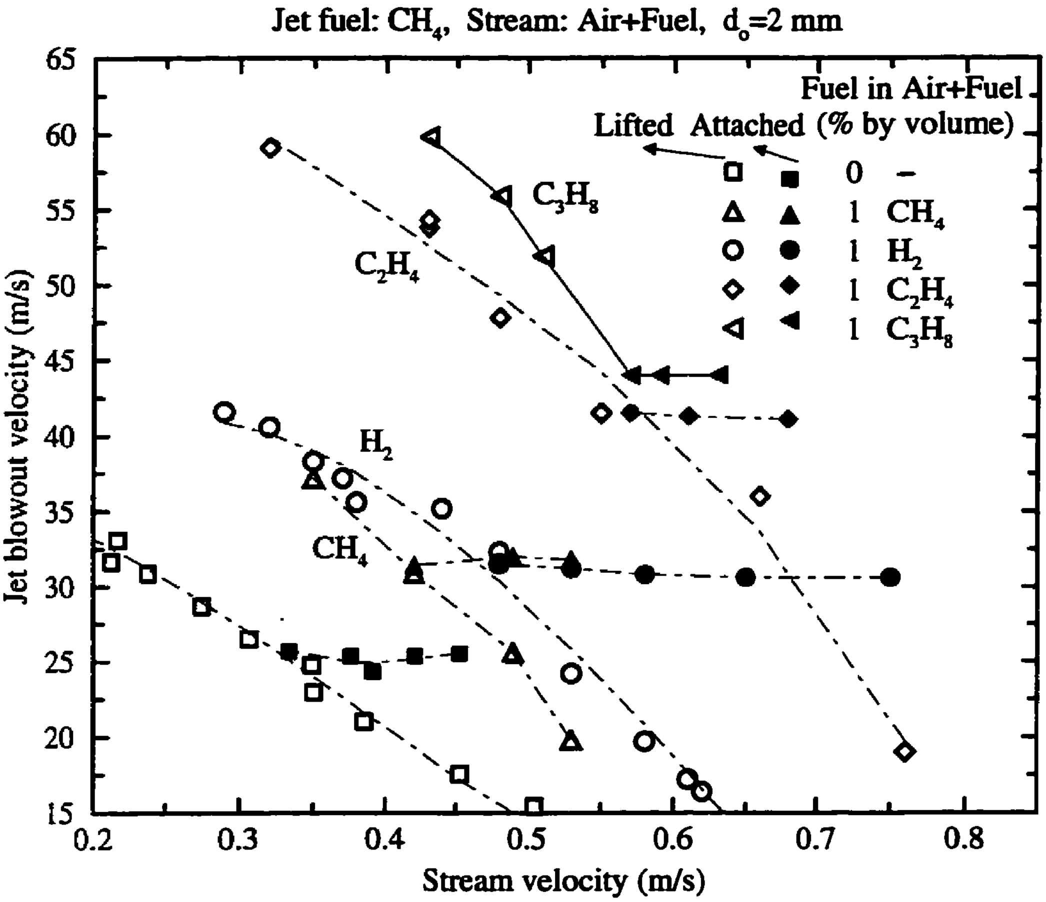

Figure 4.26: The blowout limits of methane jet flames as a function of co-flowing stream velocity for different fuels in the co-flowing stream.

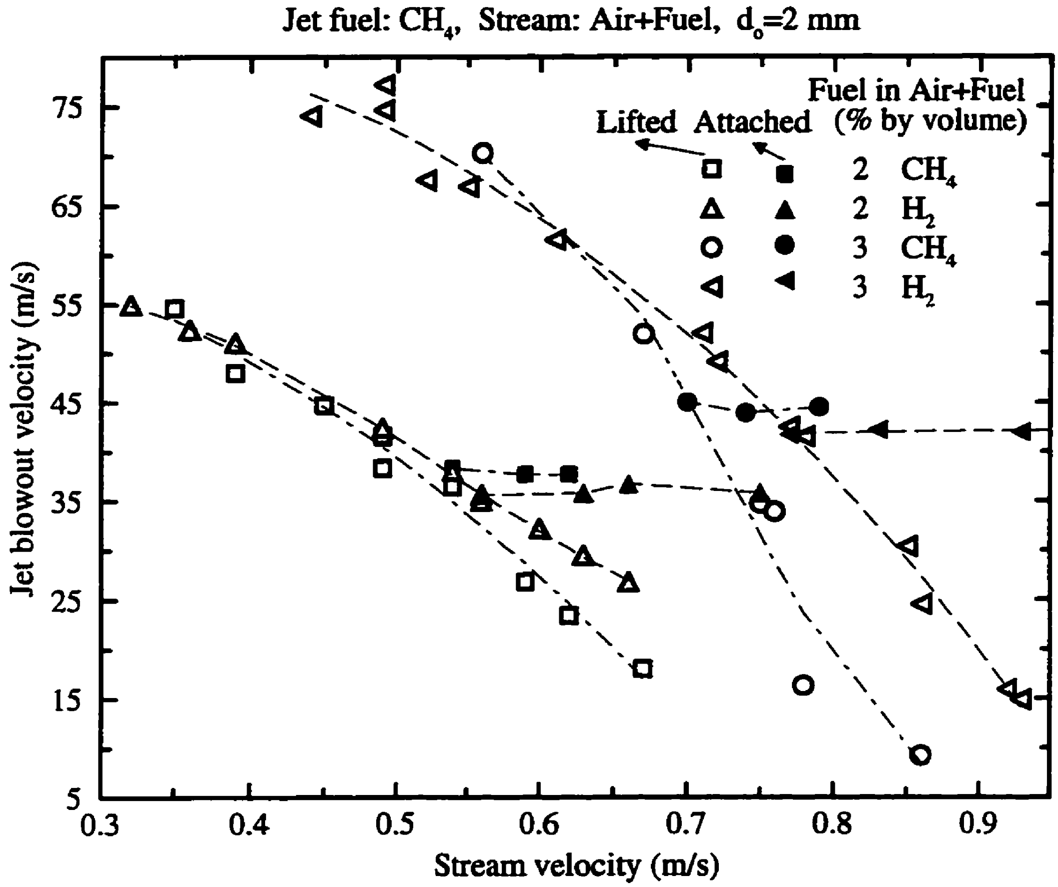

Figure 4.27: The blowout limits of methane jet flames as a function of co-flowing stream velocity for different fuels in the co-flowing stream.

the blowout limits varies with the type of auxiliary fuel involved. The most improvement on blowout limits of *lifted* flames (open symbols) was observed with propane followed by ethylene, hydrogen and methane as auxiliary fuels. However, the blowout limits of methane *attached* flames (solid symbols) were enhanced the most with propane followed by ethylene, methane and hydrogen as auxiliary fuels. The effects of methane and hydrogen in the co-flowing stream on the blowout limits of the methane jet flames are approximately the same. This is also valid for other concentrations (2% and 3%) of these fuels in the surrounding stream of air (Figure 4.27).

4.4 Effect of Diluents

Introduction of diluents either to a jet fuel or to a co-flowing air stream would affect the stability limits of non-premixed flames. This effect is discussed in Sections 4.4.1 and 4.4.2.

4.4.1 Diluent in the Jet Fuel

Diluent in Methane Jet. The effect of diluent addition to a jet fuel on the blowout limits of lifted flames was investigated with nitrogen, carbon dioxide and helium as diluents in a methane jet. The blowout limits of lifted flames for different methane-diluent mixtures are shown in Figures 4.28, 4.29 and 4.30. As expected, addition of diluents to methane jet decreased significantly its blowout limit. A higher degree of dilution leads to a higher drop in the blowout limits over the entire range of co-flowing stream velocities considered. Jet blowout velocity decreases almost linearly with an increase in the mole fraction of diluent (Figure 4.31). The slope of graphs (lines) represent the rate of this decrease which remains approximately constant for different co-flowing stream velocities (the lines are approximately parallel for each diluent). The most detrimental effect was observed with carbon dioxide as the diluent followed by nitrogen and then by helium (Figure 4.32). This trend is consistent with the variation in the transport and thermochemical properties of such fuel-diluent mixtures.

Diluent in Methane-Hydrogen Jet. The effect of addition of carbon dioxide to a methane-hydrogen fuel mixture on its blowout limits is shown in Figure 4.33. It can be seen that the addition of carbon dioxide to the jet fuel has a stronger effect on the blowout limits of methane-hydrogen flames than on those of pure methane flames. For example, at stream velocity of 0.25 m/s, an addition of 5 percent by volume of carbon dioxide to a methane jet decreased the jet blowout velocity from 30 m/s to 24 m/s (~20 percent reduction). However at the same stream velocity, a 5 percent addition of carbon dioxide to a methane-hydrogen mixture containing 50 percent hydrogen decreased the jet blowout velocity from 125 m/s to 75 m/s (~40 percent reduction).

4.4.2 Diluent in the Surrounding Air Stream

The effect of the presence of diluents - nitrogen or carbon dioxide - in the surrounding air stream on the stability limits of methane jet flames can be seen in Figures 4.34 and 4.35. The presence of these diluents in the surrounding air stream even in small quantities can be very detrimental to the flame stability. As can be observed from Figure 4.36, jet blowout velocity decreases almost linearly with an increase in the mole fraction of diluent, similar to the case of diluent addition to the jet fuel. The rate of decrease

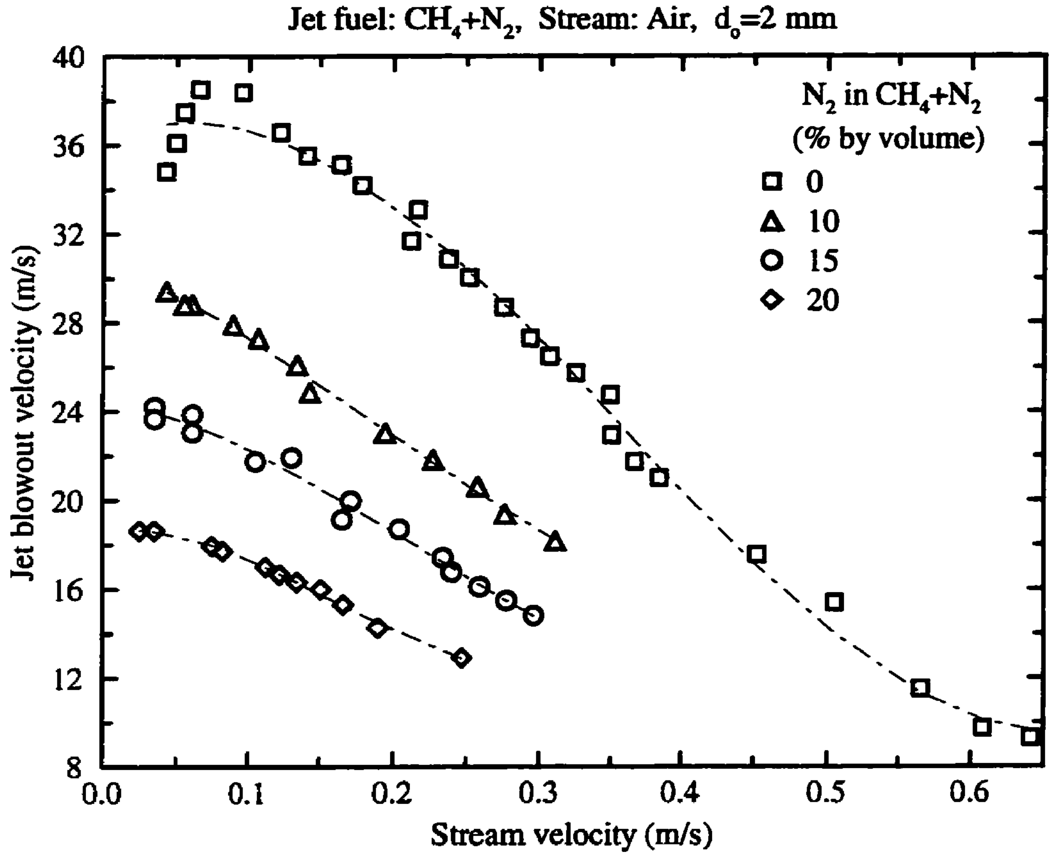

Figure 4.28: The blowout limits of methane-nitrogen lifted flames as a function of co-flowing stream velocity for different nitrogen concentrations in the fuel mixture. Jet diameter = 2.00 mm.

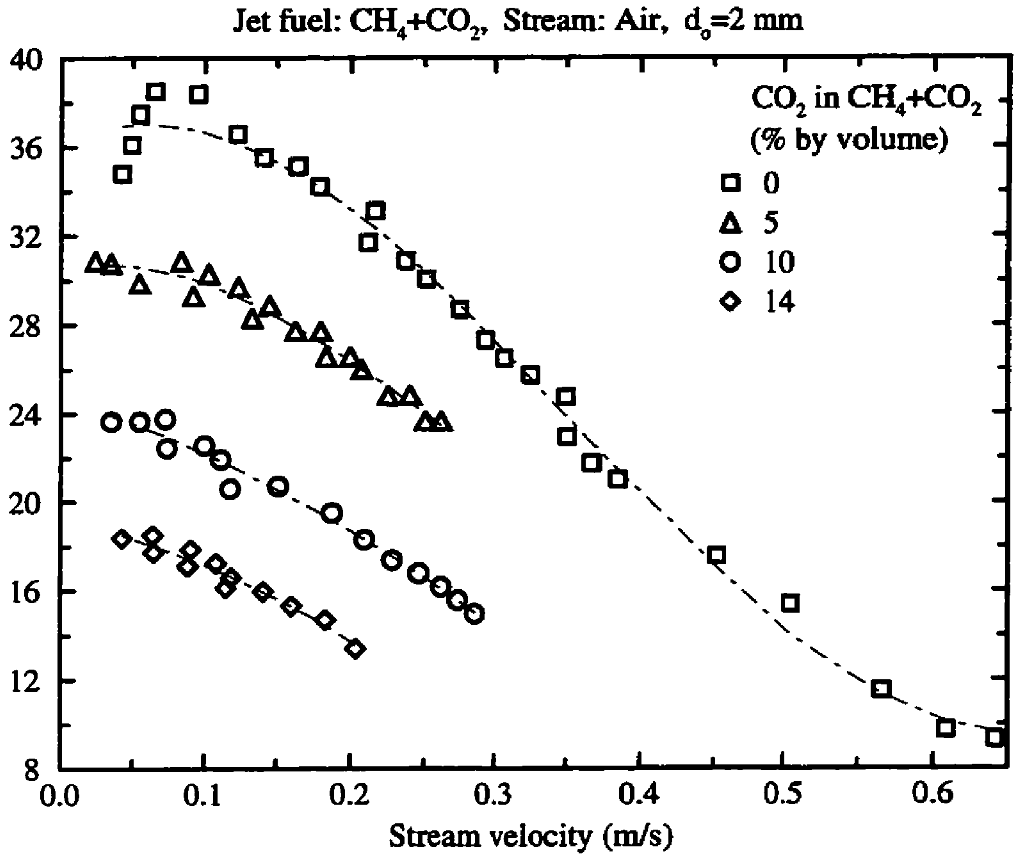

Figure 4.29: The blowout limits of methane-carbon dioxide lifted flames as a function of co-flowing stream velocity for different carbon dioxide concentrations in the fuel mixture. Jet diameter = 2.00 mm.

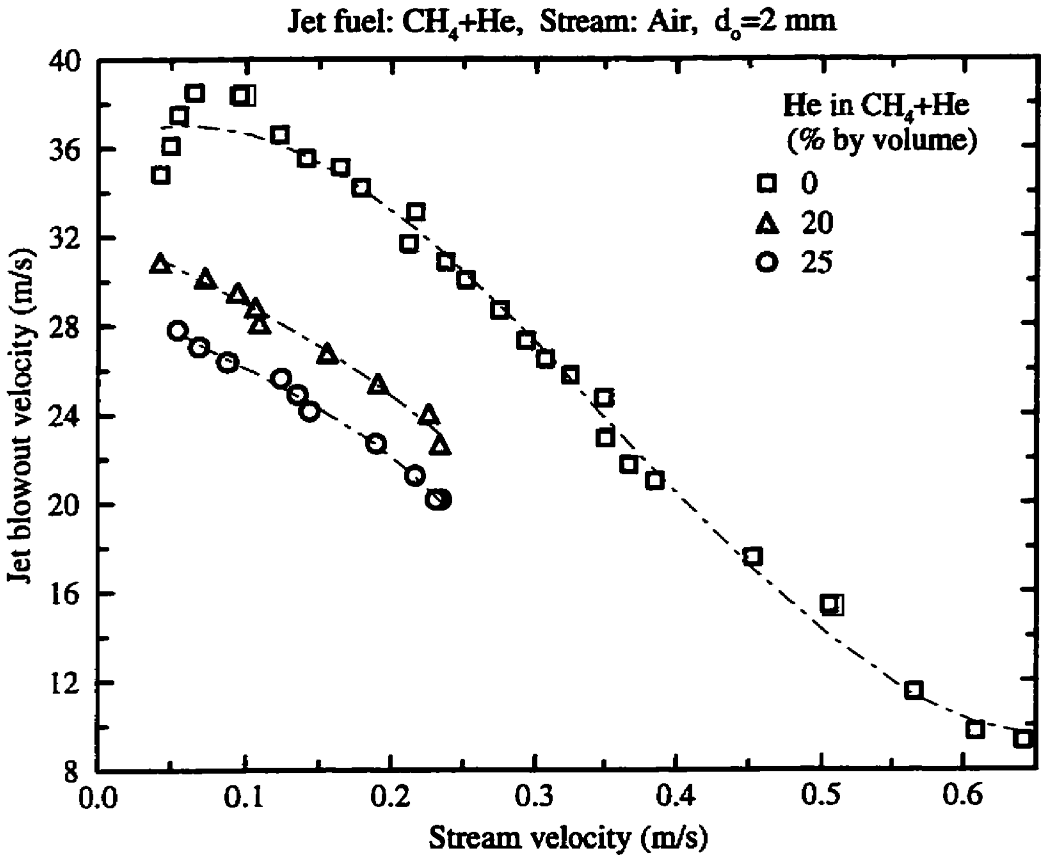

Figure 4.30: The blowout limits of methane-helium lifted flames as a function of co-flowing stream velocity for different helium concentrations in the fuel mixture. Jet diameter = 2.00 mm.

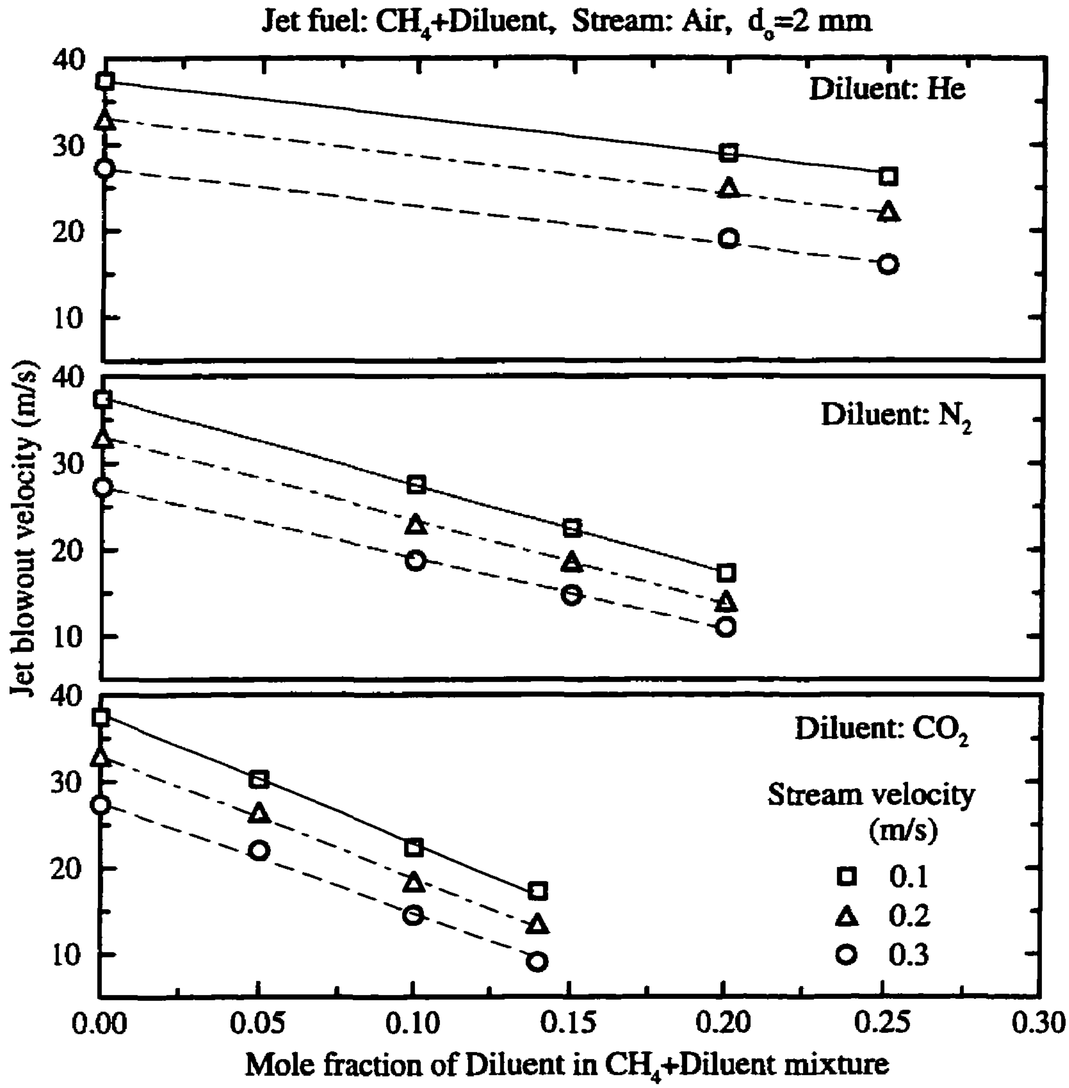

Figure 4.31: The blowout limits of methane-diluent lifted flames as a function of the mole fraction of diluent in methane-diluent mixture for different co-flowing stream velocities. Jet diameter = 2.00 mm.

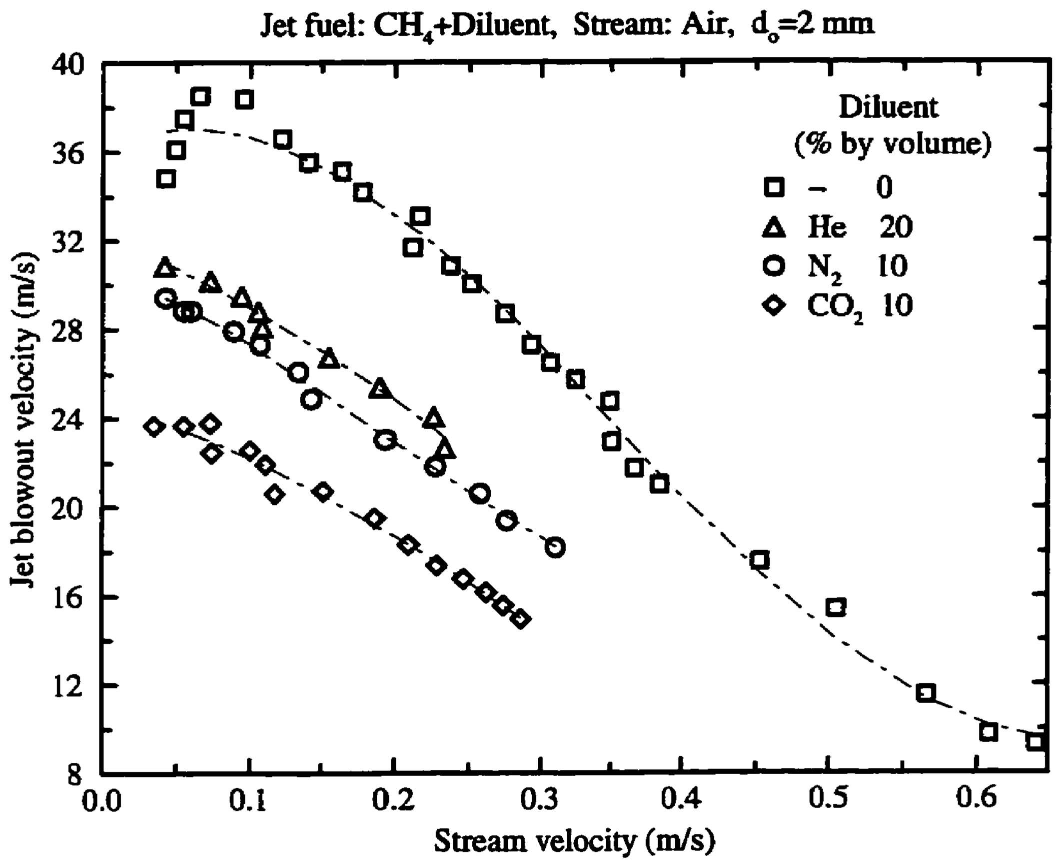

Figure 4.32: The blowout limits of methane-diluent lifted flames as a function of co-flowing stream velocity. Jet diameter = 2.00 mm.

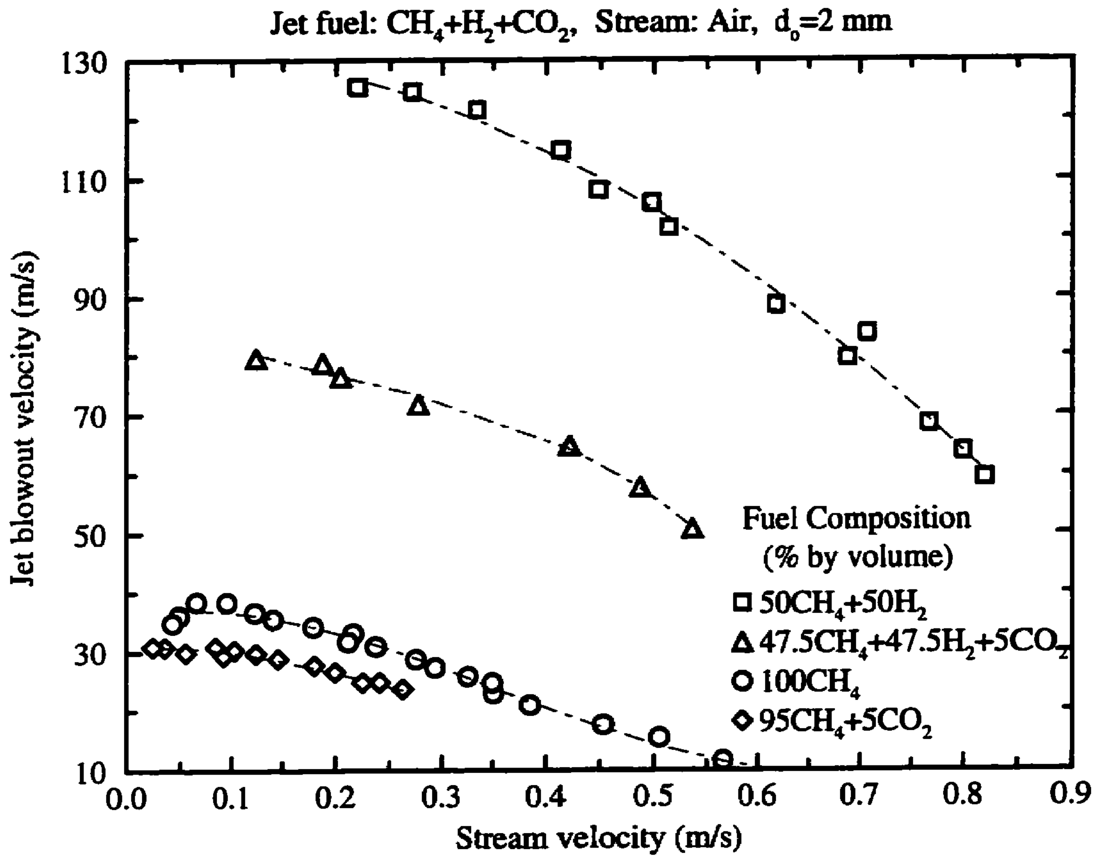

Figure 4.33: The blowout limits of lifted flames as a function of co-flowing stream velocity for different methane-hydrogen-carbon dioxide mixtures. Jet diameter = 2.00 mm.

remains approximately constant for different co-flowing stream velocities for both of these diluents.

As expected, carbon dioxide as a diluent has a more detrimental effect on the jet flame blowout limits than nitrogen. At co-flowing stream velocity of 0.3 m/s, the blowout velocity of methane flame decreased from 27 m/s to 18.5 m/s with a 4 percent addition of nitrogen to air stream (Figure 4.34). Under the same circumstances, the blowout velocity decreased from 27 m/s to 10 m/s with a 4 percent addition of carbon dioxide to the air stream (55% reduction) (Figure 4.35). The same trend was also observed for a jet diameter of 1.5 mm [69].

At the same diluent volume concentration, the presence of the diluent in the air stream affects the blowout limits more strongly than when it is present in the jet fuel. For example, at a co-flowing stream velocity of 0.2 m/s, an addition of 5 percent by volume of carbon dioxide to the jet fuel caused about 22 percent reduction in methane flame blowout limit (Figure 4.29); while the reduction was about 58 percent when the same diluent volume concentration was added to the surrounding air stream (Figure 4.35). This is due to the large entrainment of the air-diluent mixture by the jet at the location of flame stabilization before blowout.

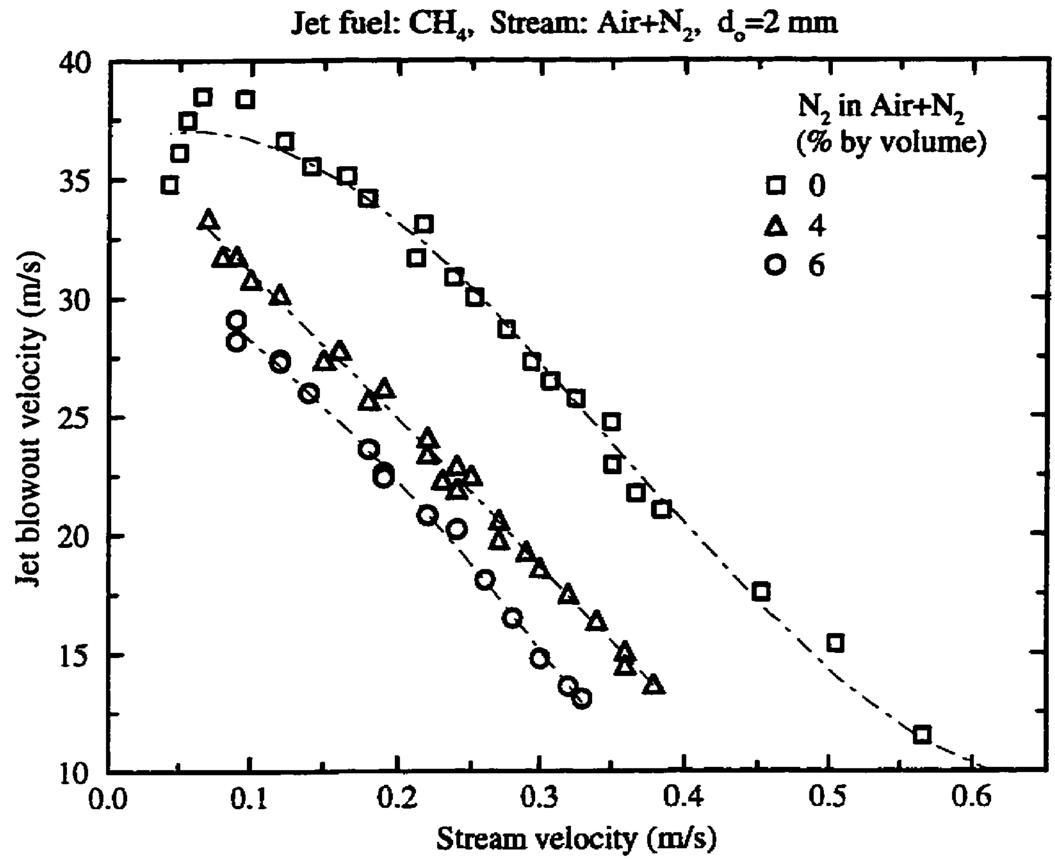

Figure 4.34: The blowout limits of methane lifted flames as a function of co-flowing stream velocity for different nitrogen concentrations in the co-flowing stream of air. Jet diameter = 2.00 mm.

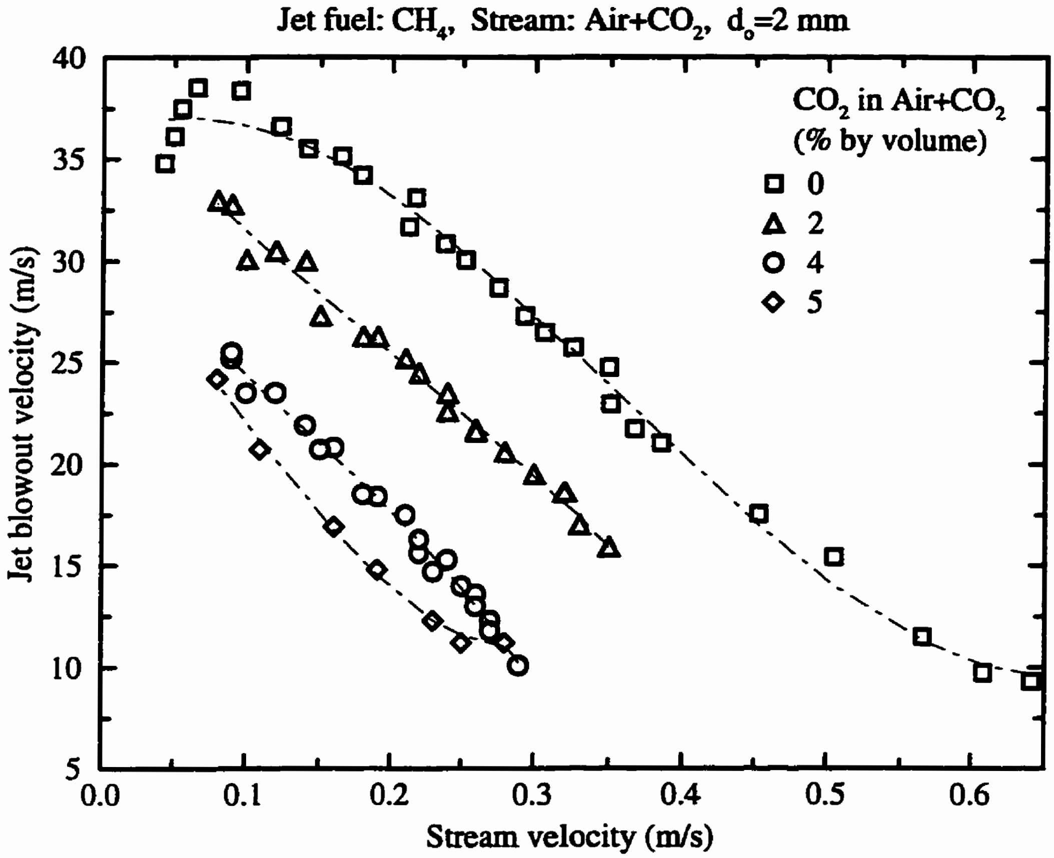

Figure 4.35: The blowout limits of methane lifted flames as a function of co-flowing stream velocity for different carbon dioxide concentrations in the co-flowing stream of air. Jet diameter = 2.00 mm.

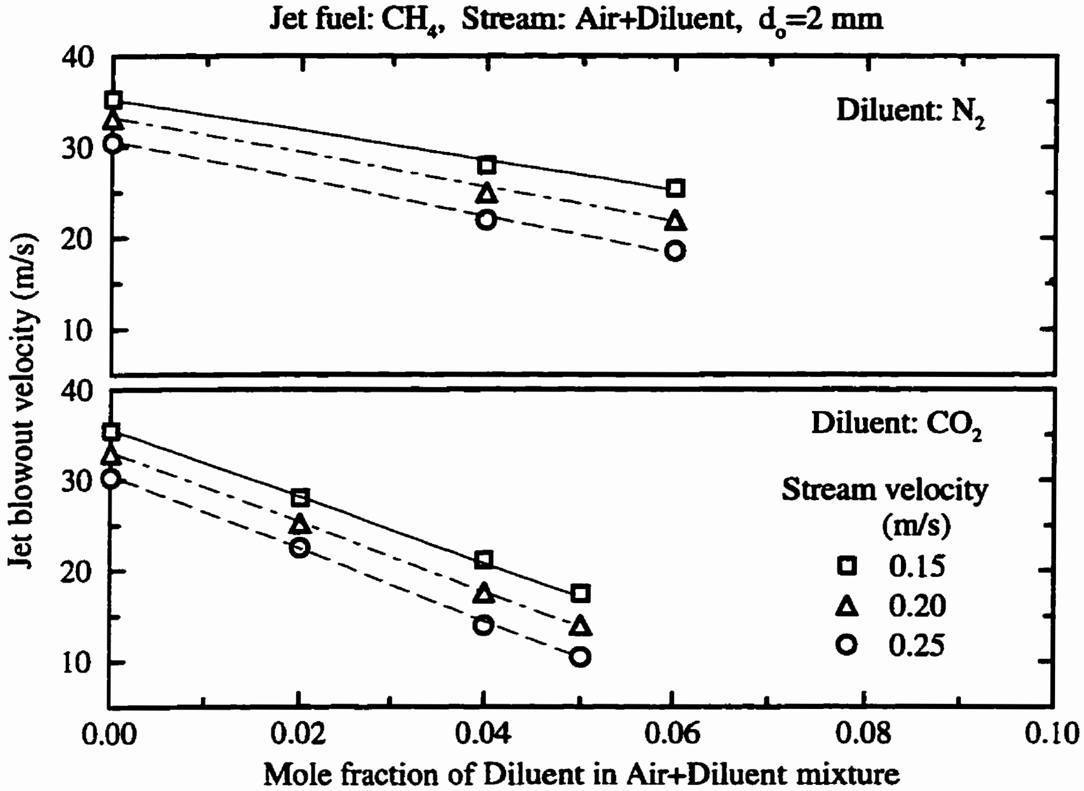

Figure 4.36: The blowout limits of methane lifted flames as a function of the mole fraction of diluent in air-diluent mixture for different co-flowing stream velocities. Jet diameter = 2.00 mm.

Chapter 5

Theoretical Study of the Blowout of Lifted Flames

As discussed in Chapter 4, two types of flames - lifted flames and attached flames - were observed experimentally before blowout. The far-field conditions, well downstream of the nozzle, are responsible for stabilization of lifted flames, while near-field conditions i.e., in the vicinity of the nozzle rim are responsible for stabilization of attached flames. Therefore, different stabilization mechanisms are responsible for the blowout limits of these flames. Hence *lifted* and *attached* flames should be modeled separately. In this chapter, the blowout limits of *lifted* flames are studied theoretically. In Section 5.1, the proposed model for prediction of these limits is described. The procedure of calculations are discussed in Section 5.2. The results of this theoretical study are presented and discussed in Section 5.3.

5.1 Modeling of the Blowout of Lifted Flames

The model proposed in the present study for the blowout of lifted flames stems from a model described by Dahm and Dibble [2]. The author modified this model significantly to achieve a more accurate prediction of experimentally determined blowout limits over a wide range of operating conditions. This model is based on the ratio of two well-recognized parameters in flame stabilization processes, i.e., the mixing time of reactants and the chemical time (combustion time).

Mixing Time. In a turbulent flow, there is a co-existence of large and small eddies. These eddies are mutually interconnected and their influence on flame propagation can not be separated. Due to fluid viscosity, the large eddies transfer their energy to smaller eddies, in turn these smaller eddies transfer energy to even smaller eddies, etc. This energy cascade driven by vortex stretching leads to viscous dissipation of energy by the smallest eddies [77]. Many different length scales have been defined in turbulent flows. The Kolmogorov microscale is the smallest length scale in turbulent motion [78]. The time scale associated with this length scale, the Kolmogorov microscale of time, can be defined as a function of the kinematic viscosity, ν, and the energy dissipation rate per unit mass, ϵ, as [77]:

$$\tau_k \equiv \left(\frac{\nu}{\epsilon}\right)^{1/2} \tag{5.1}$$

The rate of energy dissipation by the small eddies is proportional to the rate of energy supplied to them by the large eddies, and is of the order of u^3/ℓ, i.e.,

$$\epsilon \sim \frac{u^3}{\ell} \tag{5.2}$$

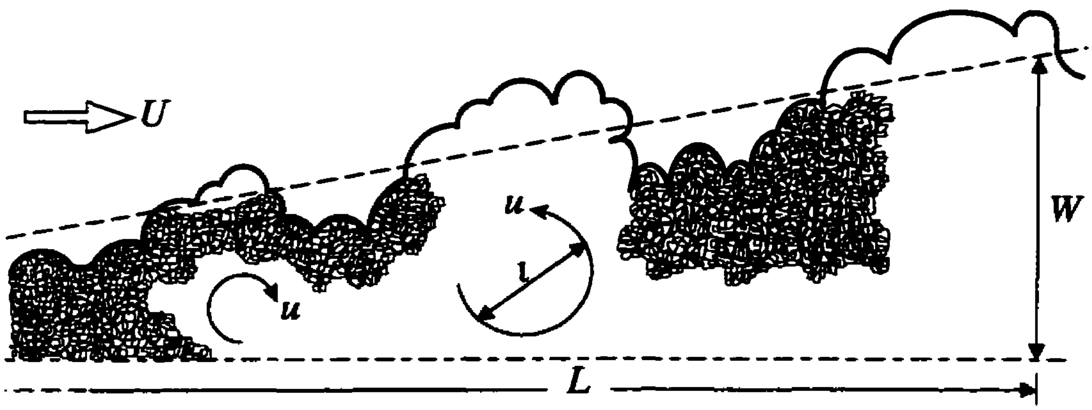

Figure 5.1: Length and velocity scales of large eddies in a turbulent flow [77].

where u and ℓ are characteristic velocity and size of turbulent large eddies, respectively (Figure 5.1). Then, the Kolmogorov microscale of time for turbulent flows can be proportional to:

$$\tau_k \sim \left(\frac{\ell \cdot \nu}{u^3}\right)^{1/2} \tag{5.3}$$

It was reported that the turbulent fine structures (small eddies) are of fundamental importance for the molecular mixing processes and flame propagation [79,80] and fine structures are concentrated in small regions (a small volume fraction of the total volume of flow) [81]. The measurement of chemiluminescence showed that the smallest highly luminous objects inside the combustion region have a size of about 1.5 mm which corresponds approximately to the Kolmogorov microscale in the region [82]. Microscopic structures in coaxial turbulent non-premixed flames were also studied in [83] and this study showed that although the surrounding air was entrained into the jet fuel by large eddy motions, combustion of fuel and air took place in a region consisting of microscopic structures.

Based on the above discussion, it can be assumed that the mixing time scale in a turbulent non-premixed flame is proportional to the Kolmogorov microscale of time,

$$\tau_m \sim \tau_k \sim \left(\frac{\ell \cdot \nu}{u^3}\right)^{1/2} \tag{5.4}$$

The large eddies size, ℓ, is comparable to the width of the flow in a direction normal to the flow field [77] (Figure 5.1). For a turbulent jet flow, the jet velocity-half radius, δ_u, at which $u - u_\infty = 1/2(u_m - u_\infty)$ does also represent the width of the jet at any distance downstream of the jet exit. Therefore δ_u can be proportional to ℓ:

$$\delta_u \sim \ell \tag{5.5}$$

Also the velocity of large eddies can be proportional to the local maximum axial velocity on the jet axis, u_m:

$$u \sim u_m \tag{5.6}$$

The local maximum axial velocity at the jet axis, u_m, and the jet velocity-half radius, δ_u, are shown in Figure 5.2. Then, from equation (5.4) the mixing time:

$$\tau_m \sim \left(\frac{\delta_u \cdot \nu}{u_m^3}\right)^{1/2} \tag{5.7}$$

Chemical Time. The characteristic chemical time (reaction time) is directly proportional to thermal diffusivity, α, and inversely proportional to

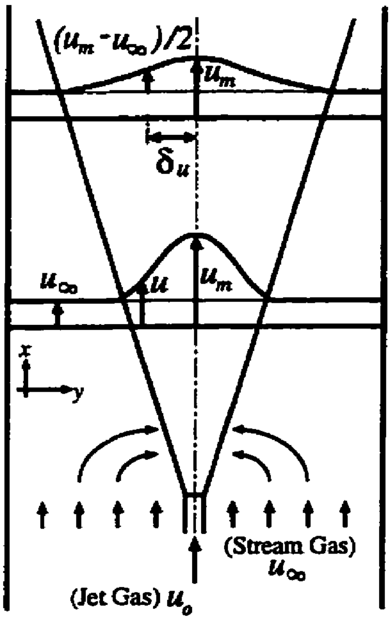

Figure 5.2: A schematic representation of a jet spreading into a moving stream of air.

the square of the laminar burning velocity, S_L^2 [76]; hence,

$$\tau_c \sim \frac{\alpha}{S_L^2} \tag{5.8}$$

Blowout Criterion. The ratio of mixing time to chemical time is generally accepted as a criterion for the blowout of jet non-premixed flames [2, 19, 43, 48, 52, 53, 56, 57, 84–87]. In the present study, a different expression for the mixing time was used to model the blowout limits of lifted flames. Using Equations (5.7) and (5.8), the above ratio can be written as:

$$\frac{\tau_m}{\tau_c} \sim \left(\frac{\delta_u \cdot \nu}{u_m^3}\right)^{1/2} \cdot \left(\frac{S_{L,St}^2}{\alpha}\right) \tag{5.9}$$

or

$$k_B^* = \left(\frac{\delta_u \cdot \nu}{u_m^3}\right)^{1/2} \cdot \left(\frac{S_{L,St}^2}{\alpha}\right) \tag{5.10}$$

Flame blowout occurs when this ratio, i.e. k_B^*, falls below a specific value called critical value $k_{B,Cr}^*$, i.e.,

$$k_B^* \leq k_{B,Cr}^* \tag{5.11}$$

This means that the mixing time becomes small enough for the mixtures of fuel, air and hot reaction products to cool rapidly with quenching of chemical reactions as a result. To examine whether at certain conditions flame blowout occurs, the value of k_B^* should be calculated at a location where the flame is stabilized before blowout and this value of k_B^* should be compared with critical value $k_{B,Cr}^*$, estimated from the experimental data. It is reasonable to assume that before blowout, the flame is stabilized at a location (blowout location) where the jet fuel concentration on the jet axis is close to its lean flammability limit (this is the last possible location for the lifted flame existence). The experimental observations reported in [88] for a hydrogen jet flame also showed that the concentration of jet fuel at the flame tip was close to its lean flammability limit. A procedure to calculate the blowout location and its corresponding blowout parameter for lifted jet flames is described in Section 5.2.

5.2 Calculation Procedure

As mentioned above the value of blowout parameter should be evaluated at the blowout location. The distance of this location from the nozzle, x, and the corresponding δ_u and u_m can be calculated from the following considerations.

Assuming a two dimensional jet (or uniform circumferential velocity and concentration values), the fuel mass flow rate balance at any axial location from the jet exit can be expressed by:

$$m_o = \int_0^{r_\infty} \rho \cdot u(r) \cdot c(r) \cdot 2\pi r dr \tag{5.12}$$

where r_∞ is the radius of the confined co-flowing oxidizing stream; $u(r)$ is the velocity at radius r; $c(r)$ is the mass fraction of jet fluid at radius r; ρ is the density; and m_o is the fuel mass flow rate at the jet exit,

$$m_o = \pi {r_o}^2 \rho_o u_o \tag{5.13}$$

where r_o is the nozzle radius; and ρ_o and u_o are the jet density and the velocity at the nozzle exit, respectively. Velocity profile $u(r)$ and mass fraction profile $c(r)$ for a non-isothermal confined jet can be calculated using correlations obtained experimentally by Steward and Guruz [72] for flow conditions close to those in this study,

$$\frac{u - u_\infty}{u_m - u_\infty} = \exp\left[-0.693\left(\frac{r}{\delta_u}\right)^{1.82}\right] \tag{5.14}$$

and

$$\frac{c - c_\infty}{c_m - c_\infty} = \exp\left[-0.693\left(\frac{r}{\delta_c}\right)^{1.82}\right] \tag{5.15}$$

where u_m and c_m are the jet velocity and mass concentration at the jet centerline, respectively; subscript ∞ stands for the co-flowing surrounding stream; δ_u is the jet velocity-half radius; δ_c is the jet concentration-half radius at which $c - c_\infty = 1/2(c_m - c_\infty)$ and δ_c is related to δ_u by $\delta_u/\delta_c = 0.825$.

Substituting m_o, $u(r)$ and $c(r)$ from Equations (5.13)-(5.15) into Equation (5.12) and assuming that the jet density at the jet far-field is close to the density of the surrounding stream ($\rho \simeq \rho_\infty$) results in:

$$r_o{}^2 \rho_o u_o = 2\rho_\infty \int_0^{r_\infty} \left[(u_m - u_\infty)e^{-0.693(r/\delta_u)^{1.82}} + u_\infty\right] \left[c_m \cdot e^{-0.693(0.825r/\delta_u)^{1.82}}\right] \cdot r dr \tag{5.16}$$

Rearranging Equation (5.16) yields:

$$\frac{r_o{}^2 \rho_o u_o}{2\rho_\infty c_m} = (u_m - u_\infty) \left[\int_0^{r_\infty} e^{-1.81(r/\delta_u)^{1.82}} r dr + \frac{u_\infty}{u_m - u_\infty} \int_0^{r_\infty} e^{-0.488(r/\delta_u)^{1.82}} r dr\right] \tag{5.17}$$

By introducing $\eta = r/\delta_u$, Equation (5.17) can be rewritten as:

$$\frac{r_o{}^2 \rho_o u_o}{2\rho_\infty c_m} = \delta_u^2 \cdot (u_m - u_\infty) \left[I_1 + I_2 \frac{u_\infty}{u_m - u_\infty}\right] \tag{5.18}$$

where

$$I_1 = \int_0^{r_\infty/\delta_u} e^{-1.181\, \eta^{1.82}} \cdot \eta d\eta = 0.44 \tag{5.19}$$

and

$$I_2 = \int_0^{r_\infty/\delta_u} e^{-0.488\, \eta^{1.82}} \cdot \eta d\eta = 1.15 \tag{5.20}$$

The above integrals were calculated numerically (see Appendix A). Therefore Equation (5.18) can be written as:

$$\frac{r_o{}^2 \rho_o u_o}{2\rho_\infty c_m} = \delta_u^2 \cdot (u_m - u_\infty) \left[0.44 + 1.15 \frac{u_\infty}{u_m - u_\infty}\right] \tag{5.21}$$

The terms $(u_m - u_\infty)$ and δ_u can be expressed from the following experimental correlations [72, 89]:

$$\delta_u = 0.084X \cdot r_\infty \left[1 + \left(\frac{X}{X_r}\right)^{5/3}\right] \tag{5.22}$$

and

$$u_m - u_\infty = \frac{u_k}{0.0725X \cdot Ct \left[1 + \left(\frac{X}{X_u}\right)^{5/3}\right]} \tag{5.23}$$

where

$$X = \frac{x}{r_\infty} \tag{5.24}$$

$$X_r = 4.07 \exp(3.54Ct) \tag{5.25}$$

$$X_u = 5.95 \exp(3.54Ct) \tag{5.26}$$

$$Ct = \frac{u_k}{\left(u_d^2 - \frac{1}{2}u_k^2\right)^{1/2}} \tag{5.27}$$

$$u_k = \frac{m_o + m_\infty}{\pi r_\infty^2 \rho_{ave}} \tag{5.28}$$

$$u_d^2 = \frac{m_o u_o + \frac{1}{2}m_\infty u_\infty}{\pi r_\infty^2 \rho_{ave}} \tag{5.29}$$

$$\rho_{ave} = \frac{m_o + m_\infty}{Q_o + Q_\infty} \tag{5.30}$$

where $m_\infty = \pi(r_\infty^2 - r_o^2)\rho_\infty u_\infty$; Q_o and Q_∞ are the volumetric flow rate of the jet and co-flowing surrounding stream, respectively. Substituting δ_u and $(u_m - u_\infty)$ from Equations (5.22) and (5.23) into Equation (5.21) results in:

$$\frac{{r_o}^2\rho_o u_o}{2\rho_\infty c_m} = 0.084^2 X^2 \cdot {r_\infty}^2 \left[1+\left(\frac{X}{X_r}\right)^{5/3}\right]^2 \cdot \left[\frac{u_k}{0.0725X\cdot Ct\left[1+\left(\frac{X}{X_u}\right)^{5/3}\right]}\right] \cdot$$
$$\left[0.44+1.15\times 0.0725X\cdot Ct\cdot\left(\frac{u_\infty}{u_k}\right)\left[1+\left(\frac{X}{X_u}\right)^{5/3}\right]\right] \tag{5.31}$$

Simplifying equation (5.31) leads to:

$$\frac{r_o^2\rho_o u_o}{2r_\infty^2\rho_\infty u_\infty c_m} = 0.043X^2\left[1+\left(\frac{X}{X_r}\right)^{5/3}\right]^2 \cdot$$
$$\left[\frac{u_k}{X\cdot Ct\cdot u_\infty\left[1+\left(\frac{X}{X_u}\right)^{5/3}\right]}+0.19\right] \tag{5.32}$$

For given velocities of jet, u_o, and co-flowing stream, u_∞, Equation (5.32) can be used to calculate the normalized distance from the jet exit, X, where the mass fraction of jet fuel at the jet axis, c_m is equal to the lean flammability limit of jet fuel in air. The mass fraction of the jet fuel on the jet centerline can be expressed as:

$$c_m = \frac{L_F\cdot M_o}{L_F\cdot M_o+(100-L_F)M_\infty} \tag{5.33}$$

where L_F is the lean flammability limit of the fuel in air (% by volume). M_o and M_∞ are the molecular weights of the jet fuel and surrounding air stream, respectively.

At the present time, there is no method available to estimate the critical value of parameter $k^*_{B,Cr}$ from a purely theoretical approach. However, this value can be estimated on the basis of known experimental blowout limits. For a known $k^*_{B,Cr}$, the jet blowout velocity, u_o, for different co-flowing stream velocities, u_∞, can be calculated using the following procedure. Equations (5.10) and (5.32), with two unknown variables u_o and X can be solved by trial and error as follows. By assuming a value for u_o, the remaining unknown, X (nondimensional blowout location), can be calculated. Then the values of δ_u and u_m corresponding to this position can be calculated using Equations (5.22) and (5.23), respectively. These values are then substituted into the right hand side of Equation (5.10). If the RHS of this equation is equal to $k^*_{B,Cr}$, the assumed value of u_o is the actual jet blowout velocity under these conditions. Otherwise, a new value for u_o is assumed and another iteration performed.

To estimate critical parameter $k^*_{B,Cr}$, typical $u_o = f(u_\infty)$ curves are calculated for different values of k^*_B parameter. These curves for a methane jet flame of 2 mm diameter and its corresponding experimental data are shown in Figure 5.3. By comparing the calculated blowout curves versus the experimental data, it can be seen that blowout limits correspond nearly to a constant value of k^*_B parameter. This value represented by $k^*_{B,Cr}$ is approximately equal to 0.24. Similar curves obtained for a 2 mm and 2.5 mm methane jet discharged into a slightly different combustor size are shown in Figures 5.4 and 5.5, respectively. The experimental data reported in [25] are also shown in these figures. As can be seen, the blowout is expected at $k^*_{B,Cr}$ parameter approximately equal to 0.24 and 0.18, respectively. Therefore, the blowout parameter, k^*_B, given by Equation (5.10), was modified to ac-

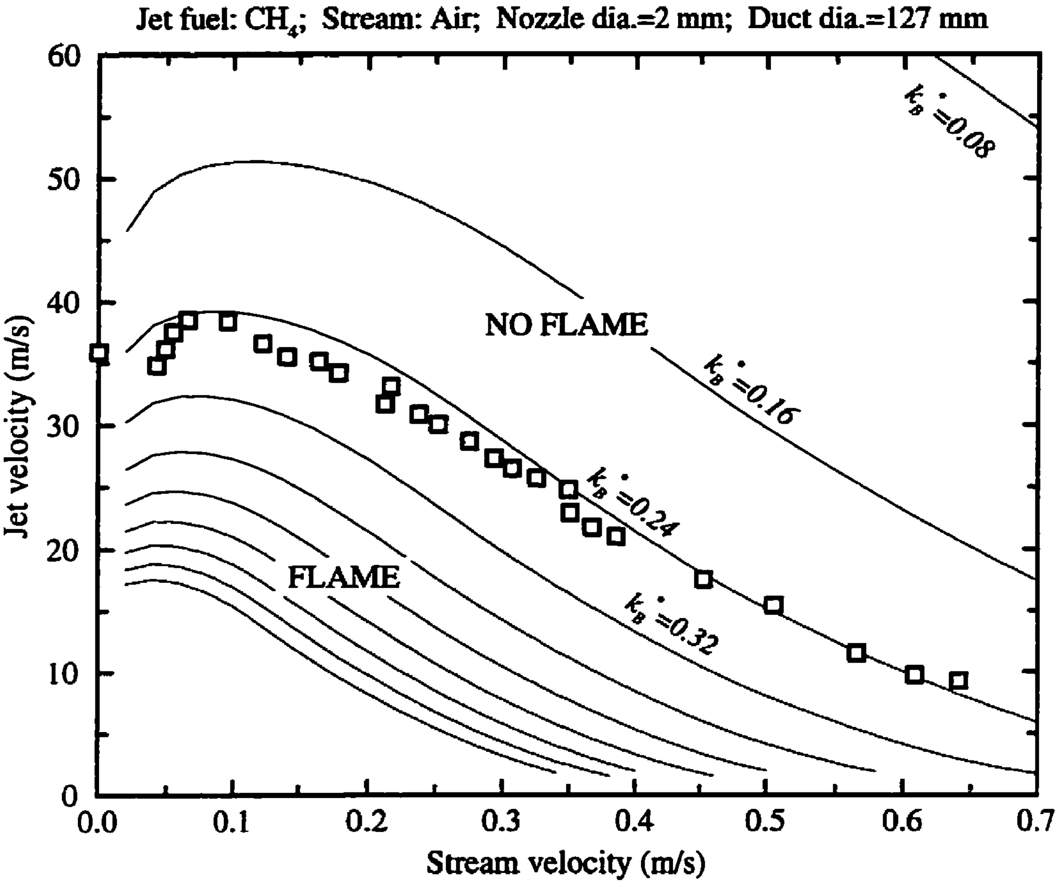

Figure 5.3: Calculated jet velocity as a function of co-flowing stream velocity for different values of blowout parameter k_B^*. Experimental data: □ - present study.

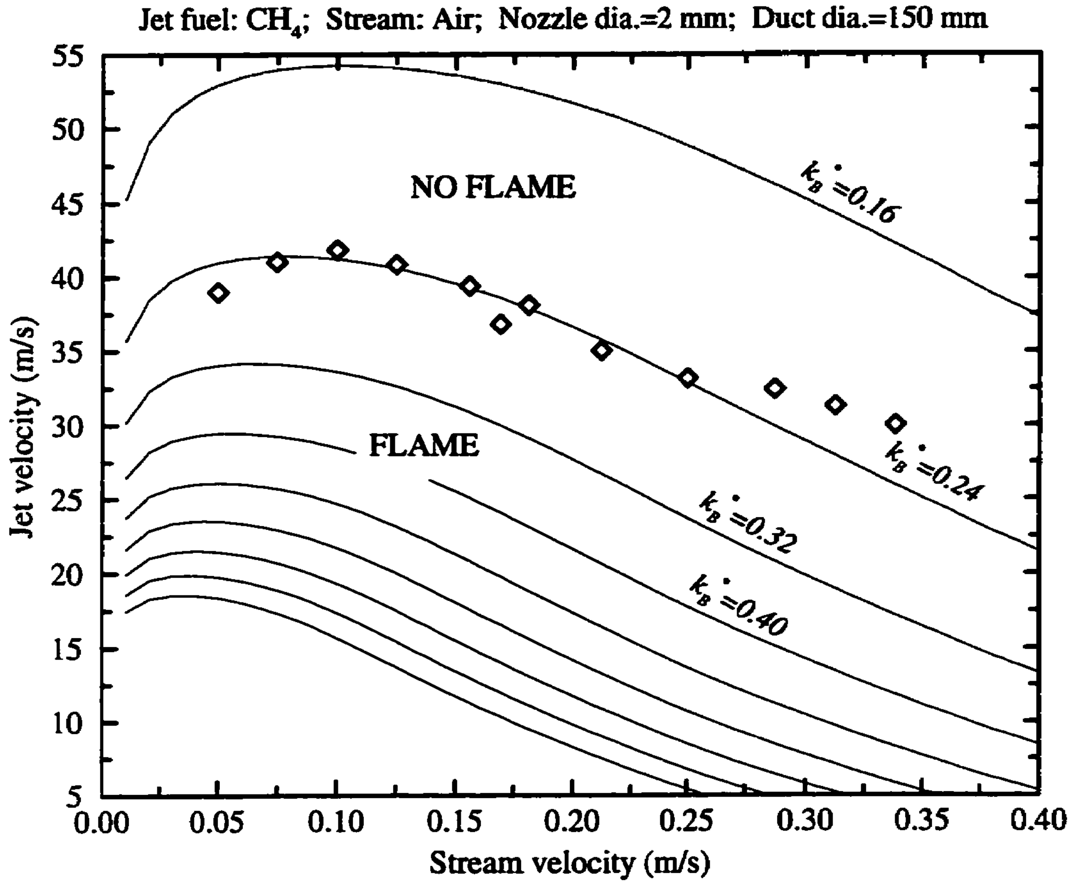

Figure 5.4: Calculated jet velocity as a function of co-flowing stream velocity for different values of blowout parameter k_B^*. Experimental data: ◇ [25].

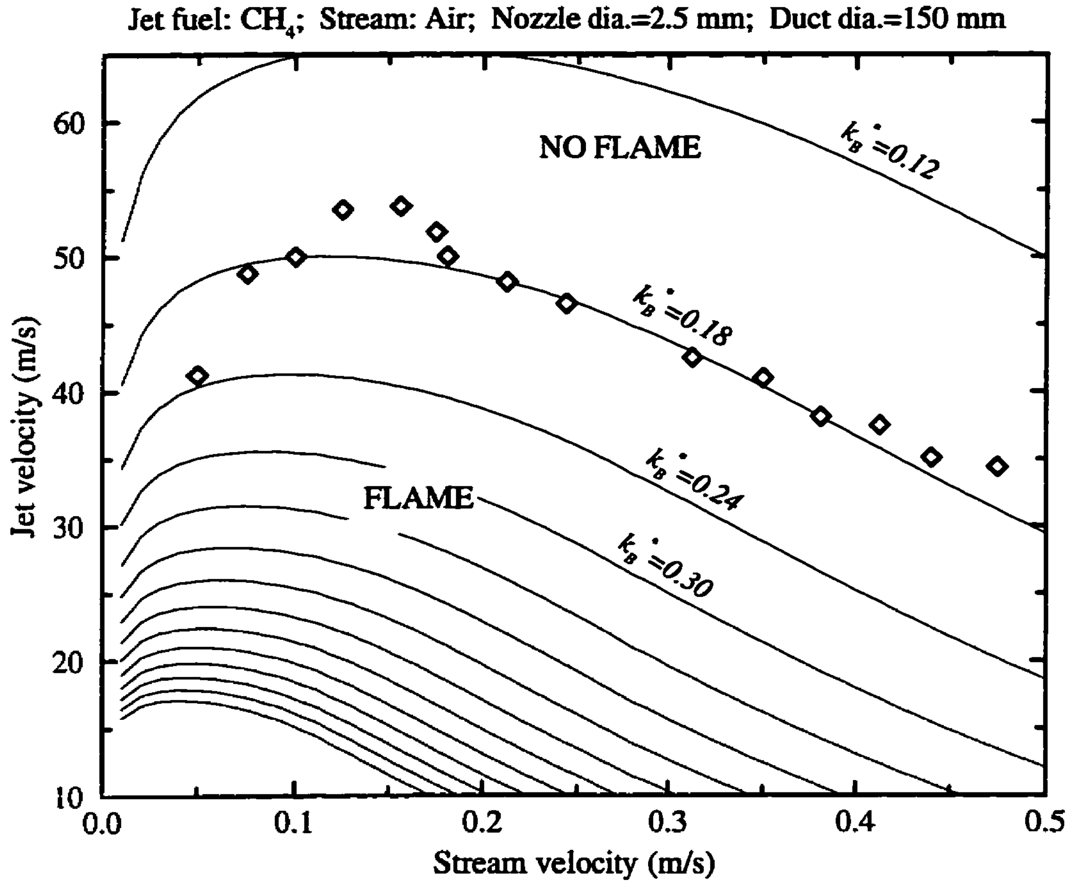

Figure 5.5: Calculated jet velocity as a function of co-flowing stream velocity for different values of blowout parameter k_B^*. Experimental data: ◇ [25].

count for the effect of nozzle radius as:

$$k_B = \left(\frac{\delta_u \cdot \nu}{u_m^3}\right)^{1/2} \cdot \left(\frac{S_{L,St}^2}{\alpha}\right) \cdot \left(\frac{r_o}{r_{ref}}\right) \tag{5.34}$$

where r_{ref} represents a radius equal to 1 mm. It can be seen that the same critical value of this modified blowout parameter ($k_B \simeq 0.24$) provides a good agreement between calculated and experimental data (Figures 5.13 and 5.14).

The flowchart of the procedure used to calculate the blowout limits of lifted jet flames in a co-flowing stream is shown in Figure 5.6. The corresponding simulation program is given in Appendix A. To clarify the details of this procedure, a numerical example is also given in Appendix B.

5.2.1 Fuel Mixtures

Addition of a second fuel to jet fuel (e.g. hydrogen to methane jet) affects the values of ρ_o, c_m and $S_{L,St}$.

Jet Density. The density of the jet fluid can be calculated as:

$$\rho_o = Y_{F_1} \cdot \rho_{F_1} + (1 - Y_{F_1}) \cdot \rho_{F_2} \tag{5.35}$$

where ρ_{F_1} and ρ_{F_2} are the density of the first and the second jet fuels, respectively; Y_{F_1} is the mole fraction of the first fuel in the jet fuel mixture.

Mass Fraction. The mass fraction of the jet fluid on the jet centerline, c_m, can be expressed in terms of lean flammability limit of the jet fuel mixture in air, $L_{F_1F_2}$, and molecular weights of the air stream, M_∞, and the jet fluid, M_o, as:

$$c_m = \frac{L_{F_1F_2} \cdot M_o}{L_{F_1F_2} \cdot M_o + (100 - L_{F_1F_2}) \cdot M_\infty} \tag{5.36}$$

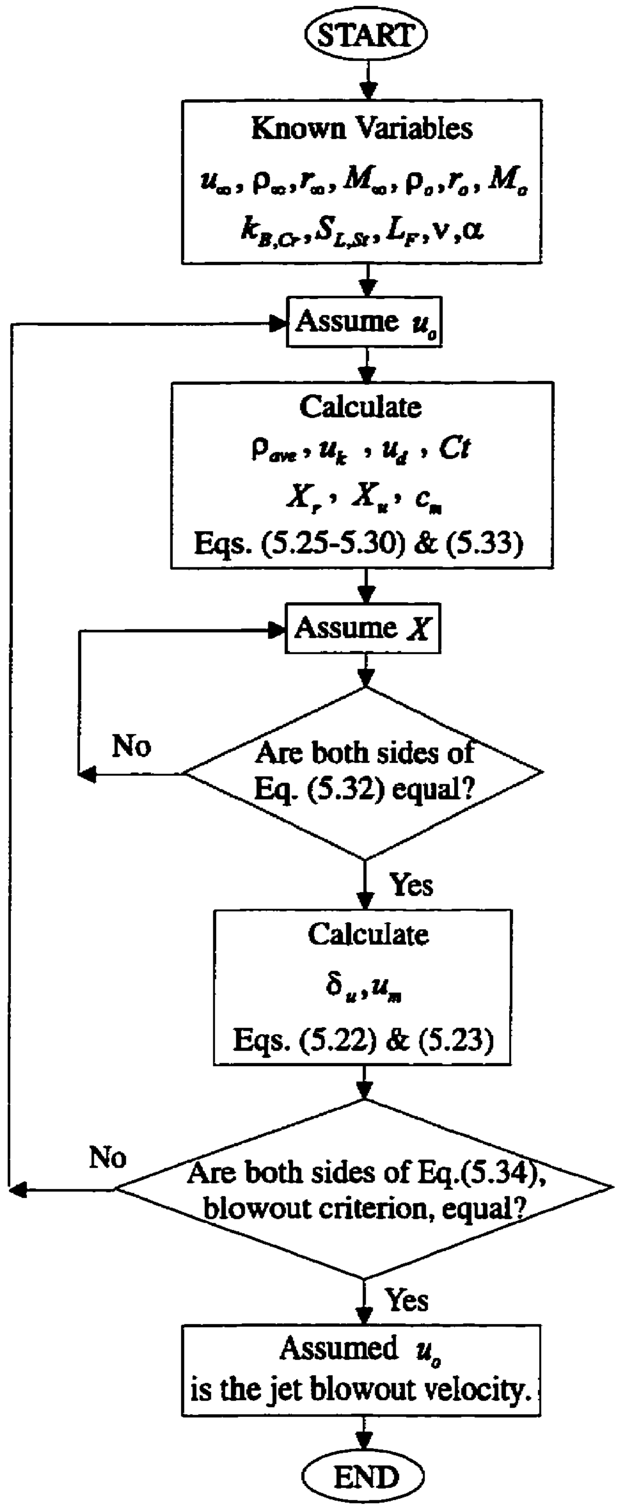

Figure 5.6: The flowchart of the procedure to calculate the blowout limits of lifted jet flames.

where $M_o = Y_{F_1} \cdot M_{F_1} + (1 - Y_{F_1}) \cdot M_{F_2}$, and the flammability limits of fuel mixtures can be calculated using the Le Chatelier mixing rule:

$$\frac{1}{L_{F_1F_2}} = \frac{Y_{F_1}}{L_{F_1}} + \frac{(1 - Y_{F_1})}{L_{F_2}} \tag{5.37}$$

where L_{F_1} and L_{F_2} are the lean flammability limits of the first fuel in air and the second fuel in air (% by volume), respectively.

Laminar Burning Velocity. Laminar burning velocities, $(S_{L,St})_{mix}$, for some fuel mixtures in air are available in the literature. Whenever data was not available for any particular fuel mixture, the burning velocity was estimated using a simple mixing rule expressed as:

$$(S_{L,St})_{mix} = Y_{F_1} \cdot (S_{L,St})_{F_1} + (1 - Y_{F_1}) \cdot (S_{L,St})_{F_2} \tag{5.38}$$

5.2.2 Fuel in the Surrounding stream

Addition of an auxiliary fuel in the surrounding stream of air will affect the values of ρ_∞, c_m and $S_{L,St}$.

Surrounding Stream Density. The density of a surrounding oxidizing stream can be calculated as:

$$\rho_\infty = Y_{F_SA} \cdot \rho_{F_S} + (1 - Y_{F_SA}) \cdot \rho_A \tag{5.39}$$

where ρ_{F_S} and ρ_A are the density of auxiliary fuel (surrounding fuel) and air, respectively; and Y_{F_SA} is the mole fraction of the surrounding fuel in the surrounding fuel-air mixture.

Mass Fraction. At the blowout location or at any distance from the jet exit, the total fluid mixture consists of jet fuel, surrounding fuel and air, i.e.,

$$Y_{F_JT} + Y_{F_ST} + Y_{AT} = 1 \tag{5.40}$$

where Y_{F_JT}, Y_{F_ST} and Y_{AT}, are the mole fraction of the jet fuel, surrounding fuel and air in the total mixture. Also at this position, the sum of concentrations of both fuels represents the lean flammability limit of the fuel mixture in air, i.e.

$$L_{F_JF_S} = 100(Y_{F_JT} + Y_{F_ST}) \tag{5.41}$$

Using Le Chatelier mixing rule, the lean flammability limits of fuel mixtures in air can be calculated as:

$$\frac{1}{L_{F_JF_S}} = \left(\frac{Y_{F_JT}}{Y_{F_JT} + Y_{F_ST}}\right) \cdot \left(\frac{1}{L_{F_J}}\right) + \left(\frac{Y_{F_ST}}{Y_{F_JT} + Y_{F_ST}}\right) \cdot \left(\frac{1}{L_{F_S}}\right) \tag{5.42}$$

where L_{F_J} and L_{F_S} are the lean flammability limits of the jet fuel and the surrounding fuel on their own in air (% by volume), respectively. Also from (5.40) and $Y_{F_SA} = Y_{F_ST}/(Y_{F_ST} + Y_{AT})$:

$$Y_{F_ST} = Y_{F_SA}(1 - Y_{F_JT}) \tag{5.43}$$

Substituting $L_{F_JF_S}$ and Y_{F_ST} from Equations (5.41) and (5.43) into Equation (5.42) results in:

$$\frac{1}{100(Y_{F_JT} + Y_{F_ST})} = \left(\frac{Y_{F_JT}}{Y_{F_JT} + Y_{F_ST}}\right) \cdot \left(\frac{1}{L_{F_J}}\right) + \left(\frac{Y_{F_SA}(1 - Y_{F_JT})}{Y_{F_JT} + Y_{F_ST}}\right) \cdot \left(\frac{1}{L_{F_S}}\right) \tag{5.44}$$

or

$$Y_{F_JT} = \frac{L_{F_J}(L_{F_S} - 100Y_{F_SA})}{100(L_{F_S} - L_{F_J} \cdot Y_{F_SA})} \tag{5.45}$$

Y_{F_JT} can be considered to be the jet fuel lean flammability limit in the mixture of air and auxiliary fuel. The corresponding mass fraction of the jet fuel is:

$$c_m = \frac{Y_{F_JT} \cdot M_o}{Y_{F_JT} \cdot M_o + (1 - Y_{F_JT}) \cdot M_\infty} \tag{5.46}$$

where $M_\infty = Y_{F_SA} \cdot M_{F_S} + (1 - Y_{F_SA}) \cdot M_A$.

Laminar Burning Velocity. The laminar burning velocities of fuel mixtures in air are usually reported as functions of the mole fraction of each fuel in the fuel mixture. To utilize these data and to find the effect of presence of an auxiliary fuel in a co-flowing air stream on the laminar burning velocity, the mole fraction of the auxiliary fuel in the fuel mixture (jet fuel - surrounding fuel mixture), Y_{F_SF}, should be expressed in terms of the mole fraction of the surrounding fuel in air, Y_{F_SA}, i.e,

$$Y_{F_SF} = \frac{Y_{F_SA} \cdot (A/F)_{St,J}}{Y_{F_SA}\left[(A/F)_{St,J} - (A/F)_{St,S} - 1\right] + 1} \tag{5.47}$$

where $(A/F)_{St,J}$ is the stoichiometric molar air to jet fuel ratio and $(A/F)_{St,S}$ is the stoichiometric molar air to surrounding fuel ratio (e.g. for methane $(A/F)_{St,J} = 9.524$). For derivation of Equation (5.47) see Appendix C.

The laminar burning velocities, $(S_{L,St})_{mix}$, for some fuel mixtures in air are available in the literature. When the data was not available, the burning velocities of fuel mixtures were estimated using a simple mixing rule as:

$$(S_{L,St})_{mix} = Y_{F_SF} \cdot (S_{L,St})_{F_S} + (1 - Y_{F_SF}) \cdot (S_{L,St})_{F_J} \tag{5.48}$$

where $(S_{L,St})_{F_S}$ and $(S_{L,St})_{F_J}$ are the stoichiometric laminar burning velocities of the surrounding fuel in air and that of the jet fuel in air, respectively.

5.2.3 Diluent in the Jet Fuel

The addition of a diluent to a jet fuel will affect the values of ρ_o, c_m and $S_{L,St}$.

Jet Density. The density of a jet fluid can be calculated using:

$$\rho_o = Y_{DF} \cdot \rho_D + (1 - Y_{DF}) \cdot \rho_F \tag{5.49}$$

where ρ_D and ρ_F are the densities of the diluent and fuel, respectively; Y_{DF} is the mole fraction of the diluent in the fuel-diluent mixture.

Mass Fraction. The centerline mass fraction of the jet fuel-diluent mixture at the blowout location, c_m, can be expressed in terms of the lean flammability limit of the jet fluid in air, L_{DF}, molecular weights of air stream, M_∞, and the jet fluid, M_o, as:

$$c_m = \frac{L_{DF} \cdot M_o}{L_{DF} \cdot M_o + (100 - L_{DF}) \cdot M_\infty} \tag{5.50}$$

where $M_o = Y_{DF} \cdot M_D + (1 - Y_{DF}) \cdot M_F$, and the flammability limit of fuel-diluent mixture can be calculated using the following formula proposed by Wierzba et al., [90]:

$$\frac{1}{L_{DF}} = \frac{1 - Y_{DF}}{L_F} + Y_{DF} \cdot a_L \tag{5.51}$$

In the above equation, L_F is the lean flammability limit of the fuel on its own in air (%by volume); and a_L is a constant that depends on the types of fuel and diluent involved. For example, for methane-diluent mixture, this constant, a_L, is equal to zero for nitrogen, 0.00033 for helium and -0.01 for carbon dioxide.

Laminar Burning Velocity. The values of laminar burning velocities (for stoichiometric mixtures) for different methane-diluent mixtures obtained from different sources are plotted as a function of the diluent concentration (in the fuel mixture) in Figures 5.7 and 5.8. It can be seen that the burning velocity decreases almost linearly with increasing diluent concentration, i.e.,

$$(S_{L,St})_{mix} = (S_{L,St})_F - H \cdot Y_{DF} \tag{5.52}$$

where $(S_{L,St})_{mix}$ is the laminar burning velocity of fuel-diluent mixture in air; $(S_{L,St})_F$ is the laminar burning velocity of fuel in air; and H is a constant. This relationship is applicable within the range of diluent concentration in the fuel-diluent mixture indicated in Figures 5.7 and 5.8, i.e., up to 60% for nitrogen, 30% for carbon dioxide and 45% for helium. However, the value of constant H derived from these experimental data varies noticeably (especially for nitrogen), as can be seen in Table 5.1.

5.2.4 Diluent in the Jet Fuel Mixture

In this case a jet fluid is a mixture of two different fuels and a diluent and the values of ρ_o, c_m and $S_{L,St}$ can be calculated as follows.

Jet Density. The density of jet fluid can be calculated as:

$$\rho_o = Y_{F_1T} \cdot \rho_{F_1} + Y_{F_2T} \cdot \rho_{F_2} + Y_{DT} \cdot \rho_D \tag{5.53}$$

Table 5.1: Values of constant H for methane-diluent mixtures.

Diluent	H	Reference
Nitrogen	0.35	Haniff et al., 1989 [91]
	0.25	Reed et al., 1971 [92]
	0.14	Fells and Rutherford, 1969 [93]
	0.44	Gerry and Walter, 1952 [94]
Carbon dioxide	0.48	Haniff et al., 1989 [91]
	0.44	Reed et al.,1971 [92]
	0.42	Fells and Rutherford, 1969 [93]
Helium	0.20	Gerry and Walter, 1952 [94]

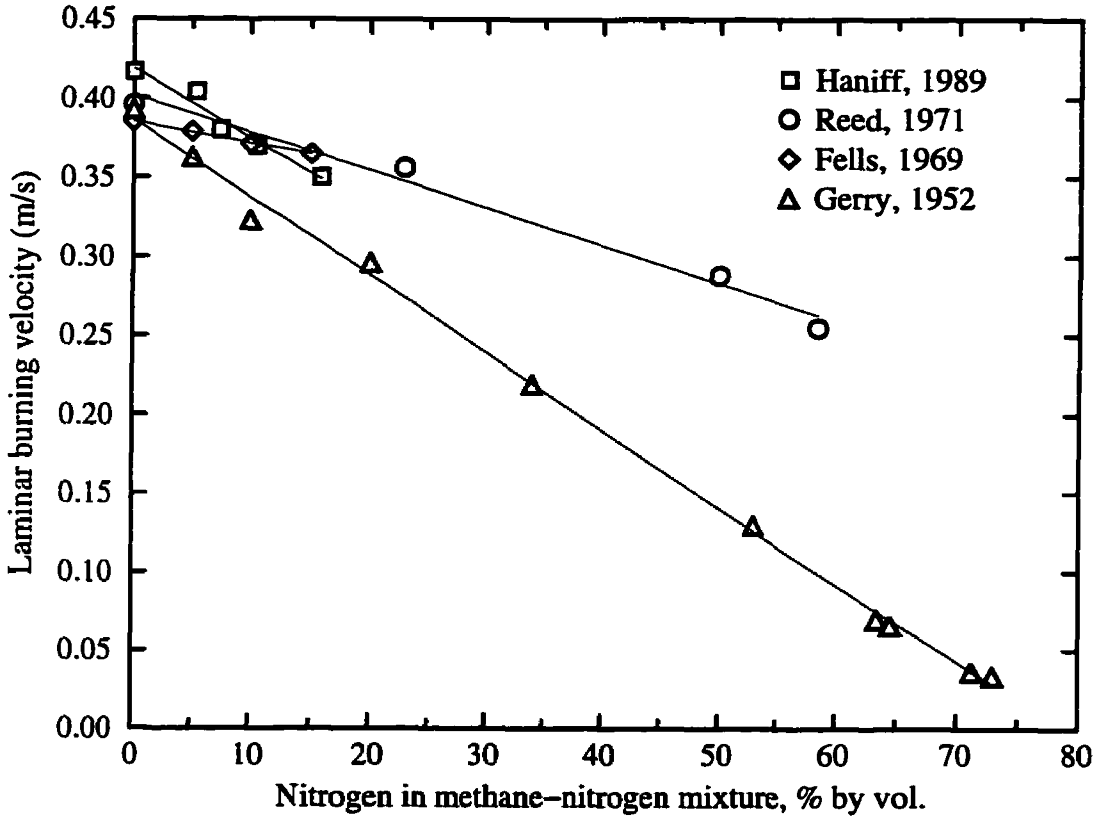

Figure 5.7: Stoichiometric laminar burning velocities of methane-nitrogen mixtures in air as a function of nitrogen concentration in a methane-nitrogen mixture. Data are from [91–94].

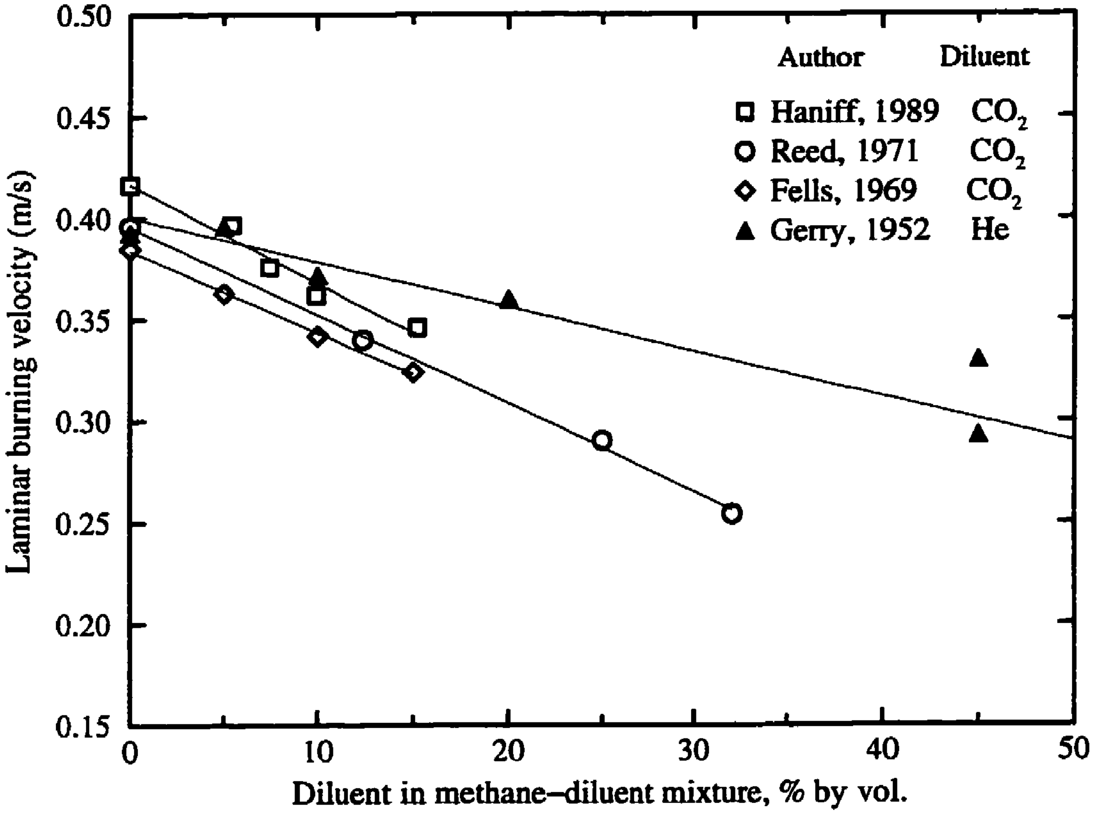

Figure 5.8: Stoichiometric laminar burning velocities of methane-diluent mixtures in air as a function of diluent concentration in a methane-diluent mixture. Data are from [91–94].

where Y_{F_1T}, Y_{F_2T} and Y_{DT} are the mole fractions of first fuel, second fuel and diluent in the total fuel mixture, respectively.

Mass Fraction. The mass fraction of the jet fluid on the jet centerline, c_m can be expressed as:

$$c_m = \frac{L_{F_1F_2D} \cdot M_o}{L_{F_1F_2D} \cdot M_o + (100 - L_{F_1F_2D}) \cdot M_\infty} \tag{5.54}$$

where $L_{F_1F_2D}$ is the lean flammability limit of the jet fluid (mixture of the first fuel, the second fuel and diluent) in air, M_∞ is the molecular weight of air stream and M_o is the molecular weight of jet fluid, i.e., $M_o = Y_{F_1T} \cdot M_{F_1} + Y_{F_2T} \cdot M_{F_2} + Y_{DT} \cdot M_D$.

The lean flammability limit, $L_{F_1F_2D}$, can be calculated as follows:

1. The first fuel and the diluent can be combined to form a fuel-diluent mixture. The lean flammability limit of this mixture, L_{F_1D}, can be calculated using,

$$\frac{1}{L_{F_1D}} = \frac{1 - Y_{DF_1}}{L_{F_1}} + Y_{DF_1} \cdot a_L \tag{5.55}$$

   where L_{F_1} is the lean flammability limit of the first fuel on its own in air (%by volume); and $Y_{DF_1} = Y_{DT}/(Y_{F_1T} + Y_{DT})$.

2. The above mixture (mixture of the first fuel and diluent) and the second fuel can be combined to form a mixture with lean flammability of $L_{F_1F_2D}$ which can be calculated using:

$$\frac{1}{L_{F_1F_2D}} = \frac{(1 - Y_{F_2T})}{L_{F_1D}} + \frac{Y_{F_2T}}{L_{F_2}} \tag{5.56}$$

where L_{F_2} is the lean flammability limit of the second fuel on its own in air (%by volume).

Laminar Burning Velocity. The laminar burning velocities for some of such mixtures are available in the literature.

5.2.5 Diluent in the Surrounding stream

An addition of a diluent to a co-flowing stream of air affects the values of ρ_∞, c_m and $S_{L,St}$.

Surrounding Stream Density. The density of surrounding oxidizing stream can be calculated using expression,

$$\rho_\infty = Y_{DA} \cdot \rho_D + (1 - Y_{DA}) \cdot \rho_A \tag{5.57}$$

where Y_{DA} is the mole fraction of diluent in the diluent-air mixture.

Mass Fraction. The total mixture within the jet consists of jet fuel, diluent and air. Assuming that their mole fractions in the mixture are Y_{FT}, Y_{DT} and Y_{AT}, respectively:

$$Y_{FT} + Y_{DT} + Y_{AT} = 1 \tag{5.58}$$

Also at the blowout location, the sum of concentrations of the diluent and the fuel represents the lean flammability limit of the fuel-diluent mixture in air,

$$L_{DF} = 100(Y_{FT} + Y_{DT}) \tag{5.59}$$

The lean flammability limits of fuel-diluent mixtures in air can also be calculated using Equation (5.51):

$$\frac{1}{L_{DF}} = \left(\frac{Y_{FT}}{Y_{FT}+Y_{DT}}\right) \cdot \frac{1}{L_F} + \left(\frac{Y_{DT}}{Y_{FT}+Y_{DT}}\right) \cdot a_L \qquad (5.60)$$

Substituting L_{DF} from Equations (5.59) into Equation (5.60) results in:

$$\frac{1}{100(Y_{FT}+Y_{DT})} = \left(\frac{Y_{FT}}{Y_{FT}+Y_{DT}}\right) \cdot \frac{1}{L_F} + \left(\frac{Y_{DT}}{Y_{FT}+Y_{DT}}\right) \cdot a_L \qquad (5.61)$$

Simplifying this equation yields:

$$\frac{1}{100} = \frac{Y_{FT}}{L_F} + Y_{DT} \cdot a_L \qquad (5.62)$$

The mole fraction of the diluent in the total mixture, Y_{DT}, can be expressed in terms of the mole fraction of the diluent in the diluent-air mixture, Y_{DA}, by using Equations (5.58) and $Y_{DA} = Y_{DT}/(Y_{DT} + Y_{AT})$, as:

$$Y_{DT} = Y_{DA}(1 - Y_{FT}) \qquad (5.63)$$

Substituting Y_{DT} from this equation into Equation (5.62) and some rearrangement result in:

$$Y_{FT} = \frac{L_F(1 - 100Y_{DA} \cdot a_L)}{100(1 - L_F \cdot Y_{DA} \cdot a_L)} \qquad (5.64)$$

The mole fraction of the jet fuel Y_{FT} can be considered as its lean flammability limit in a surrounding of air-diluent mixture. The mass fraction of the jet fuel corresponding to this concentration at the blowout location on the jet centerline can be evaluated from:

$$c_m = \frac{Y_{FT} \cdot M_o}{Y_{FT} \cdot M_o + (1 - Y_{FT}) \cdot M_\infty} \tag{5.65}$$

where $M_\infty = Y_{DA} \cdot M_D + (1 - Y_{DA}) \cdot M_A$.

Laminar Burning Velocity. Available experimental data in the literature on laminar burning velocities of fuel-diluent mixtures in air are reported as a function of the mole fraction of diluent in fuel-diluent mixture. The mole fraction of diluent in fuel-diluent mixture can be determined from the following considerations. In the total fuel-air-diluent mixture, fuel and diluent can be combined to form a so-called diluted fuel. The mole fraction of diluent in such fuel, Y_{DF}, can be expressed in terms of the mole fraction of diluent in air, Y_{DA}.

Using Equation (5.64), the stoichiometric mole fraction of a jet fuel in an ambient of air and diluent can be written as:

$$Y_{FT} = \frac{\left(\frac{100}{1 + (A/F)_{St,J}}\right) \cdot (1 - 100 Y_{DA} \cdot a_L)}{100 \left[1 - \left(\frac{100}{1 + (A/F)_{St,J}}\right) \cdot Y_{DA} \cdot a_L\right]} \tag{5.66}$$

where the term $100/(1 + (A/F)_{St,J})$ represents the stoichiometric concentration of jet fuel in air (% by volume). Using Equation (5.63), the concentration Y_{DF} can be expressed as:

$$Y_{DF} = \frac{Y_{DA} \cdot (1 - Y_{FT})}{Y_{DA} \cdot (1 - Y_{FT}) + Y_{FT}} \tag{5.67}$$

Substituting Y_{FT} from Equation (5.66) and simplifying this equation results in:

$$Y_{DF} = \frac{Y_{DA} \cdot (A/F)_{St,J}}{Y_{DA} \cdot (A/F)_{St,J} + (1 - 100Y_{DA} \cdot a_L)} \tag{5.68}$$

Therefore the laminar burning velocity of a jet fuel in a surrounding stream of air-diluent mixture can be calculated using Equations (5.52) and (5.68):

$$(S_{L,St})_{mix} = (S_{L,St})_F - H \cdot \left[\frac{Y_{DA} \cdot (A/F)_{St,J}}{Y_{DA} \cdot (A/F)_{St,J} + (1 - 100Y_{DA} \cdot a_L)}\right] \tag{5.69}$$

5.3 Results and Discussion

Using the described model and following the calculation procedure presented, calculations of jet blowout velocity of lifted flames were conducted for different co-flowing stream velocities, jet fluid and stream compositions as well as different combustor and nozzle sizes for various values of parameter k_B. The critical value of k_B is equal to 0.24 for all these cases.

The results of calculations for pure fuels and fuel mixtures in a stream of air are presented in Sections 5.3.1 and 5.3.2, respectively. The effect of an auxiliary fuel in air stream on blowout limits is investigated in Section 5.3.3. Addition of a second fuel to jet fuel and/or surrounding air stream is the subject of Section 5.3.4. The effect of diluent in either the jet fuel or the co-flowing stream is discussed in Section 5.3.5.

5.3.1 Pure Fuels

The combustion properties of the fuels used in the calculations are listed in Table 5.2 [74–76, 95]. The kinematic viscosity, ν, and the thermal diffusivity, α, were taken for pure air at 2000 K, since the properties of fuel-air mixture at the lean limit are approximately the same as those of air.

Table 5.2: Properties of gaseous fuels used in calculations of blowout limits of lifted flames.

Gaseous fuel	Stoich. laminar burning velocity $S_{L,St}$ (m/s)	Lean flammability limit L_F (% by vol.) [76]
CH_4	0.385	5
C_3H_8	0.45	2.1
C_2H_4	0.78	2.7
H_2	1.7	4

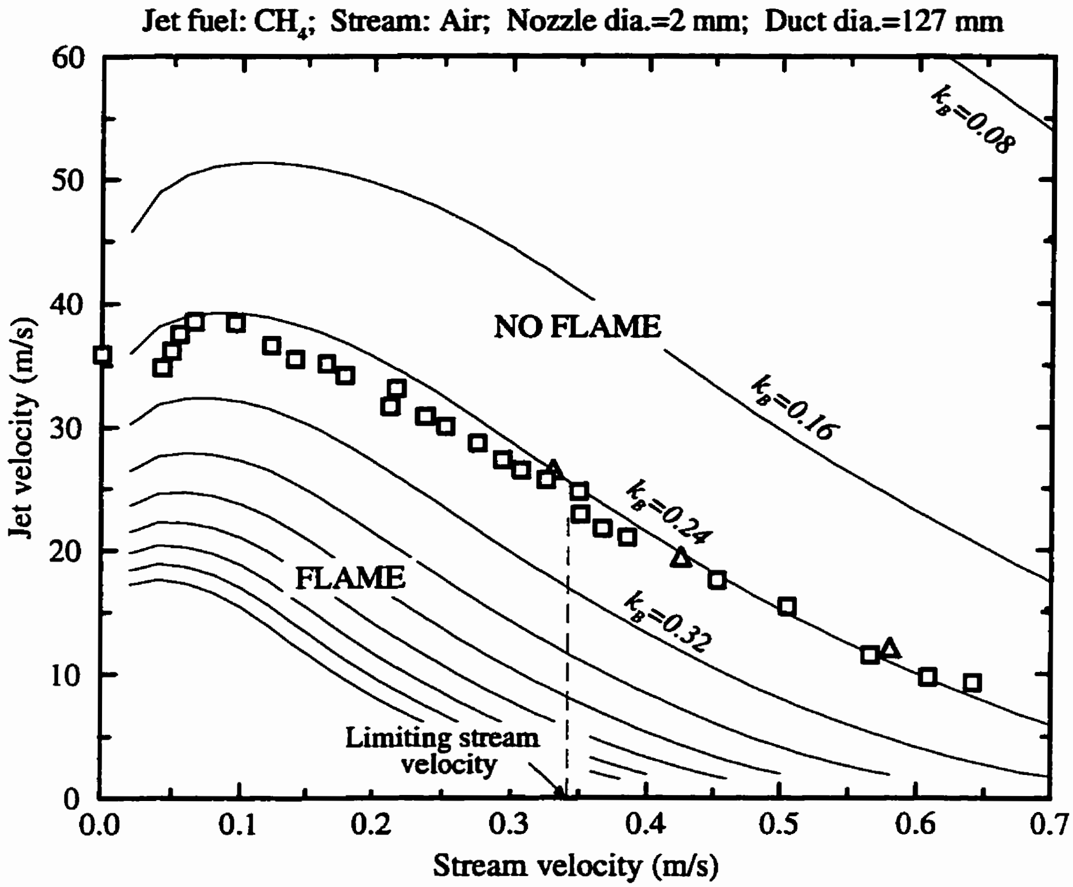

Figure 5.9: The calculated jet blowout velocity of a methane jet flame as a function of co-flowing air stream velocity for different values of the blowout parameter k_B. Experimental data: △ - [27], ◻ - the present study; — Calculated.

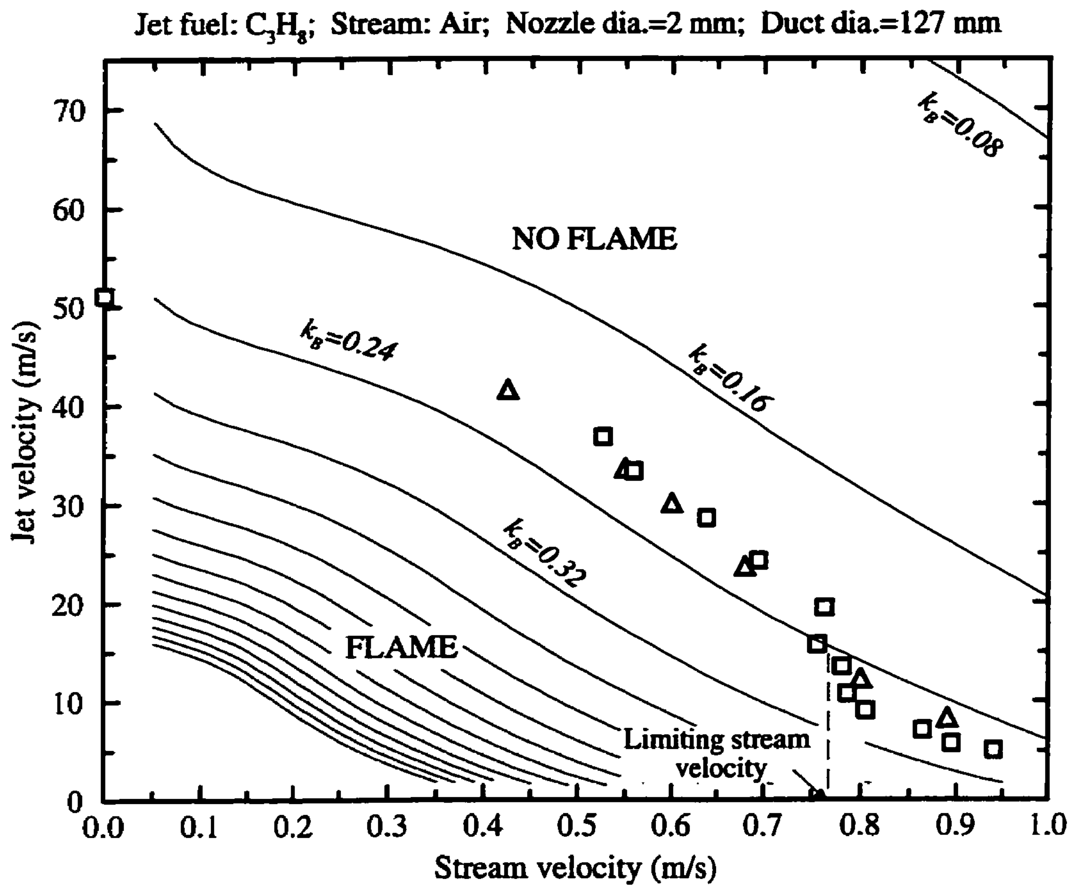

Figure 5.10: The calculated jet blowout velocity of a propane jet flame as a function of co-flowing air stream velocity for different values of the blowout parameter k_B. Experimental data: $\triangle$ - [27], $\square$ - the present study; — Calculated.

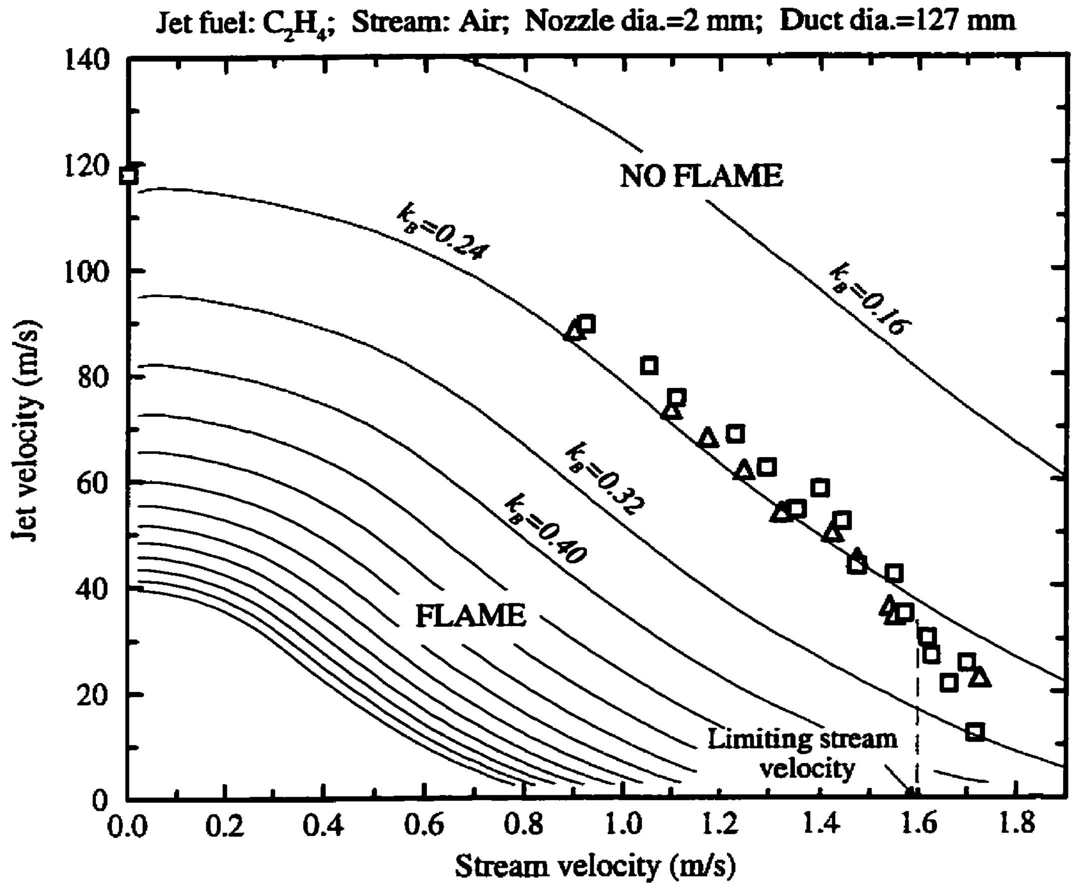

Figure 5.11: The calculated jet blowout velocity of an ethylene jet flame as a function of co-flowing air stream velocity for different values of the blowout parameter k_B. Experimental data: △ - [27], □ - the present study; — Calculated.

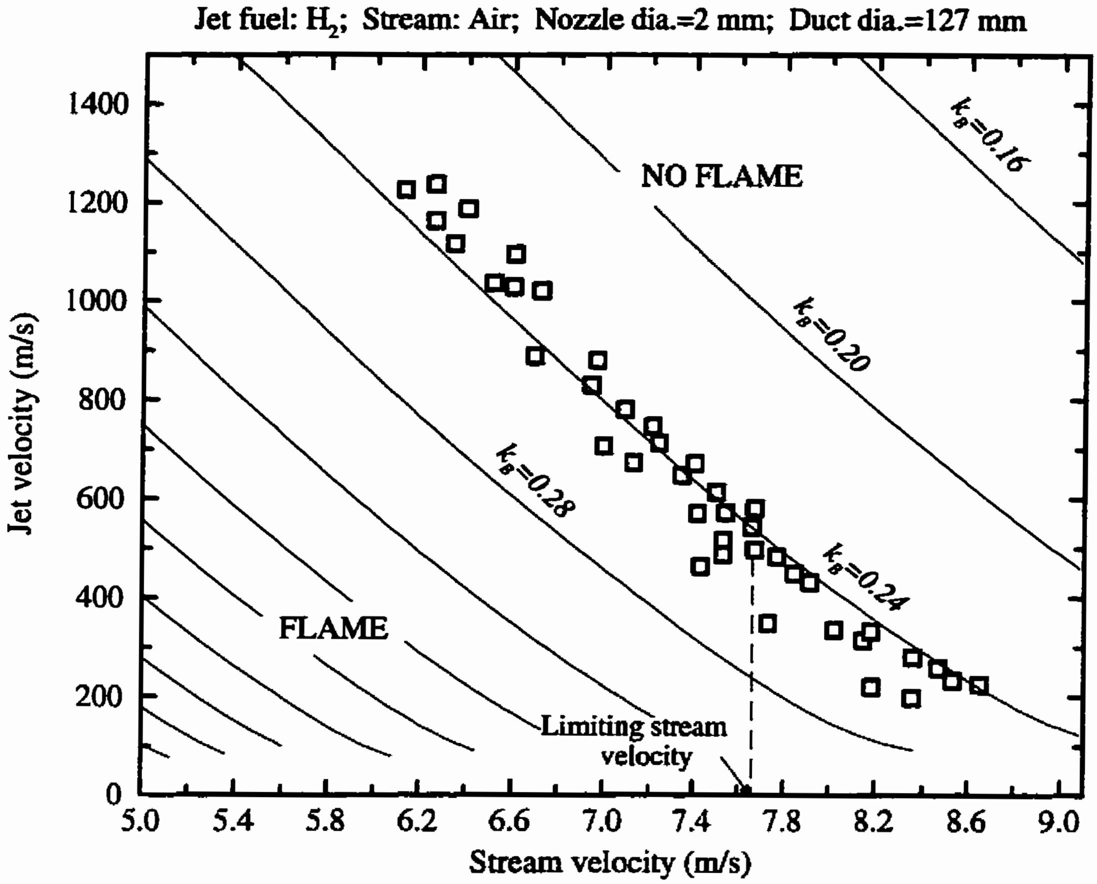

Figure 5.12: The calculated jet blowout velocity of hydrogen jet flame as a function of co-flowing air stream velocity for different values of the blowout parameter k_B. Experimental data: □ - the present study; — Calculated.

The results of calculations in the form of $u_o = f(u_\infty)$ curves are presented in Figures 5.9, 5.10, 5.11 and 5.12 for methane, propane, ethylene and hydrogen jet flames, respectively. In each case, a jet of 2 mm diameter issued into a combustor (duct) with hydraulic diameter of 127 mm. The corresponding experimental values obtained in the current research as well as the available data in the literature [27] are also shown in these figures. It can be seen that the experimental data are aligned with a curve of constant k_B. This supports the validity of the assumption stating that flame blowout is associated with a constant value of k_B parameter. The blowout of lifted flames occurs at an average value of $k_B \simeq 0.24$ for different experimental data measured by the author as well as those given in [27].

It appears that agreement between experimental and calculated data is good except for co-flowing stream velocities larger than the limiting co-flowing stream velocity (region II). This could be due to the limited range of applicability of the experimental correlations for jet velocity and concentration profiles used in the calculations of blowout limits. These correlations were obtained for a range of $0.22 < Ct < 1.2$ [72]. For co-flowing stream velocities larger than limiting stream velocity, the value of Ct is larger than 1.2 and this could result in an additional uncertainty in the value of blowout velocities. It should be noted that lifted flames in region II have no practical importance, since attached flames with higher blowout limits were preferred in this region. As a result, any discrepancy between the model predictions and the actual experimental data in this region can be overlooked.

The proposed model was also verified using some additional experimental data on blowout limits of jet flames in a co-flowing air stream available in the literature. For example, the blowout limits of methane lifted flames for

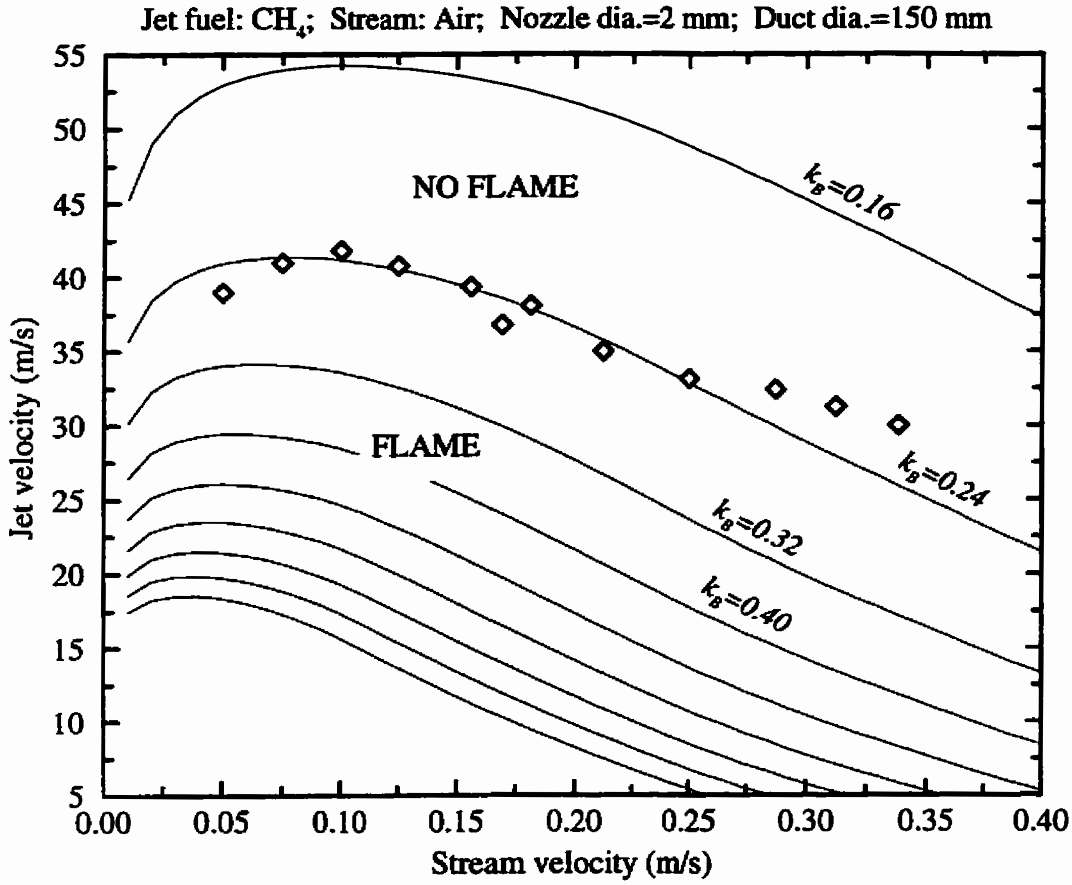

Figure 5.13: The calculated jet blowout velocity of a methane jet flame as a function of co-flowing air stream velocity for different values of the blowout parameter k_B. Experimental data: $\diamond$ - [25].

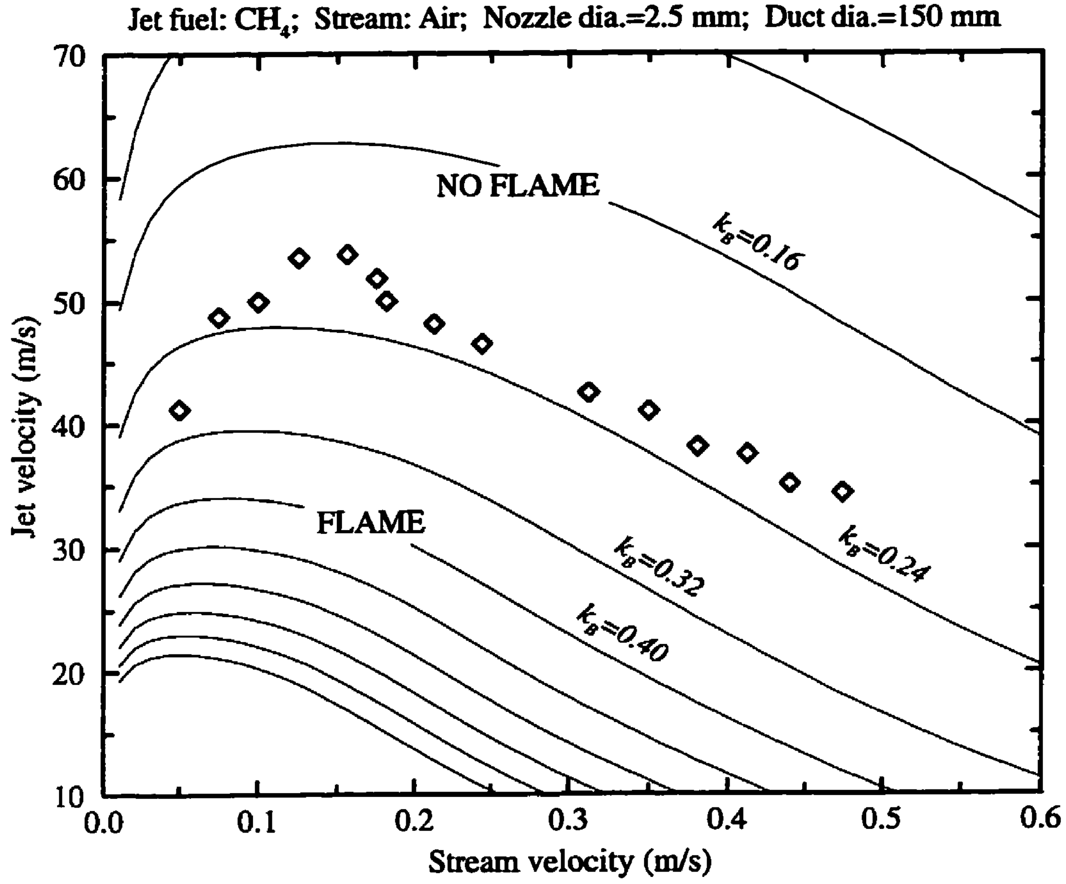

Figure 5.14: The calculated jet blowout velocity of a methane jet flame as a function of co-flowing stream velocity for different values of the blowout parameter k_B. Experimental data: ◇ - [25].

two different jet diameters of 2 mm and 2.5 mm issued into a combustor with 150 mm diameter were also calculated and compared with the experimental data reported in [25] (Figures 5.13 and 5.14). It appears that the critical value of k_B is approximately 0.24 for a jet of 2 mm diameter, while it is approximately 0.23 for a jet of 2.5 mm diameter. In Figure 5.13, the last three experimental points associated with higher co-flowing stream velocities are deviating from the predicted curve for blowout limits. However, for the experiment performed by the author under the same conditions (but with a slight difference in the combustor size), a good agreement was observed between experiment and calculation even at these stream velocities (Figure 5.9).

Moreover, the blowout limits of a larger jet of 3.3 mm issuing into a larger combustor of 300 mm hydraulic diameter were calculated and compared with the available experimental data [2]. The results for a propane and a methane jet are shown in Figures 5.15 and 5.16, respectively. In addition, Figure 5.17 shows the results of calculation for a methane jet of 5.2 mm, as well as the available experimental data obtained from [2]. The critical values of parameter k_B is almost constant for different nozzle and combustor diameters, co-flowing stream velocities and fuels. An exception was observed for methane jets of 3.3 and 5.2 mm diameters employed in [2] for which $k_{B,Cr}$ oscillates around 0.24.

It can be seen that the model reproduces fairly accurately the existing trend between the blowout limits of lifted flames and the co-flowing stream velocity.

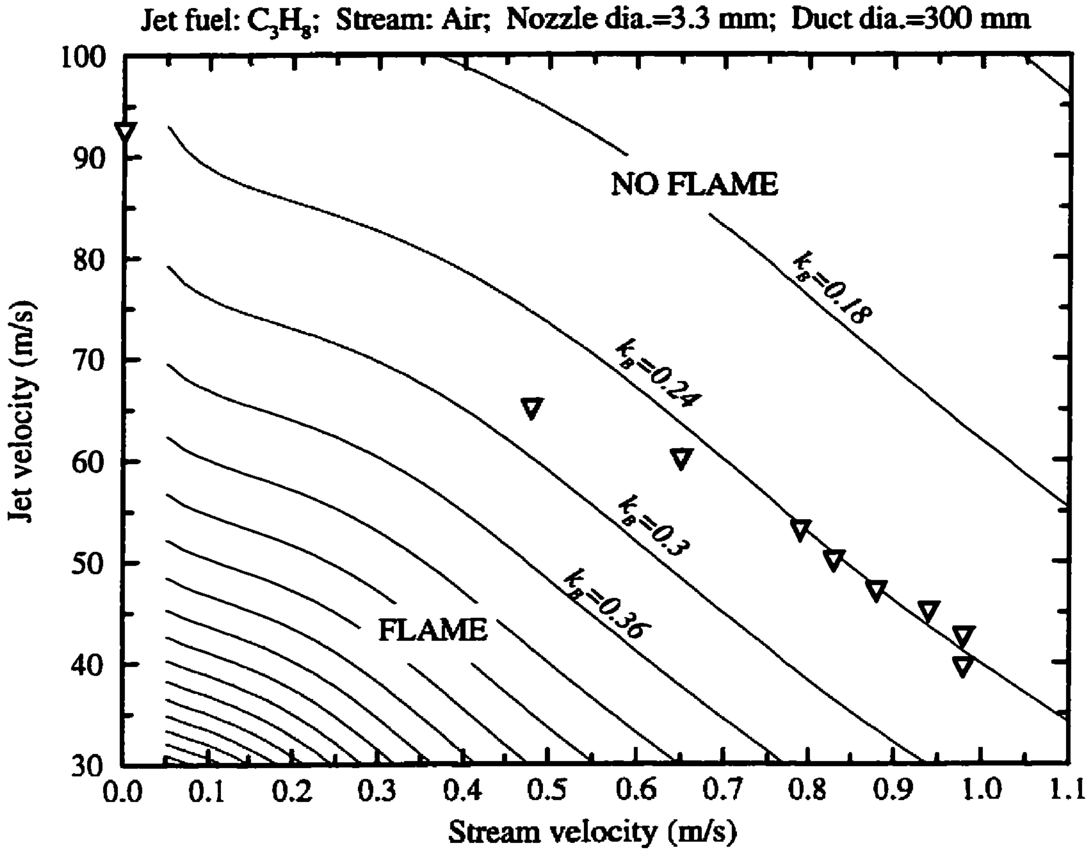

Figure 5.15: The calculated jet blowout velocity of a propane jet flame as a function of co-flowing air stream velocity for different values of the blowout parameter k_B. Experimental data: ∇ - [2]; — Calculated.

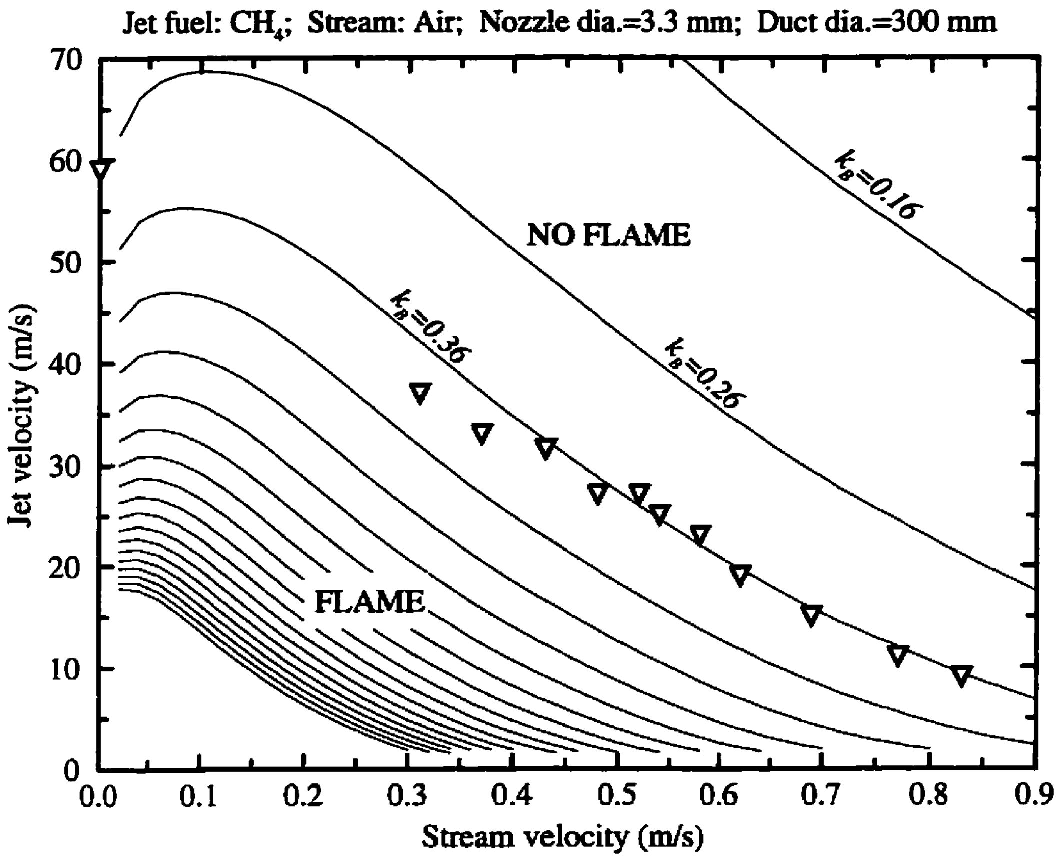

Figure 5.16: The calculated jet blowout velocity of a methane jet flame as a function of co-flowing air stream velocity for different values of the blowout parameter k_B. Experimental data: ∇ - [2]; — Calculated.

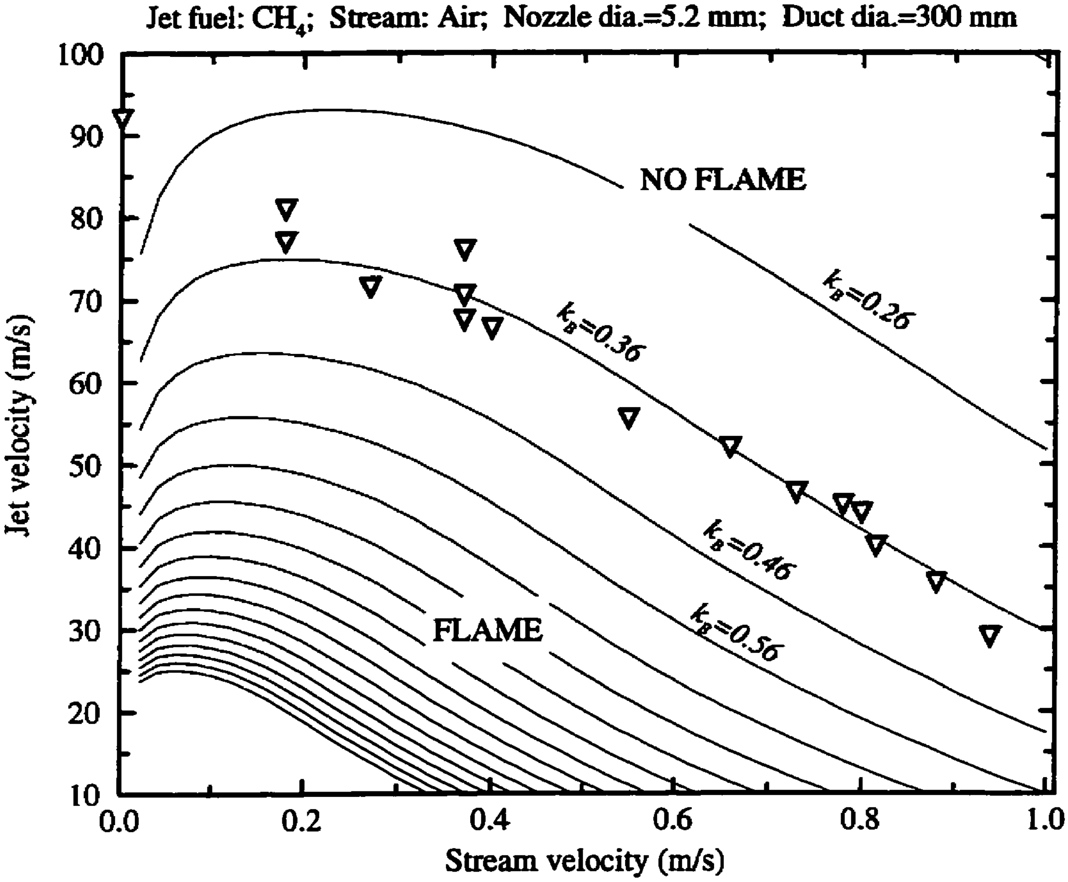

Figure 5.17: The calculated jet blowout velocity of a methane jet flame as a function of co-flowing air stream velocity for different values of the blowout parameter k_B. Experimental data: ∇ - [2]; — Calculated.

Effect of Co-flowing Stream Velocity on Jet Blowout Velocity

Generally, the jet blowout velocity of lifted flames decreases with an increase in the co-flowing stream velocity as observed experimentally (Chapter 4). This behavior can be explained with the help of the proposed model.

Consider a methane jet flame issuing into a co-flowing stream of air. The calculated jet blowout velocities for such a flame are shown by a dash line curve in Figure 5.18. Point 1 on this curve can be chosen arbitrarily as a starting point. Assume that the actual trend of variation of blowout limit with the co-flowing stream velocity is unknown. Starting at point 1, with an increase in the co-flowing stream velocity, the corresponding jet blowout velocity might increase, remain constant or decrease.

These three possible scenarios are shown in Figure 5.18 by three arrows 1-2, 1-3 and 1-4. Among these three trends, only one of them can fulfill the flame stability requirement. To find the right trend, parameters δ_u and u_m were calculated using Equations (5.22) and (5.23) for points 1, 2, 3 and 4 at a position downstream of the jet exit, x, where the jet centerline concentration is equal to the lean flammability limit of methane in air. The position x was calculated using Equation (5.32). The values of proposed blowout criterion for lifted flames,

$$k_B = \left(\frac{\delta_u \cdot \nu}{u_m^3}\right)^{1/2} \cdot \left(\frac{S^2{}_{L,St}}{\alpha}\right) \cdot \left(\frac{r_o}{r_{ref}}\right)$$

were also calculated for all these points. The results of these calculations are shown in Table 5.3. It can be seen that increasing the stream velocity (from $u_\infty = 0.3$ m/s to $u_\infty = 0.5$ m/s) at the same jet velocity ($u_o = 28.7$ m/s) causes an increase in the jet velocity on the jet centerline (from $u_m = 1.765$

Table 5.3: Jet parameters corresponding to points 1, 2, 3 and 4 shown in Figure 5.18 at the blowout position. Jet Fuel: CH_4; Stream: Air; Nozzle dia.=2.00 mm; Duct dia.=127 mm

Point	u_∞ (m/s)	u_o (m/s)	x (m)	δ_u (mm)	u_m (m/s)	k_B
1	0.3	28.7	0.1997	16.823	1.765	0.240
2	0.5	43.74	0.1955	16.446	2.781	0.120
3	0.5	28.7	0.1739	14.613	2.171	0.164
4	0.5	15.15	0.1415	11.888	1.572	0.240

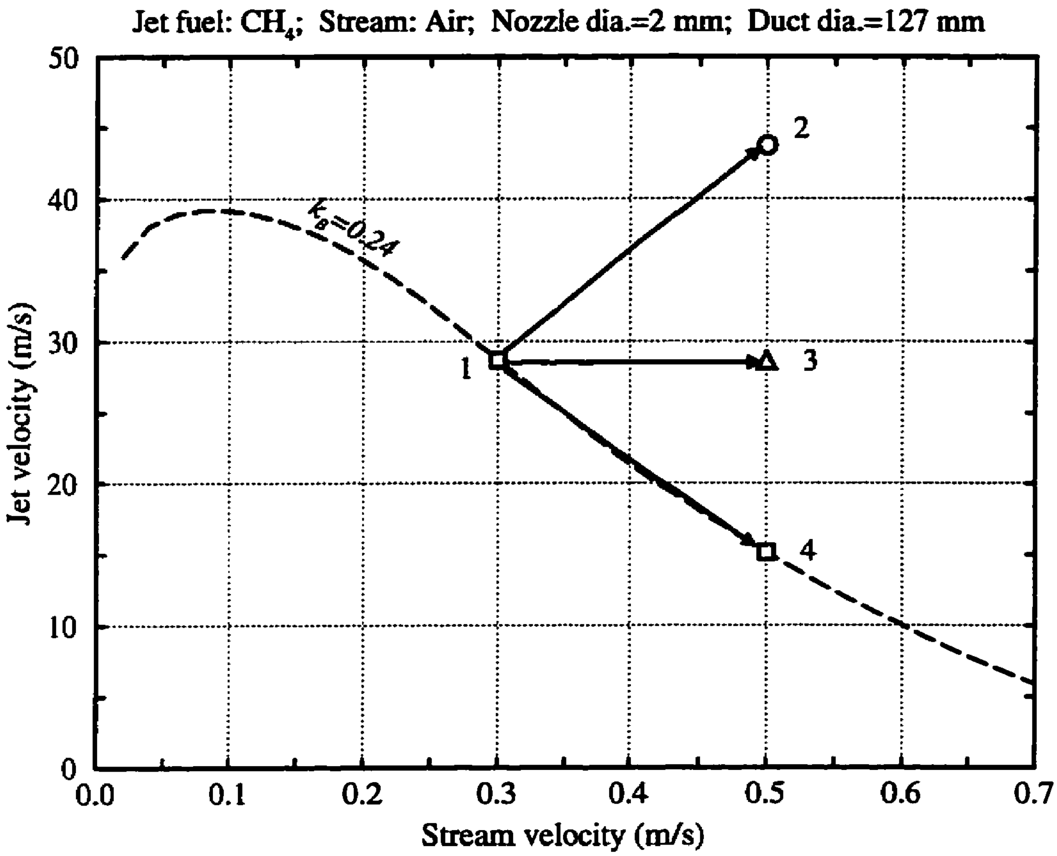

Figure 5.18: Calculated jet velocities of methane jet as a function of co-flowing air stream velocity. Dashed line represents the jet blowout velocity curve.

m/s to $u_m = 2.171$ m/s) and a decrease in the jet velocity half radius (from $\delta_u = 16.823$ mm to $\delta_u = 14.613$ mm) both resulting in a smaller value of blowout parameter (from $k_B = 0.240$ to $k_B = 0.164$). In this case, due to smaller blowout parameter than its critical value, the mixing process of cold air and fuel with hot products occurs in a time shorter than the chemical time and the mixture cools quickly and ignition becomes impossible. As a result, with increasing the stream velocity, the jet blowout cannot remain constant and it should either increase or decrease.

Since increasing stream velocity at a constant jet velocity (from point 1 to 3) resulted in a larger value of u_m, obviously increasing both jet and stream velocities (from point 1 to 2) would result in a larger value of u_m. Based on the same reasoning, point 2 cannot be the jet blowout velocity at $u_\infty = 0.5$ m/s either. Therefore, the only possible scenario can be decreasing of the jet blowout velocity with an increase in the stream velocity (from point 1 to 4). This decrease should insure a constant blowout parameter k_B.

Additionally, based on flame stabilization mechanism, a stable flame can be sustained when the local jet velocity is equal to the burning velocity. It is assumed that for the same type of fuel, the burning velocity at the blowout location does not change significantly from point 1 to 2, 3 or 4. Since the values of jet velocity (u_m) at the blowout location only for points 1 and 4 are almost the same, line 1-4 shows the actual trend of blowout velocity variation with the stream velocity.

Effect of Fluid Properties on Jet Blowout Velocity

The effect of variations in fluid properties such as density of jet fluid, density of surrounding stream, laminar burning velocity and lean flammability limit of jet fluid on the flame blowout limit were investigated analytically. The effect of variations in each property on the blowout limit was studied one at a time and by assuming the same value of blowout parameter $k_{B,Cr} = 0.24$ in all calculations. Calculations showed that the blowout limit of lifted flames increases with an increase in the laminar burning velocity of jet fuel and the density of the co-flowing stream as well as with a decrease in the lean flammability limit of jet fuel and the jet fuel density. The following is an explanation of the above effects based on the proposed model that suggests flame blowout occurs whenever k_B becomes equal to its critical value at the blowout location.

Laminar Burning Velocity. An increase in the laminar burning velocity decreases the chemical time. To keep k_B parameter constant, the mixing time should be decreased by increasing the jet blowout velocity.

This trend can be seen by simplifying Equation (5.34) for a constant value of k_B as:

$$S_L^2 \sim \frac{u_m^{3/2}}{\delta_u^{1/2}} \tag{5.70}$$

With increasing the laminar burning velocity, the RHS of the above relation should increase as well. The latter increases by increasing the jet blowout velocity, since increasing the jet velocity increases u_m, and decreases δ_u, at the blowout location.

Lean Flammability Limit. Any decrease in the lean flammability limit of a jet fuel means that the blowout location (at which the jet centerline fuel concentration is equal to the lean flammability limit) will be farther away from the nozzle. Moving downstream of the jet exit, the jet velocity decays and becomes smaller and the jet width becomes larger. Both of these result in a larger mixing time at this position. To keep k_B parameter constant, this effect should be canceled by increasing the jet velocity.

Density of Jet Fluid. Variation in the density of jet affects the jet blowout velocity in two ways:

- A decrease in the density of jet results in a faster decay of jet flow concentration [72,73]. In other words, blowout location is moving closer to the jet exit. By moving closer to the jet exit, velocity on the jet centerline is larger and the jet width is smaller. This results in a larger mixing time at this position. To cancel this effect and keep the k_B parameter constant, the mixing time should increase. This is possible if the jet blowout velocity decreases.

- Since the mass fraction of jet fluid on the jet axis, c_m, at the blowout location is proportional to the jet density, a decrease in density results in a decrease in c_m value. As discussed above (see discussion related to the lean flammability limit), this results in an increase in the jet blowout velocity.

Although a faster decay of jet fluid velocity due to its smaller density decreases the jet blowout velocity, this velocity increases due to smaller c_m at the blowout location, i.e., the overall effect is an increase in the jet blowout velocity.

Density of Co-flowing Stream Fluid. An increase in the density of surrounding stream results in both a faster decay of jet flow [72,73] and a smaller c_m at the blowout location. As discussed above, the overall effect is an improvement in the flame blowout limits.

Effect of Combustor Size

The effect of combustor (duct) size on the blowout limits of methane lifted flames is shown in Figure 5.19 for a range of combustor diameters and two different jet diameters. As can be seen, an increase in the duct diameter increases the blowout limits only at lower co-flowing stream velocities and these limits do not change at higher co-flowing stream velocities. When the combustor size becomes sufficiently large compared to the nozzle size, any further increase in the combustor size does not affect the blowout limits of lifted flames. For example, for a nozzle of 2 mm diameter, the blowout limit curve remains the same for combustors of 600 mm diameter and larger.

Validation of Flame Stabilization Location before Blowout

Earlier an assumption was made that the blowout location is a position where the jet fuel concentration on the jet axis is close to its lean flammability limit. To investigate the validity of this assumption, the following calculations and experiments were conducted.

For a methane jet issuing into a co-flowing air stream, the calculated jet blowout velocities (at $k_B = 0.24$) are shown in Figure 5.20. The calculated blowout location where the concentration of jet fuel on the jet axis, c_m, is equal to lean flammability limit ($c_m = L_f = 5$), is also shown in this figure. As can be seen, both the jet blowout velocity and the blowout location are decreasing with an increase in the stream velocity.

The flame length which was measured visually at jet velocities close to 95 percent of the jet blowout velocities is also shown in Figure 5.20. The measured flame lengths have an uncertainty of at least ± 2.5 cm, due to the brushy and flickering flame tip. The jet velocities associated with these flame

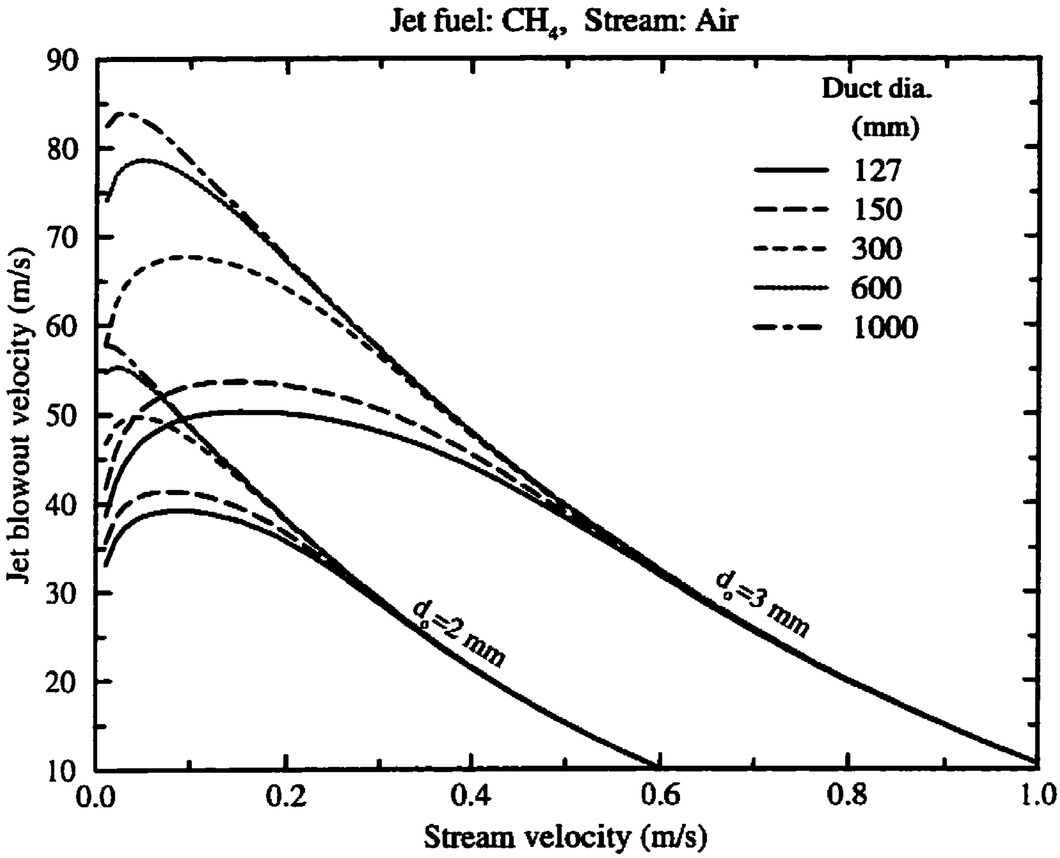

Figure 5.19: The blowout velocities of methane lifted flames as a function of co-flowing air stream velocities for different combustor and nozzle diameters.

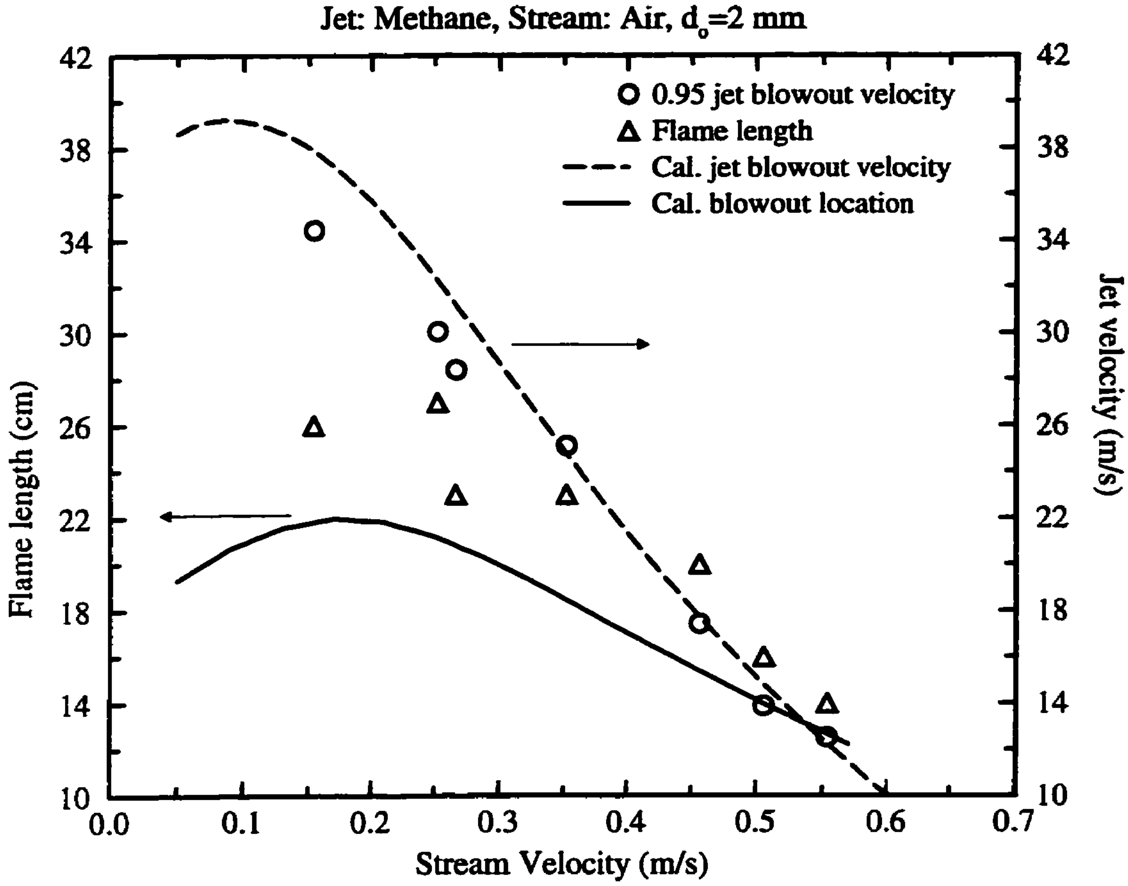

Figure 5.20: The variation of lifted flame length with the co-flowing stream velocity at jet velocities of about 95 percent of the jet blowout velocities.

lengths are also shown in this figure.

Comparison of measured flame lengths (triangle symbols) with calculated blowout locations (solid line) shows that both have the same trend with an increase in the stream velocity. However, the values of measured flame lengths and calculated blowout locations cannot be compared quantitively, since relatively crude measurements of the flame lengths were conducted. Taking this into consideration, the trends of calculated and experimental data are in good agreement.

5.3.2 Fuel Mixtures

In this section, the blowout limit calculations for different fuel mixtures issued from a jet of 2 mm diameter into a combustor with hydraulic diameter of 127 mm are conducted. The value of the blowout parameter, k_B, used in these calculations is equal to 0.24 as for all the other cases. The values of the stoichiometric laminar burning velocity for methane-hydrogen mixtures containing 15, 25, 50 and 75 percent of hydrogen are considered as 0.41, 0.46, 0.56 and 0.91 m/s, respectively [96]. The burning velocities of methane-ethylene and methane-propane mixtures were calculated using the simple rule of mixing.

Methane-Hydrogen Mixtures. Calculated blowout limits for methane-hydrogen mixtures containing 15, 25, 50 and 75 percent of hydrogen are presented in Figures 5.21, 5.22, 5.23 and 5.24, respectively. The corresponding experimental data obtained in the current research are also shown in the same figures for comparison. The agreement can be seen to be satisfactory. This shows that the proposed model can be used to calculate the improving effect of the addition of hydrogen to a methane jet on its blowout limits.

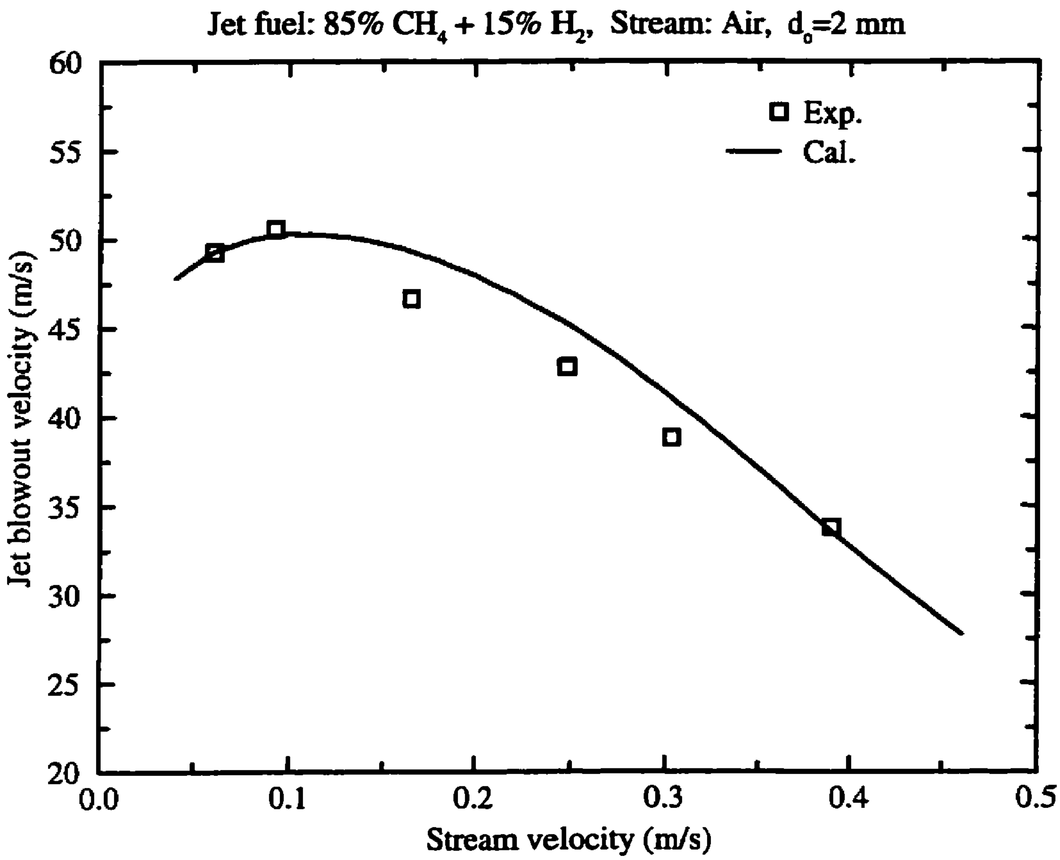

Figure 5.21: The blowout limits of lifted flames as a function of the co-flowing air stream velocity for a fuel mixture containing 85% of methane and 15% of hydrogen.

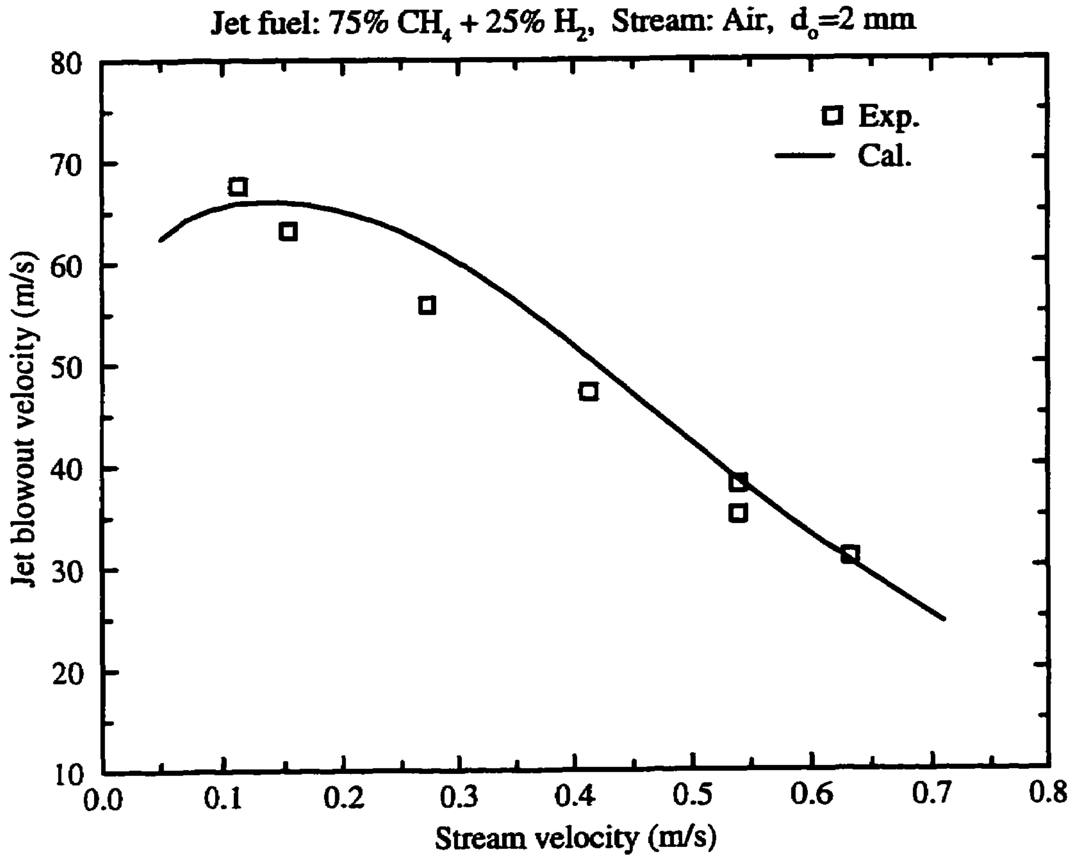

Figure 5.22: The blowout limits of lifted flames as a function of co-flowing air stream velocity for a fuel mixture containing 75% of methane and 25% of hydrogen.

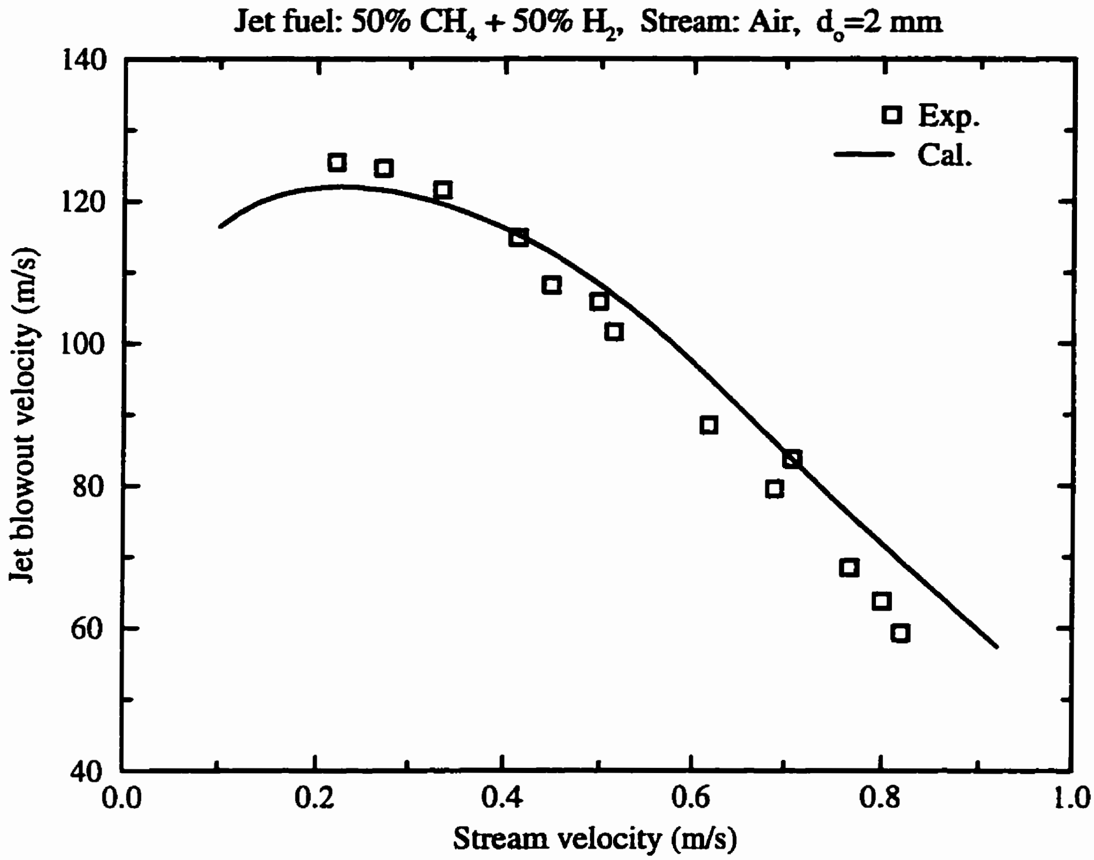

Figure 5.23: The blowout limits of lifted flames as a function of co-flowing air stream velocity for a fuel mixture containing 50% of methane and 50% of hydrogen.

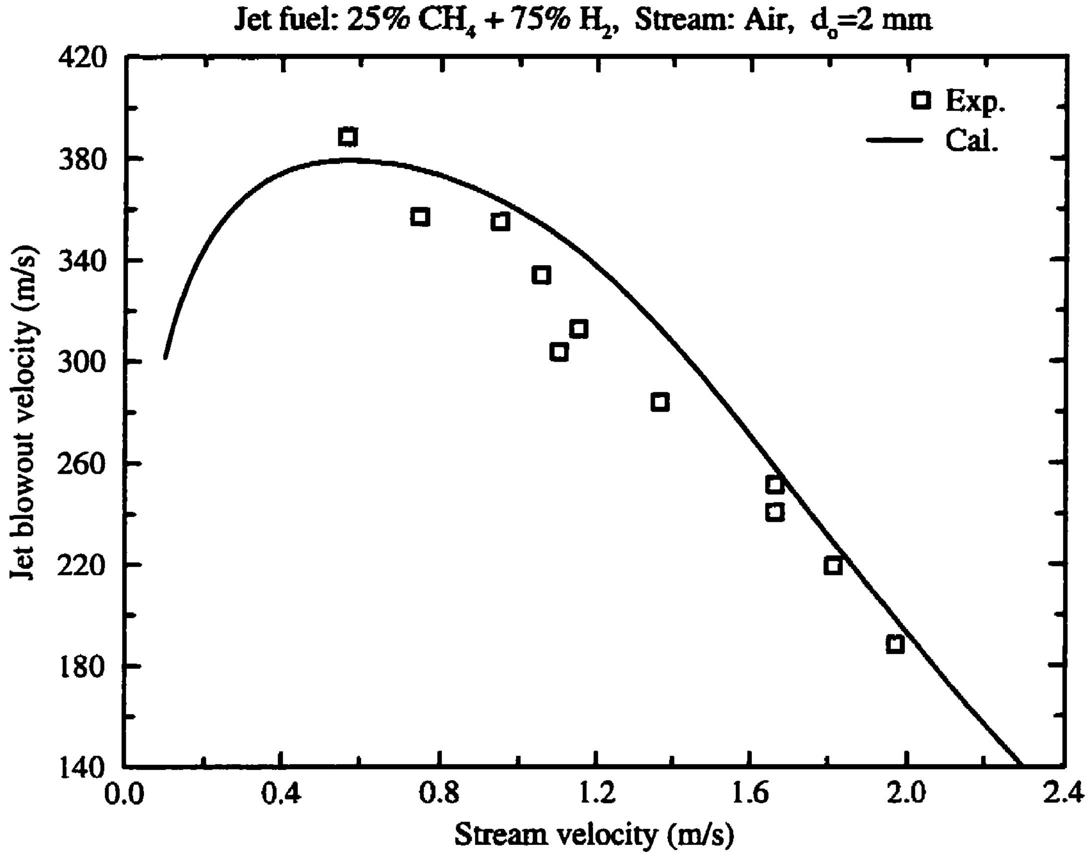

Figure 5.24: The blowout limits of lifted flames as a function of co-flowing air stream velocity for a fuel mixture containing 25% of methane and 75% of hydrogen.

This effect is due to not only the small density and lean flammability limit of hydrogen but also its large burning velocity both having an enhancing effect on the blowout limits (see Section 5.3.1).

Methane-Ethylene Mixtures. The calculated blowout limits for methane-ethylene mixtures containing 7.5, 11.7, 29.5 and 31.6 percent of ethylene as well as those for pure methane are shown in Figure 5.25. A few experimentally measured data points are also shown for comparison. As can be seen, the addition of ethylene to a methane jet flame substantially increases its blowout limits. Agreement between calculated blowout limits and the limits obtained experimentally is fairly good. Although the larger density of ethylene has a diminishing effect on these limits, its larger burning velocity and smaller lean flammability limit have enhancing effects. As a result, the overall effect is an increase in the blowout limits.

Methane-Propane Mixtures. The calculated blowout velocities for different methane-propane mixtures containing 12, 30, 50 and 75 percent of propane as well as those for pure methane are shown in Figure 5.26. As expected, an addition of propane to a methane jet flame increases its blowout limit (like an addition of hydrogen or ethylene) over the whole range of co-flowing stream velocities considered. This is due to the larger burning velocity and the smaller lean flammability of propane compared to methane.

Comparison of Various Fuel Mixtures. The effect of the type of a second fuel added to the methane jet on its blowout limit is shown in Figure 5.27. For each methane-fuel mixture, concentration of the second fuel in the jet fuel mixtures is 25 percent by volume. The biggest improvement on the blowout limits was observed for hydrogen followed by ethylene and

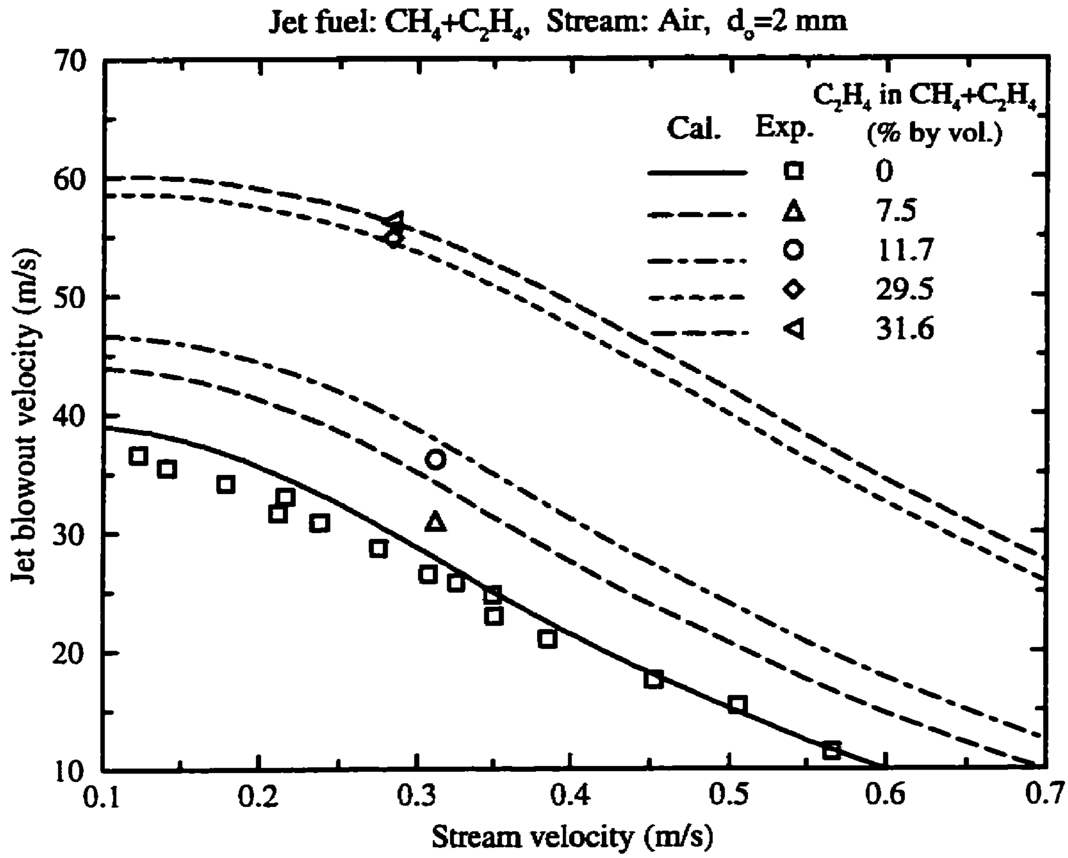

Figure 5.25: The blowout limits of lifted flames as a function of co-flowing air stream velocity for different methane-ethylene mixtures.

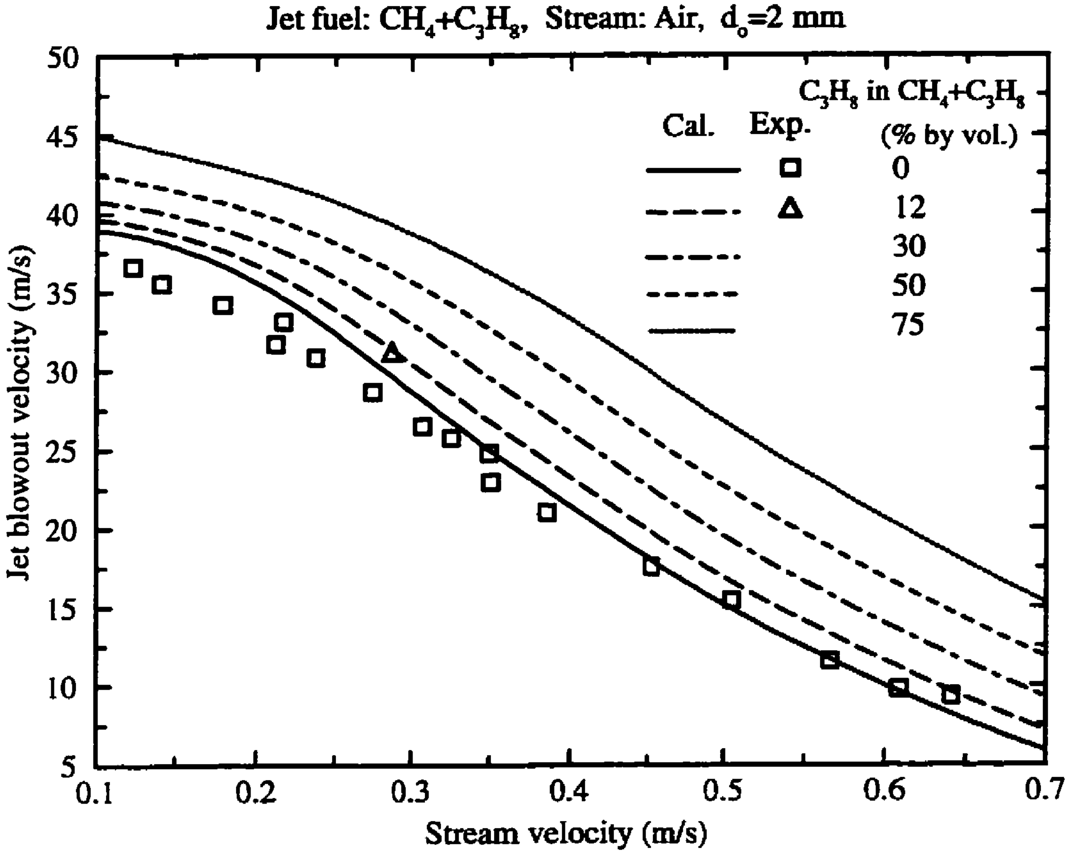

Figure 5.26: The blowout limits of lifted flames as a function of co-flowing air stream velocity for different methane-propane mixtures.

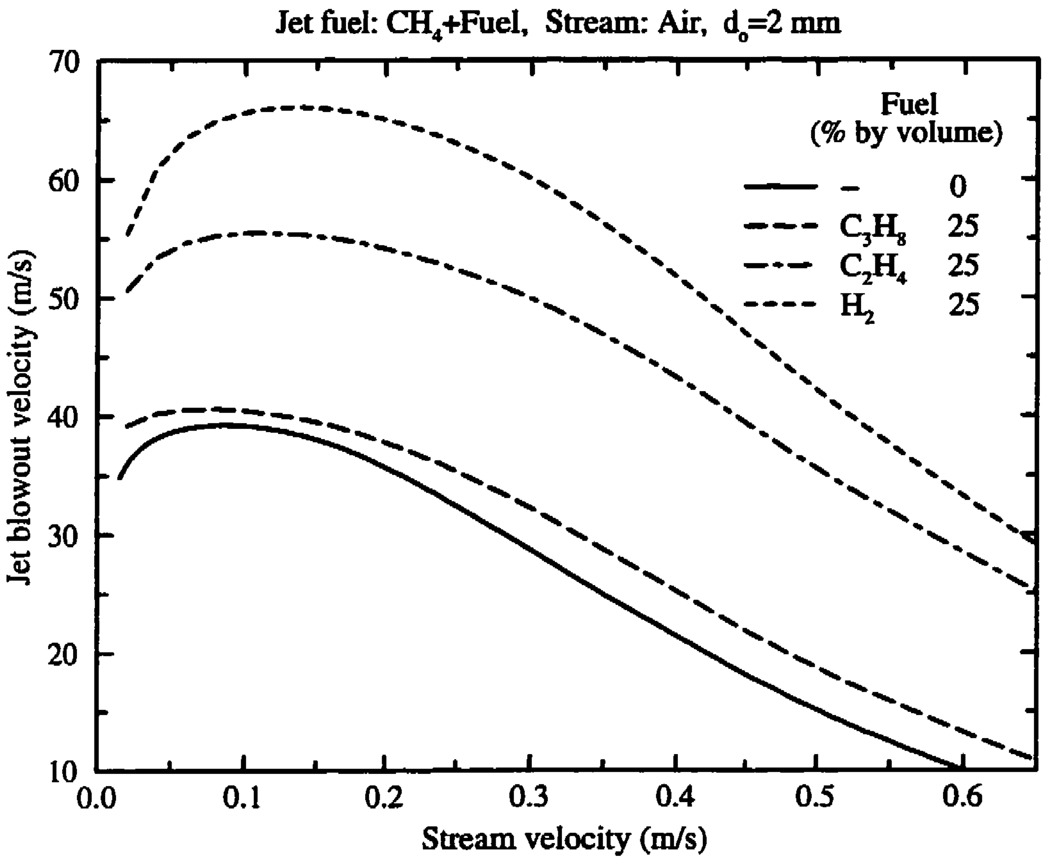

Figure 5.27: The blowout limits of lifted flames as a function of the co-flowing air stream velocity for different fuel mixtures.

propane. As discussed in Section 5.2.1, the addition of a second fuel to a jet fuel affects the value of jet density, burning velocity and lean flammability limit. The effect of these parameters on the jet blowout velocity was also discussed in Section 5.3.1. Based on these discussions, the obtained trend for different fuel mixtures can be explained as follows. Although propane has the smallest lean flammability limit, hydrogen has the most improving effect on the blowout limits of methane jet due to its higher burning velocity and smaller density compared to the other fuels. The obtained trend for various fuel mixtures show that variations in the value of burning velocity is a dominant factor, since the burning velocity of hydrogen is the highest followed by ethylene and propane.

5.3.3 Fuel in the Surrounding Stream

In this section, the effect of the introduction of an auxiliary fuel into a surrounding air stream on blowout limits is investigated analytically. The calculations were conducted for a methane jet discharged from a 2 mm diameter nozzle into a co-flowing stream of air-fuel mixture in a combustor with a 127 mm hydraulic diameter. The critical value of k_B is equal to 0.24 exactly as for the case of pure fuels and fuel mixtures. Methane, propane, ethylene and hydrogen were used as auxiliary fuels. The laminar burning velocities were calculated using the simple mixing rule except for the methane-hydrogen-air mixtures that were taken from [96].

The results of calculation are presented in Figures 5.28-5.31. To avoid the occurrance of flashback in the co-flowing stream, auxiliary fuels were used at relatively small concentrations. The calculated blowout limits are in good agreement with those obtained experimentally except for hydrogen

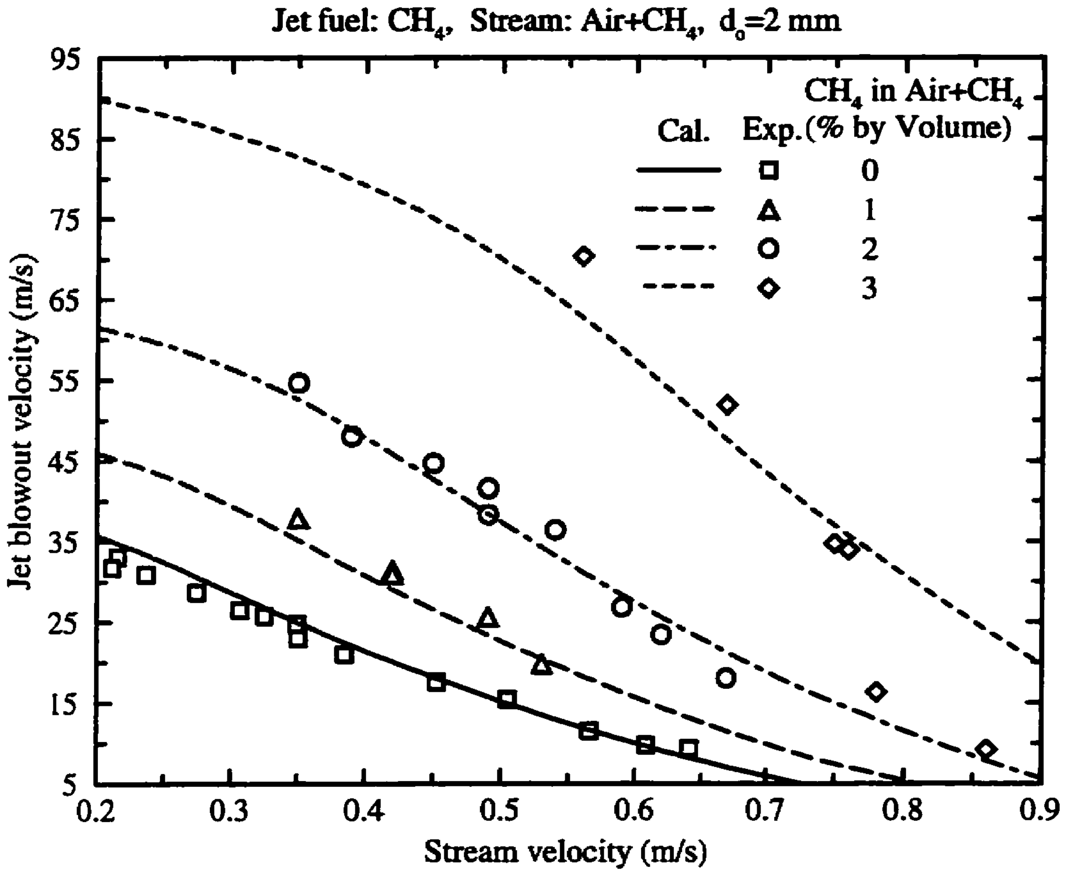

Figure 5.28: The blowout limits of methane lifted flames as a function of co-flowing stream velocity for different concentrations of methane in the co-flowing stream of air.

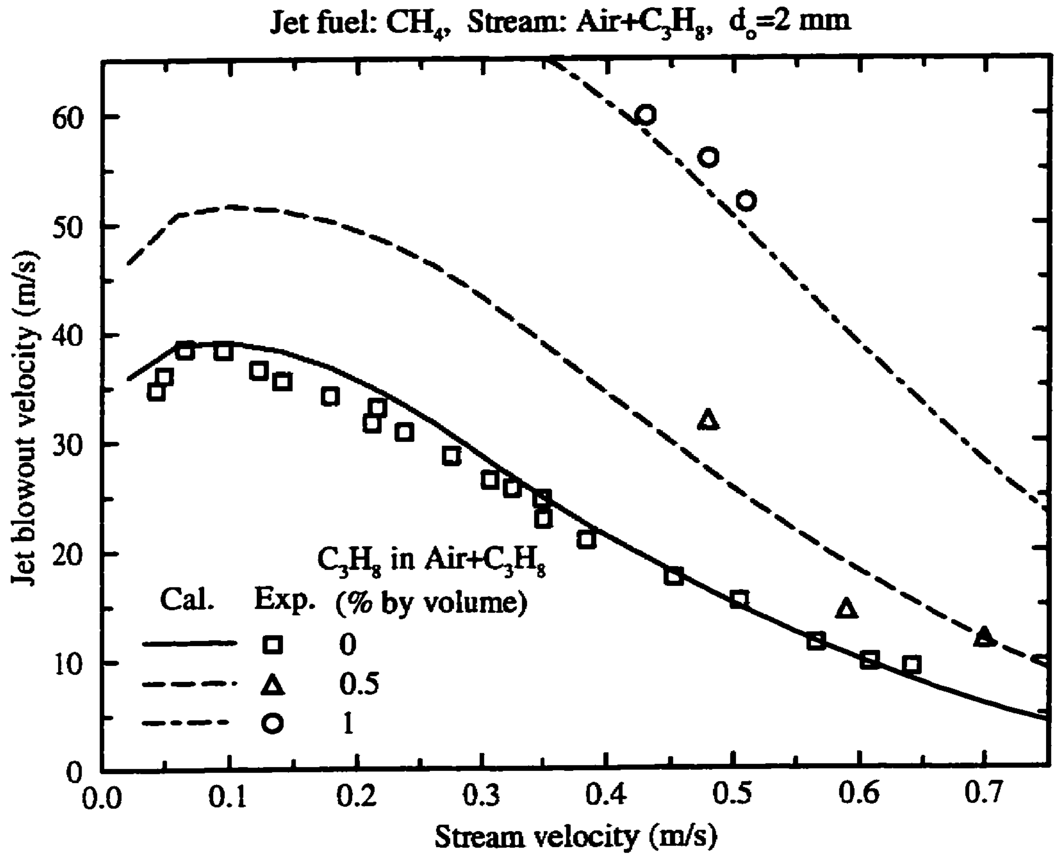

Figure 5.29: The blowout limits of methane lifted flames as a function of co-flowing stream velocity for different concentrations of propane in the co-flowing stream of air.

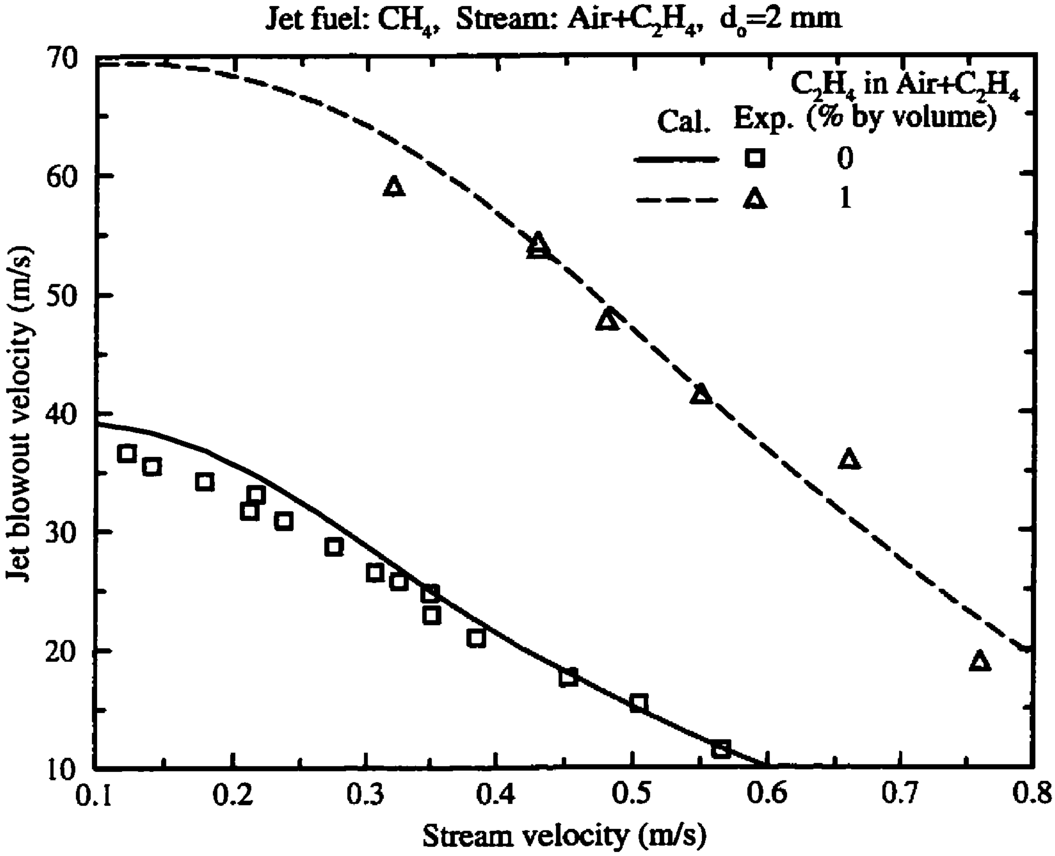

Figure 5.30: The blowout limits of methane lifted flames as a function of co-flowing stream velocity for different concentrations of ethylene in the co-flowing stream of air.

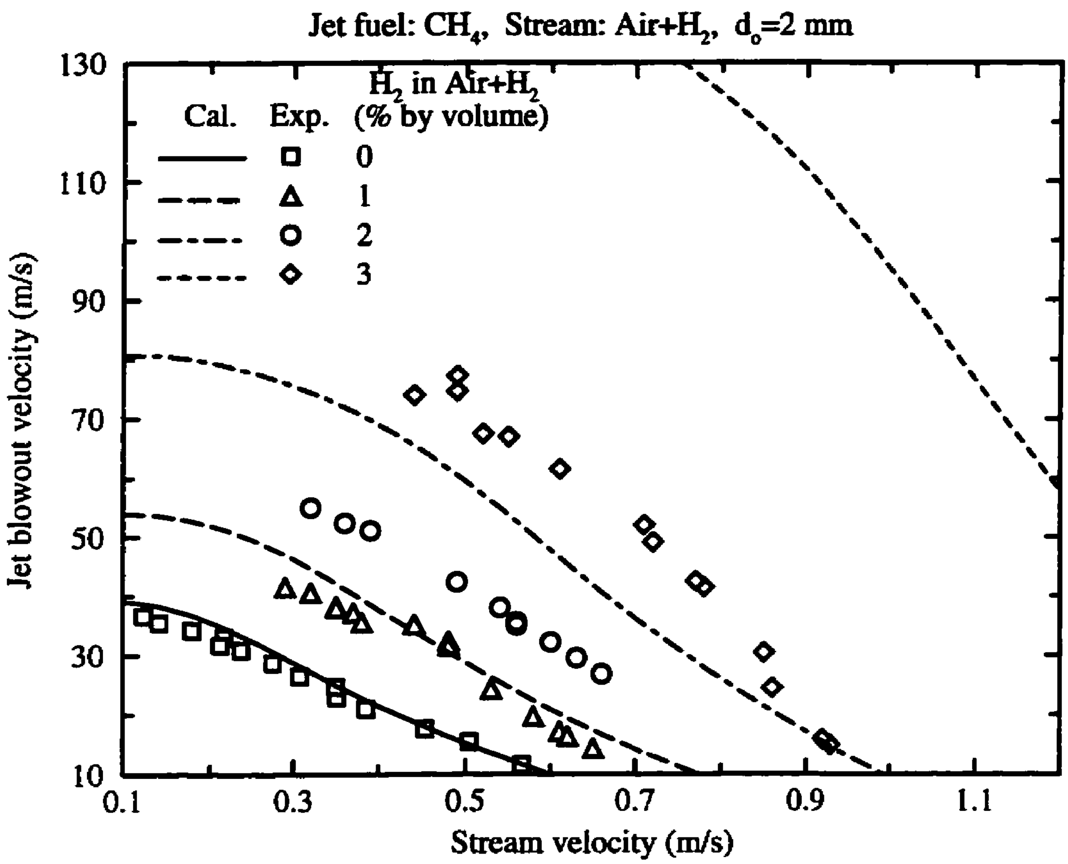

Figure 5.31: The blowout limits of methane lifted flames as a function of co-flowing stream velocity for different concentrations of hydrogen in the co-flowing stream of air.

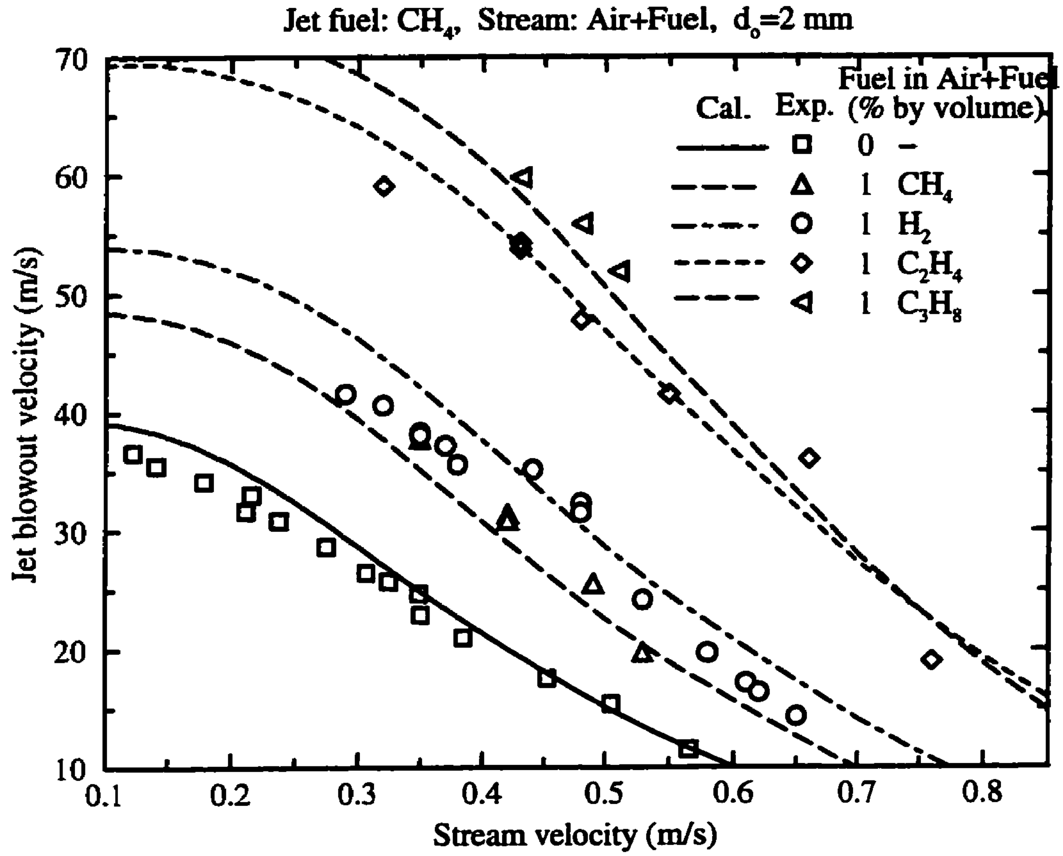

Figure 5.32: The blowout limits of methane lifted flames as a function of co-flowing stream velocity for different auxiliary fuels in the co-flowing stream of air.

followed by ethylene and propane (variation in the burning velocity is a dominent parameter) while in the second case, the most improvement on the blowout limits was observed for propane followed by ethylene and hydrogen (variation in the lean flammability limit is a dominent parameter).

5.3.4 A Second Fuel in Jet and/or Co-flowing Stream

A Second Fuel in Jet or Co-flowing Stream. The effects of ethylene addition to a methane jet and to a surrounding stream are compared in Figure 5.33. As can be seen, an addition of 40 percent ethylene to the methane jet flame increases its blowout limits as much as when 1 percent of ethylene is added to the air stream. The following is a comparison of the flow rate of consumed fuels in each case to achieve an economically efficient choice. At a stream velocity of 0.4 m/s, when a mixture of 40 percent ethylene and 60 percent methane was used as a jet fuel, the fuel flow rates were 0.258 m^3/h for ethylene and 0.386 m^3/h for methane. However, at the same stream velocity, when a methane jet issued into a co-flowing stream of 1 percent ethylene and 99 percent of air, the fuel flow rates were 0.644 m^3/h for methane and 0.182 m^3/h for ethylene. However, not of all this ethylene was entrained in the jet flame. The total fuel flow rate in the first case is less than the total fuel flow rate in the second one. As a result, the first case is more efficient if the reduction of total flow rate is the objective. On the other hand, since ethylene is a relatively expensive fuel the second choice would be economically efficient if cost reduction is the goal.

A Second Fuel in both Jet and Co-flowing Stream. The effect of a second fuel addition to both methane jet flame and co-flowing air stream on blowout limits is shown in Figures 5.34 and 5.35. As can be seen, when 25

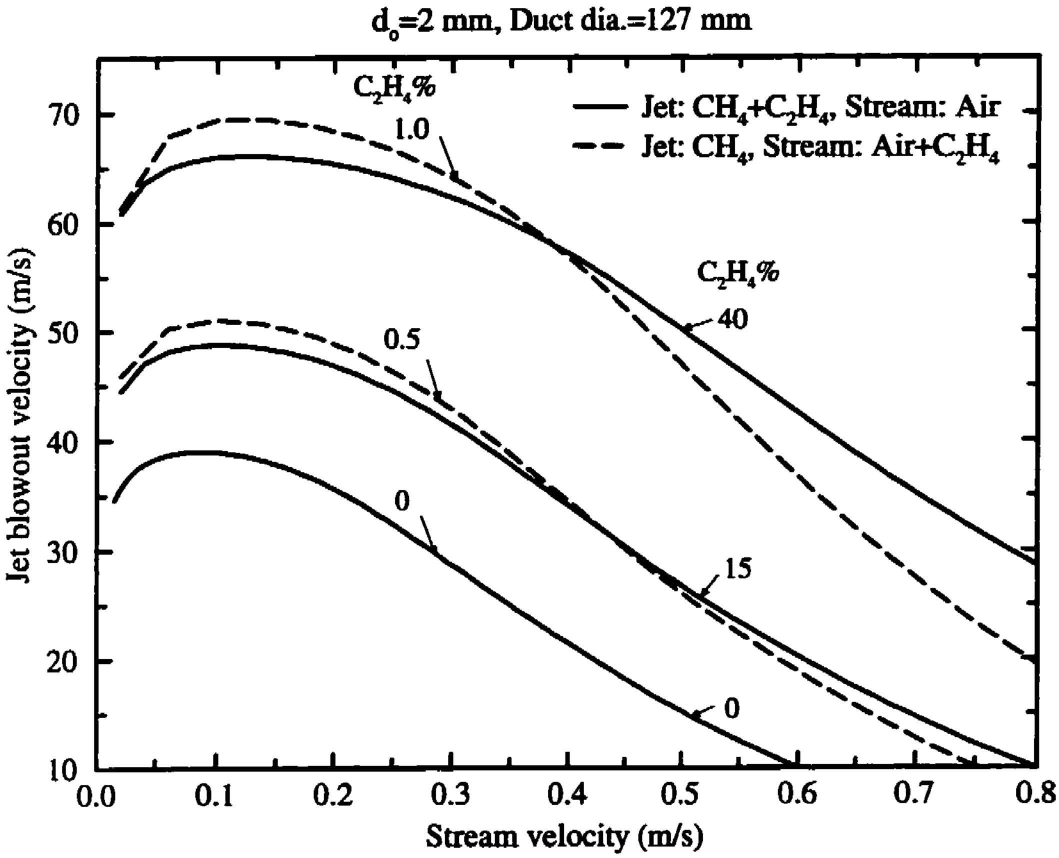

Figure 5.33: The blowout limits of methane or methane-ethylene lifted flames as a function of co-flowing air or air-ethylene stream velocity for different concentrations of ethylene.

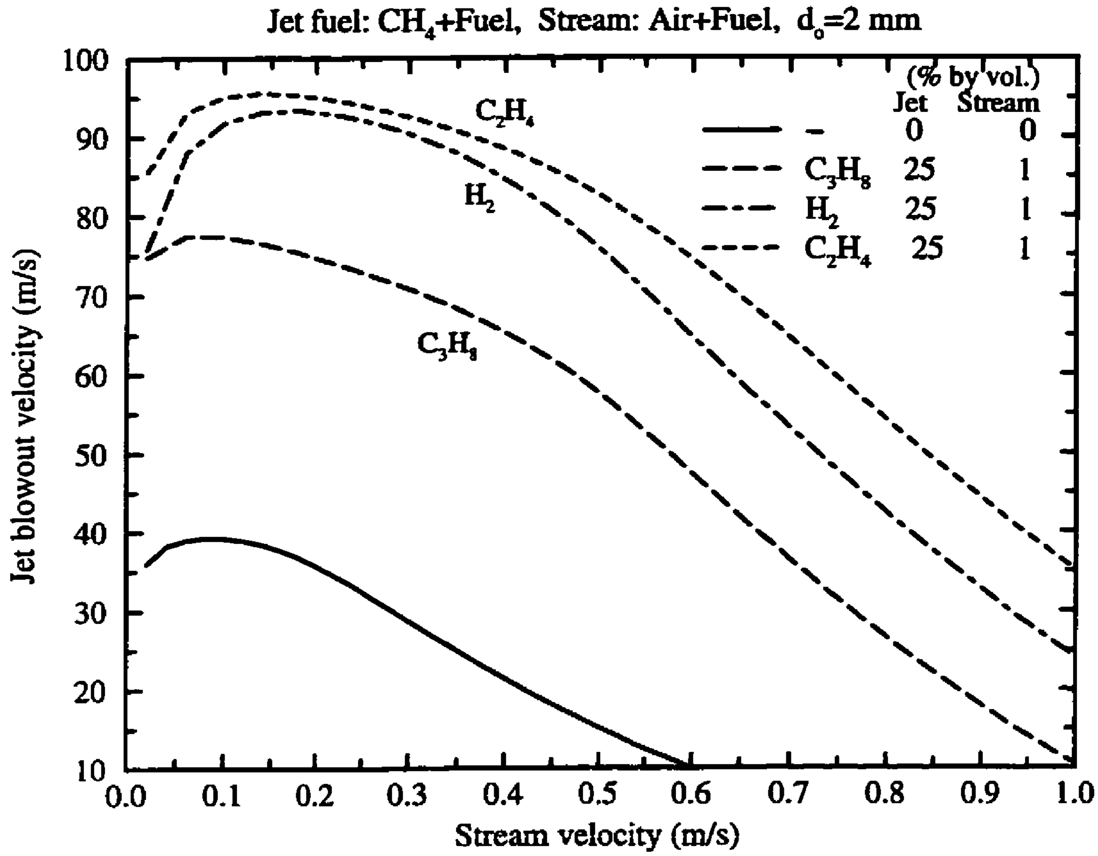

Figure 5.34: The blowout limits of methane-fuel lifted flames as a function of co-flowing air-fuel stream velocity. Concentration of the second fuel is 25% in the methane jet and 1% in the co-flowing air stream.

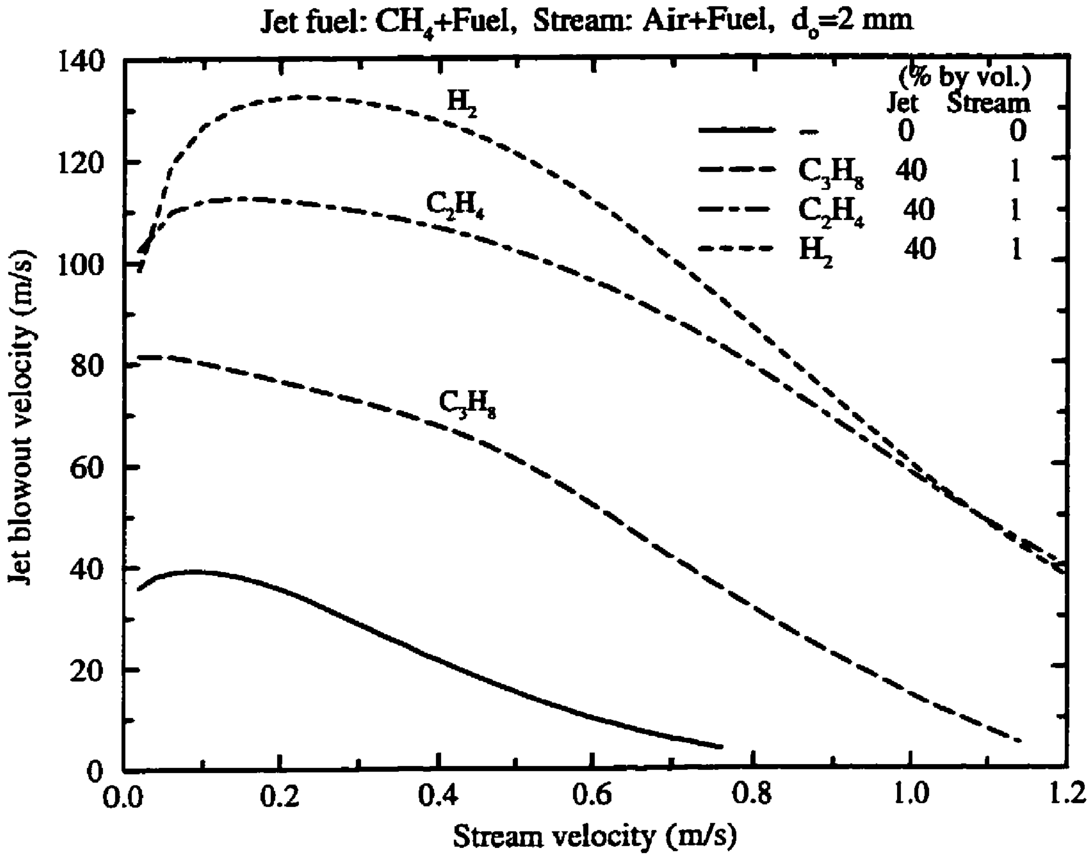

Figure 5.35: The blowout limits of methane-fuel lifted flames as a function of co-flowing air-fuel stream velocity. Concentration of the second fuel is 40% in the methane jet and 1% in the co-flowing air stream.

percent of a second fuel is added to the methane jet and 1 percent to the co-flowing air stream, the most improvement in blowout limits was observed with ethylene followed by hydrogen and then propane (Figure 5.34). However, with increasing the percentage of a second fuel in the methane jet from 25 percent to 40 percent, the most improvement in blowout limits was observed with hydrogen followed by ethylene and then propane (Figure 5.35). These trends show that at higher concentrations of a second fuel in the methane jet, hydrogen leads to the most improvement in blowout limits while at lower concentrations ethyelne improves blowout limits the most. This is due to the higher burning velocity of methane-hydrogen mixtures than that of methane-ethylene mixtures at larger concentrations of a second fuel. Although in the case when a fuel is added only to the co-flowing air stream, propane resulted in the most improvement in blowout limits (Figure 5.32), it lead to the least improvement when fuel was added to both jet and co-flowing stream. This is due to a smaller lean flammability limit of propane compared to the other fuels in the former case and due to a smaller burning velocity of propane compared to the other fuels in the latter.

5.3.5 Effect of Diluent

Calculations were conducted to predict the effect of diluent addition to the jet fuel or surrounding stream on the blowout limits of lifted flames. Calculations were for a jet of 2 mm diameter issuing into a combustor of 127 mm hydraulic diameter. The same critical value of k_B parameter equal to 0.24 was used in these calculations. The values of laminar burning velocities for methane-diluent mixtures were calculated using Equations (5.52) and (5.69) in which H is 0.25 for nitrogen, 0.44 for carbon dioxide and 0.20 for helium [92,94].

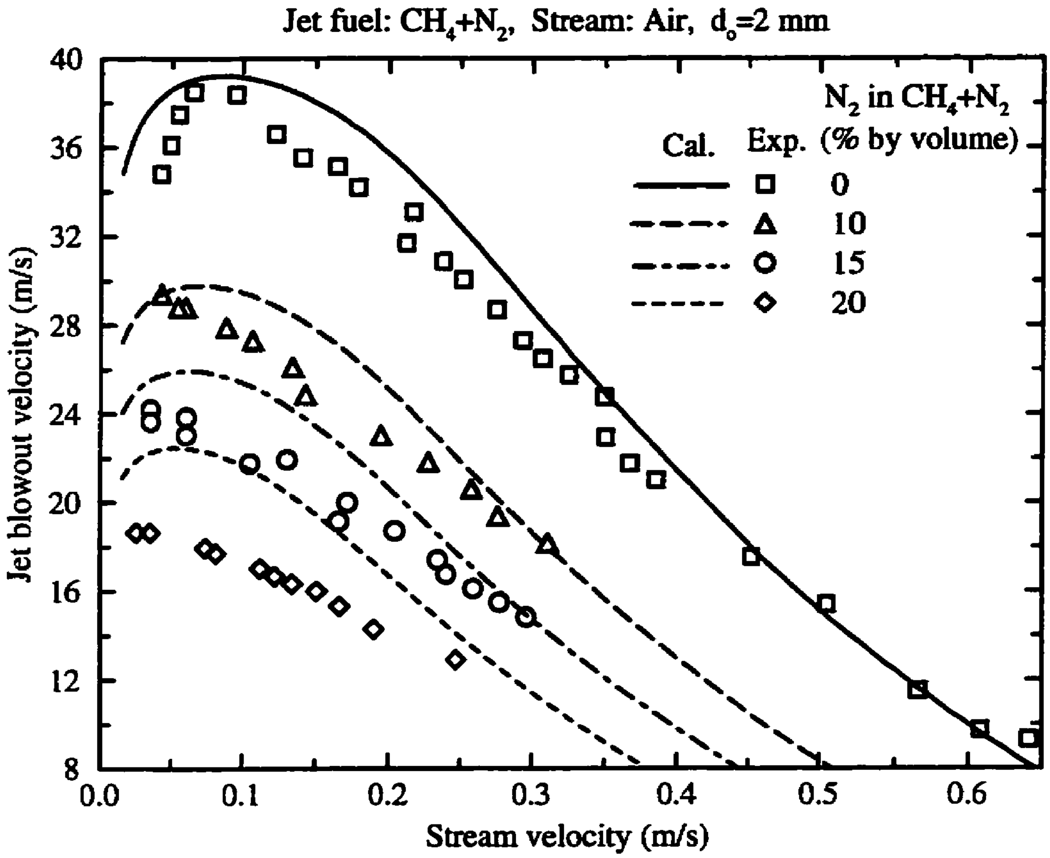

Figure 5.36: The blowout limits of methane-nitrogen lifted flames as a function of co-flowing air stream velocity for different nitrogen concentrations in the fuel mixture.

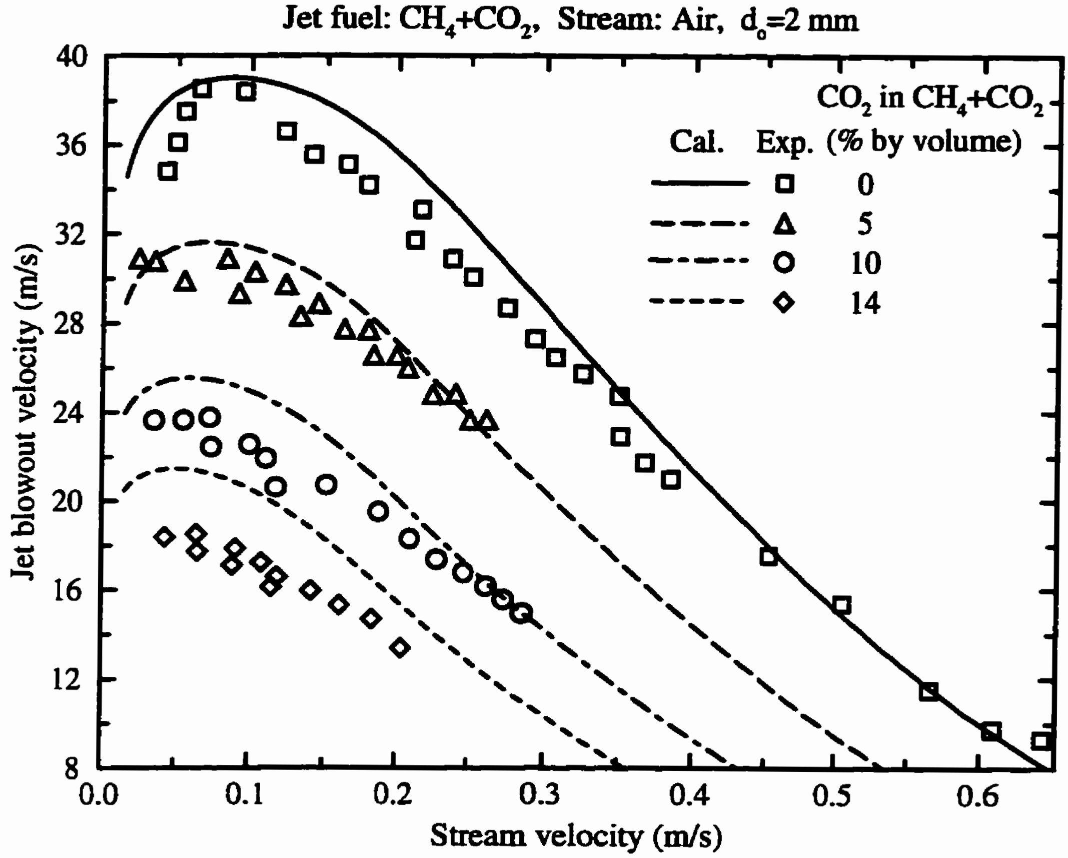

Figure 5.37: The blowout limits of methane-carbon dioxide lifted flames as a function of co-flowing air stream velocity for different carbon dioxide concentrations in the fuel mixture.

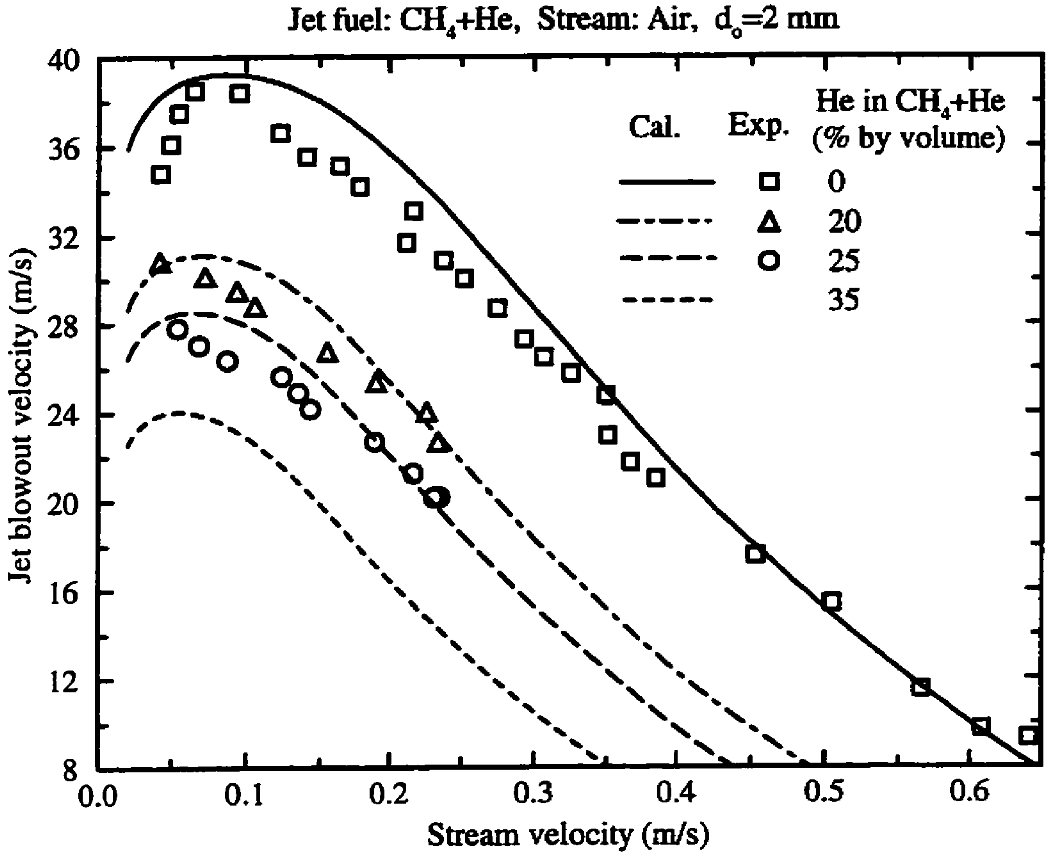

Figure 5.38: The blowout limits of methane-helium lifted flames as a function of co-flowing air stream velocity for different helium concentrations in the fuel mixture.

Diluent in Jet Fuel. The calculated results for nitrogen, carbon dioxide and helium as a diluent in a methane-diluent jet are presented in Figure 5.36, 5.37 and 5.38, respectively. The experimental results are also shown for comparison. It can be seen that the model predicts satisfactorily the blowout limits at higher co-flowing stream velocities while there is a deviation at smaller co-flowing stream velocities and higher diluent concentrations. The deviation could be due to the large uncertainty in the value of laminar burning velocities for fuel-diluent mixtures.

The effect of diluent type on the blowout limits of methane-diluent jet flames in a co-flowing air stream is shown in Figure 5.39. Concentration of all diluents in the jet fuel is 15 percent by volume. The most detrimental effect on the blowout limits is associated with carbon dioxide as a diluent, followed by nitrogen and then helium. This is due to the small laminar burning velocity and large lean flammability limit and density of methane-carbon dioxide mixtures in comparison with other methane-diluent mixtures. For the same reason, the effect of nitrogen on the blowout limits is less significant than the effect of carbon dioxide and more significant than the effect of helium.

Diluent in Fuel Mixture. The results of calculations for different methane-hydrogen-carbon dioxide mixtures are shown in Figure 5.40. It can be seen that an addition of 5 percent carbon dioxide to methane-hydrogen mixture containing 50 percent of hydrogen has more detrimental effect on the blowout limits than when the same amount (percent by volume) of this diluent is added to pure methane jet. For a methane-hydrogen jet, a replacement of 5 percent of fuel mixture with carbon dioxide results in about 19.4 percent increase in the density of jet fluid, while for a methane jet, a replacement of

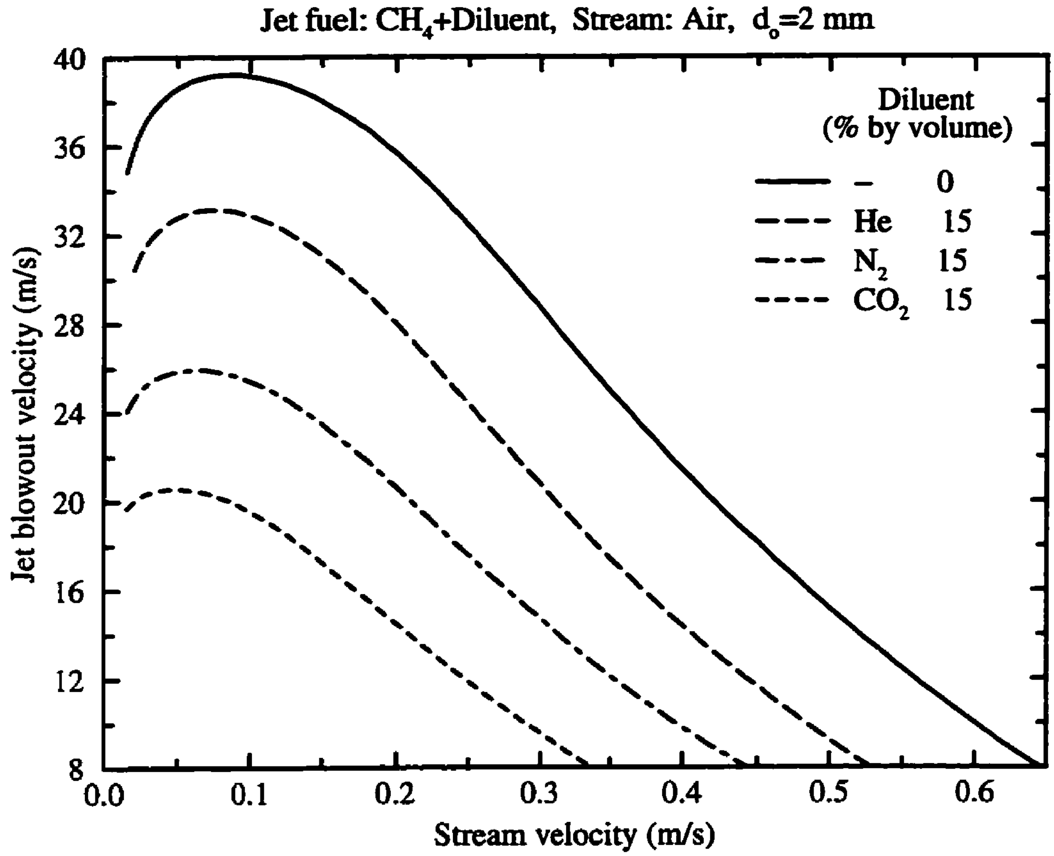

Figure 5.39: Calcualted blowout limits of methane-diluent lifted flames as a function of co-flowing air stream velocity for different diluents.

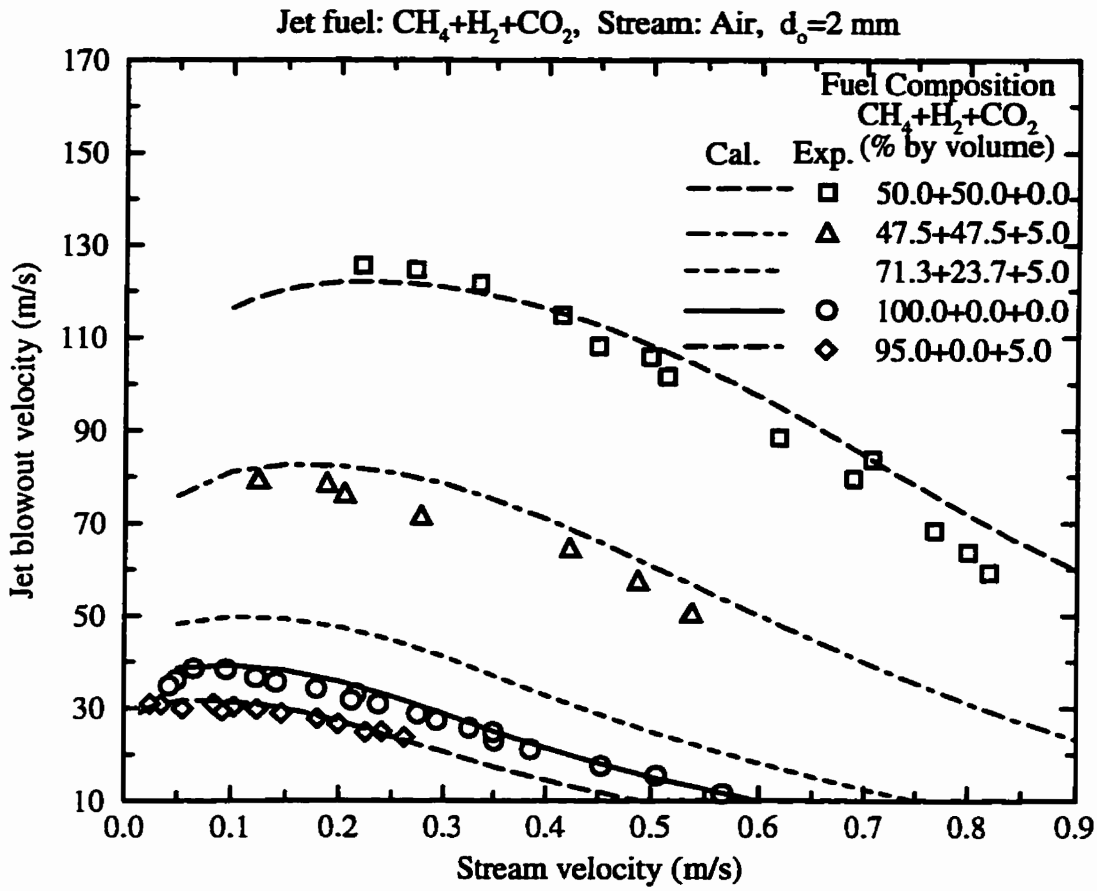

Figure 5.40: The blowout limits of lifted flames as a function of the co-flowing air stream velocity for different methane-hydrogen-carbon dioxide mixtures.

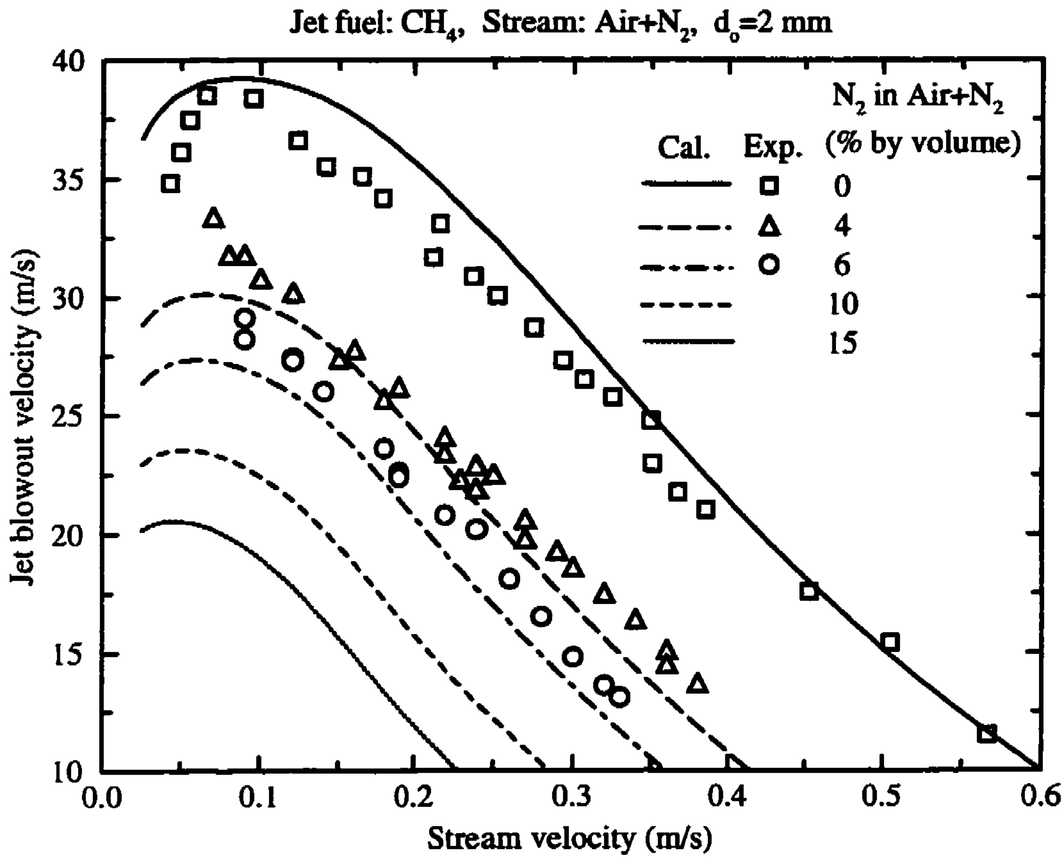

Figure 5.41: The blowout limits of methane lifted flames as a function of co-flowing stream velocity for different concentrations of nitrogen in the co-flowing stream of air.

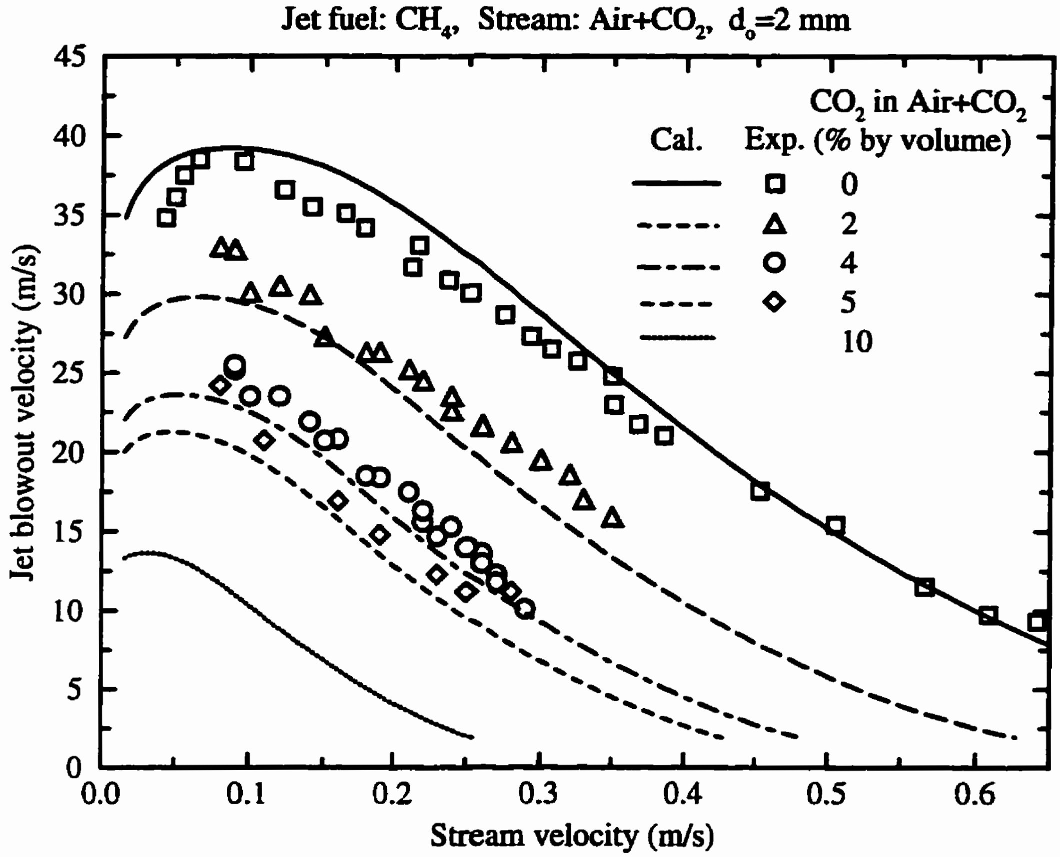

Figure 5.42: The blowout limits of methane lifted flames as a function of co-flowing stream velocity for different concentrations of carbon dioxide in the co-flowing stream of air.

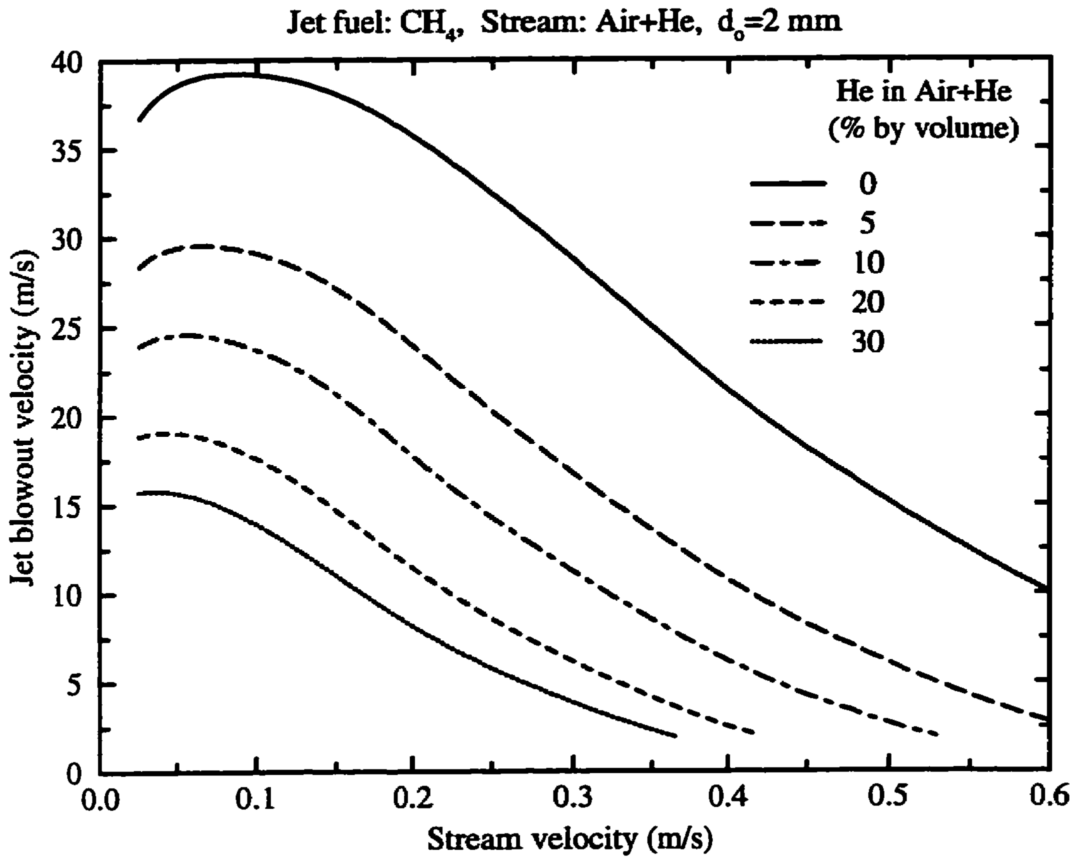

Figure 5.43: The blowout limits of methane lifted flames as a function of co-flowing stream velocity for different concentrations of helium in the co-flowing stream of air.

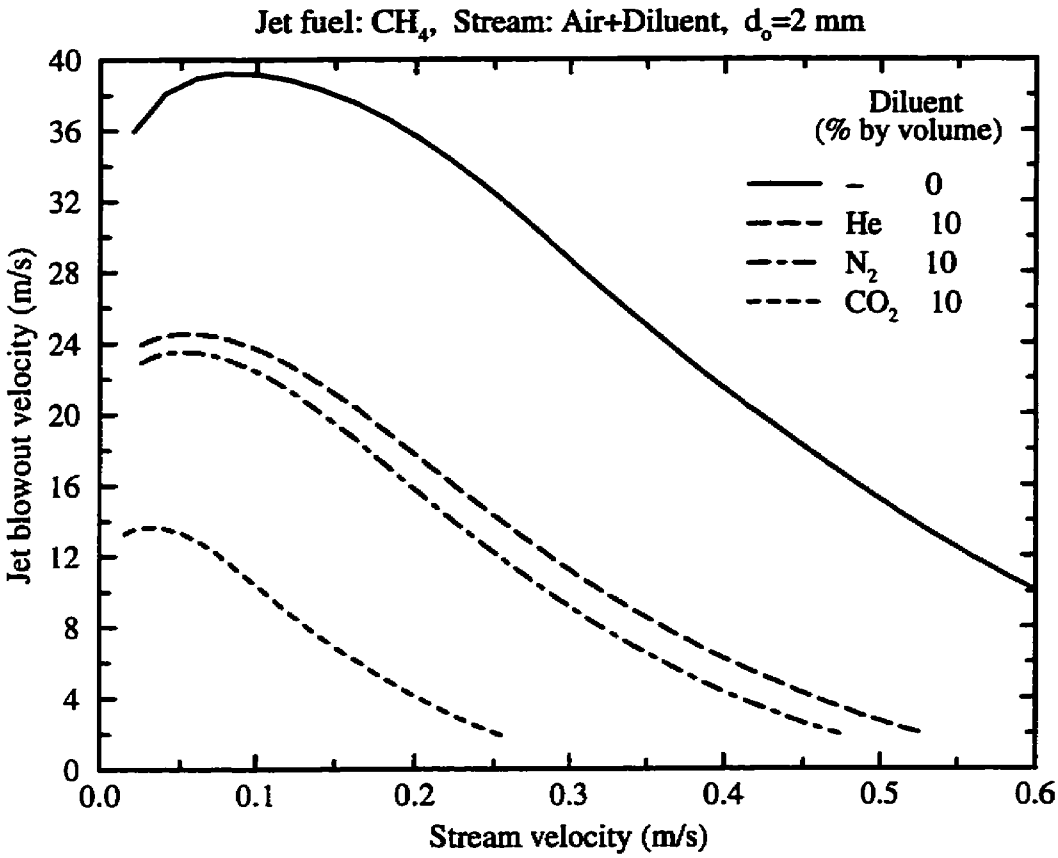

Figure 5.44: The calcualted blowout limits of methane lifted flames as a function of co-flowing air-diluent stream velocity for different diluents.

the jet flames. For example, the addition of 15 percent carbon dioxide to methane jet decreases its blowout limit as much as when 4.5 percent of carbon dioxide is added to the air stream. As a result, the presence of a diluent in the air stream affects the blowout limits more strongly than when it is present in the jet fuel at the same volume concentrations. This is due to the large entrainment of diluents in the oxidizing stream to the jet fuel at the blowout location.

The addition of a diluent to both jet fuel and co-flowing stream affects significantly the blowout limits of methane jet flame. This effect is shown in Figure 5.48. Concentration of the diluent in both the jet fuel and the co-flowing stream is 5 percent by volume for each diluent. Similar to the cases when a diluent is added to the jet fuel or to the co-flowing stream, the most detrimental effect on blowout limits was observed with carbon dioxide followed by nitrogen and then helium.

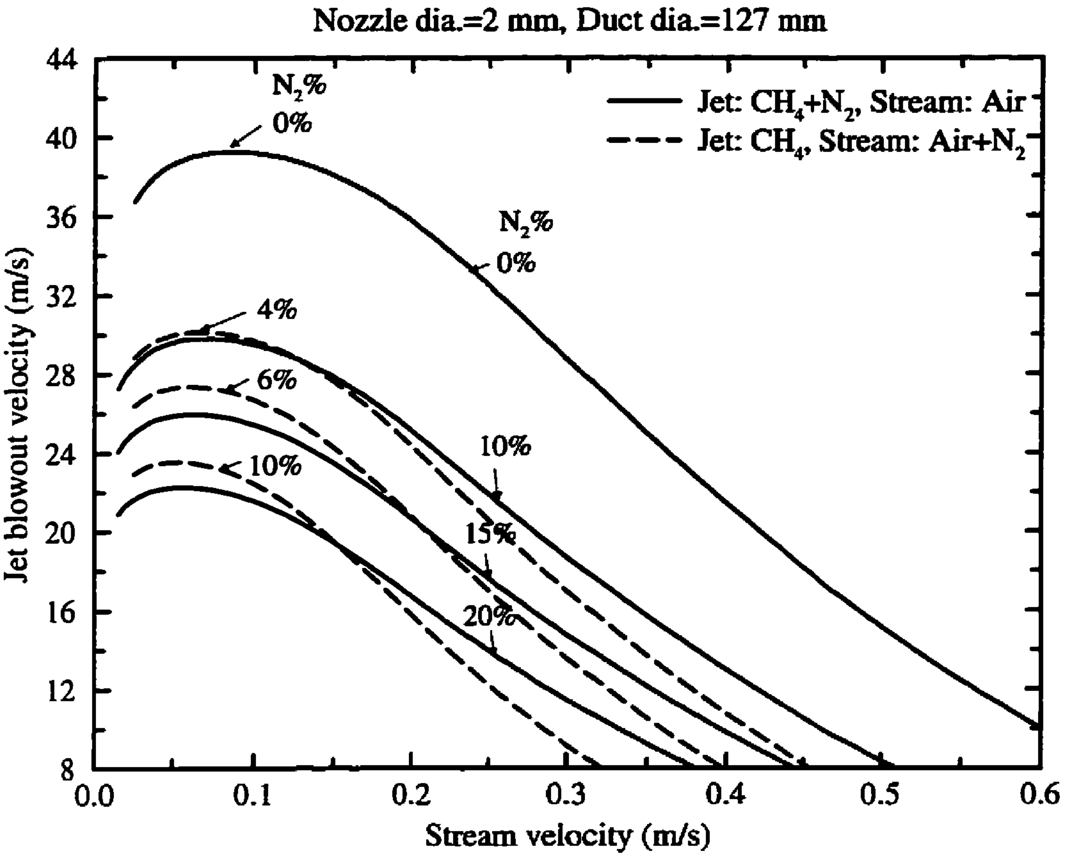

Figure 5.45: The blowout limits of methane or methane-nitrogen lifted flames as a function of co-flowing air or air-nitrogen stream velocity for different concentrations of nitrogen.

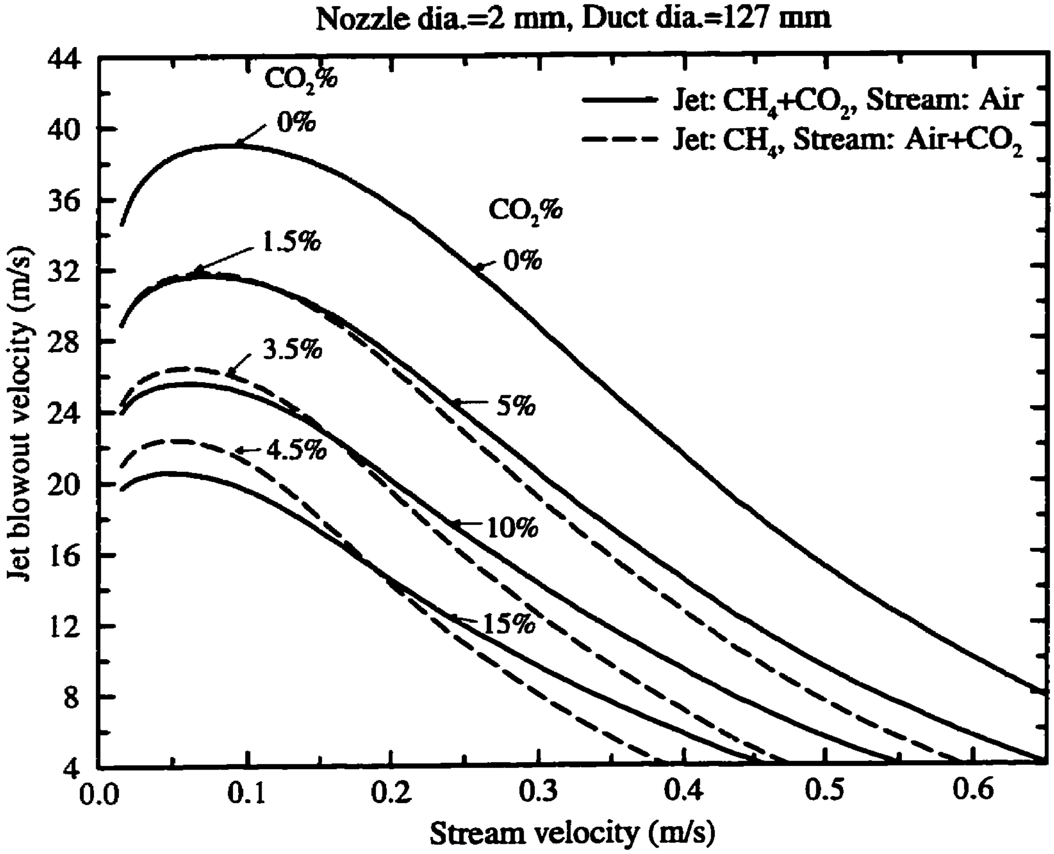

Figure 5.46: The blowout limits of methane or methane-carbon dioxide lifted flames as a function of co-flowing air or air-carbon dioxide stream velocity for different concentrations of carbon dioxide.

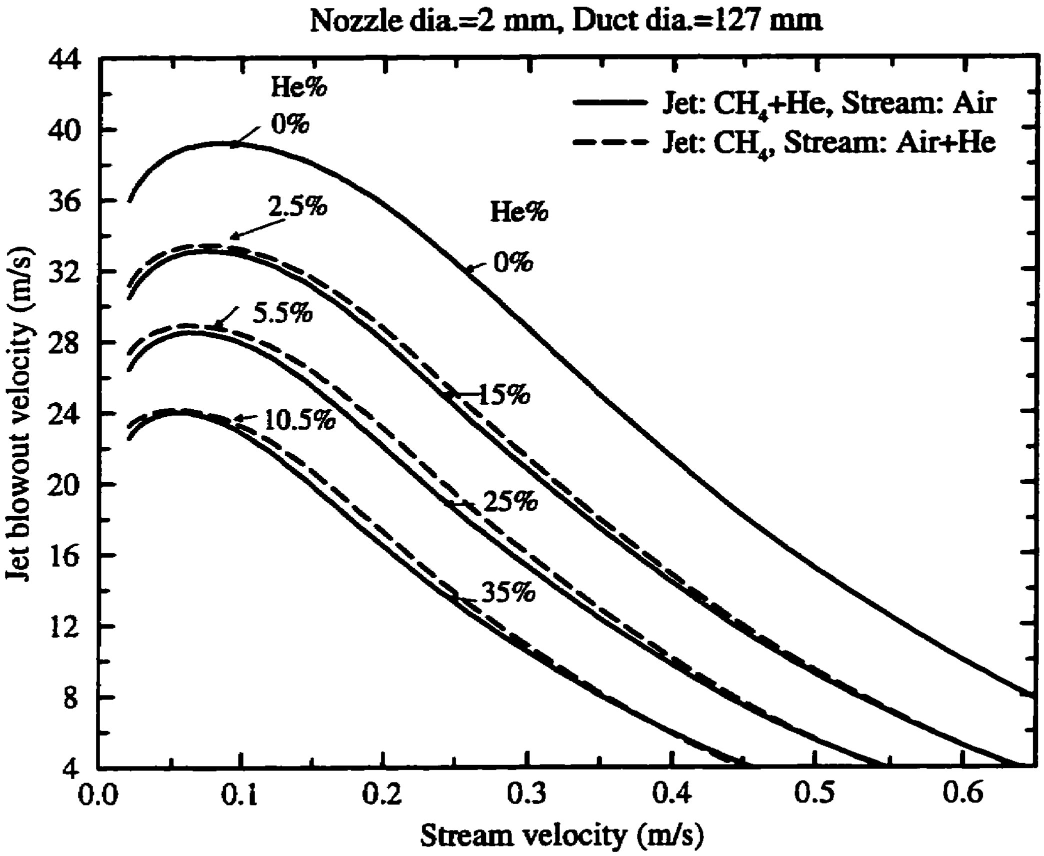

Figure 5.47: The blowout limits of methane or methane-helium lifted flames as a function of co-flowing air or air-helium stream velocity for different concentrations of helium.

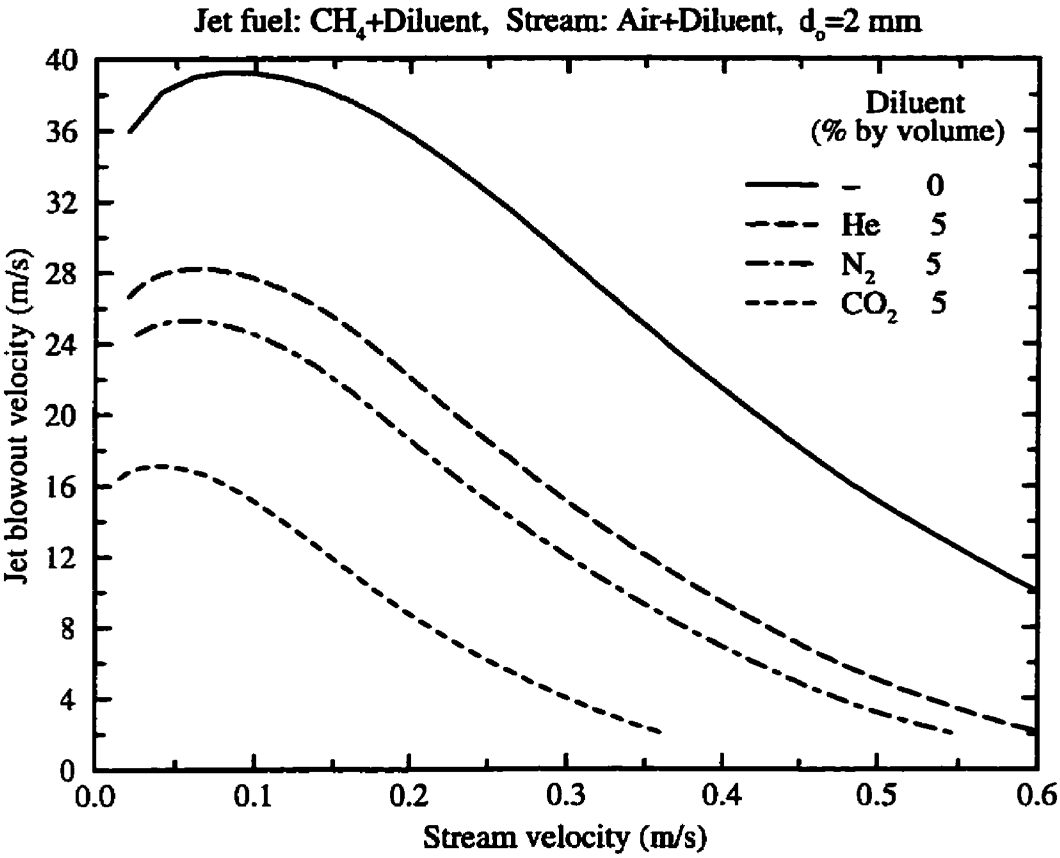

Figure 5.48: The blowout limits of methane-diluent lifted flames as a function of co-flowing air-diluent stream velocity for different diluents.

Chapter 6

Theoretical Study of Liftoff, Reattachment and the Blowout of Attached Flames

There are two stability limits for attached flames: liftoff limit and blowout limit. The liftoff limit corresponds to co-flowing stream velocities less than *limiting co-flowing stream velocity*, while the blowout limit corresponds to stream velocities larger than the limiting co-flowing stream velocity. The blowout of attached flames can be considered as a continuation of the liftoff curve. As mentioned before, the near-field conditions, i.e., in the vicinity of the nozzle rim, are responsible for stabilization of attached flames. Also these conditions are responsible for the reattachment phenomenon of lifted flames. Therefore in this chapter a single criterion is proposed to calculate the liftoff, the blowout of attached flames and the reattachment limits for a non-premixed jet flame into a co-flowing stream of air. This criterion is described in Section 6.1. The associated procedure of calculations is discussed in Section 6.2. Finally, the results are presented and discussed in Section 6.3.

6.1 Modeling of Stability Limits

An attempt was made to correlate experimentally established values of liftoff and reattachment limits as well as the blowout limits of attached flames. Using the velocity-gradient concept described in [44, 45, 66], in the present research, a dimensionless group was proposed to predict these limits at different operating conditions. This dimensionless group can be expressed as:

$$k_{LBR} = \frac{u_m \cdot \delta_u}{S_{L,max}(r_o \cdot r_\infty)^{1/2}} \tag{6.1}$$

The flame liftoff and blowout occur when this parameter, k_{LBR}, becomes larger than a certain critical value, i.e.,

$$k_{LBR} \geq (k_{LBR})_{Cr} \tag{6.2}$$

and the flame reattachment occur when,

$$k_{LBR} \leq (k_{LBR})_{Cr} \tag{6.3}$$

It is known that flame extinction takes place when the flame stretch exceeds a certain critical value. Also, it is reasonable to assume that the flame stretch is proportional to the flame length which itself is proportional to the distance (from the nozzle exit) where the concentration of jet fuel is close to its stoichiometric value. For attached flames the larger this distance, the larger is the stretch. Therefore, the product of $\delta_u \cdot u_m$ was evaluated at this distance.

6.2 Calculation Procedure

As mentioned before, the value of the proposed dimensionless criterion should be evaluated at a position where the concentration of jet fuel on the jet axis is equal to its stoichiometric value. This position can be calculated from Equation (5.32), i.e.,

$$\begin{aligned}\frac{r_o^2\rho_o u_o}{2r_\infty^2\rho_\infty u_\infty c_m} &= 0.043X^2\left[1+\left(\frac{X}{X_r}\right)^{5/3}\right]^2 \cdot \\ &\left[\frac{u_k}{X\cdot Ct\cdot u_\infty\left[1+\left(\frac{X}{X_u}\right)^{5/3}\right]}+0.19\right]\end{aligned}$$

where

$$c_m = \frac{L_{St}\cdot M_o}{L_{St}\cdot M_o+(100-L_{St})M_\infty} \tag{6.4}$$

where L_{St} is the stoichiometric limit of the fuel in air (% by volume).

Presently, there is no method available to estimate the critical value of $(k_{LBR})_{Cr}$ parameter from a purely theoretical approach. However, this value can be estimated on the basis of known experimental stability limits of jet flames. With this value, $(k_{LBR})_{Cr}$, known, the jet velocity at the stability limits, u_o, for different co-flowing stream velocities, u_∞, can be calculated using the above equations and Equation (6.1) with two unknown variables of u_o and X. The procedure and flowchart of calculations are similar to those described for the blowout of *lifted* flames in Section 5.2. The simulation program is given in Appendix A.

For attached flames, the jet flow in the nozzle near-field region is hot before the liftoff or the blowout but it is cold before the reattachment of lifted flames. Due to this fact the jet density was calculated at 2000 K to determine the liftoff and blowout limits while the jet density was calculated at 300 K to obtain the reattachment limits. To estimate the critical parameter $(k_{LBR})_{Cr}$, typical $u_o = f(u_\infty)$ curves were calculated for different values of k_{LBR} parameter and were compared with flame stability curves obtained experimentally. As a typical example, Figure 6.1 shows that for a methane jet discharged from a nozzle of type A, the value of $(k_{LBR})_{Cr}$ is about 2.8. The same method was used to determine the value of $(k_{LBR})_{Cr}$ for other conditions as well.

6.3 Results and Discussion

Calculations of liftoff, reattachment and blowout velocities of attached flames were conducted for different fuels, nozzle configurations, combustor sizes and co-flowing stream velocities. The results of calculations for methane, propane, ethylene and hydrogen jets are shown in Figures. 6.2, 6.3, 6.4 and 6.5 for a jet of 2 mm diameter issued into a duct of 127 mm hydraulic diameter. In these calculations, the maximum laminar burning velocities were assumed to be 0.41 m/s for methane, 0.46 m/s for propane, 0.79 m/s for ethylene and 2.8 m/s for hydrogen [75, 95, 97, 98]. The corresponding experimental data measured by the author are also shown in these figures for the sake of comparison. The nozzle A (Figure 3.2a) with a lip-thickness of 1.82 mm was used in these measurements.

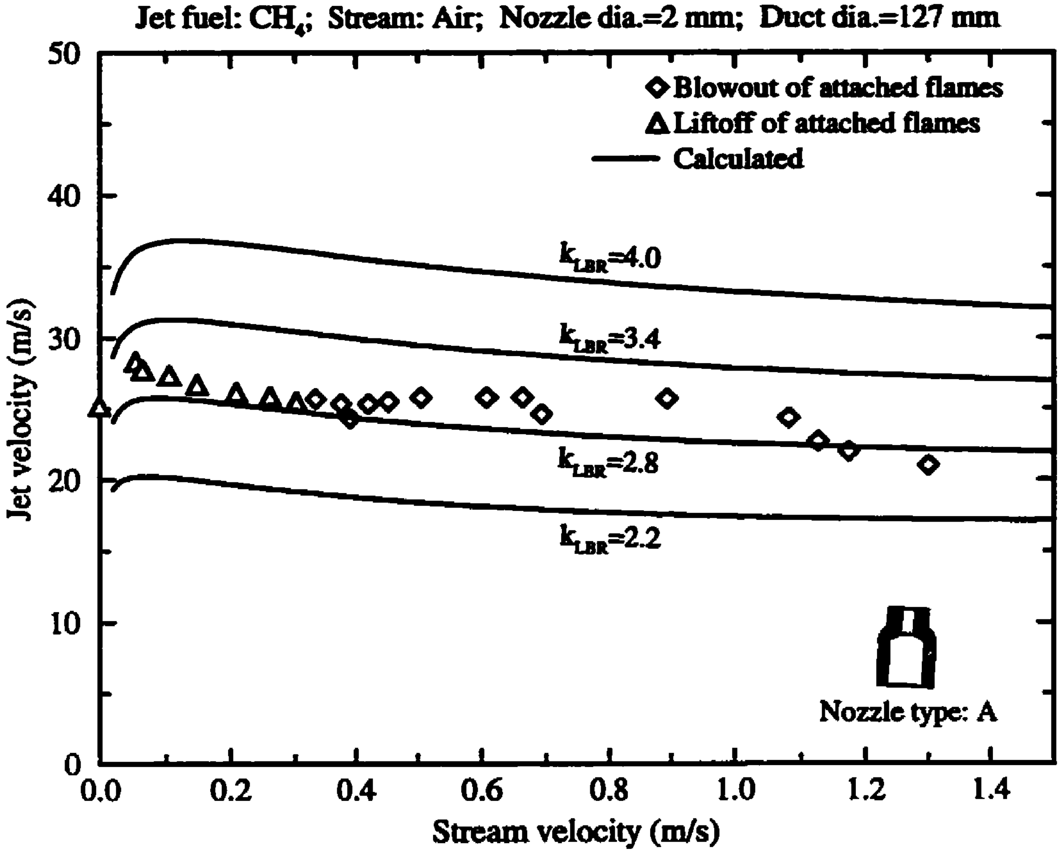

Figure 6.1: Calculated stability limits of methane jet flame as a function of co-flowing air stream velocity for different values of k_{LBR} parameter.

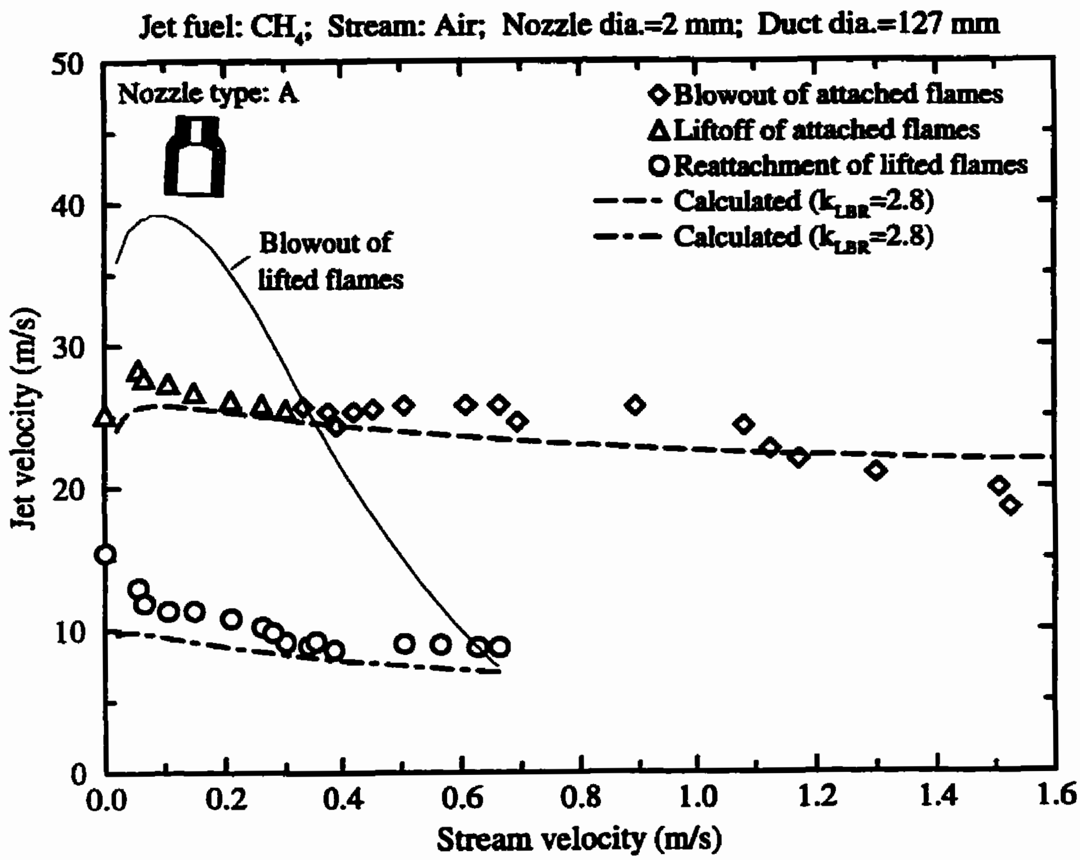

Figure 6.2: Calculated and experimental stability limits of methane jet flame as a function of co-flowing air stream velocity.

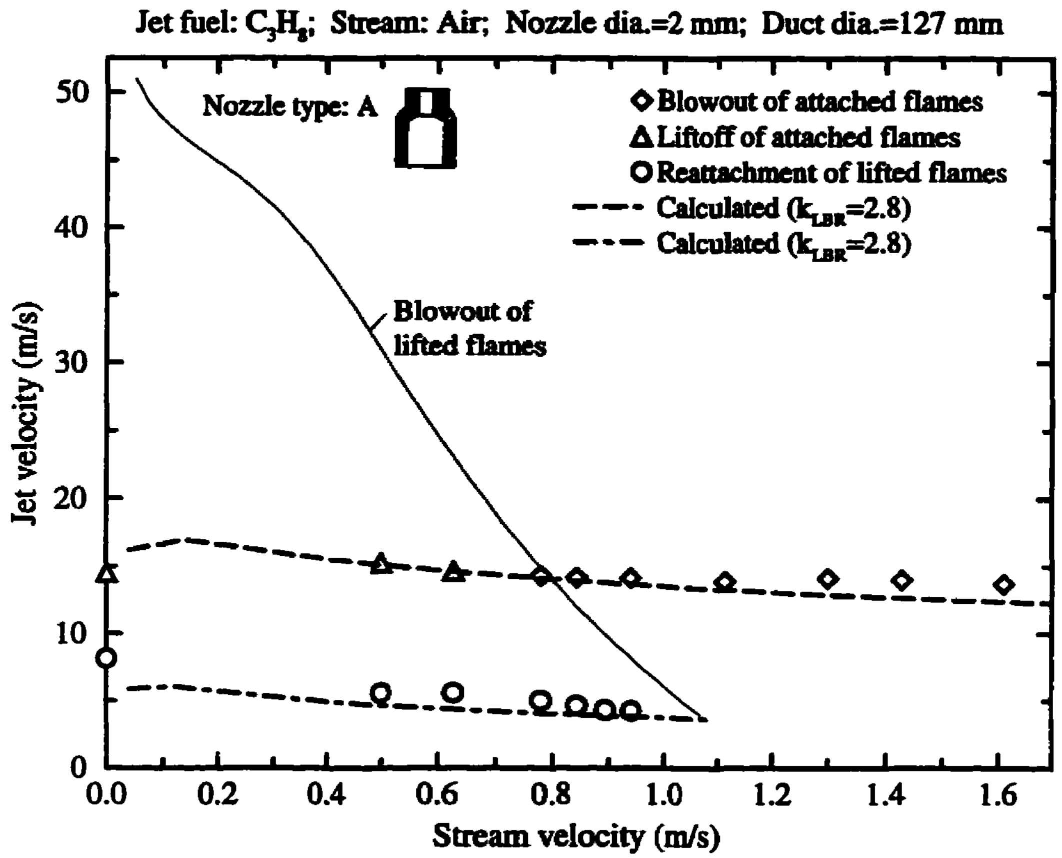

Figure 6.3: Calculated and experimental stability limits of propane jet flame as a function of co-flowing air stream velocity.

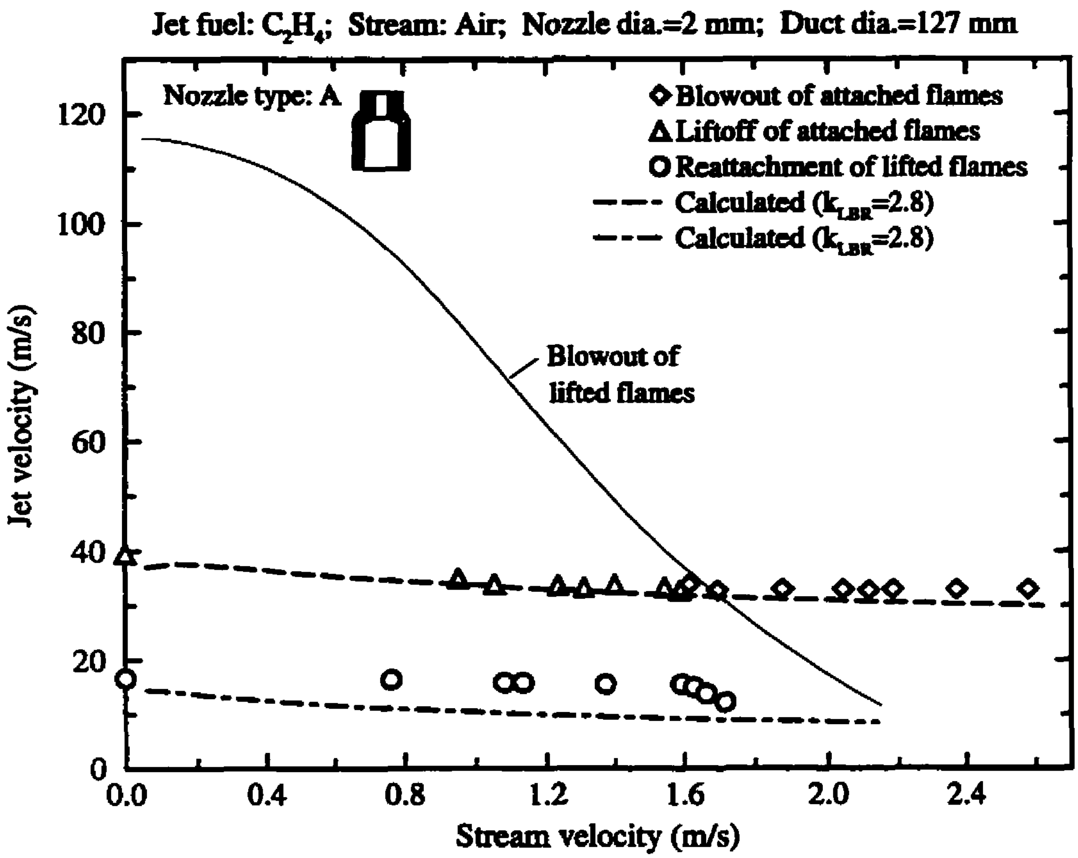

Figure 6.4: Calculated and experimental stability limits of ethylene jet flame as a function of co-flowing air stream velocity.

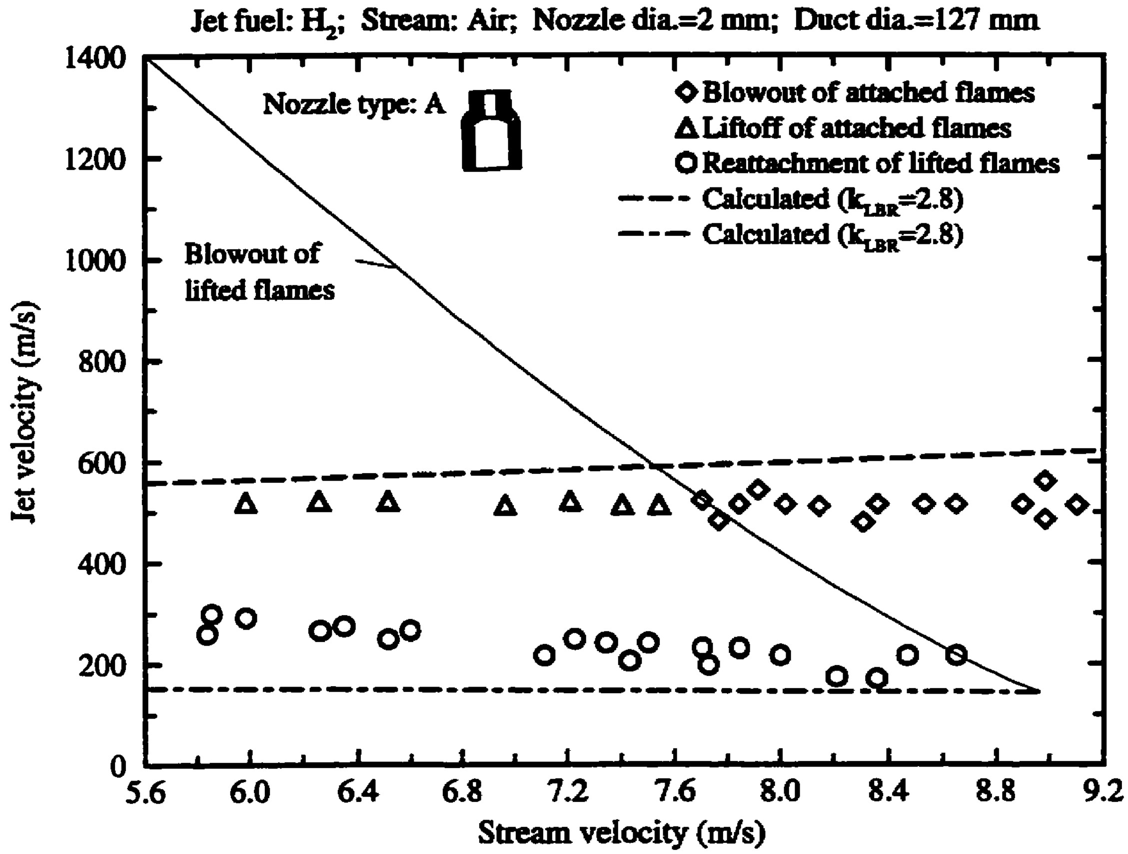

Figure 6.5: Calculated and experimental stability limits of hydrogen jet flame as a function of co-flowing air stream velocity.

It can be seen that for the range of co-flowing stream velocities shown in these figures, the calculated values of flame liftoff, blowout and reattachment velocities by assuming $(k_{LBR})_{Cr} = 2.8$ are in fairly good agreement with the experimental data. However, for methane and hydrogen jet flames, the calculated blowout velocities deviate somewhat (up to 12%) from those obtained experimentally. The precise measurement of these limits especially for hydrogen was extremely difficult. The hydrogen flame appeared in light blue and was hardly visible and its liftoff, blowout and reattachment phenomena took place suddenly.

As a result of the above discussion, the effect of co-flowing stream velocity and the fuel type on the liftoff, reattachment and blowout limits of attached flames can be estimated using the described method at a critical value of $k_{LBR} = 2.8$ for nozzle A.

6.3.1 Effect of Nozzle Shape and size

An attempt was made to verify the proposed method by the experimental data available in the literature for nozzles of different shapes and sizes [25,27, 30]. The experimental data for a nozzle B with 2 mm diameter and 0.2 mm lip-thickness (Figure 3.2b) and a combustor of 127 mm hydraulic diameter were reported in [27]. These data for methane, propane and ethylene jet flames are shown in Figures 6.7, 6.8 and 6.9, respectively. The liftoff data [25] for methane jet discharged from nozzle C (Figure 6.6a) are shown in Figure 6.10 for different nozzle diameters. The blowout limits of attached flames [30] for a methane jet discharged from nozzle D (Figure 6.6b) are also shown in Figure 6.11 for different nozzle diameters and lip-thicknesses.

Using the procedure described in Section 6.2 for determining the critical

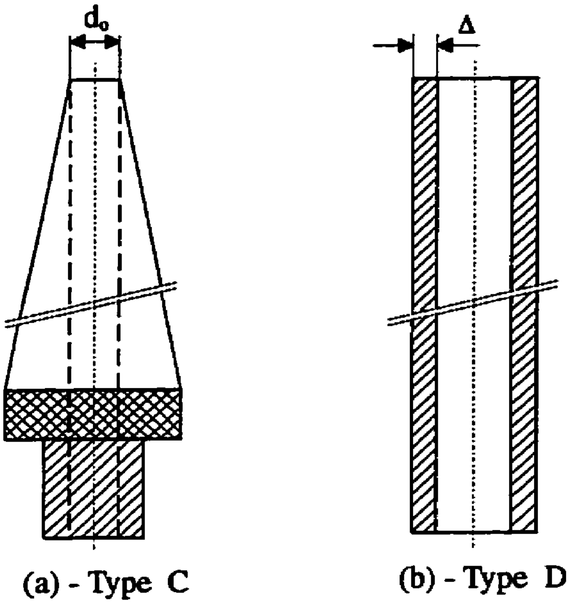

Figure 6.6: Configuration of nozzles used in: (a) - [25], (b) - [30].

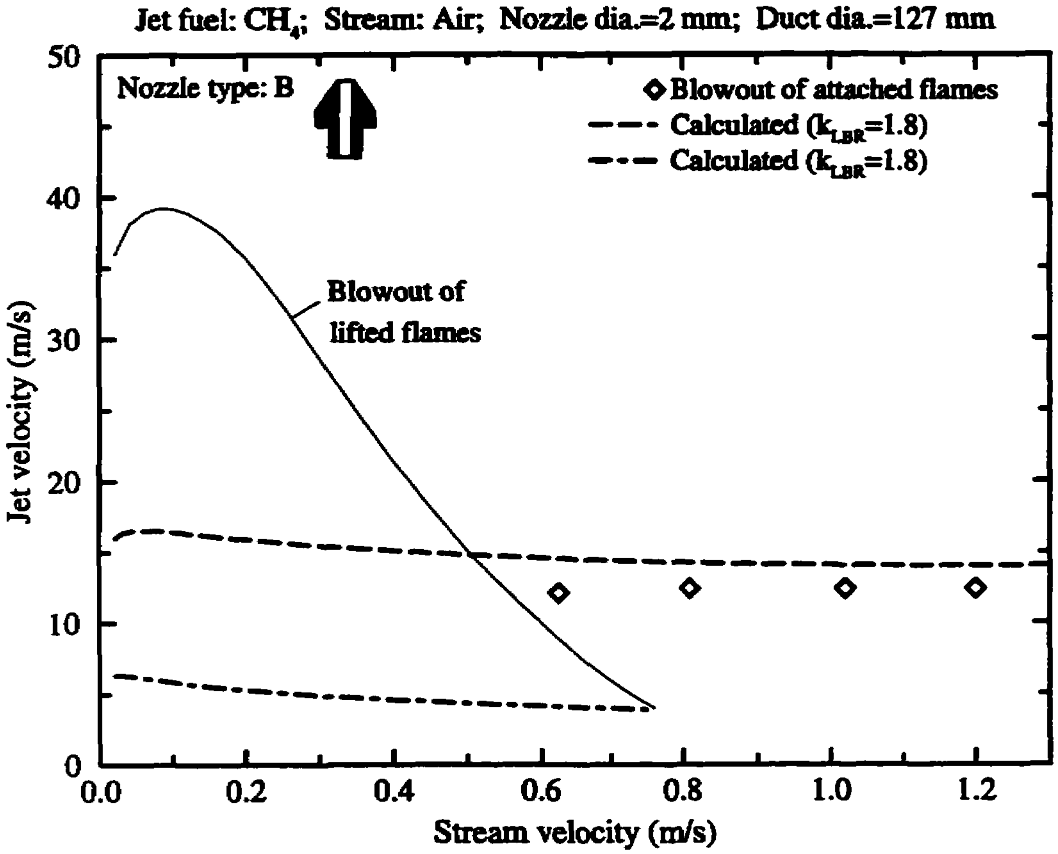

Figure 6.7: Calculated and experimental stability limits of methane jet flame as a function of co-flowing air stream velocity. Experimental data are from [27].

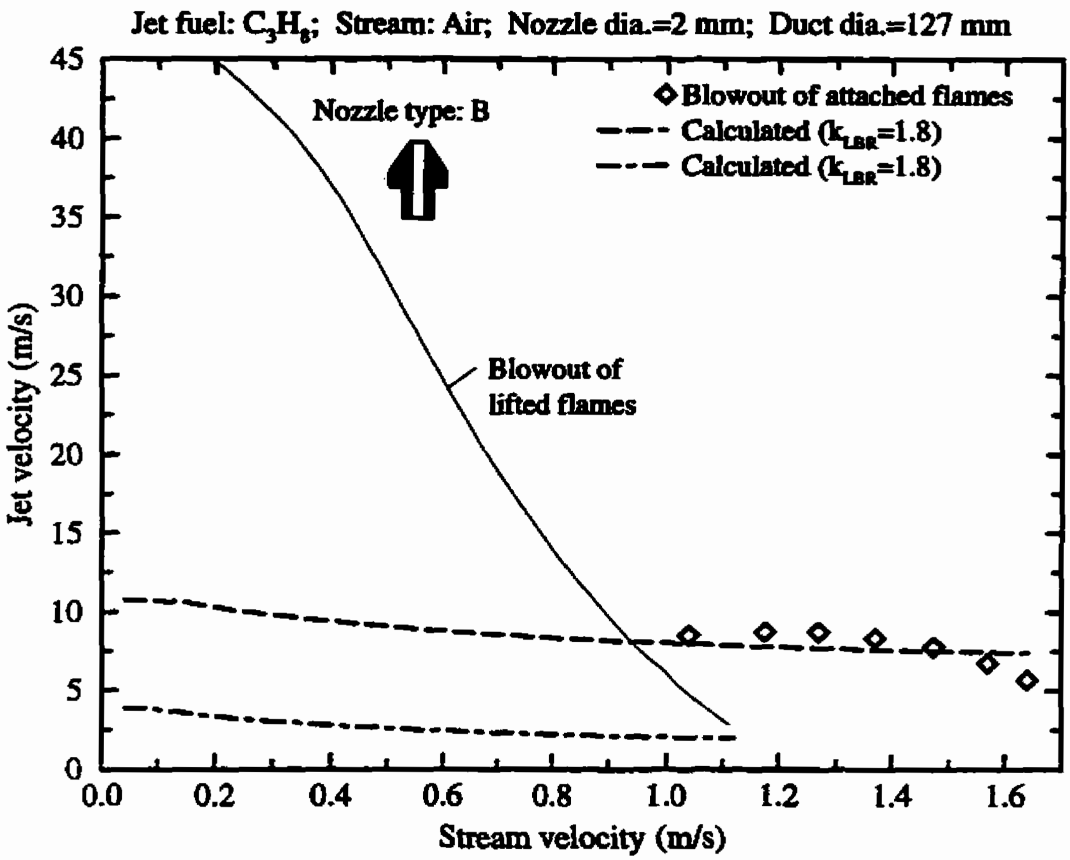

Figure 6.8: Calculated and experimental stability limits of propane jet flame as a function of co-flowing air stream velocity. Experimental data are from [27].

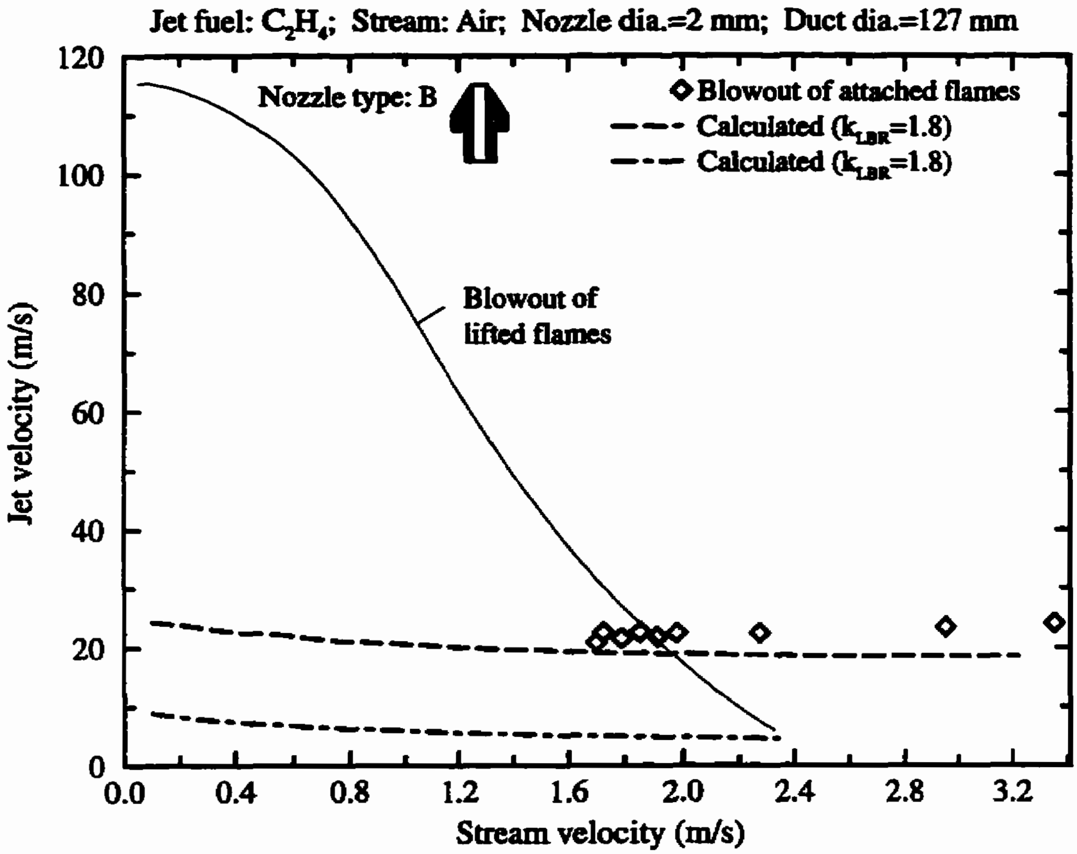

Figure 6.9: Calculated and experimental stability limits of ethylene jet flame as a function of co-flowing air stream velocity. Experimental data are from [27].

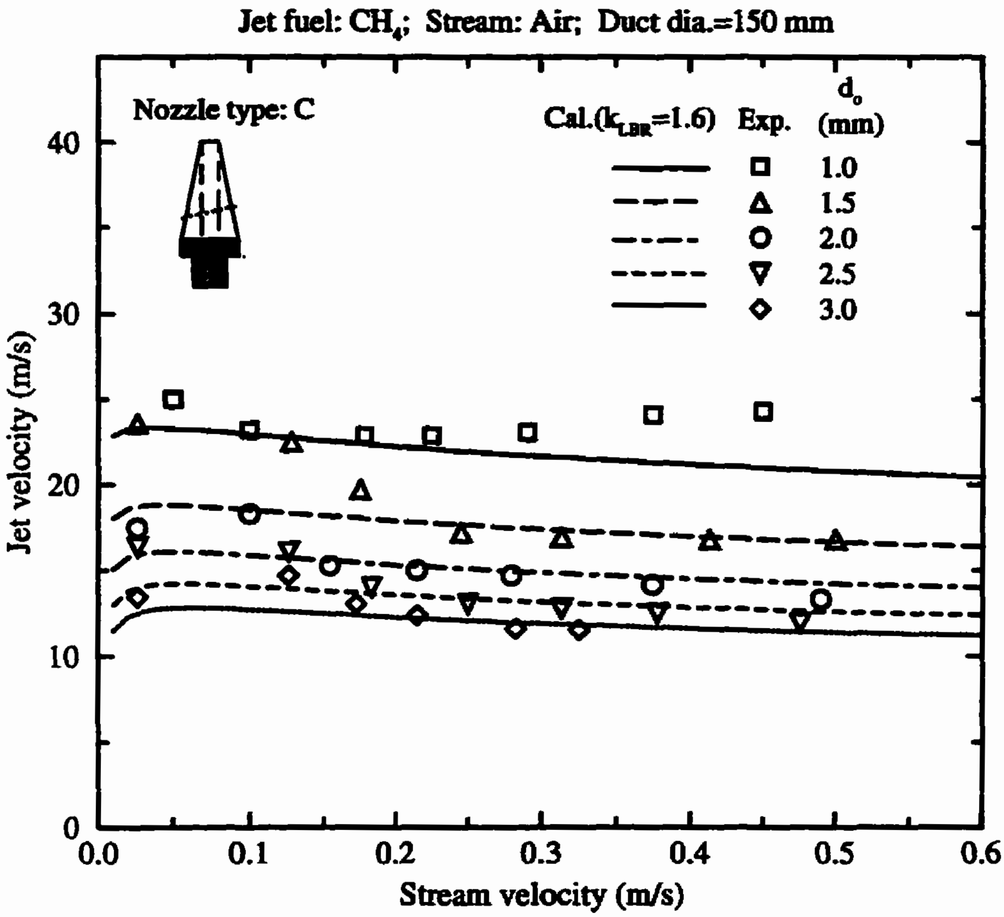

Figure 6.10: Calculated and experimental liftoff limits of methane jet flames as a function of co-flowing air stream velocity for different nozzle sizes. Experimental data are from [25].

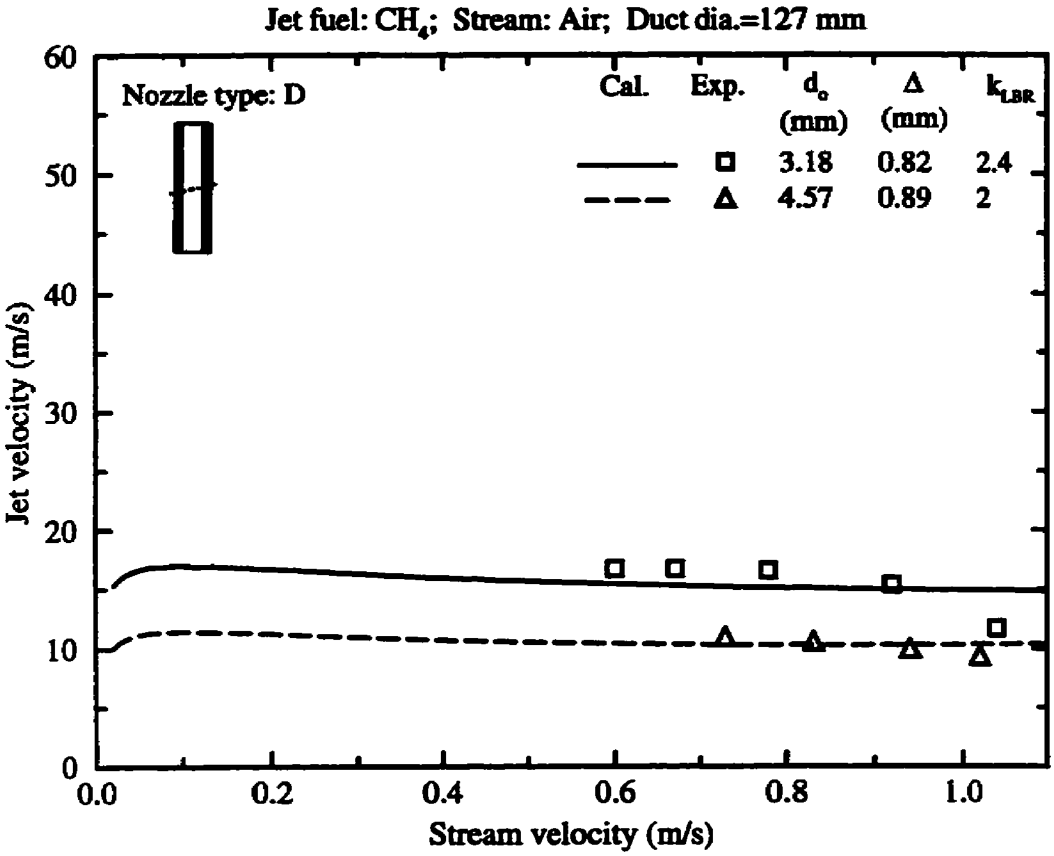

Figure 6.11: Calculated and experimental blowout limits of attached methane jet flames as a function of co-flowing air stream velocity for nozzles with different sizes and lip-thicknesses. Experimental data are from [30].

value of k_{LBR} parameter, it was found that $(k_{LBR})_{Cr}$ values are different for different nozzle shapes. It was found that $(k_{LBR})_{Cr}$ is approximately equal to 1.8 for nozzle B and 1.6 for nozzle C. Two different lip-thicknesses of nozzle D leads to two distinct values of 2.4 and 2 for $(k_{LBR})_{Cr}$.

The calculated blowout limits of attached flames are slightly higher than the experimental limits for methane jet flame as shown in Figure 6.7, but the agreement is good for ethylene and propane. Also, as can be seen in Figure 6.10, the effect of nozzle size on liftoff limit can be predicted fairly accurately using the same value of $(k_{LBR})_{Cr}$ (at co-flowing stream velocities larger than 0.15 m/s).

One of the applications of the proposed criterion, k_{LBR}, is in prediction of certain limits which were not investigated experimentally. For example, the experimental reattachment limits associated with the operating conditions of Figures 6.7, 6.8 and 6.9 are not reported. The value of $k_{LBR} = 1.8$ obtained for these conditions can be used to predict the reattachment limits. The calculation results for methane, propane and ethylene are shown in these figures.

The experimental stability limits of methane attached flames obtained by the author for nozzle A with two diameters of 2 and 2.82 mm and two respective lip-thicknesses of 1.82 and 1.33 mm are shown in Figure 6.12. In the same figure, the calculated stability limits for these two nozzles are shown using $(k_{LBR})_{Cr} = 2.8$ for the 2 mm nozzle and $(k_{LBR})_{Cr} = 2.6$ for the 2.82 mm nozzle. The effect of the size of nozzle A on the stability limits of attached flames was investigated by calculating these limits for different jet diameters and with the same value of $(k_{LBR})_{Cr} = 2.8$. The calculated results are shown in Figure 6.12. It can be seen that with an increase in the nozzle

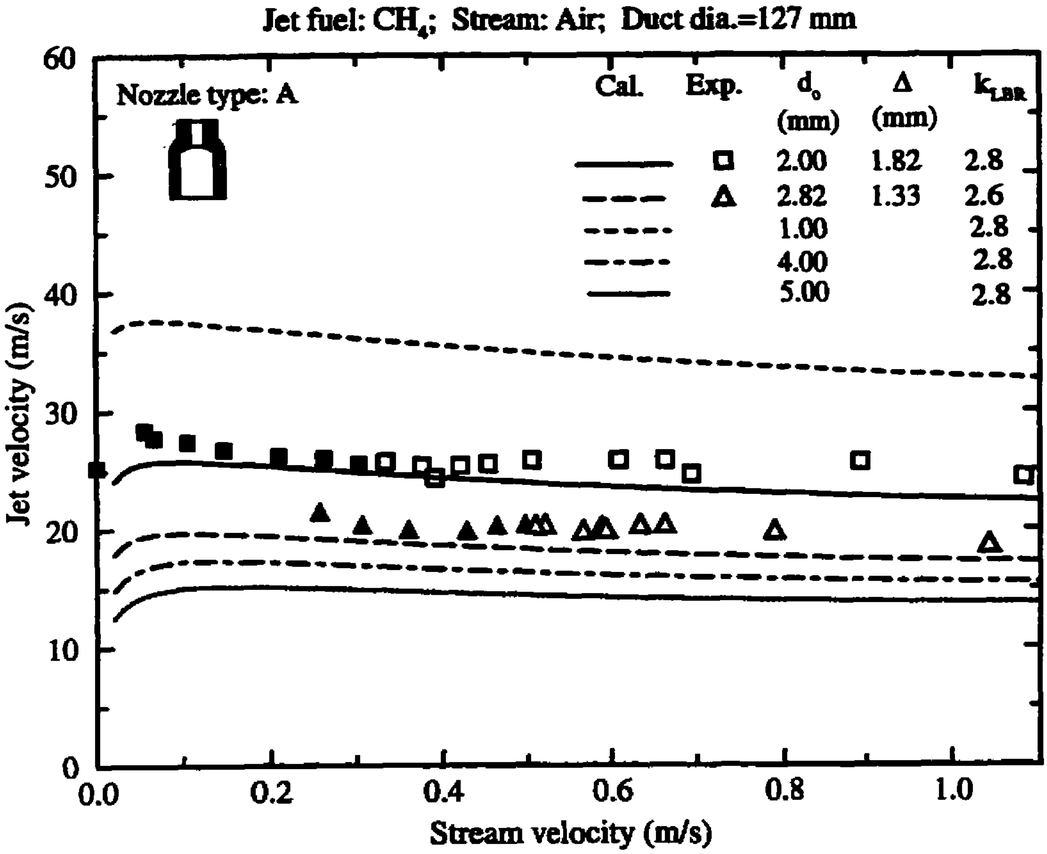

Figure 6.12: Calculated and experimental stability limits of attached methane jet flames as a function of co-flowing air stream velocity for nozzles with different sizes and lip-thicknesses. Solid symbols: liftoff limits; Open symbols: blowout limits.

size, the liftoff and the blowout limits of attached flames decrease.

For each nozzle shape used in the experimental measurements one unique value for $(k_{LBR})_{Cr}$ was obtained. These values are presented in Table 6.1. As can be seen nozzle A has the largest value of k_{LBR} followed by nozzle D, nozzle B and nozzle C. A larger value of $(k_{LBR})_{Cr}$ corresponded to a nozzle with a larger ratio of lip-thickness to diameter (Δ/d_o). Also, if the lip-thickness of a nozzle reduces over a larger length of the nozzle tube, the corresponding $(k_{LBR})_{Cr}$ is smaller (type C). Calculations showed that with an increase in the value of k_{LBR}, the stability limit of attached flames increases. Then the nozzle A results in the largest stability limits of attached flames followed by nozzle D, nozzle B and nozzle C. This can be due to the recirculation zone formed between co-flowing air and fuel jet in the case of thick-walled nozzles. This zone provides a significant stabilizing effect on the attached flame [18].

As a result, the same value of k_{LBR} can be used in the prediction of the stability limits of attached flames as a function of the co-flowing stream velocity for different fuels and nozzle diameters provided that the employed nozzles have the same shape.

Effect of Combustor Size. The experimental liftoff limits [25] obtained for nozzle C and a combustor size of 150 mm in diameter as well as the experimental blowout limits of attached flames [27] obtained for nozzle B and a combustor size of 127 mm in hydraulic diameter are shown in Figure 6.13 for comparison. As can be seen at a stream velocity of ~ 0.6 m/s, these limits are the same, i.e., the blowout curve is a continuation of the liftoff curve. This may conflict with the previous conclusion that nozzle B could result in slightly larger stability limit than nozzle C. But it should be noted that the measured stability limits with nozzle B and C correspond to

Table 6.1: The values of $(k_{LBR})_{Cr}$ obtained for different nozzle configurations.

Type of Nozzle	Shape of Nozzle	d_o (mm)	Δ (mm)	Δ/d_o	$(k_{LBR})_{Cr}$	d_∞(mm)
A		2	1.82	0.91	2.8	127
		2.82	1.33	0.47	2.6	127
B		2	0.2	0.1	1.8	127
C		2	$\approx$0.2	$\approx$0.1	1.6	150
D		3.18	0.82	0.26	2.4	127
		4.57	0.89	0.195	2	127

different combustor sizes. Calculations showed that for the same k_{LBR} the stability limits increase with an increase in combustor size (Figure 6.13). In spite of larger stability limits for nozzle B compared to nozzle C, utilization of a larger combustor size with nozzle C has lead to a better stability limit compared to the case utilizing nozzle B with a smaller combustor size. Since the difference between the stability limits for different nozzle shapes and combustor sizes are very small and comparable to experimental uncertanity, the above argument is not conclusive and further investigation is required.

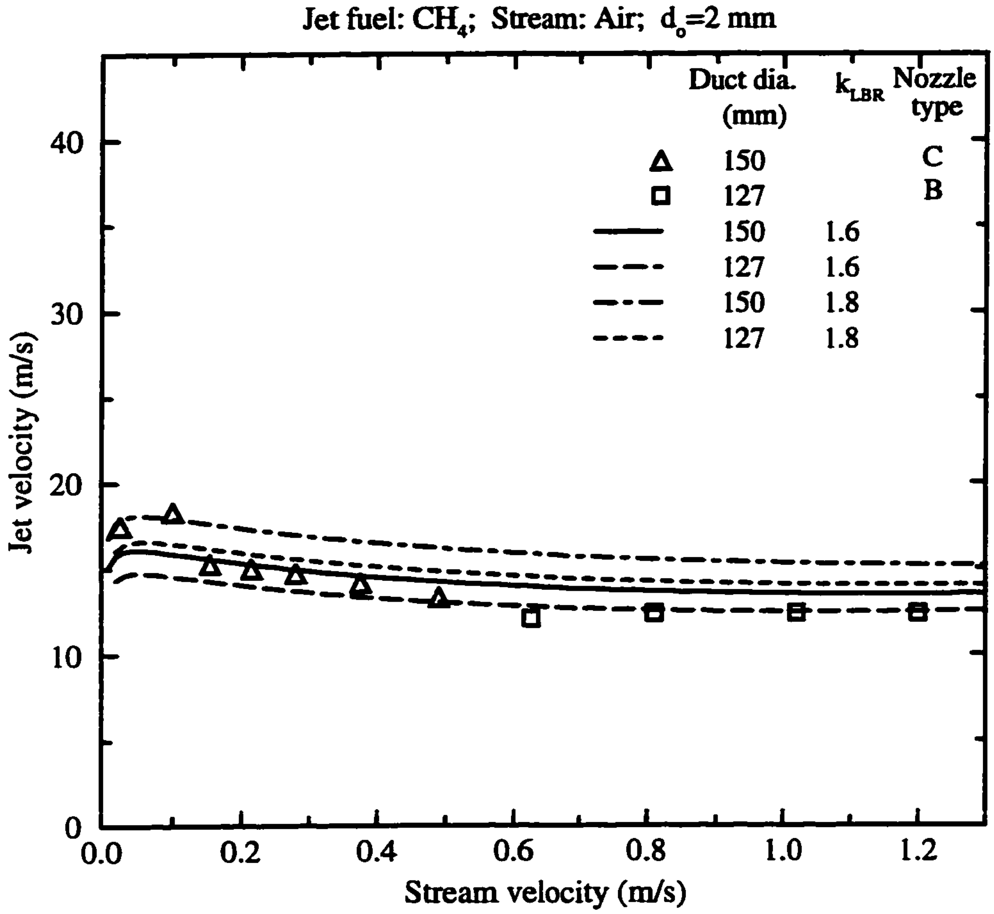

Figure 6.13: Calculated and experimental stability limits of attached methane jet flames as a function of co-flowing air stream velocity for different combustor sizes. △ - the liftoff data [25], □ - the blowout of attached flames [27].

In summary, obtaining a constant k_{LBR} for each nozzle shape provides an opportunity to predict the stability limits of attached flames and reattachment limits as a function of co-flowing stream velocity for different fuels, combustor sizes and nozzle diameters.

Chapter 7

Conclusions

7.1 Summary and General Conclusions

Based on the results obtained from both analytical modeling and experimental investigations in the present study, a number of conclusions can be made:

- For non-premixed jet flames in a co-flowing stream, four different types of flame stability limits were observed: liftoff, reattachment, the blowout of *lifted* flames and the blowout of *attached* flames. The co-flowing stream velocity has a significant effect on the stability behavior of a non-premixed jet flame. Depending on the magnitude of this velocity, three different regions were recognized. At low co-flowing stream velocities (region I), the blowout of *lifted* flames was observed while at higher co-flowing stream velocities (region III), the blowout of *attached* flames occurred. For mid values of stream velocities (region II), both types of blowout were experienced. The lifted flames were much less stable than the attached flames and should be avoided (in region II).

- Depending on the ignition conditions (i.e., the jet and stream velocities and ignitor position), the ignition of a jet fuel can result in either a *lifted* flame or an *attached* flame. The optimum ignition conditions for increased blowout limits of jet flames are a small jet velocity and placing the ignitor close to the nozzle rim. An ignition limit was recognized for attached flames. At jet velocities larger than this limit, no attached flames could be produced.

- Generally the blowout limits of a jet flame decrease with an increase in the stream velocity. The rate of decrease depends on whether the flame is *lifted* or *attached* before blowout. The blowout limits of *lifted* flames deteriorated very significantly with a small increase in the co-flowing stream velocity, while those for *attached* flames were much less sensitive to changes in the co-flowing stream velocities. The liftoff and reattachment limits were decreased slightly due to increasing the co-flowing stream velocity.

- The minimum stream velocity for occurrence of the blowout of *attached* flames (the limiting co-flowing stream velocity) was found to be dependent on the type of jet fuel, surrounding stream composition, nozzle diameter, but independent of the nozzle shape. The limiting stream velocity was higher for fuels with higher burning velocity and density and for nozzles with larger sizes. A correlation was proposed in this research to estimate the limiting stream velocity for different operational conditions. The limiting stream velocity was decreased to some extent with an addition of hydrogen (less than 50% addition) and then was increased with further addition of hydrogen (more than 50% addition). An addition of auxiliary fuel into surrounding air resulted in an increase in the limiting stream velocity.

- No significant effect of the nozzle shape was observed on the blowout of *lifted* flames; while the liftoff and blowout limits of *attached* flames were significantly affected by the nozzle shape especially by nozzle lip-thickness. An increase in nozzle lip-thickness enhanced flame stability limits. With increasing the nozzle diameter, the blowout velocities of *lifted* flames increased while the liftoff and blowout velocities of *attached* flames showed a reverse trend.

- The stability limits depends on the type of jet fuel. The blowout limits of *lifted* flames were the highest for hydrogen followed by ethylene, propane and methane. The liftoff, the reattachment and the blowout limits of *attached* flames were the highest for hydrogen followed by ethylene, methane and propane.

- An addition of an auxiliary fuel to the co-flowing air stream enhanced the blowout limits of the *lifted* flames more significantly than those of the *attached* flames. Individual additions of propane and ethylene with the same percentage to the co-flowing stream improved the methane jet flame blowout limits approximately by the same amount. Furthermore, hydrogen and methane when used as auxiliary fuels look alike for their improving effects on these limits. However, the enhancing effects on the blowout limit with propane and ethylene as auxiliary fuels were higher than that with hydrogen and methane.

- The diluent addition to the jet fuel and/or to the surrounding air stream decreased substantially the blowout limits of *lifted* flames. A higher degree of dilution leads to a higher drop in these limits. The most detrimental effect was observed with carbon dioxide as the diluent followed by nitrogen and then by helium. The presence of a diluent in the air stream affects the blowout limit more strongly than when it is present in the jet fuel at the same volume concentration.

- A model of *lifted* flames extinction was developed on the base of a well-recognized criterion. This criterion states that the ratio of the mixing time scale to characteristic combustion time scale is equal to its critical value at the blowout. Moreover, an original expression for the mixing time scale was proposed. The mixing time was calculated at the blowout location using experimentally derived correlations (available in the literature) for jet velocity and concentration profiles at any distance from nozzle. The model indicated that the jet fluid and the surrounding stream fluid properties such as laminar burning velocity, lean flammability limit and density have significant effects on the value of blowout limits. The effect of variations in the jet fuel composition and surrounding stream composition on the blowout limits was reflected on the value of blowout limits through these properties.

  The proposed model allowed calculation of the blowout limits of *lifted* flames for a wide range of operating conditions. This model was able to predict fairly accurately the effect on the blowout limits of *lifted* flames of many parameters such as co-flowing stream velocity, jet fuel type, nozzle diameter and combustor size as well as addition of a second fuel and/or diluent to the jet fuel and/or to the surrounding air stream. The advantages of the proposed model are its simplicity and short calculation time.

- A dimensionless criterion was also proposed to predict the liftoff, the blowout of *attached* flames and the reattachment limits of jet flames in a co-flowing air stream. To the knowledge of the author to date, no model has been reported for predicting these limits for non-premixed jet flames in a co-flowing air stream. The critical value of this criterion was only affected by the nozzle shape.

- Good agreement between calculated and experimental values of jet flame stability limits was obtained throughout.

7.2 Future Work

It was shown that the proposed models have the potential to predict the stability limits of non-premixed flames in a co-flowing stream. Further improvements in the accuracy of these models and their validities over a wider range of operating conditions are required.

In this research, the correlations used to calculate velocity and concentration profiles along the jet have been obtained from experimental results for a relatively narrow range of jet to stream velocities, nozzle and combustor sizes and density of jet and surrounding stream. Also, the effects of preferential diffusion on these profiles when hydrogen exists in air stream or in jet fuel were not investigated. Therefore, more precise and thorough correlations of these profiles are needed to minimize uncertainties in the estimation of flame stability limits. An effort has been made by the author to achieve more accurate velocity and concentration profiles using the FLUENT code. The results were encouraging, however, further investigation is required in order to achieve more accurate results.

Further investigations are also required to develop a correlation which describes the effect of nozzle shape on the stability limits of non-premixed *attached* jet flames and reattachment limits.

References

[1] Feikema, D., Chen, R., and Driscoll, J.F., "Blowout of nonpremixed flames: Maximum coaxial air velocities achievable, with and without swirl", *Combustion and Flame*, vol. 86, pp. 347–358, 1991.

[2] Dahm, W.J.A. and Dibble, R.W., "Coflowing turbulent jet diffusion flame blowout", in *Twenty-Second Symposium (International) on Combustion, The Combustion Institute*, 1988, p. 801.

[3] Karim, G.A., Wierzba, I., and Hanna, M., "The blowout limit of a jet diffusion flame in a coflowing stream of lean gaseous fuel-air mixtures", *Combustion and Flame*, vol. 57, pp. 283–288, 1984.

[4] Karim, G.A., Kibrya, M., Lapucha, R., and Wierzba, I., "Examination of the combustion of a fuel jet in a homogeneously premixed lean fuel-air stream", in *Proceedings of the International Fuels and Lubricants Meeting and Exposition, SAE paper No. 881662*, 1988, p. 1.

[5] Wierzba, I., Kar, K., and Karim, G.A., "An experimental investigation of the blowout limits of a jet diffusion flame in co-flowing streams of different velocity and composition", *Journal of Energy Resources Technology, Transactions of A.S.M.E.*, vol. 115, pp. 142–147, 1993.

[6] Feikma, D., Chen, R., and Driscoll, J.F., "Enhancement of flame blowout limits by use of swirl", *Combustion and Flame*, vol. 80, pp. 183–195, 1990.

[7] Kalghatgi, G.T., "Blow-out stability of gaseous jet diffusion flames. part I: In still air", *Combustion Science and Technology*, vol. 26, pp. 233–239, 1981.

[8] Kalghatgi, G.T., "Lift-off heights and visible lengths of vertical turbulent jet diffusion flames in still air", *Combustion Science and Technology*, vol. 41, pp. 17–29, 1984.

[9] Gollahalli, S.R., Savas, O., Huang, R.F., and Rodriquez, J.L., "Structure of attached and lifted gas jet flames in hysteresis region", in *Twenty-first Symposium (International) on Combustion, The Combustion Institute*, 1986, pp. 1463–1471.

[10] Eickhoff, H., Lenze, B., and Leuckel, W., "Experimental investigation on the stabilization mechanism of jet diffusion flames", in *Twentieth Symposium (International) on Combustion, The Combustion Institute*, 1984, p. 311.

[11] Savas, S.S.O and Gollahalli, S.R., "Structure of a split gas flame", *Combustion and Flame*, vol. 73, pp. 221–232, 1988.

[12] Lee, B.J., Kim, J.S., and Chung, S.H., "Effect of dilution on the liftoff of non-premixed jet flames", in *Twenty-Fifth Symposium (International) on Combustion, The Combustion Institute*, 1994, pp. 1175–1181.

[13] Vranos, A., Taback, E.D., and Shipman, C.W., "An experimental study of the stability of hydrogen-air diffusion flames", *Combustion and Flame*, vol. 12, No.3, pp. 253–260, 1968.

[14] Yuasa, S., "Effects of swirl on the stability of jet diffusion flames", *Combust. Flame*, vol. 66, pp. 181–192, 1986.

[15] Takahashi, F., Mizomoto, M., and Ikai, S., "Stability of hydrogen jet diffusion flames", in *Hydrogen Energy Progress, Proceedings of the 3rd World Hydrogen Energy Conference, Tokyo, Japan*, 1980, pp. 1156–1176.

[16] Takahashi, F., Mizomoto, M., Ikai, S., and Futaki, N., "Lifting mechanism of free jet diffusion flames", in *Twentieth Symposium (International) on Combustion, The Combustion Institute*, 1984, p. 295.

[17] Takahashi, F., Mizomoto, M., Ikai, S., and Tsuruyama, K., "Stability limits of hydrogen/air coflow jet diffusion flames", *AIAA paper, No. 90-0034*, 1990.

[18] Takahashi, F. and Schmoll, W.J., "Lifting criteria of jet diffusion flames", in *Twenty-Third Symposium (International) on Combustion, The Combustion Institute*, 1990, p. 677.

[19] Takahashi, F. and Goss, L.P., "Near-field turbulent structures and the local extinction of jet diffusion flames", in *Twenty-Fourth Symposium (International) on Combustion, The Combustion Institute*, 1992, p. 351.

[20] Takeno, T. and Kotani, Y., "An experimental study on the stability of jet diffusion flame", *Acta Astronautica*, vol. 2, pp. 999–1008, 1975.

[21] Coats, C.M. and Zhao, H., "Transition and stability of turbulent jet diffusion flames", in *Twenty-Second Symposium (International) on Combustion, The Combustion Institute*, 1988, p. 685.

[22] Prasad, A., Gundavelli, S., and Gollahalli, S.R., "Characteristics of diluent-caused lifted gas jet flames", *Journal of Propulsion and Power*, vol. 7,No. 5, pp. 659–667, 1991.

[23] Chao, Y. and Jeng, M., "Behavior of the lifted jet flame under acoustic excitation", in *Twenty-Fourth Symposium (International) on Combustion, The Combustion Institute*, 1992, pp. 333–340.

[24] Chen, T.H., Goss, L.P., Talley, D.G., and Mikolaitis, D.W., "Dynamic stabilization zone structure of jet diffusion flames from liftoff to blowout", *Journal of Propulsion and power*, vol. 8, No. 3, pp. 548–552, 1992.

[25] Kibrya, M.G., *An experimental and analytical examination of jet diffusion flames in non-quiescent environments of fuel and air*, PhD thesis, Department of Mechanical Engineering, University of Calgary, Jan. 1987.

[26] Seaba, J.P., Chen, L.D., and Roquemore, W.M., "Liftoff characteristics of methane jet diffusion flames", *Journal of Propulsion and Power*, vol. 9, No. 4: Technical notes, pp. 654–656, 1993.

[27] Wierzba, I. and Oladipo, A.B., "Blowout of jet diffusion flames in coflowing air stream", in *Proceedings of 24th ASME Energy-Sources Technology Conference*, Jan. 1994, vol. PD-57, p. 29.

[28] Yoon, Y., Donbar, J.M., and Driscoll, J.F., "Blowout stability limits of a hydrogen jet flame in a supersonic, heated, coflowing air stream", *Combustion Science and Technology*, vol. 97, pp. 137–156, 1994.

[29] Papanikolaou, N. and Wierzba, I., "Effect of burner geometry on the blowout limits of jet diffusion flames in a co-flowing oxidizing stream", *Proceedings of ASME Energy & Environmental Expo 95, Emerging Energy Technology Symposium*, vol. 66, pp. 29–35, 1995.

[30] Papanikolaou, N. and Wierzba, I., "The effects of burner geometry and fuel composition on the stability of a jet diffusion flame", *Proceedings of ASME Energy week conference, Emerging Energy Technology*, vol. I, pp. 8–13, 1996.

[31] Kim, S.J. and Shin, H.D., "A visual study of the structure of turbulent nonpremixed flame near jet exit", *Combustion Science and Technology*, vol. 99, pp. 37–49, 1994.

[32] Dimotakis, P.E., Miake-Lye, R.C., and Papantoniou, D.A., "Structure and dynamics of round turbulent jets", *Physics of fluids*, vol. 26, No.11, pp. 3185–3192, 1983.

[33] Mungal, M.G., Karasso, P.S., and Lozano, A., "The visible structure of turbulent jet diffusion flames: Large-scale organization and flame tip oscillation", *Combustion Science and Technology*, vol. 76, pp. 165–185, 1991.

[34] Mungal M.G. and O'Neil J.M., "Visual observations of a turbulent diffusion flame", *Combustion and Flame*, vol. 78, pp. 377–389, 1989.

[35] Schefer, R.W., Namazian, M., Filtopoulos, E.E.J., and Kelly, J., "Temporal evolution of turbulence/chemistry interactions in lifted, turbulent-jet flames", in *Twenty-Fifth Symposium (International) on Combustion, The Combustion Institute*, 1994, pp. 1223–1231.

[36] Schefer, R.W., Namazian, M., and Kelly, J., "Stabilization of lifted turbulent-jet flames", *Combustion and flame*, vol. 99, pp. 75–86, 1994.

[37] Pitts, W.M., "Larg-scale turbulent structures and the stabilization of lifted turbulent jet diffusion flames", in *Twenty-Third Symposium (International) on Combustion, The Combustion Institute*, 1990, p. 661.

[38] Karbasi, M. and Wierzba, I., "Prediction and validation of blowout limits of co-flowing jet diffusion flames - effect of dilution", *accepted for publication in Journal of Energy Resources Technology, ASME*, 1997.

[39] Karbasi, M. and Wierzba, I., "The effect of hydrogen addition on the stability limits of methane jet diffusion flames", *accepted for publication in International Journal of Hydrogen Energy*, 1997.

[40] Vanquickenborne, L. and Van Tiggelen, A., "The stabilization mechanism of lifted diffusion flames", *Combustion and Flame*, vol. 10, pp. 59–69, 1966.

[41] Günther, R., Horch, K., and Lenze, B., "The stabilization mechanism of free jet diffusion flames", in *Combustion Institute (U.S.), 1ST Meeting, University of Bordeaux, France*, 1981, pp. 117–122.

[42] Günther, R. and Lenze, B., "The stability of free jet diffusion flames", in *14th World Gas Conference, Toronto, International Gas Union*, 1979, pp. 1–15.

[43] Miake-Lye, R.C. and Hammer, J.A., "Lifted turbulent jet flames: A stability criterion based on the jet large-scale structure", in *Twenty-Second Symposium (International) on Combustion, The Combustion Institute*, 1988, p. 817.

[44] Kremer, H., Minx, E., and Rawe, R., "Stabilization of parallel-flow turbulent jet diffusion flames by means of flame-holders", in *Combustion Institute European Symposium*, 1973, p. 536.

[45] Rawe, R. and Kremer, H., "Stability limits of natural gas diffusion flames with swirl", in *Eighteenth Symposium (International) on Combustion, The Combustion Institute*, 1981, pp. 667–677.

[46] Dahm, W.J.A. and Mayman, A.G., "Blowout limits of turbulent jet diffusion flames for arbitrary source conditions", *AIAA Journal*, vol. 28, No.7, no. 7, pp. 1157–1162, 1990.

[47] Kaplan, C.R., Oran, E.S., and Baek, S.W., "Stabilization mechanism of lifted jet diffusion flames", in *Twenty-Fifth Symposium (International) on Combustion, The Combustion Institute*, 1994, pp. 1183–1189.

[48] Byggstoyl, S. and Magnussen, B.F., "A model for flame extinction in turbulent flow", in *Turbuelnt Shear Flows 4, International Symposium on Turbulent Shear Flows, Berlin, Springer-Verlag, (L.J.S. Bradbury et al. ed.)*, 1985, pp. 381–395.

[49] Peters, N., "Partially premixed diffusion flamelets in non-premixed turbulent combustion", in *Twentieth Symposium (International) on Combustion, The Combustion Institute*, 1984, p. 353.

[50] Muller, C.M., Breitbach, H., and Peters, N., "Partially premixed turbulent flame propagation in jet flames", in *Twenty-Fifth Symposium (International) on Combustion, The Combustion Institute*, 1994, pp. 1099–1106.

[51] Sanders, J.P.H. and Lamers, A.P.G.G., "Modeling and calculation of turbulent lifted diffusion flames", *Combustion and Flame*, vol. 96, pp. 22–33, 1994.

[52] Broadwell, J.E., Dahm, W.J.A., and Mungal, M.G., "Blowout of turbulent diffusion flames", in *Twentieth Symposium (International) on Combustion, The Combustion Institute*, 1984, p. 303.

[53] Pitts, W.M., "Importance of isothermal mixing processes to the understanding of lift-off and blowout of turbulent jet diffusion flames", *Combustion and Flame*, vol. 76, pp. 197–212, 1989.

[54] Gran, I.R., Melaaen, M.C., and Magnussen, B.F., "Numerical simulation of local extinction effects in turbulent combustor flows of methane and air", in *Twenty-Fifth Symposium (International) on Combustion, The Combustion Institute*, 1994, pp. 1283–1291.

[55] Peters, N. and Williams, F.A., "Liftoff characteristics of turbulent jet diffusion flames", *AIAA Journal*, vol. 21, No.3, pp. 423–429, 1983.

[56] Byggstoyl, S. and Magnussen, B.F., "A model for flame extinction in turbulent flow", in *Fourth Symposium on Turbulent Shear Flows*, 1983, p. 10.32.

[57] Lockwood, F.C. and Megahed, I.E.A., "Extinction in turbulent reacting flows", *Combustion Science and Technology*, vol. 19, pp. 77–80, 1978.

[58] Karbasi, M. and Wierzba, I., "Prediction of blowout of jet diffusion flames in a confining stream of air", *Proceedings of 1994 Spring Technical Meeting of the Combustion Institute, Canadian Section, Kingston*, 1994.

[59] Karbasi, M. and Wierzba, I., "Prediction of the blowout of jet diffusion flames in a coflowing stream of air", *Proceedings of ASME Energy & Environmental Expo 95, Emerging Energy Technology Symposium*, vol. 66, pp. 21–27, Jan. 1995.

[60] Karbasi, M. and Wierzba, I., "Prediction and measurement of blowout limit of fuel-diluent jet diffusion flames in co-flowing stream of air-diluent mixtures", *Proceedings of 1995 Spring Technical Meeting of the Combustion Institute, Canadian Section, Victoria*, pp. 165–169, 1995.

[61] Karbasi, M. and Wierzba, I., "Prediction and validation of blowout limits of co-flowing jet diffusion flames - effect of dilution", *ASME Energy Week Conference & Exhibition, Emerging Energy Technology*, vol. I, pp. 1–7, 1996.

[62] Karbasi, M. and Wierzba, I., "The stability of diffusion flames of methane-hydrogen mixtures", *Proceedings of 1996 Spring Technical Meeting of the Combustion Institute, Canadian Section, Waterloo, Ontario*, p. 26, 1996.

[63] Scholefield, D.A. and Garside, J.E., "The structure and stability of diffusion flames", in *Third Symposium on Combustion, Flame and Explosion Phenomena*, 1949, pp. 102–110.

[64] Karbasi, M. and Wierzba, I., "The effect of hydrogen addition on the stability limits of methane jet diffusion flames", *Hydrogen Energy Progress*

XI, the 11th World Hydrogen Energy Conference, Germany, vol. 2, pp. 1557–1567, 1996.

[65] Lewis, B. and von Elbe, G., "Stability and structure of burner flames", *Journal of Chemical Physics*, vol. 11, pp. 75–97, 1943.

[66] Putnam, A.A. and Jensen, R.A., "Application of dimensionless numbers to flash-back and other combustion phenomena", in *Third Symposium (International) on Combustion, The Combustion Institute*, 1949, p. 89.

[67] Pitts, W.M., "Assessment of theories for the behavior and blowout of lifted turbulent jet diffusion flames", in *Twenty-Second Symposium (International) on Combustion, The Combustion Institute*, 1988, p. 809.

[68] Biringen, S., "An experimental study of a turbulent axisymmetric jet issuing into a coflowing airstream", *Von Karman Institute for Fluid Dynamics, Tech. Note 110*, 1975.

[69] Kar, K., "Experimental study of flame-blowout and flashback in a system involving fuel jet within homogeneous turbulent stream of air and fuel", Master's thesis, Department of Mechanical Engineering, University of Calgary, Dec. 1990.

[70] Wohl, K., Kapp, N.M., and Gazley, C., "Flame stabilization and quenching", in *Third Symposium on Combustion and Flame and Explosion Phenomena*, 1949, pp. 3–21.

[71] Field, M.A., Gill, D.W., Morgan, B.B., and Hawksley, P.G.W., *Combustion of Pulverised Coal*, The British Coal Utilisation Research Association, 1967.

[72] Steward, F.R. and Guruz, A.G., "Aerodynamics of a confined jet with variable density", *Combustion Science and Technology*, vol. 16, pp. 29–45, 1977.

[73] Gladnick, P.G., Enotiadis, A.C., LaRue, J.C., and Samuelsen, G.S., "Near-field characteristics of a turbulent coflowing jet", *AIAA Journal*, vol. 28, No. 8, pp. 1405–1414, 1990.

[74] Tseng, L.K., Ismall, M.A., and Faeth, G.M., "Laminar burning velocities and Markstein Numbers of hydrocarbon / air flames", *Combustion and flame*, vol. 95, pp. 410–426, 1993.

[75] Raezer, S.D. and Olsen, H.L., "Measurement of laminar flame speeds of ethylene-air and propane-air mixtures by double kernel method", *Combustion and Flame*, vol. 6, pp. 227–232, 1962.

[76] Glassman, I., *Combustion*, Academic press, Second Editiion, 1987.

[77] Tennekes, H. and Lumley, J.L., *A First Course in Turbulence*, M.I.T. Press, Cambridge, 1972.

[78] Turns, S.R., *An Introduction to Combustion*, McGraw-Hill, Inc., 1996.

[79] Chomiak, J., "Dissipation fluctuation and the structure and propagation of turbulent flames in premixed gases at high Renolds Numbers", in *Sixteenth Symposium (International) on Combustion, The Combustion Institute*, 1976, pp. 1665–1673.

[80] Namazian, M., Kelly, J.T., and Schefer, R.W., "Near-field instantaneous flame and fuel concentration structures", in *Twenty-Second Symposium (International) on Combustion, The Combustion Institute*, 1988, p. 627.

[81] Chomiak, J., "A possible propagation mechanism of turbulent flames at high Reynolds Numbers", *Combustion and Flame*, vol. 15, pp. 319–321, 1970.

[82] Chomiak, J., "Application of chemiluminescence measurement to the study of turbulent flame structure", *Combustion and Flame*, vol. 18, pp. 429–433, 1972.

[83] Ida, T. and Ohtake, K., "Microscopic structures in turbulent diffusion flames", *JSME International Journal, Series B: Fluid and Thermal Engineering*, vol. 37, No.3, pp. 629–635, 1994.

[84] Magre, P. and Dibble, R., "Finite chemical kinetics effects in a subsonic turbulent hydrogen flame", *Lecture Notes In Engineering: Turbulent Reactive Flows*, vol. 40, pp. 10–32, 1987.

[85] Karlovitz, B., Denniston, D.W., Knapschaefer, D.H., and Wells, F.E., "Studies on turbulent flames", in *Fourth Symposium (International) on Combustion, The Combustion Institute*, 1953, pp. 613–620.

[86] Chomiak, J. and Jarosinski, J., "Flame quenching by turbulence", *Combustion and Flame*, vol. 48, pp. 241–249, 1982.

[87] Radhakrishnan, K., Heywood, J.B., and Tabaczynski, R.J., "Premixed turbulent flame blowoff velocity correlation based on coherent structures in turbulent flows", *Combustion and Flame*, vol. 42, pp. 19–33, 1981.

[88] Cheng, T.S., Wehrmeyer, J.A., and Pitz, R.W., "Simultaneous temperature and multispecies measurement in a lifted hydrogen diffusion flame", *Combustion and Flame*, vol. 91, pp. 323–345, 1992.

[89] Guruz, A.G., Guruz, H.K., Osuwan, S., and Steward, F.R., "Aerodynamics of a confined burning jet", *Combustion Science and Technology*, vol. 9, pp. 103–110, 1974.

[90] Wierzba, I., Karim, G.A., and Cheng, H., "Correlating the flammability limits of fuel-diluent mixtures", *Journal of Energy Resources Technology*, vol. 110, pp. 157–160, 1988.

[91] Haniff, M.S., Melvin, A., Smith, D.B., and Williams, A., "The burning velocities of methane and SNG mixtures with air", *Journal of The Institute of Energy*, vol. LXII, No. 435, pp. 229–236, 1989.

[92] Reed, S.B., Mineur, J., and McNaughton, J.P., "The effect on the burning velocity of methane of vitiation of combustion air", *Journal of the Institute of Fuel*, vol. 44, pp. 149–155, 1971.

[93] Fells, I. and Rutherford A.G., "Burning velocity of methane-air flames", *Combustion and Flame*, vol. 13, pp. 130–138, 1969.

[94] Gerry, H.M. and Walter, R.K., "Some effects of inert diluents on flame speeds and temperatures", in *Fourth Symposium (International) on Combustion, The Combustion Institute*, 1952, pp. 313–320.

[95] Egolfopoulos, F.N., Zhu, D.L., and Law, C.K., "Experimental and numerical determination of laminar flame speed: mixtures of C_2-hydrocarbons with oxygen and nitrogen", in *Twenty-Third Symposium (International) on Combustion, The Combustion Institute*, 1990, pp. 471–478.

[96] Scholte, T.G. and Vaags, P.B., "Burning velocities of mixtures of hydrogen, carbon monoxide and methane with air", *Combustion and Flame*, vol. 3, pp. 511–524, 1959.

[97] Oostendorp, D.L. and Levinsky, H.B., "The effects of fuel and non-fuel gases on the laminar burning velocity of methane-air flames", *Journal of The Institute of Energy*, vol. 63, pp. 160–166, 1990.

[98] Dowdy, D.R., Smith, D.B., Taylon, S.C., and Williams, A., "The use of expanding spherical flames to determine burning velocities and stretch effects in hydrogen/air mixtures", in *Twenty-Third Symposium (International) on Combustion, The Combustion Institute*, 1990, pp. 325–332.

Appendix A

Simulation Programs

A.1 Simulation Program for the Blowout of Lifted Flames

```
# include <stdio.h>
# include <math.h>
main ()
{
  FILE  *fptr1 ;
  int i,n ;
  double ua, ub, ee, cr, ubmin, ubmax, k=0.24,
         uamin=0.05, uamax=0.6, step=0.01, fun() ;
  fptr1 = fopen ("curve-ub", "w") ;
  n = (int)((uamax-uamin)/step) ;
  ua = uamin ;
  for ( i=1; i<=n+2 ; i++ )
   {
```

```
ubmin =1 ;
ubmax = 4000 ;
ub = (ubmin+ubmax)/2 ;
cr = fun(ua,ub) ;
ee = fabs(cr-k) ;
while ( ee>=.0000001 )
  {
   if ( cr<k )
{
      ubmax = ub ;
      ub = (ubmin+ubmax)/2 ;
      cr = fun(ua,ub) ;
      ee = fabs(cr-k) ;
     }
   else if ( cr>k )
{
      ubmin = ub ;
      ub = (ubmin+ubmax)/2 ;
      cr = fun(ua,ub) ;
      ee = fabs(cr-k) ;
     }
   else { break ; }
  }
fprintf (fptr1, "%f\t %f\n", ua , ub) ;
if (ub<2.) {break ;}
ua = ua + step  ;
```

```
}
}
 double fun(ua,uj)
 double ua,uj;
{
 double rj=0.001 , ra=0.064 , Mf=16 , Ma=29 , rhoj=0.584 ,
        rhoa=1.06, s=0.385 , Lf=5. , Xmin=.001 , Xmax=80 ,
        Qj , Qa , mj , ma , rho1 , uk , ud , ct1 , ct , y ,
        e , g() , X , um , a , delta , cm , Tm , kb  ;
 Qj = rj*rj*uj ;
 Qa = (ra*ra-rj*rj)*ua  ;
 mj = Qj * rhoj ;
 ma = Qa * rhoa ;
 rho1 = (mj + ma) / (Qj + Qa) ;
 uk = (mj + ma) / (ra*ra*rho1)  ;
 ud = (mj*uj + 0.5*ma*ua) / (ra*ra*rho1) ;
 ct1 = ud-0.5*uk*uk ;
 ct = uk/(pow(ct1, (double)0.5))  ;
 cm = (Lf*Mf)/(Lf*Mf + (100-Lf)*Ma) ;
 y = (0.5*mj)/(cm*rhoa*ua*ra*ra) ;
 e = fabs(Xmax-Xmin) ;
 X = (Xmax+Xmin)/2. ;
 if ( y>=g(Xmin,ct,uk,ua) && y<=g(Xmax,ct,uk,ua) )
 {
   while (e>= 0.0000001)
   {
```

```
    if (y>g(X,ct,uk,ua))
     {
      Xmin = X   ;
      X = (Xmax+X)/2.   ;
      e = fabs(X-Xmin) ;
     }
    else if (y< g(X,ct,uk,ua))
     {
      Xmax = X   ;
      X = (Xmin+X)/2.   ;
      e = fabs(X-Xmax)   ;
     }
     else { break ; }
  }
 }
 else { printf ("out of range") ;}
 a = 1+ pow( (X/(5.95*exp(3.54*ct))),(double)1.67 ) ;
 um = ( uk/(ct*.0725*X*a) ) + ua ;
 delta = 0.084*ra*X*(1+pow((X/(4.07*exp(3.54*ct))),(double)1.67)) ;
 Tm = (4.2/10000.)* delta / (um*um*um) ;
 kb = (pow(Tm,(double).5)) * (s*s*10000./7.) * (rj/0.001) ;
 return ( kb ) ;
}
 double g(xx,ct,uk,ua)
  double xx, ct,uk,ua ;
  {
```

```
  double Xu1, Xu, Xr1, Xr, g1 ;
  Xu1 = xx/(5.95*exp(3.54*ct)) ;
  Xu = 1 + pow(Xu1,(double)1.67) ;
  Xr1 = xx/(4.07*exp(3.54*ct)) ;
  Xr = 1+pow(Xr1,(double)1.67)  ;
  g1 = 0.043*xx*xx*Xr*Xr*( (uk/(xx*ct*ua*Xu)) +0.19 ) ;
  return (g1) ;
 }
```

A.2 Simulation Program for Liftoff, Reattachment and the Blowout of Attached Flames

```
# include <stdio.h>
# include <math.h>
main ()
{
  FILE  *fptr1 ;
  int i,n ;
  double ua, ub, ee, cr, ubmin, ubmax, k=2.8 ,
         uamin=.05, uamax=1.3, step=.01, fun() ;
  fptr1 = fopen ("curve-ulbr", "w") ;
  n = (int)((uamax-uamin)/step) ;
  ua = uamin ;
  for ( i=1; i<=n+2 ; i++ )
   {
    ubmin =1 ;
```

```
    ubmax = 4000 ;
    ub = (ubmin+ubmax)/2 ;
    cr = fun(ua,ub) ;
    ee = fabs(cr-k) ;
    while ( ee>=.0000001 )
      {
       if ( cr>k )
 {
          ubmax = ub ;
          ub = (ubmin+ubmax)/2 ;
          cr = fun(ua,ub) ;
          ee = fabs(cr-k) ;
        }
       else if ( cr<k )
 {
          ubmin = ub ;
          ub = (ubmin+ubmax)/2 ;
          cr = fun(ua,ub) ;
          ee = fabs(cr-k) ;
        }
       else { break ; }
      }
    fprintf (fptr1, "%f\t %f\n", ua , ub) ;
    if (ub<2.) {break ;}
    ua = ua + step  ;
}
```

```
}
 double fun(ua,uj)
 double ua,uj;
{
  /*  For Reattachment: rhoj=0.584  */
 double rj=0.001 , ra=0.064 , Mf=16 , Ma=29 , rhoj=0.088 ,
        rhoa=1.06, s=0.41 , Lst=9.53 , Xmin=.001 , Xmax=300 ,
        Qj , Qa , mj , ma , rho1 , uk , ud , ct1 , ct , y ,
        e , g() , X , um , a , delta , cm , Tm , klbr  ;
 Qj = rj*rj*uj ;
 Qa = (ra*ra-rj*rj)*ua  ;
 mj = Qj * rhoj ;
 ma = Qa * rhoa ;
 rho1 = (mj + ma) / (Qj + Qa) ;
 uk = (mj + ma) / (ra*ra*rho1)  ;
 ud = (mj*uj + 0.5*ma*ua) / (ra*ra*rho1) ;
 ct1 = ud-0.5*uk*uk ;
 ct = uk/(pow(ct1, (double)0.5))  ;
 cm = (Lst*Mf)/(Lst*Mf + (100-Lst)*Ma) ;
 y = (0.5*mj)/(cm*rhoa*ua*ra*ra) ;
 e = fabs(Xmax-Xmin) ;
 X = (Xmax+Xmin)/2. ;
 if ( y>=g(Xmin,ct,uk,ua) && y<=g(Xmax,ct,uk,ua) )
 {
   while (e>= 0.0000001)
   {
```

```
      if (y>g(X,ct,uk,ua))
       {
        Xmin = X  ;
        X = (Xmax+X)/2.  ;
        e = fabs(X-Xmin) ;
       }
      else if (y< g(X,ct,uk,ua))
       {
        Xmax = X  ;
        X = (Xmin+X)/2.  ;
        e = fabs(X-Xmax)  ;
       }
       else { break ; }
    }
  }
  else { printf ("out of range") ;}
  a = 1+ pow( (X/(5.95*exp(3.54*ct))),(double)1.67 ) ;
  um = ( uk/(ct*.0725*X*a) ) + ua ;
  delta = 0.084*ra*X*(1+pow((X/(4.07*exp(3.54*ct))),(double)1.67)) ;
  klbr = (delta*um) / (s*pow((ra*rj),(double)0.5)) ;
  return ( klbr ) ;
}
  double g(xx,ct,uk,ua)
   double xx, ct,uk,ua ;
   {
    double Xu1, Xu, Xr1, Xr, g1 ;
```

```
  Xu1 = xx/(5.95*exp(3.54*ct)) ;
  Xu = 1 + pow(Xu1,(double)1.67) ;
  Xr1 = xx/(4.07*exp(3.54*ct)) ;
  Xr = 1+pow(Xr1,(double)1.67)  ;
  g1 = 0.043*xx*xx*Xr*Xr*( (uk/(xx*ct*ua*Xu)) +0.19 ) ;
  return (g1) ;
 }
```

A.3 Calculation of Constants I_1 and I_2

```
/*  SIMPSON'S RULE  */
# include <stdio.h>
# include <math.h>
main ()
{
   int i;
   double h=0.0001, x1, x2=0., s=0., fun(), I ;
   for (i=1; i<=40000 ; i++)
     {
      x1=x2 ;
      x2=x1+h ;
      s+=(h/6)*(fun(x1)+4*fun((x1+x2)/2)+fun(x2)) ;
     }
      I = s ;
      printf("x1=%f\t I=%f\n", x1, I) ;
}
```

```
double fun(x)
double x ;
  {
   double power ;
   power = -1.181 ;
   /*  For I2: power = -0.488  */
   return(x*exp(power*pow(x,(double)1.82))) ;
  }
```

Appendix B

Numerical Example for the Blowout of Lifted Flames

Determination of the blowout limit of a methane jet into a co-flowing stream of air for the following conditions:

u_{∞}=0.3 m/s	$S_{L,St}$=0.385 m/s
d_o=2 mm	L_F=5% by volume
d_{∞}=127 mm	$\nu = 4.2 \times 10^{-4}$ m^2/s
ρ_o=0.584 kg/m^3	$\alpha = 7 \times 10^{-4}$ m^2/s
ρ_{∞}=1.06 kg/m^3	$k_{B,Cr}$=0.24

Solution:

The jet blowout velocity can be calculated using a trial and error method. Assuming a value for this velocity, u_o=28.7 m/s, the following variables can be calculated using Equations (5.25 - 5.27) and (5.33), as:

$$Q_o = \pi r_o^2 u_o = \pi \times 0.001^2 \times 28.7 = 9.016 \times 10^{-5} \text{ m}^3/\text{s}$$

$$Q_\infty = \pi(r_\infty^2 - r_o^2)u_\infty = \pi \times (0.064^2 - 0.001^2) \times 0.3 = 3.85 \times 10^{-3} \text{ m}^3/\text{s}$$

$$m_o = Q_o \cdot \rho_o = 9.016 \times 10^{-5} \times 0.584 = 5.268 \times 10^{-5} \text{ kg/s}$$

$$m_\infty = Q_\infty \cdot \rho_\infty = 3.85 \times 10^{-3} \times 1.06 = 4.08 \times 10^{-3} \text{ kg/s}$$

$$\rho_{ave} = \frac{m_o + m_\infty}{Q_o + Q_\infty} = \frac{5.268 \times 10^{-5} + 4.08 \times 10^{-3}}{9.016 \times 10^{-5} + 3.85 \times 10^{-3}} = 1.049 \text{ kg/m}^3$$

$$u_k = \frac{m_o + m_\infty}{\pi r_\infty^2 \rho_{ave}} = \frac{5.268 \times 10^{-5} + 4.08 \times 10^{-3}}{\pi \times 0.064^2 \times 1.049} = 0.307 \text{ m/s}$$

$$\begin{aligned} u_d^2 &= \frac{m_o u_o + \frac{1}{2} m_\infty u_\infty}{\pi r_\infty^2 \rho_{ave}} \\ &= \frac{5.268 \times 10^{-5} \times 28.7 + 0.5 \times 4.08 \times 10^{-3} \times 0.3}{\pi \times 0.064^2 \times 1.049} \\ &= 0.157 \text{ m}^2/\text{s}^2 \end{aligned}$$

$$Ct = \frac{u_k}{\left(u_d^2 - \frac{1}{2}u_k^2\right)^{1/2}} = \frac{0.307}{(0.157 - 0.5 \times 0.307^2)^{1/2}} = 0.925$$

$$X_r = 4.07 \exp(3.54 Ct) = 4.07 \exp(3.54 \times 0.925) = 107.4$$

$$X_u = 5.95 \exp(3.54 Ct) = 5.95 \exp(3.54 \times 0.925) = 157$$

$$\begin{aligned} c_m &= \frac{L_L \cdot M_o}{L_L \cdot M_o + (100 - L_L) M_\infty} \\ &= \frac{5 \times 16}{5 \times 16 + (100 - 5) \times 29} = 0.028 \end{aligned}$$

The normalized distance from jet exit, X, where the jet fuel concentration at the jet axis is equal to its lean flammability limit can be calculated using Equation (5.32),

$$\frac{r_o^2 \rho_o u_o}{2 r_\infty^2 \rho_\infty u_\infty c_m} = 0.043 X^2 \left[1 + \left(\frac{X}{X_r}\right)^{5/3}\right]^2 .$$

$$\left[\frac{u_k}{X \cdot Ct \cdot u_\infty \left[1 + \left(\frac{X}{X_u}\right)^{5/3}\right]} + 0.19\right]$$

Substituting the values of calculated parameters into this equation results in:

$$\begin{aligned}\frac{0.001^2 \times 0.584 \times 28.7}{2 \times 0.064^2 \times 1.06 \times 0.3 \times 0.028} &= 0.043X^2\left[1 + \left(\frac{X}{107.4}\right)^{5/3}\right]^2 \cdot \\ &\left[\frac{0.307}{X \times 0.925 \times 0.3 \left[1 + \left(\frac{X}{157}\right)^{5/3}\right]} + 0.19\right]\end{aligned}$$

This equation can be solved for X by trial and error method. The results of calculation for normalized axial distance is:

$$X = 3.12$$

and the corresponding axial distance is:

$$\begin{aligned} x &= X \cdot r_\infty \\ x &= 3.12 \times 0.064 = 0.2 \text{ m} \end{aligned}$$

The values of δ_u and u_m corresponding to this position can be calculated from Equations (5.22) and (5.23) as:

$$\begin{aligned}\delta_u &= 0.084X \cdot r_\infty \left[1 + \left(\frac{X}{X_r}\right)^{5/3}\right] \\ &= 0.084 \times 3.12 \times 0.064 \left[1 + \left(\frac{3.12}{107.4}\right)^{5/3}\right] = 1.682 \times 10^{-2} \text{ m}\end{aligned}$$

$$
\begin{aligned}
u_m &= \frac{u_k}{0.0725X \cdot Ct\left[1+\left(\frac{X}{X_u}\right)^{5/3}\right]} + u_\infty \\
&= \frac{0.307}{0.0725 \times 3.12 \times 0.925\left[1+\left(\frac{3.12}{157}\right)^{5/3}\right]} + 0.3 = 1.765 \text{ m/s}
\end{aligned}
$$

Substituting δ_u, u_m and k_B into Equation (5.34) results in:

$$
\begin{aligned}
k_B &= \left(\frac{\delta_u \cdot \nu}{u_m^3}\right)^{1/2} \cdot \left(\frac{S_{L,St}^2}{\alpha}\right) \cdot \left(\frac{r_o}{r_{ref}}\right) \\
0.24 &= \left(\frac{1.682 \times 10^{-2} \times 4.2 \times 10^{-4}}{1.765^3}\right)^{1/2} \cdot \left(\frac{0.385^2}{7 \times 10^{-4}}\right) \cdot \left(\frac{0.001}{0.001}\right) \\
0.24 &= 0.24
\end{aligned}
$$

Since the value of both sides of the above equation (blowout criterion) are the same, the assumed u_o is the jet blowout velocity at these conditions.

Appendix C

Derivation of $Y_{F_S F}$

The combustion reaction of a general hydrocarbon $(C_nH_m)_J$ as the jet fuel in an ambient of air premixed with a hydrocarbon $(C_nH_m)_S$ can be expressed as:

$$\phi_J(C_nH_m)_J + \mathbf{x}\left[(1 - Y_{F_S A})(0.21O_2 + 0.79N_2) + Y_{F_S A}(C_nH_m)_S\right] \rightarrow$$
$$A_1(CO_2) + A_2(H_2O) + A_3(N_2) + ... \quad (C.1)$$

where ϕ_J is the equivalence ratio of the jet fuel (the molar fuel to air ratio to the molar stoichiometric fuel to air ratio); $Y_{F_S A}$ is the mole fraction of surrounding fuel in surrounding fuel-air mixture. $\mathbf{x}$ should be evaluated in such a way that both the jet fuel and the surrounding fuel burn in their equivalence ratio, ϕ_J and ϕ_S, respectively. The combustion reaction of the jet fuel in air on its own at equivalence ratio of ϕ_J can be expressed as:

$$\phi_J(C_nH_m)_J + [A/F]_{St,J}(0.21O_2 + 0.79N_2) \rightarrow$$
$$B_1(CO_2) + B_2(H_2O) + B_3(N_2) + ... \quad (C.2)$$

where $[A/F]_{St,J}$ is the stoichiometric molar air to jet fuel ratio (e.g. for methane, $[A/F]_{St,J} = 9.524$). Also, the combustion reaction of the surrounding fuel in air on its own at equivalence ratio of ϕ_S can be expressed as:

$$[\mathbf{x} \cdot Y_{F_SA}]\,(\mathrm{C_nH_m})_S + \left[\mathbf{x} \cdot Y_{F_SA} \cdot \left(\frac{[A/F]_{St,S}}{\phi_S}\right)\right](0.21\mathrm{O_2} + 0.79\mathrm{N_2}) \rightarrow \mathrm{C_1(CO_2) + C_2(H_2O) + C_3(N_2)} + \dots \quad \text{(C.3)}$$

The sum of the air coefficient in the left hand side of chemical equations of (C.2) and (C.3) should be equal to that of chemical equation of (C.1), i.e.,

$$[A/F]_{St,J} + \mathbf{x} \cdot Y_{F_SA} \cdot \left(\frac{[A/F]_{St,S}}{\phi_S}\right) = \mathbf{x}(1 - Y_{F_SA}) \qquad \text{(C.4)}$$

Rearrangement of this equation yields to:

$$\mathbf{x} = \frac{[A/F]_{St,J}}{1 - Y_{F_SA}\left(1 + \frac{[A/F]_{St,S}}{\phi_S}\right)} \qquad \text{(C.5)}$$

Substituting the value of $\mathbf{x}$ into equation (C.1) results in:

$$\phi_J(\mathrm{C_nH_m})_J + \left[\frac{[A/F]_{St,J}(1 - Y_{F_SA})}{1 - Y_{F_SA}\left(1 + \frac{[A/F]_{St,S}}{\phi_S}\right)}\right](0.21\mathrm{O_2} + 0.79\mathrm{N_2}) + \left[\frac{[A/F]_{St,J} \cdot Y_{F_SA}}{1 - Y_{F_SA}\left(1 + \frac{[A/F]_{St,S}}{\phi_S}\right)}\right](\mathrm{C_nH_m})_S \rightarrow \mathrm{A_1(CO_2) + A_2(H_2O) + A_3(N_2)} + \dots \qquad \text{(C.6)}$$

In the total jet fuel, air and surrounding fuel mixture, jet fuel and surrounding fuel can be combined to form a fuel mixture. The mole fraction of surrounding fuel in such fuel mixture, Y_{F_SF}, can be expressed as:

$$Y_{F_SF} = \frac{Y_{F_S}}{Y_{F_S} + Y_{F_J}} \tag{C.7}$$

Y_{F_S} and Y_{F_J} can be found from Equation (C.6), and replaced into Equation (C.7). As a result,

$$Y_{F_SF} = \frac{\left[\frac{[A/F]_{St,J} \cdot Y_{F_SA}}{1 - Y_{F_SA}(1 + [A/F]_{St,S}/\phi_S)}\right]}{\left[\frac{[A/F]_{St,J} \cdot Y_{F_SA}}{1 - Y_{F_SA}(1 + [A/F]_{St,S}/\phi_S)}\right] + \phi_J} \tag{C.8}$$

Simplifying this equation results in:

$$Y_{F_SF} = \frac{Y_{F_SA} \cdot [A/F]_{St,J}}{Y_{F_SA} \cdot [A/F]_{St,J} + [1 - Y_{F_SA}(1 + [A/F]_{St,S}/\phi_S)] \cdot \phi_J} \tag{C.9}$$

and for stochiometric condition:

$$Y_{F_SF} = \frac{Y_{F_SA} \cdot [A/F]_{St,J}}{Y_{F_SA}\{[A/F]_{St,J} - [A/F]_{St,S} - 1\} + 1} \tag{C.10}$$

This expression for Y_{F_SF} as a function of Y_{F_SA} can be used in calculations of the laminar burning velocity of a jet fuel in a surrounding stream of air premixed with fuel.

IMAGE EVALUATION
TEST TARGET (QA-3)

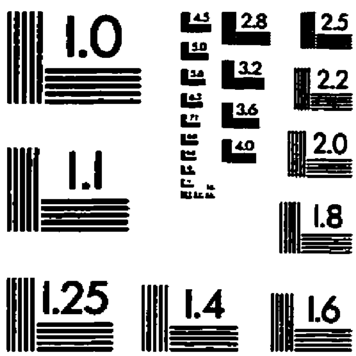

150mm

6"

APPLIED IMAGE . Inc
1653 East Main Street
Rochester, NY 14609 USA
Phone: 716/482-0300
Fax: 716/288-5989